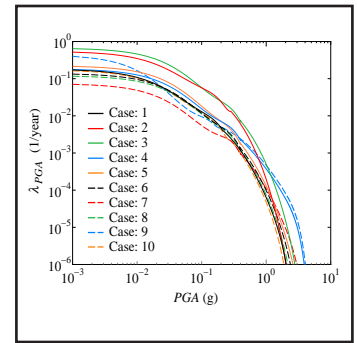
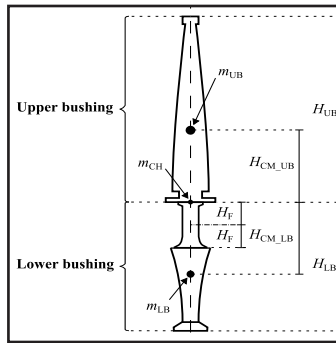
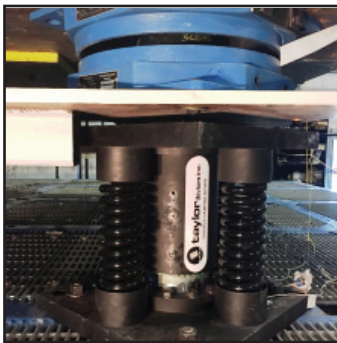


Procedures and Results of Assessment of Seismic Performance of Seismically Isolated Electrical Transformers with Due Consideration for Vertical Isolation and Vertical Ground Motion Effects

by
**Shoma Kitayama, Michael C. Constantinou
 and Donghun Lee**



Technical Report MCEER-16-0010

December 31, 2016

NOTICE

This report was prepared by the University at Buffalo, State University of New York, as a result of research sponsored by MCEER. Neither MCEER, associates of MCEER, its sponsors, University at Buffalo, State University of New York, nor any person acting on their behalf:

- a. makes any warranty, express or implied, with respect to the use of any information, apparatus, method, or process disclosed in this report or that such use may not infringe upon privately owned rights; or
- b. assumes any liabilities of whatsoever kind with respect to the use of, or the damage resulting from the use of, any information, apparatus, method, or process disclosed in this report.

Any opinions, findings, and conclusions or recommendations expressed in this publication are those of the author(s) and do not necessarily reflect the views of MCEER, the National Science Foundation or other sponsors.

**Procedures and Results of Assessment of
Seismic Performance of Seismically Isolated
Electrical Transformers with Due Consideration for
Vertical Isolation and Vertical Ground Motion Effects**

by

Shoma Kitayama,¹ Michael C. Constantinou² and Donghun Lee¹

Publication Date: December 31, 2016

Submittal Date: August 15, 2016

Technical Report MCEER-16-0010

MCEER Thrust Area 3: Innovative Technologies

- 1 PhD Candidate, Department of Civil, Structural and Environmental Engineering, University at Buffalo, State University of New York
- 2 Samuel P. Capen Professor and SUNY Distinguished Professor, Department of Civil, Structural and Environmental Engineering, University at Buffalo, State University of New York

MCEER

University at Buffalo, State University of New York

212 Ketter Hall, Buffalo, NY 14260

E-mail: mceer@buffalo.edu; Website: <http://mceer.buffalo.edu>

Preface

MCEER is a national center of excellence dedicated to the discovery and development of new knowledge, tools and technologies that equip communities to become more disaster resilient in the face of earthquakes and other extreme events. MCEER accomplishes this through a system of multidisciplinary, multi-hazard research, in tandem with complimentary education and outreach initiatives.

Headquartered at the University at Buffalo, The State University of New York, MCEER was originally established by the National Science Foundation in 1986, as the first National Center for Earthquake Engineering Research (NCEER). In 1998, it became known as the Multidisciplinary Center for Earthquake Engineering Research (MCEER), from which the current name, MCEER, evolved.

Comprising a consortium of researchers and industry partners from numerous disciplines and institutions throughout the United States, MCEER's mission has expanded from its original focus on earthquake engineering to one which addresses the technical and socio-economic impacts of a variety of hazards, both natural and man-made, on critical infrastructure, facilities, and society.

The Center derives support from several Federal agencies, including the National Science Foundation, Federal Highway Administration, Department of Energy, Nuclear Regulatory Commission, and the State of New York, foreign governments and private industry.

This report presents an analytical study of the response of seismically isolated electrical transformers with particular emphasis on comparing the performance of equipment that are non-isolated to equipment that are isolated only in the horizontal direction or are isolated by a three-dimensional isolation system. The failure characteristics of transformers were determined by calibrating a failure model using fragility data of non-isolated transformers that were based on field data and are used in the seismic performance of electrical equipment by utilities in the Western U.S.

The performance was assessed by calculating the probability of failure as a function of the seismic intensity with due consideration of (a) horizontal and vertical ground seismic motion effects, (b) displacement capacity of the seismic isolation system, including uplift capacity, (c) acceleration limits for failure of electrical bushings, (d) details of construction of the isolation system that allow or restrain rocking of the isolated structure, (e) weight of the isolated transformer in the range of 320 to 520 kip, (f) bushings with as-installed frequencies of 2.6 to 11.3 Hz, (g) inclined and vertical placed bushings and (h) various details of the isolators, including upper and lower bound properties and details of construction of the isolators.

ABSTRACT

This report presents an analytical study of the response of seismically isolated electrical transformers with particular emphasis on comparing the performance of equipment that are non-isolated to equipment that are isolated only in the horizontal direction or are isolated by a three-dimensional isolation system. The failure characteristics of transformers were determined by calibrating a failure model using fragility data of non-isolated transformers that were based on field data and are used in the seismic performance of electrical equipment by utilities in the western US. The performance was assessed by calculating the probability of failure as a function of the seismic intensity with due consideration of (a) horizontal and vertical ground seismic motions, (b) displacement capacity of the seismic isolation system, (c) acceleration limits for failure of electrical bushings, (d) details of construction of the isolation system that allow or restrain rocking of the isolated structure, (e) weight of isolated transformer in the range of 320 to 520kip, (f) inclined and vertical electrical bushings, (g) as-installed frequency of bushings and (h) various details of the isolators, including upper and lower bound properties and details of construction of the isolators. Moreover, calculations of the probability of failure within the lifetime of isolated and non-isolated transformers at various locations in the western US were performed.

The results of this study demonstrates primarily that a) seismic isolation systems, and particularly systems which isolate in both the horizontal and vertical ground directions, can improve the seismic performance in terms of reducing the probability of failure, and b) combined horizontal-vertical seismic isolation systems consistently improve the probability of failure of transformers for a wide range of parameters.

The methodologies and results presented in this report (a) may be used to decide on the benefits offered by the seismic protective system depending on the limits of the protected equipment, location of the equipment (value of PGA) and configuration and properties of the seismic protective system, and (b) may be used to calculate the mean annual frequency of functional failure and the corresponding probability of failure over the lifetime of the equipment. The information produced by these methodologies may be used to assess the seismic performance of electric transmission networks under scenarios of component failures.

“This Page Intentionally Left Blank”

ACKNOWLEDGEMENTS

This work was made possible with financial support by the Bonneville Power Administration (BPA) with Dr. Leon Kempner, Jr. and Mr. Michael Riley as the responsible technical officers. This support is gratefully acknowledged.

We acknowledge the contributions of Dr. Leon Kempner, Mr. Michael Riley and Professor Anshell Schiff in providing numerous comments and suggestions during the course of this study that resulted in substantial improvements in the final product.

“This Page Intentionally Left Blank”

TABLE OF CONTENTS

SECTION 1	INTRODUCTION	1
SECTION 2	METHODOLOGY FOR FAILURE PERFORMANCE EVALUATION OF SEISMICALLY ISOLATED ELECTRICAL TRANSFORMERS	5
SECTION 3	MODELING OF ELECTRICAL TRANSFORMERS FOR FAILURE ASSESSMENT	11
3.1	Modeling of Bushings.....	11
3.2	Failure of Transformers	16
3.3	Modeling the Transformer	25
SECTION 4	DESCRIPTION OF SEISMIC ISOLATION SYSTEM	29
4.1	Triple Friction Pendulum Bearings.....	29
4.2	Behavior of Triple Friction Pendulum Bearings.....	31
4.3	Description of Spring-Damper Device	32
SECTION 5	MODEL FOR SIMULATING THE ULTIMATE BEHAVIOR OF TRIPLE FRICTION PENDULUM BEARINGS.....	37
5.1	Introduction.....	37
5.2	Description of Element	37
5.3	Example of Application and Investigation of Axial-Shear Force Interaction.....	42
5.4	Calculation of Uplift Displacement	60
SECTION 6	MODEL FOR SIMULATING THE ULTIMATE BEHAVIOR OF SPRING-DAMPER UNIT IN THREE-DIMENSIONAL SEISMIC ISOLATION SYSTEM	63
SECTION 7	SELECTION AND SCALING OF GROUND MOTIONS.....	69
SECTION 8	FRAGILITY ANALYSIS RESULTS	75

TABLE OF CONTENTS (CONT'D)

SECTION 9	SUMMARY OF RESULTS AND SAMPLE PROBABILITY OF FAILURE LIFETIME RISK CALCULATIONS.....	97
SECTION 10	SUMMARY AND CONCLUSIONS	109
SECTION 11	REFERENCES.....	111
APPENDIX A	MODIFIED SERIES MODEL PARAMETERS	117
A.1	Case of Bearing without Inner Restrainer Ring (Figure 4-2).....	117
A.1.1	Model with Axial-Shear Force Interaction	117
A.1.2	Model without Axial-Shear Force Interaction	120
A.2	Case of Bearing with Inner Restrainer Ring (Figure 4-1).....	122
A.2.1	Model with Axial-Shear Force Interaction	122
A.2.2	Model without Axial-Shear Force Interaction	125

LIST OF FIGURES

Figure 1-1 Horizontal-Only and Horizontal-Vertical Isolation Systems	1
Figure 2-1 Moderate and High Required Response Spectra per IEEE 693 (5% Damped).....	5
Figure 2-2 Example of Fragility Curve.....	7
Figure 2-3 Seismic Hazard Curves for Zero Period for Locations of Table 2-1.....	9
Figure 3-1 Definition of Dimensions of Bushing	13
Figure 3-2 Bushing Models: (a) Fixed Condition; (b) As-Installed Condition.....	15
Figure 3-3 Test Results on Vertical and Rocking Frequency of As-Installed Bushings (From Kong, 2010 and Fahad, 2013).....	15
Figure 3-4 Main Failure Modes of Porcelain Bushings.....	17
Figure 3-5 Relation between Acceleration at Center of Mass and Normalized Moment of Upper Bushing in Combined Horizontal-Vertical Seismic Isolation System with Unrestrained Rocking in the Isolation System for Case of Motion Beverly Hills - Mulhol	18
Figure 3-6 Relation between Acceleration at Center of Mass and Normalized Moment of Upper Bushing in Combined Horizontal-Vertical Seismic Isolation System with Restrained Rocking in the Isolation System for Case of Motion Beverly Hills – Mulhol	19
Figure 3-7 Relation between Acceleration at Center of Mass and Normalized Moment of Upper Bushing in Combined Horizontal-Vertical Seismic Isolation System with Unrestrained Rocking in the Isolation System for Case of Motion Arcelik	19
Figure 3-8 Relation between Acceleration at Center of Mass and Normalized Moment of Upper Bushing in Combined Horizontal-Vertical Seismic Isolation System with Restrained Rocking in the Isolation System for Case of Motion Arcelik	20
Figure 3-9 5%-Damped Acceleration Spectra of Motions Recorded at Station Beverly Hills–Mulhol in the 1994 Northridge Earthquake and Recorded at Station Arcelik in the 1999 Kocaeli Earthquake (as recorded).....	21
Figure 3-10 Calculation of Longitudinal and Lateral Bushing Accelerations and Their Limit.....	22
Figure 3-11 Two-Dimensional Transformer Models.....	26
Figure 4-1 Section and Plan of Triple FP Bearing with Inner Restrainer	29

LIST OF FIGURES (CONT'D)

Figure 4-2 Section and Plan of Smallest Size Triple FP Bearing without Inner Restrainer	30
Figure 4-3 Sections of Larger Size Triple FP Bearings without Inner Restrainer	31
Figure 4-4 Schematic of Spring-Viscous Damper Device	34
Figure 4-5 Installation Method that Freely Allows Rocking	35
Figure 4-6 Installation Method that Restrains Rocking	35
Figure 4-7 View of Isolation System with Installation Method that Allows Free Rocking.....	36
Figure 4-8 View of Isolation System with Installation Method that Restrains Rocking	36
Figure 5-1 Organization of Elements of Modified Series Model in OpenSees	38
Figure 5-2 Three Springs in Parallel Element to Replace Single FP Element when Axial-Shear Force Interaction is Neglected	38
Figure 5-3 Bi-Linear Elastic Spring for Simulating Vertical Behavior	39
Figure 5-4 Definition of Parameters of Triple FP Bearing	40
Figure 5-5 Force-Displacement Loops of Individual Isolators and Total Base Shear-Displacement Loop of Transformer with Horizontal Isolation System in Horizontal Only Ground Motion.....	45
Figure 5-6 Acceleration Histories at Bushing Center of Mass of Transformer with Horizontal Isolation System in Horizontal Only Ground Motion.....	46
Figure 5-7 Force-Displacement Loops of Individual Isolators and Total Base Shear-Displacement Loop of Transformer with Horizontal-Vertical Isolation System with Rocking in Horizontal Only Ground Motion.....	47
Figure 5-8 Acceleration Histories at Bushing Center of Mass of Transformer with Horizontal-Vertical Isolation System with Rocking in Horizontal Only Ground Motion	48
Figure 5-9 Force-Displacement Loops of Individual Isolators and Total Base Shear-Displacement Loop of Transformer with Horizontal-Vertical Isolation System without Rocking in Horizontal Only Ground Motion.....	49
Figure 5-10 Acceleration Histories at Bushing Center of Mass of Transformer with Horizontal-Vertical Isolation System without Rocking in Horizontal Only Ground Motion	50
Figure 5-11 Force-Displacement Loops of Individual Isolators and Total Base Shear-Displacement Loop of Transformer with Horizontal Isolation System in Horizontal-Vertical Ground Motion	52
Figure 5-12 Acceleration Histories at Bushing Center of Mass of Transformer with Horizontal Isolation System in Horizontal-Vertical Ground Motion.....	53

LIST OF FIGURES (CONT'D)

Figure 5-13 Force-Displacement Loops of Individual Isolators and Total Base Shear-Displacement Loop of Transformer with Horizontal-Vertical Isolation System with Rocking in Horizontal-Vertical Ground Motion.....	54
Figure 5-14 Acceleration Histories at Bushing Center of Mass of Transformer with Horizontal-Vertical Isolation System with Rocking in Horizontal-Vertical Ground Motion	55
Figure 5-15 Force-Displacement Loops of Individual Isolators and Total Base Shear-Displacement Loop of Transformer with Horizontal-Vertical Isolation System without Rocking in Horizontal-Vertical Ground Motion.....	56
Figure 5-16 Acceleration Histories at Bushing Center of Mass of Transformer with Horizontal-Vertical Isolation System without Rocking in Horizontal-Vertical Ground Motion.....	57
Figure 5-17 Force-Displacement Loops of Individual Isolators and Total Base Shear-Displacement Loop of Transformer with Horizontal-Vertical Isolation System without Rocking in Another Horizontal-Vertical Ground Motion Scaled to PGA=1.0g so that there is Uplift.....	58
Figure 5-18 Acceleration Histories at Bushing Center of Mass of Transformer with Horizontal-Vertical Isolation System without Rocking in Another Horizontal-Vertical Ground Motion Scaled to PGA=1.0g so that there is Uplift.....	59
Figure 5-19 Measurement of Uplift Displacement	61
Figure 5-20 Example Uplift Displacement History of Triple FP Bearing	61
Figure 6-1 Elements Connected in parallel to Represent the Ultimate Behavior of Springs.....	63
Figure 6-2 Force-Displacement Relation Produced by Spring Element	64
Figure 6-3 Ultimate Behavior of Viscous Damper Element (Viscous Force not Depicted).....	65
Figure 6-4 Force-Displacement Loops Produced by Damper Element	66
Figure 6-5 Force-Displacement Loops Produced by Combined Spring-Damper Element.....	67
Figure 6-6 Force-Displacement Loops Produced by Combined Spring-Damper Element Supporting a Triple FP Isolator.....	68
Figure 7-1 Horizontal Acceleration Response Spectra of Selected 20 Ground Motions (Total of 40 Components).....	72
Figure 7-2 Vertical Acceleration Response Spectra of Selected 20 Ground Motions (Total of 20 Components).....	72

LIST OF FIGURES (CONT'D)

Figure 7-3 Average Vertical to Horizontal (V/H) Ratio of Spectral Accelerations of 40 Sets of Motions	73
Figure 7-4 Comparison of Horizontal and Vertical Average Spectra to IEEE High Required Response Spectra.....	74
Figure 8-1 Fragility Curves for 420kip Transformer with 7.7Hz Bushing (No. 8) Inclined at 20 Degrees, Triple FP Bearings without Inner Restrainer, Lower Bound Friction Properties and Isolator Ultimate Displacement Capacity of 17.7inch	77
Figure 8-2 Fragility Curves for 420kip Transformer with 7.7Hz Bushing (No. 8) Inclined at 20 Degrees, Triple FP Bearings without Inner Restrainer, Lower Bound Friction Properties and Isolator Ultimate Displacement Capacity of 27.7inch	83
Figure 8-3 Fragility Curves for 420kip Transformer with 7.7Hz Bushing (No. 8) Inclined at 20 Degrees, Triple FP Bearings without Inner Restrainer, Lower Bound Friction Properties and Isolator Ultimate Displacement Capacity of 31.3inch	84
Figure 8-4 Fragility Curves for 420kip Transformer with Vertically Placed 7.7Hz Bushing (No. 8), Triple FP Bearings without Inner Restrainer, Lower Bound Friction Properties and Isolator Ultimate Displacement Capacity of 17.7inch	85
Figure 8-5 Fragility Curves for 420kip Transformer with Vertically Placed 7.7Hz Bushing (No. 8), Triple FP Bearings without Inner Restrainer, Lower Bound Friction Properties and Isolator Ultimate Displacement Capacity of 27.7inch	86
Figure 8-6 Fragility Curves for 420kip Transformer with Vertically Placed 7.7Hz Bushing (No. 8), Triple FP Bearings without Inner Restrainer, Lower Bound Friction Properties and Isolator Ultimate Displacement Capacity of 31.3inch	87
Figure 8-7 Fragility Curves for 320, 420, 520kip Transformer with 7.7Hz Bushing (No. 8) Inclined at 20 Degrees, Triple FP Bearings without Inner Restrainer, Lower Bound Friction Properties and Isolator Ultimate Displacement Capacity of 17.7inch, Bushing Lateral Acceleration Limit=1g	88
Figure 8-8 Fragility Curves for 420kip Transformer with 2.6Hz, 4.3Hz, 7.7Hz and 11.3Hz Bushings (No. 7, 3, 8 and 6) Inclined at 20 Degrees, Triple FP Bearings without Inner Restrainer, Lower Bound Friction Properties and Isolator Ultimate Displacement Capacity of 17.7inch, Bushing Lateral Acceleration Limit=1g	90

LIST OF FIGURES (CONT'D)

Figure 8-9 Fragility Curves for 420kip Transformer with 2.6Hz, 4.3Hz, 7.7Hz and 11.3Hz Bushings (No. 7, 3, 8 and 6) Inclined at 20 Degrees, Triple FP Bearings without Inner Restrainer, Lower Bound Friction Properties and Isolator Ultimate Displacement Capacity of 17.7inch, Bushing Lateral Acceleration Limit=2g	91
Figure 8-10 Fragility Curves for 420kip Transformer with 7.7Hz Bushing (No. 8) Inclined at 20 Degrees, Triple FP Bearings without Inner Restrainer, Lower and Upper Bound Friction Properties and Isolator Ultimate Displacement Capacity of 17.7inch, Bushing Lateral Acceleration Limit=1g	92
Figure 8-11 Fragility Curves for 420kip Transformer with 7.7Hz Bushing (No. 8) Inclined at 20 Degrees, Triple FP Bearings without Inner Restrainer, Lower Bound Friction Properties and Isolator Ultimate Displacement Capacity of 17.7, 27.7, 31.3inch, Bushing Lateral Acceleration Limit=2g	93
Figure 8-12 Fragility Curves for 420kip Transformer with 7.7Hz Bushing (No. 8) Inclined at 20 Degrees, Triple FP Bearings without Inner Restrainer, Lower Bound Friction Properties and Isolator Ultimate Displacement Capacity of 17.7, 27.7, 31.3inch, Bushing Lateral Acceleration Limit=1g	94
Figure 8-13 Fragility Curves for 420kip Transformer with 7.7Hz Bushing (No. 8) Inclined at 20 Degrees, Triple FP Bearings with and without Inner Restrainer, Lower Bound Friction Properties and Isolator Ultimate Displacement Capacity of 17.7inch, Bushing Lateral Acceleration Limit=1g	96
Figure 9-1 Fragility Curves for 420kip Transformer with 11.3Hz Bushing (No. 6) Inclined at 20 Degrees, Triple FP Bearings without Inner Restrainer, Lower Bound Friction Properties and Isolator Ultimate Displacement Capacity of 17.7 or 27.7 inch, Horizontal Isolation, Bushing Lateral Acceleration Limit=2g	108
Figure 9-2 Fragility Curves for 420kip Transformer with 11.3Hz Bushing (No. 6) Inclined at 20 Degrees, Triple FP Bearings without Inner Restrainer, Lower Bound Friction Properties and Isolator Ultimate Displacement Capacity of 17.7 or 27.7 inch, Horizontal-Vertical Isolation with Rocking, Bushing Lateral Acceleration Limit=2g	108

LIST OF TABLES

Table 2-1 Location and Coordinates (not shown in the publicly available report) of Ten Sites in Western US	8
Table 3-1 Characteristics of Tested Bushings (based on Kong, 2010 and Fahad, 2013).....	12
Table 3-2 Parameters of Analytically Constructed Fragility Curves for Several Non-Isolated Transformers	23
Table 3-3 Parameters of Empirical Fragility Curves based of Field Earthquake Performance Data for Bushings of Seven Types of Non-Isolated Transformers (program SERA, Kempner, 2016) ...	24
Table 4-1 Lower Bound Frictional Properties of Triple Friction Pendulum Bearings	32
Table 4-2 Parameters of Spring-Damper Device	33
Table 5-1 Properties of Triple FP Bearings (Values in Parenthesis are for Bearing without Inner Restrainer Ring)	42
Table 5-2 Material/Element Parameter Values in Program OpenSees for Model Considering Axial-Shear Force Interaction (Values in Parenthesis are for Bearing without Inner Restrainer Ring)	43
Table 5-3 Input Material/Element Parameter Values in Program OpenSees for Model Considering Axial-Shear Force Interaction (Values in Parenthesis are for Bearing without Inner Restrainer Ring).....	44
Table 6-1 Parameters for Viscous Damper	65
Table 7-1 Ground Motions Used in Dynamic Analysis.....	70
Table 8-1 Analyzed Cases of Non-Isolated and Isolated Transformers.....	75
Table 8-2 Number of Failures for Case of 1g Transverse and 5g Longitudinal Bushing Acceleration Limits for 420kip Transformer with 7.7Hz Inclined Bushing (No. 8), Triple FP Bearings without Inner Restrainer, Lower Bound Friction Properties and Isolator Ultimate Displacement Capacity of 17.7inch.....	79
Table 8-3 Number of Failures for Case of 2g Transverse and 5g Longitudinal Bushing Acceleration Limits for 420kip Transformer with 7.7Hz Inclined Bushing (No. 8), Triple FP Bearings without Inner	

LIST OF TABLES (CONT'D)

Restrainer, Lower Bound Friction Properties and Isolator Ultimate Displacement Capacity of 17.7inch.....	81
Table 9-1 Fragility Data for Analyzed Transformers in Case of Lower Bound Friction, Bushing Inclined at 20 Degrees and FP Isolators without Inner Restrainer.....	97
Table 9-2 Fragility Data for Analyzed Transformers in Case of Lower Bound Friction, Vertical Bushing and FP Isolators without Inner Restrainer.....	98
Table 9-3 Fragility Data for Analyzed Transformers in Case of Upper Bound Friction, Bushing Inclined at 20 Degrees and FP Isolators without Inner Restrainer.....	98
Table 9-4 Fragility Data for Analyzed Transformers in Case of Lower Bound Friction, Bushing Inclined at 20 Degrees and FP Isolators with Inner Restrainer.....	98
Table 9-5 Values of Probability of Failure of Transformer with Bushing Inclined at 20 Degrees, FP Isolators without Inner Restrainer in Lower Bound Conditions for Seismic Intensity with $PGA=0.6g$, $P_{F/PGA=0.6g}$	99
Table 9-6 Probability of Failure (in %) in 50 Years PF of 420 kip Transformer with 2.6Hz Bushing for Locations in Western US with 1g Transverse Acceleration Limit.....	101
Table 9-7 Probability of Failure (in %) in 50 Years PF of 420 kip Transformer with 2.6Hz Bushing for Ten Locations in Western US with 2g Transverse Acceleration Limit.....	101
Table 9-8 Probability of Failure (in %) in 50 Years PF of 420 kip Transformer with 4.3Hz Bushing for Ten Locations in Western US with 1g Transverse Acceleration Limit.....	102
Table 9-9 Probability of Failure (in %) in 50 Years PF of 420 kip Transformer with 4.3 Hz Bushing for Ten Locations in Western US with 2g Transverse Acceleration Limit.....	102
Table 9-10 Probability of Failure (in %) in 50 Years PF of 420 kip Transformer with 7.7 Hz Bushing for Ten Locations in Western US with 1g Transverse Acceleration Limit	103
Table 9-11 Probability of Failure (in %) in 50 Years PF of 420 kip Transformer with 7.7 Hz Bushing for Ten Locations in Western US with 2g Transverse Acceleration Limit	104
Table 9-12 Probability of Failure (in %) in 50 Years PF of 420 kip Transformer with 11.3 Hz Bushing for Ten Locations in Western US with 1g Transverse Acceleration Limit	105
Table 9-13 Probability of Failure (in %) in 50 Years PF of 420 kip Transformer with 11.3 Hz Bushing for Ten Locations in Western US with 2g Transverse Acceleration Limit	105

SECTION 1 INTRODUCTION

This report presents an analytical study of the response of seismically isolated electrical transformers with particular emphasis on comparing the performance of equipment that are non-isolated to equipment that are isolated only in the horizontal direction or are isolated by a three-dimensional isolation system. The performance is assessed by constructing failure fragility curves. The isolation systems considered are triple Friction Pendulum (FP) isolators for the horizontal isolation system and an independent vertical-only spring-damper system that supports the triple FP isolators to form the three-dimensional isolation system. Figure 1-1 illustrates the two isolation systems and the motion of the isolated transformer with respect to the ground.

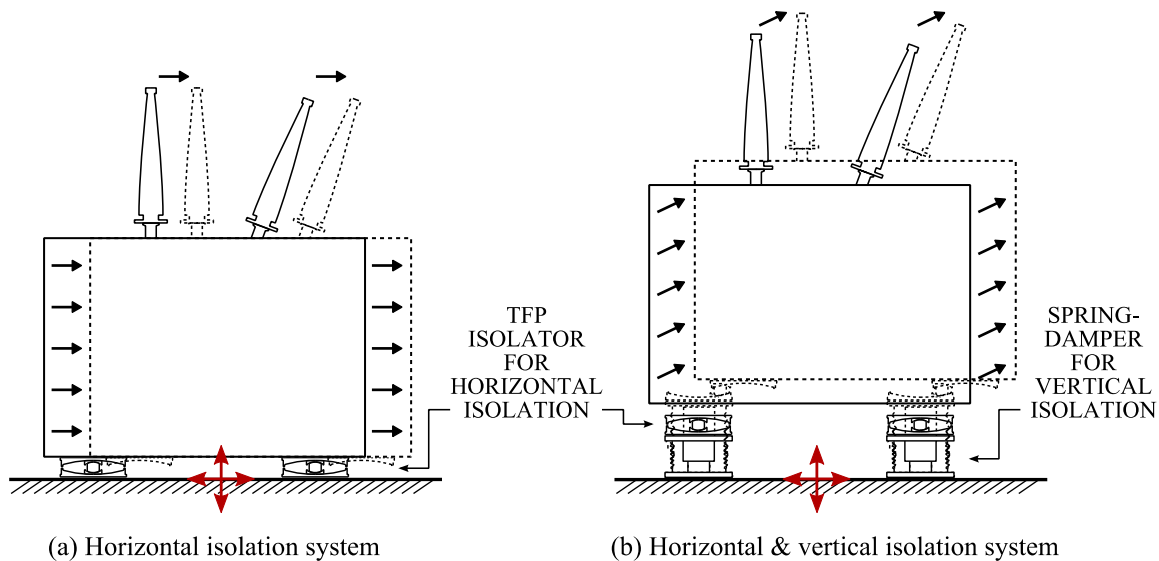


Figure 1-1 Horizontal-Only and Horizontal-Vertical Isolation Systems

As shown in Figure 1-1, the combined horizontal-vertical isolation system is allowed to undergo horizontal and vertical motions. In reality, two versions of the system will be discussed and analyzed in the report: (a) one that allows for clearly separated horizontal and vertical motions without (or with limited) rocking and (b) another in which rocking of the supported equipment is freely allowed.

Past studies of the seismic performance of electrical equipment demonstrated that horizontal isolation systems can improve the seismic performance in terms of reduction of absolute acceleration and relative displacement of bushings and the transformer body (e.g., Murota et al., 2005; Ersoy et al., 2008; Oikonomou et al., 2016). This reduction of response only applied to the

horizontal direction, whereas there was no reduction of response in the vertical direction. However, these studies did not relate the selective reduction of response to prevention of failure of components of the equipment or failure of the equipment itself. Moreover, experimental studies of Kong (2010) and Fahad (2013) investigated the failure modes of electrical bushings but their studies did not relate the findings of component failure to the seismic response of transformers. Information on the field performance of electrical equipment in past earthquakes exists (e.g, Anagnos, 1999; Kempner et al, 2006) and has been used to develop empirical fragility curves for conventionally supported electrical equipment which are then used in seismic vulnerability assessments by electric utility companies. One notable example is the earthquake assessment program SERA (Kempner et al, 2006) that is used by many west coast utility companies (BPA, PG&E, SDG&E, BC Hydro, Pacific Corp, etc.). Information utilized in program SERA for non-isolated electrical transformers is used in this study to calibrate the failure model, which is then used for constructing fragility curves for seismically isolated transformers.

This study utilizes advanced models for the isolators that can simulate the ultimate characteristics of the isolation system components in order to perform an assessment of performance based on a probabilistic method using incremental dynamic analysis (Vamvatsikos and Cornell, 2002), the statistical assessment methodologies in FEMA P695 (FEMA, 2009) and FEMA P58 (FEMA, 2012) and studies for the safety assessment of building structures (e.g., Krawinkler et al., 2006). An important feature of the study is that the vertical ground motion is included in the analysis. The study utilizes advanced models for the ultimate behavior of the isolators to assess the seismic performance of transformers equipped by horizontal-only and with horizontal and vertical isolation systems. The seismic intensities that cause functional failure of the transformers with fixed base and the two types of isolation systems are compared. A number of parameters are considered: (a) transformer weight (plus additional weight to implement the isolation system) in the range of 320 to 520kip, (b) bushing failure limits in terms of the peak acceleration at the center of mass of the upper part of 1g and 2g in the direction perpendicular to the longitudinal axis and 5g in the longitudinal direction (the selection of these limits is based on available field empirical data which will be discussed later in this report), (c) as-installed bushing frequency 2.6, 4.3, 7.7 and 11.3Hz, (d) vertical and inclined bushings (at 20 degree angle) and (e) horizontal isolation system (triple FP isolators) with ultimate displacement capacity of 17.7, 27.7 and 31.3 inch by selecting standard concave plates of increasing diameter, while maintaining the properties of the vertical isolation system unchanged.

The results of the study are fragility curves; that is, graphs of the probability of failure versus the intensity of the seismic shaking. The intensity of the seismic motion is measured by the peak ground acceleration (PGA) in order to relate to the seismic spectra used in IEEE (2005) for the design and qualification of electrical equipment. Failure is defined as either exceeding the acceleration limit set for the bushings or exceeding the displacement capacity of the triple FP isolators or failure of the vertical isolation system in tension, whichever occurs first. The fragility curves may be used to:

- (a) Decide on the benefits offered by the seismic protective system depending on the limits of the protected equipment, location of the equipment (value of PGA) and configuration and properties of the seismic protective system.
- (b) Calculate the mean annual frequency of functional failure and the corresponding probability of failure over the lifetime of the equipment. This calculation requires knowledge of the seismic hazard curves that are available for any location in the US from the United States Geological Survey. Sample calculations for selected locations are presented in this document.
- (c) The information can be used to assess the seismic performance of electric transmission networks under scenarios of component failures (e.g., Kempner, 2006; Shinozuka et al, 2007).

SECTION 2

METHODOLOGY FOR FAILURE PERFORMANCE EVALUATION OF SEISMICALLY ISOLATED ELECTRICAL TRANSFORMERS

The failure performance evaluation is based on the procedures of FEMA P695 (2009) for collapse performance evaluation. These procedures require to perform Incremental Dynamic Analysis (IDA; Vamvatsikos and Cornell, 2002) and to detect collapse of the analyzed structure and failure of its critical components either by direct or indirect (non-simulated failure) simulation (Haselton, 2006; Haselton and Deierlein, 2007; Haselton et al., 2008 and 2009; Liel et al., 2011; Lignos and Kranwinkler, 2013).

The procedure followed is to conduct IDA to obtain information on the number of failures for each level of seismic intensity considered. For the work in this report, failure is considered either when the maximum value of acceleration at the center of gravity of the upper part of the bushing in the transverse or the longitudinal directions reaches a specified limit, or when the isolation system fails by exceeding the horizontal or the vertical (uplift) displacement capacity, whichever occurs first. The intensity of the ground motion is measured in terms of the peak ground acceleration PGA, or per the terminology used in IEEE (2005), the zero-period acceleration ZPA.

The 5%-damped high required and moderate required IEEE response spectra (IEEE, 2005) are shown in Figure 2-1. The corresponding spectra in the vertical direction are identical in shape to the horizontal spectra but scaled in amplitude by a factor of 0.8.

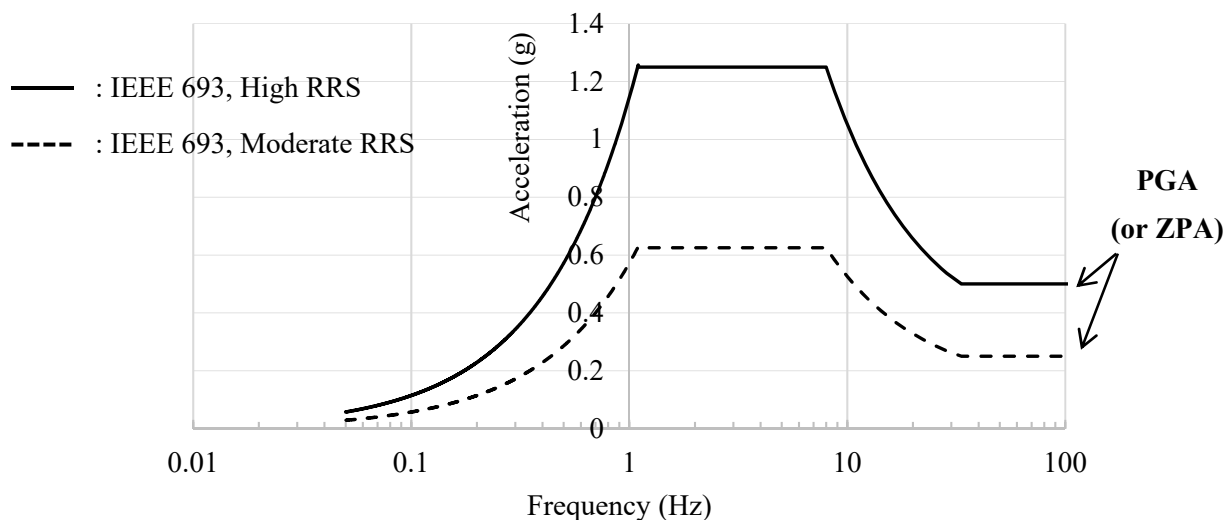


Figure 2-1 Moderate and High Required Response Spectra per IEEE 693 (5% Damped)

IDA is conducted for a set of ground motions, each one of which consists of a horizontal and a vertical component as originally recorded and progressively increased in intensity while maintaining the original ratio of peak vertical to peak horizontal acceleration. The intensity is defined as the peak value of the horizontal ground acceleration, the PGA. Failure is defined when either the acceleration reaches a limit based on calibration of the model using field empirical data (1g or 2g in the transverse direction and 5g in the longitudinal bushing direction) or the lateral displacement of the isolators exceeds the stability limit of the isolators or the vertical isolation system fails in tension (uplift), whichever occurs first. The empirical fragility curves (cumulative distribution functions) are then generated from information obtained from the IDA and analytical descriptions of the fragility curves are obtained by fitting the empirical data with lognormal representations. The fragility curves present the probability of failure (actually the probability of exceeding a threshold of either acceleration or isolator displacement) versus the PGA, where the probability of failure is determined at each PGA level as the number of analyses that resulted in failure divided by the total number of analyses.

Note that the presentation of the fragility curves (probability of failure versus the intensity of ground motion) is based on the use of the PGA for the measure of ground motion intensity. This differs from the approach in FEMA P695 (2009) where the intensity is measured by the spectral acceleration at the fundamental period of the studied system. The reasons for selecting PGA as the intensity measure are:

- 1) PGA (or ZPA) is the ground motion intensity measure typically used in fragility analysis of electrical equipment (e.g., Kempner et al, 2006; Shinozuka et al, 2007).
- 2) It facilitates use of the IEEE 693 (2005) spectra, which are described by PGA (or ZPA) and unlike the ASCE 7 (2010) spectra used for building design which are described by the spectral acceleration values at 0.2sec and 1.0sec.
- 3) It allows presentation of fragility analysis results when the analyzed system has two distinct modes of vibration at two very different frequencies (horizontal and vertical).
- 4) Fragility analysis results are valid for any location and are only dependent on the PGA.

An example of a fragility curve is shown in Figure 2-2.

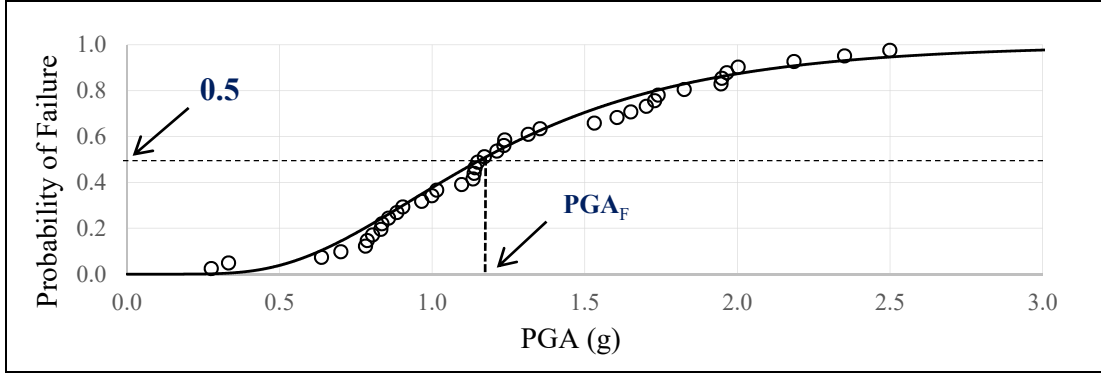


Figure 2-2 Example of Fragility Curve

In the fragility analysis, the following parameters are calculated:

- 1) PGA_F is the measure of intensity (PGA) for which at least 50% of the analyses resulted in failure (is the value of PGA for which the probability of failure is 0.5).
- 2) The dispersion factor β is calculated as the standard deviation of the natural logarithm of the values of PGA causing failure of the transformer (failure of bushings or collapse of isolator). Note that a number of analyses are conducted with motions of increasing intensity (IDA analysis). In the analyses of this report the number of motions is 40.

The analytical fragility curve (cumulative distribution function or CDF) representing the empirical data is calculated as:

$$CDF(x) = \int_0^x \frac{1}{s\beta\sqrt{2\pi}} \exp\left[-\frac{(\ln s - \ln PGA_F)^2}{2\beta^2}\right] ds \quad (2-1)$$

The fragility curves present information on the probability of failure for specific levels of earthquake intensity, as measured by the PGA. This information is very useful and obtained in computationally intensive analysis. However, engineers, utility officials, government officials, owners and insurers are interested in assessing risk, defined in this case as the mean annual frequency of failure, λ_F . The mean annual frequency is related to another important parameter, the probability of failure for a given number of years, n , P_F (n years). Assuming that the earthquake occurrence follows a Poisson distribution, the following equation relates the mean annual frequency to the probability of failure:

$$P_F(n \text{ years}) = 1 - e^{-\lambda_F n} \quad (2-2)$$

The calculation of the mean annual frequency requires consideration of the hazard from all possible seismic events. The hazard data are obtained from the USGS website

(<http://geohazards.usgs.gov/hazardtool/application.php>) in the form of the annual frequency of exceedance λ_{S_a} as function of the spectral acceleration S_a for specific values of the period (zero, 0.1, 0.2, 0.3, 0.5, 0.75, 1.0, 2.0, 3.0, 4.0 and 5.0 second). The zero period spectral value is the PGA (and the corresponding λ_{S_a} is hereafter written as λ_{PGA}).

The calculation of the mean annual frequency of failure, λ_F , requires integration of the failure fragility of the structure over the seismic hazard curve (Medina and Krawinkler, 2002; Ibarra and Krawinkler, 2005; Krawinkler *et al.*, 2006; Champion and Liel, 2012; Eads *et al.*, 2013; Elkady and Lignos, 2014):

$$\lambda_F = \int_0^{\infty} (P_F | PGA) \cdot \left| \frac{d\lambda_{PGA}}{d(PGA)} \right| \cdot d(PGA) \quad (2-3)$$

In Equation (2-3), $|d\lambda_{PGA}(PGA)/d(PGA)|$ is the absolute value of the slope of the seismic hazard curve for the specific case of zero period.

For example, the zero-period seismic hazard curves were obtained from the USGS website (United States Geological Survey website, accessed November 11, 2015, July 16, 2016 and August 14, 2016) for several locations in the western US as described in Table 2-1.

Table 2-1 Location and Coordinates (not shown in the publicly available report) of Ten Sites in Western US

Case No.	Location	Latitude	Longitude	Soil Type
1	Vancouver, WA	██████████	██████████	D
2	Saranap, CA	██████████	██████████	D
3	Loma Linda, CA	██████████	██████████	D
4	Aberdeen, WA	██████████	██████████	D
5	Chehalis, WA	██████████	██████████	D
6	Hillsboro, OR	██████████	██████████	D
7	Eugene, OR	██████████	██████████	D
8	Wilsonville, OR	██████████	██████████	D
9	Curry County, OR	██████████	██████████	D
10	Troutdale, OR	██████████	██████████	D

The obtained hazard curves are shown in Figure 2-3. Note that λ_{PGA} is the number of times that exceeds a specific PGA in one year (differs per location: Cases 1 to 10).

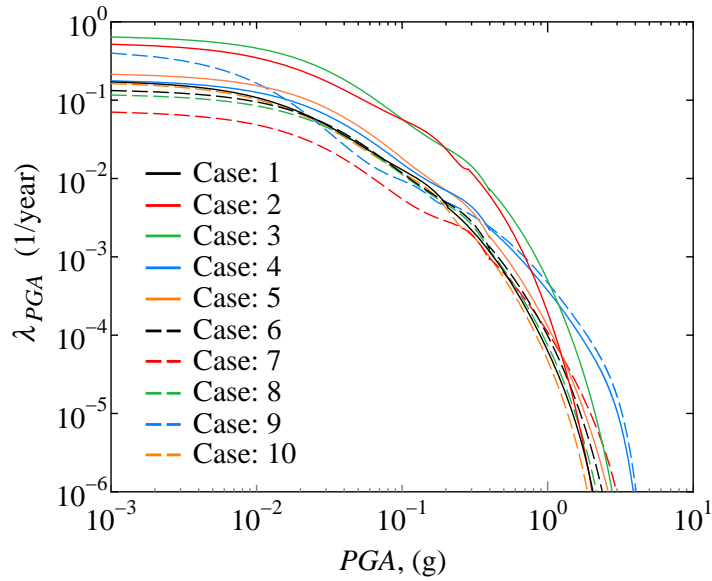


Figure 2-3 Seismic Hazard Curves for Zero Period for Locations of Table 2-1

The IEEE 693 standard (2005) defines the life of equipment as over 30 years. Accordingly, sample calculations of probabilities of failure over the lifetime of the equipment are performed for 50 years of lifetime (i.e., $n=50$ in Equation (2-2)) for the locations listed in Table 2-1 above. The information is provided to demonstrate one use of the fragility curves presented in this report.

SECTION 3

MODELING OF ELECTRICAL TRANSFORMERS FOR FAILURE ASSESSMENT

3.1 Modeling of Bushings

This section describes the model of bushings used in the analysis of electrical transformers for failure assessment. Bushings are critical components of electrical transformers. Damage or failure of bushings is considered to be failure for the transformer (Shumuta, 2007). The model utilizes the test results of Kong (2010) and Fahad (2013) who examined the characteristics of bushings installed in a variety of conditions. Particular emphasis is placed at properly representing the rotational and vertical frequencies of bushings in their installed condition and accounting for the effects of the flexibility of the supporting plate.

Figure 3-1 illustrates a bushing and defines its parts and some of its important dimensions (not in scale). The bushing is divided into upper and lower parts that are separated by the plate to which the bushing is connected to. This plate is shown in Figure 3-1 to have a thickness $2H_F$. Other geometric parameters are: H_{UB} is the length of the bushing's upper part, H_{LB} is the length of the bushing's lower part, H_{CM_UB} is the distance of the flange to the center of gravity of the bushing's upper part, H_{CM_LB} is the distance of the flange to the center of gravity of the bushing's lower part, m_{UB} is the mass of the bushing's upper part, m_{LB} is the mass of the bushing's lower part and m_{CH} is the mass of the connection housing.

Data in Kong (2010) and Fahad (2013) for several bushings include geometric properties, masses and frequencies of free vibration when installed fixed (f_{FIX}) and when installed connected to a flexible plate (called as-installed frequency, f_{AI}). Table 3-1 presents information on the properties of nine tested bushings. Some of the parameters of these bushing were not available and were estimated by the authors.

Table 3-1 Characteristics of Tested Bushings (Based on Kong, 2010 and Fahad, 2013)

Property	Unit	Bushing 1	Bushing 2	Bushing 3	Bushing 4a	Bushing 4b	Bushing 5	Bushing 6	Bushing 7	Bushing 8
Manufacturer		G.E.	G.E.	G.E.	HSP	HSP	Trench	ABB	ABB	ABB
Material of insulator		Porcelain	Porcelain	Porcelain	Composite	Composite	Composite	Porcelain	Porcelain	Porcelain
Voltage capacity (kV)		500	550	550	230	230	500	196/230	550	550
Designation		GE-500 - TypeU	GE-500 - TypeU	GE-500 - TypeU	HSP-230-1200	HsSP-230-1200	500D004C_3	196w0800bz	T550W2000UD	T550Z3000SE
Total height (in)	in	290.0	244.8	244.8	150.7	150.7	257.2	151.4	295.0	255.2
Length over mounting flange: H_{UB}	in	204.0	194.8	194.8	91.2	91.2	192.2	91.4	208.3	190.2
Length below mounting flange: H_{LB}	in	86.0	50.0	50.0	59.5	59.5	65.0	60.0	86.7	65.0
Max dia. Over mounting flange	in	20.0	25.0	25.0	11.6	11.6	19.8	11.8	23.0	18.7
Max. dia. Below mounting flange	in	20.0	18.8	18.8	8.3	8.3	12.4	10.0	23.0	16.8
Diameter of mounting flange	in	35.0	33.0	33.0	24.0	24.0	28.5	24.0	34.2	27.0
Total weight	lbs	4000	2800	2810	510	385	1850	840	4330	2180
Location of CG. (above flange)	in	57.5	57.5	57.5	17.0	17.0	65.5	14.0	47.0	54.8
Upper bushing weight: m_{UB}^*g	lbs	2744	2148	2156	248	172	1307	447	3012	1570
Location of upper bushing CG: $H_{CM_{UB}}$	in	96.0*	87.6*	87.6*	45.0	45.0	96.0	34.0	90.0	85.2
Lower bushing weight: m_{LB}^*g	lbs	1156	552	554	162	113	443	293	1218	510
Location of lower bushing CG: $H_{CM_{LB}}$	in	38.9*	59.2*	59.2*	27.0	27.0	24.5	28.0	59.0	39.0
Connection housing weight: m_{CH}^*g	lbs	100	100	100	100	100	100	100	100	100
Weight per unit length	lb/in	13.45	11.03	11.07	2.72	1.89	6.80	4.89	14.34	8.15
Distance to the flange (half of center pocket): H_F	in	13.6*	11.5*	11.5*	8.25	8.25	11.5	13.4	13.6	11.5
Fixed base frequency: f_{Fix}	Hz	5.15*	9.36*	9.36*	8.32	8.04	5.15	21.00	9.37	9.35
As-installed frequency: f_{AI}	Hz	3.30-3.90	4.20	4.25	7.75	6.79	3.25	11.25	2.57	7.70
*Values estimated by authors										

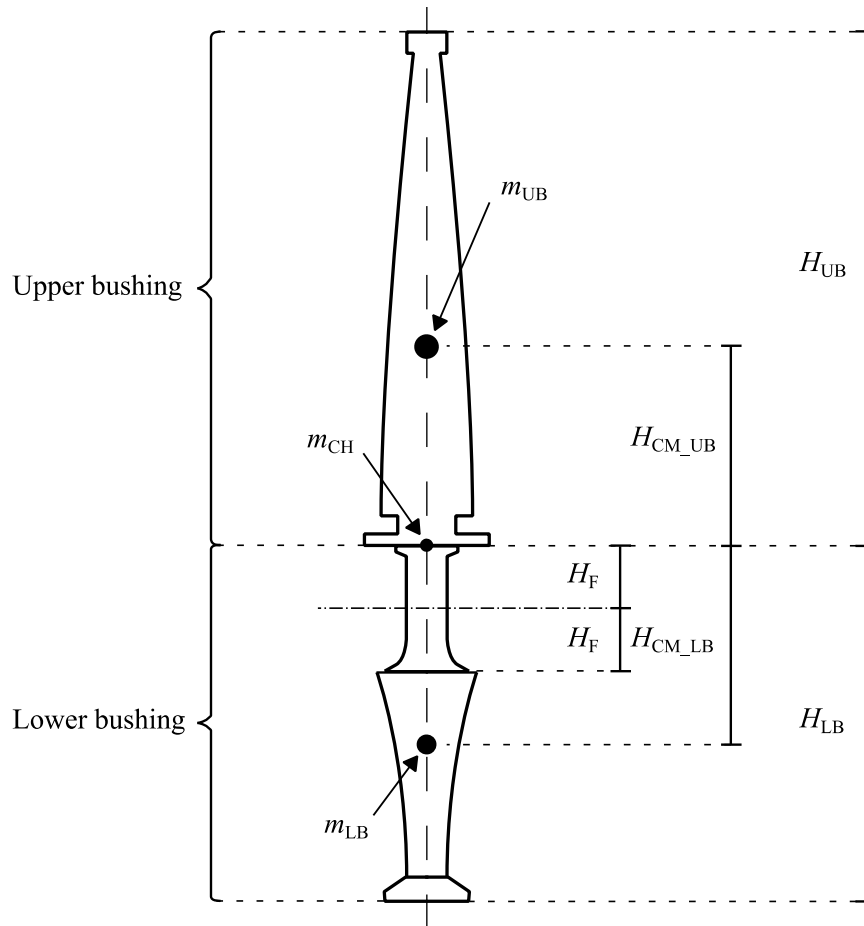


Figure 3-1 Definition of Dimensions of Bushing

Figure 3-2 illustrates two models that can be used to represent a bushing in its fixed condition at the connecting plate or in its flexible condition at the connecting plate (the latter called “as-installed” condition). Inherent damping was specified by adding vertical and rotational linear viscous dampers at the connection between the bushing and the transformer body, and horizontal linear viscous dampers between the nodes representing masses m_{CH} and m_{UB} , as shown in Figure 3-2, so that each mode of vibration is damped at 3% of critical damping. This value of damping ratio is consistent with observations in field studies (Villaverde et al., 2001). Note that specification of damping using the option of Rayleigh damping in program Opensees resulted in significant “leakage of damping” in the isolated modes that incorrectly affected the calculated isolator displacement (Sarlis and Constantinou, 2010).

Calibration of the as-installed model of the bushing is performed as follows. Given the geometry of a bushing and the values of the frequencies for the fixed and the as-installed conditions, f_{Fix}

and f_{AI} , respectively, as for example in Table 3-1, properties useful in constructing the analytical models of Figure 3-2 are obtained in the following steps:

- a) Assume the value of young's modulus for upper bushing E_{UB} (e.g., $E_{UB}=29000\text{ksi}$ or any other value) and calculate the moment of inertia of the upper bushing I_{UB} using the expression for the fixed condition frequency in Equation (3-1).

$$f_{\text{Fix}} = \frac{1}{2\pi} \sqrt{\frac{3E_{UB}I_{UB}}{H_{CM_UB}^3 m_{UB}}} \quad (3-1)$$

- b) Construct the as-installed model shown in Figure 3-2(b) using the values of E_{UB} and I_{UB} from step 1. The vertical stiffness K_V is calculated from the following equation where f_V is the vertical frequency of the as-installed bushing.

$$K_V = (2\pi f_V)^2 \cdot (m_{UB} + m_{CH} + m_{LB}) \quad (3-2)$$

If the vertical frequency of the as-installed bushing is not known, assume that is in the range of 10 to 20Hz. Justification for this value is provided in Figure 3-3, which is based on the test results of Kong (2010) and Fahad (2013) who examined the rotational and vertical frequencies of bushings in the as-installed condition. These data are shown in Figure 3-3 which presents the rotational and vertical frequencies in the testing of 33 bushings. The figure of 15Hz may represent a reasonable estimate for the vertical frequency in the absence of any better information.

- c) Assume a value for the rotational stiffness K_θ , calculate the fundamental frequency and compare it to the known value of the as-installed frequency f_{AI} . Adjust the value of K_θ and repeat until the calculated value of frequency is sufficiently close to the known value.

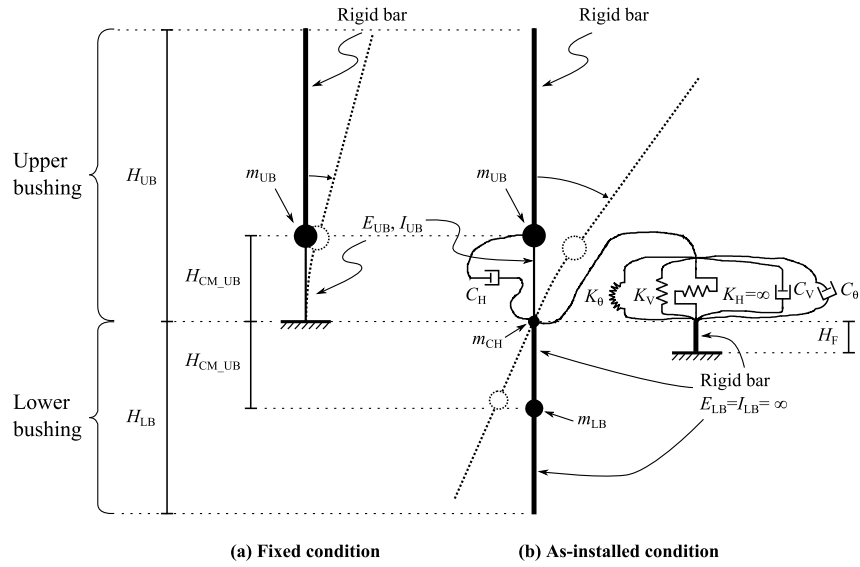


Figure 3-2 Bushing Models: (a) Fixed Condition; (b) As-Installed Condition

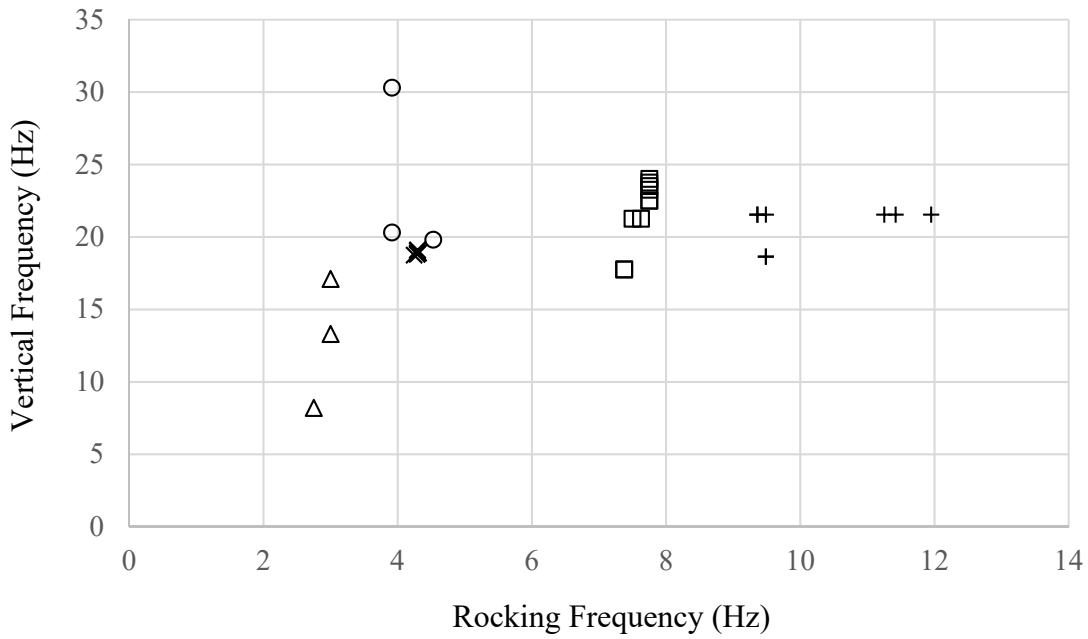


Figure 3-3 Test Results on Vertical and Rocking Frequency of As-Installed Bushings
(From Kong, 2010 and Fahad, 2013)

d) The vertical linear viscous damper constant C_V was calculated using:

$$C_V = 4\pi m_V \cdot \beta_V \cdot f_V \quad (3-3)$$

where β_v is the damping ratio in a purely vertical mode (0.03 is used), f_v is the vertical frequency (15 Hz is used for this study) and m_v is the effective mass in the vertical direction given by Equation (3-4):

$$m_v = m_{UB} + m_{CH} + m_{LB} \quad (3-4)$$

Masses m_{UB} , m_{CH} and m_{LB} are identified in Figures 3-1 and 3-2.

- e) The circular frequency ω_θ at the joint of bushing and transformer body is calculated as follows. Note that this frequency is the as-installed frequency ($\omega_\theta = 2\pi f_{AI}$).

$$\omega_\theta = \sqrt{K_\theta / I} \quad (3-5)$$

where I is the moment of inertia of the bushing.

The rotational linear viscous damper constant C_θ is given by:

$$C_\theta = 2I \cdot \beta_\theta \cdot \omega_\theta \quad (3-6)$$

where β_θ is the damping ratio in a purely rotational mode (0.03 is used). Use of Equation (3-5) results in:

$$C_\theta = \frac{K_\theta \cdot \beta_\theta}{\pi \cdot f_{AI}} \quad (3-7)$$

- f) The horizontal linear damper constant C_H is similarly given by:

$$C_H = 4\pi\beta_H m_{UB} f_{Fix} \quad (3-8)$$

where β_H is the damping ratio in a purely horizontal mode (0.03 is used).

3.2 Failure of Transformers

Transformers may fail in an earthquake in a variety of ways. Herein we assume that failure of the bushings represents the main contributor to failure of the transformer. The major failure modes of bushing are shown in Figure 3-4 based on the observations in past earthquakes (Schiff, 1977; Kong, 2010).

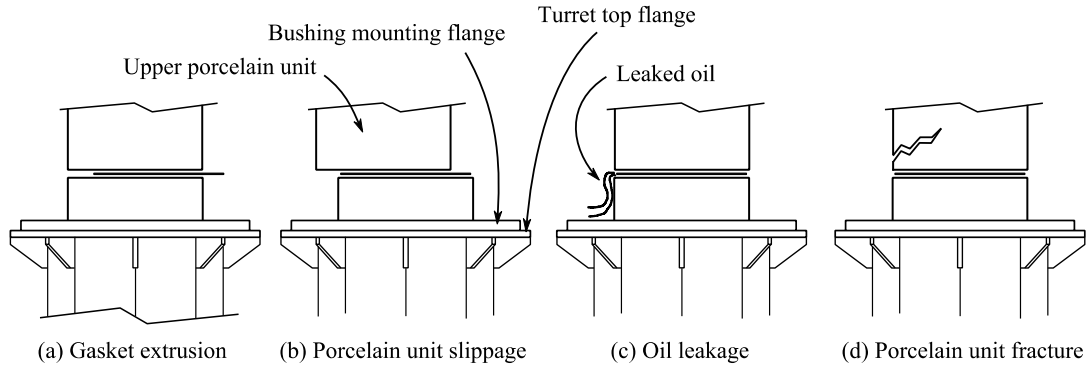


Figure 3-4 Main Failure Modes of Porcelain Bushings

The modes of failure shown in Figure 3-4 are the result of the development of large overturning moment and/or shear force at the base of the bushings. The moment and shear force are the resultants of the distributed inertia forces in the transverse direction along the height of the bushing. Herein we assume that bushings are acceleration-sensitive components so that their failure is caused by the acceleration exceeding some critical value. In this work, the peak acceleration at the center of mass of the upper portion of the bushing is used as the single critical parameter for assessing failure. This represents a correct choice when the distribution of lateral acceleration over the height of the bushing is constant so that the peak value at the center of mass represents a good measure for both the shear force and the overturning moment. When the bushing experiences significant rocking acceleration in addition to translational acceleration, the use of this single parameter will tend to underestimate the overturning moment effects when rocking and translation are in phase and will otherwise likely overestimate the overturning moment effects, while correctly estimating the shear force effects.

Consider a vertical bushing as shown in Figure 3-2 and let the acceleration at the center of mass of the upper bushing in the transverse direction be A . If the bushing experiences a constant acceleration over its height, the overturning moment at the interface of the upper bushing to the supporting plate is $OM = m_{UB} H_{CM_UB} A$ where m_{UB} is the mass of the upper bushing and H_{CM_UB} is the distance of the center of mass of the upper bushing to the plate as shown in Figure 3-1. Accordingly, another parameter that could describe the failure of a transformer is the normalized overturning moment $OM / m_{UB} H_{CM_UB}$ which has dimensions of acceleration. A comparison then of the transverse upper bushing acceleration at the center of mass A and the normalized overturning moment at the bushing base $OM / m_{UB} H_{CM_UB}$ can reveal the differences between the two measures of bushing failure. Such comparisons are presented in Figures 3-5 and 3-6 for the case of an isolated transformer of 420kip total weight equipped with a three-dimensional

isolation system allowed to rock and then restrained against rocking (see description in Section 4 that follows) and a vertical bushing having an as-installed frequency of either 2.6Hz or 7.7Hz. The horizontal isolator is smallest considered in this study (shown in Figure 4-2) with its lower bound properties. One of the 40 pairs of horizontal-vertical used in the fragility analysis in this report was used and applied incrementally as described in Section 7 later in this report until the peak acceleration of the upper bushing at the center of mass reached about 3g. The motion was Beverly Hills - Mulhol of the 1994 Northridge Earthquake (see Table 7-1). The calculated value of acceleration at each increment is plotted in Figures 3-5 and 3-6 versus the calculated normalized overturning moment $OM/m_{UB}H_{CM_UB}$. Another set of results is presented in Figures 3-7 and 3-8 for another of the motions used in the fragility analysis: the Arcelik station motion in the 1999 Kocaeli earthquake. The two motions used in the analysis include a vertical component of excitation as recorded and the two components were scaled incrementally as described in Section 7. Figure 3-9 compares the 5%-damped acceleration response spectra of the components of the two motions used in the analysis in order to demonstrate the differences in their characteristics.

In the results of Figures 3-5 to 3-8, when the two compared quantities of acceleration and normalized moment are exactly equal, the distribution of acceleration over the bushing height is constant. The deviation from the equal value line in these graphs indicates whether the measure

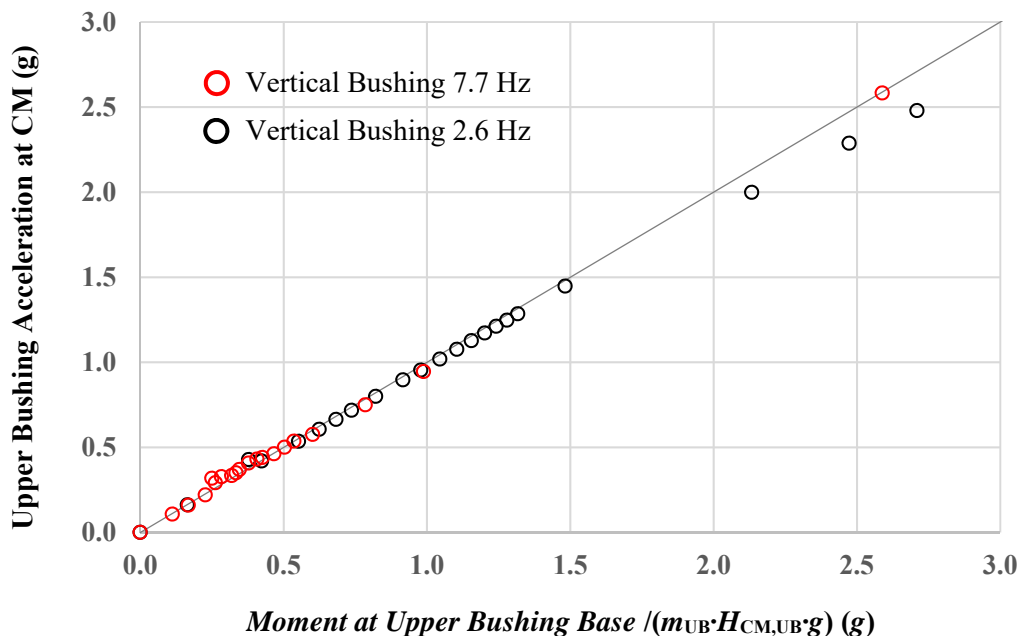


Figure 3-5 Relation between Acceleration at Center of Mass and Normalized Moment of Upper Bushing in Combined Horizontal-Vertical Seismic Isolation System with Unrestrained Rocking in the Isolation System for Case of Motion Beverly Hills - Mulhol

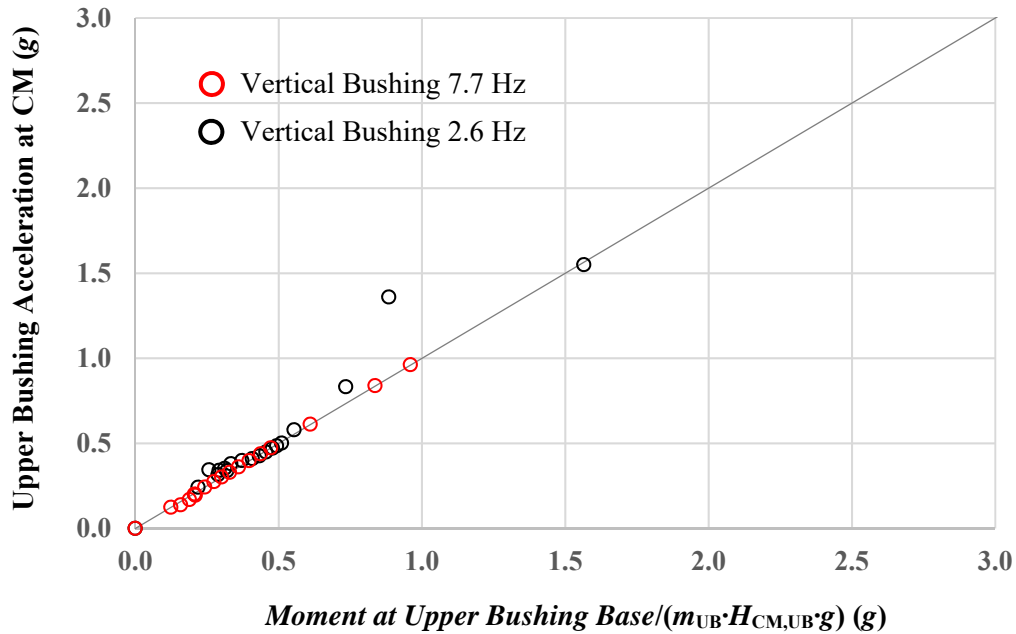


Figure 3-6 Relation between Acceleration at Center of Mass and Normalized Moment of Upper Bushing in Combined Horizontal-Vertical Seismic Isolation System with Restrained Rocking in the Isolation System for Case of Motion Beverly Hills – Mulhol

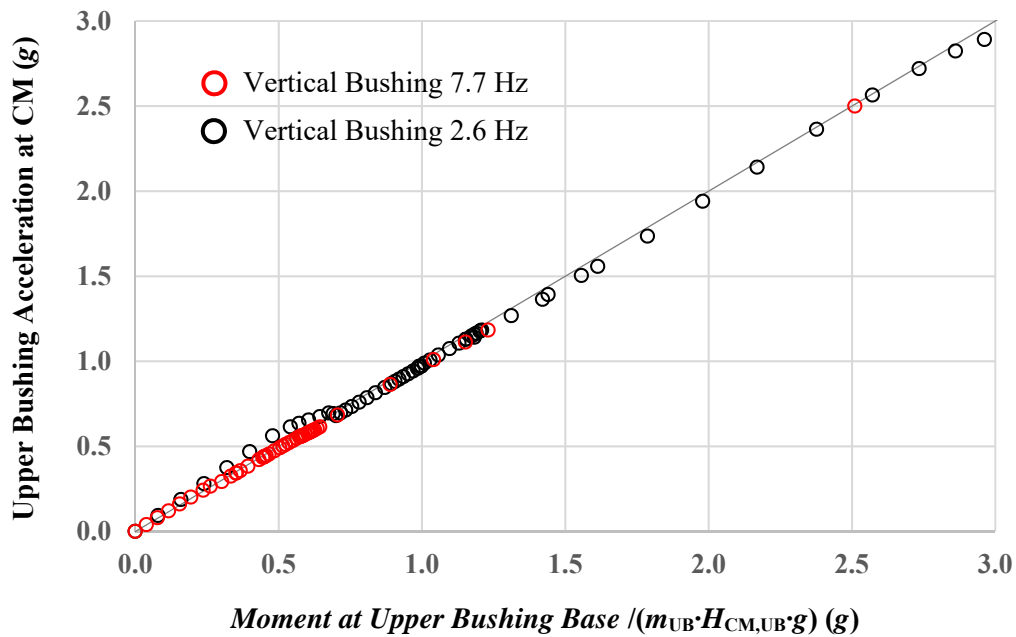


Figure 3-7 Relation between Acceleration at Center of Mass and Normalized Moment of Upper Bushing in Combined Horizontal-Vertical Seismic Isolation System with Unrestrained Rocking in the Isolation System for Case of Motion Arcelik

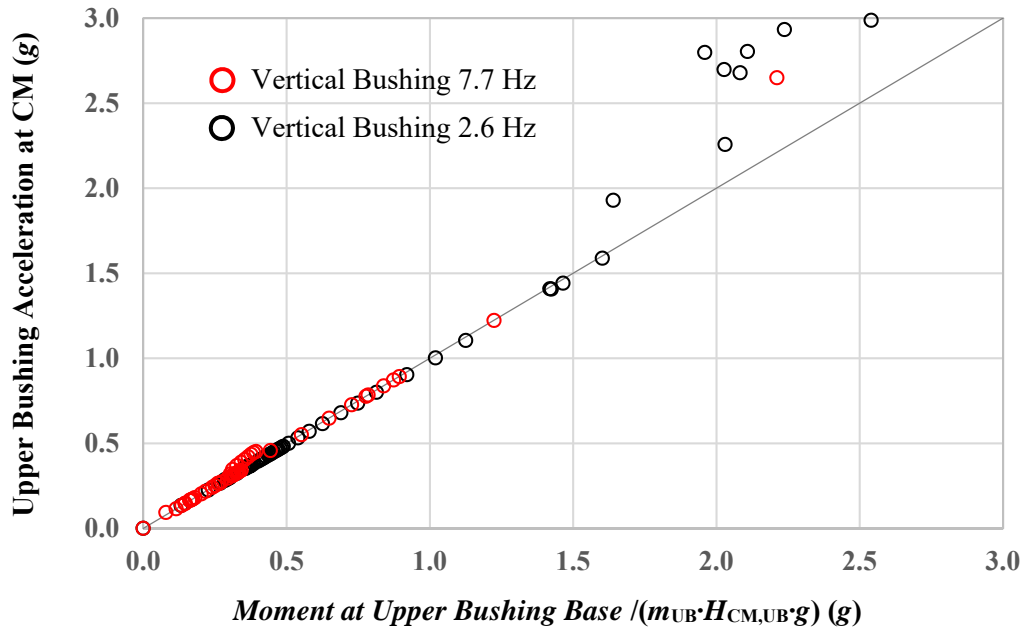


Figure 3-8 Relation between Acceleration at Center of Mass and Normalized Moment of Upper Bushing in Combined Horizontal-Vertical Seismic Isolation System with Restrained Rocking in the Isolation System for Case of Motion Arcelik

of acceleration at the center of mass is conservative (points above line of equal values) or un-conservative (points below line of equal values). The results in Figures 3-5 to 3-8 clearly indicate a close correlation between the acceleration at the center of mass of the upper bushing and the normalized bending moment at the upper bushing base so that the acceleration at the center of mass of the upper bushing may be used to describe failure of the transformer.

Having accepted that the bushing acceleration at the center of mass of the upper bushing is a good indicator for failure of the transformer, a variety of options for the limits of acceleration in the longitudinal and transverse bushing directions of the bushing were considered and fragility curves were constructed for the non-isolated transformer model (see Fig. 3-11 (a)). These curves were then compared to empirical fragility curves based on field observations in earthquakes and used in program SERA (Kempner et al, 2006) so that the bushing acceleration limits are established. Specifically, the study considered that the bushings fail when the acceleration at the center of mass of the upper part per Figure 3-1 reaches the limit of 1g or 2g or 3g in the lateral (or transverse) direction (perpendicular to the longitudinal bushing axis) and when it reaches the limit of 5g in the bushing longitudinal direction. The reason for the distinction between the limits in the lateral and longitudinal directions is based on observations of bushing failures in which failures like those depicted in Figure 3-4 are caused by bending, and shear force which are the

result of inertia forces in the lateral direction. The calculation of the accelerations in the longitudinal and lateral bushing directions from values in the vertical and horizontal directions, and the acceleration limits, are illustrated in Figure 3-10.

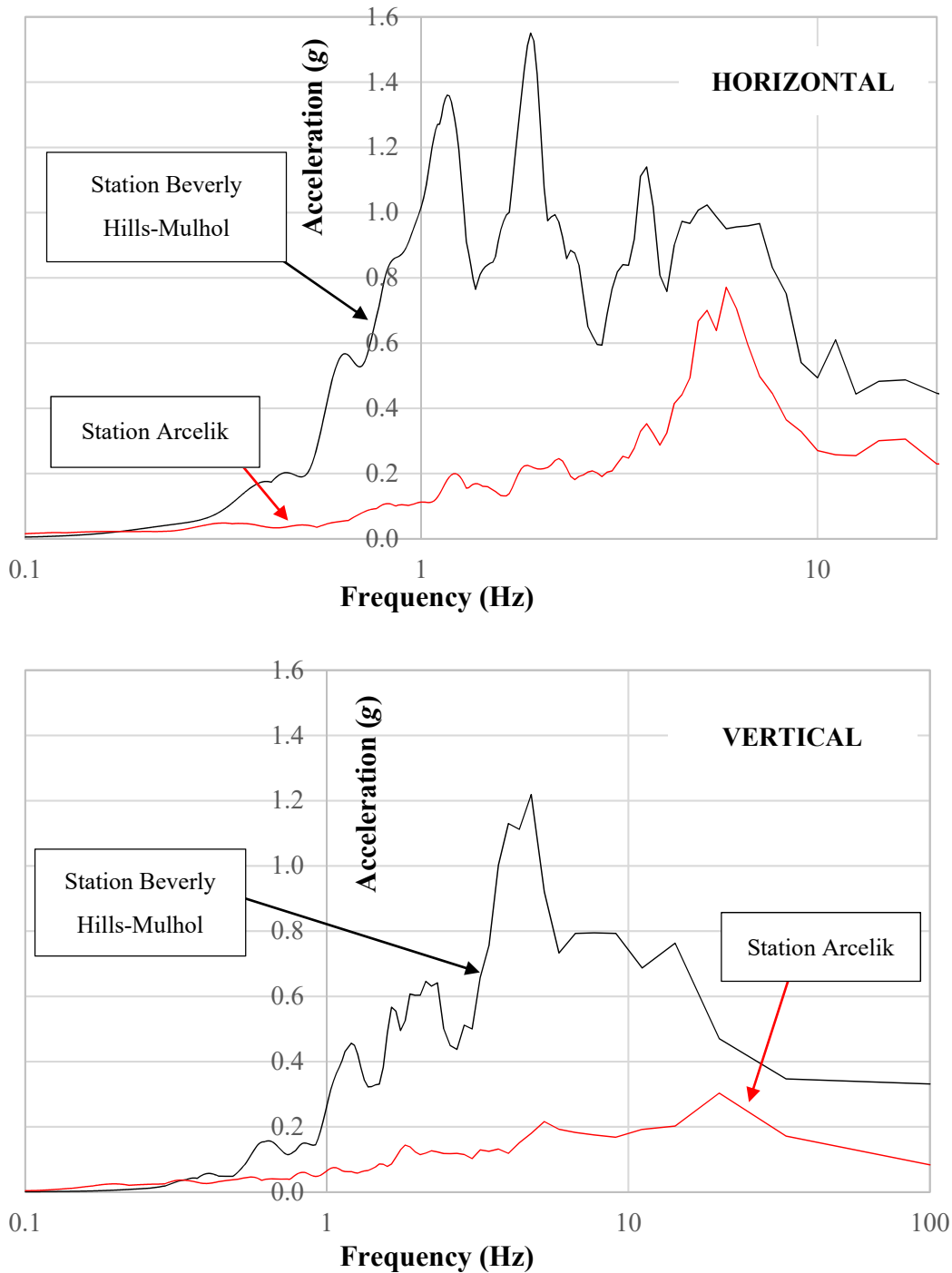
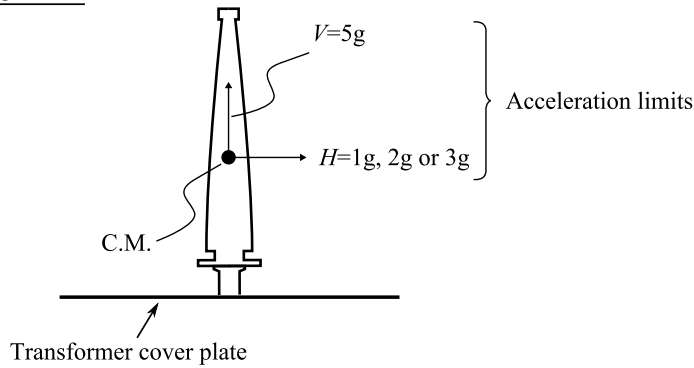


Figure 3-9 5%-Damped Acceleration Spectra of Motions Recorded at Station Beverly Hills–Mulhol in the 1994 Northridge Earthquake and Recorded at Station Arcelik in the 1999 Kocaeli Earthquake (as recorded)

Vertical Bushing Limits



Inclined Bushing Limits

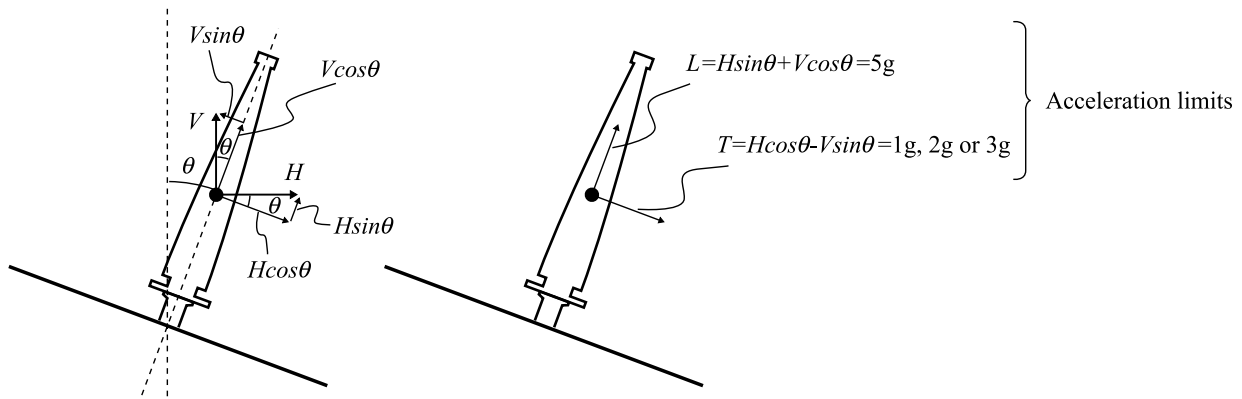


Figure 3-10 Calculation of Longitudinal and Lateral Bushing Accelerations and Their Limit

Table 3-2 presents values of the median PGA_F and the dispersion coefficient β of the analytically constructed fragility curves of several non-isolated transformer models (details of the model and analysis are provided in the remaining of Section 3 and in Section 7 of this report).

Program SERA (Kempner et al, 2006) utilizes empirical fragility curves that are based on observations of damage to electrical equipment in earthquakes over the past several years. These were made available (Kempner, 2016) from which Table 3-3 was prepared. Only data for failures of bushings of 230 and 500kV voltage are included in the table. The data are based on seven types of transformers as shown in photographs in the table. (Note that all bushings in the photographs of transformers in Table 3-3 are center-clamped porcelain bushings.) The data in the table include the median value of PGA_F and the dispersion factor. The lower limit of the median PGA_F in Table 3-3 corresponds to failure attributed to gasket leakage, whereas the upper limit of the median PGA_F corresponds to failures attributed to breakage of the bushing. Higher values of up to 1g of the median PGA_F exist in the SERA database and all correspond to failures attributed to radiator breakage.

Table 3-2 Parameters of Analytically Constructed Fragility Curves for Several Non-Isolated Transformers

Transformer Weight (kip)	Bushing Inclination (degrees)	Bushing As-Installed Frequency (Hz)	Bushing Transverse Acceleration Limit (g)	Median PGA_F (g)	Dispersion Factor β
320	20	7.7	3.0	1.20	0.45
			2.0	0.80	0.45
			1.0	0.40	0.45
420	20	2.6	3.0	1.69	0.32
			2.0	1.13	0.32
			1.0	0.56	0.32
420	20	4.3	3.0	1.47	0.34
			2.0	0.98	0.34
			1.0	0.49	0.34
420	20	7.7	3.0	1.20	0.45
			2.0	0.80	0.45
			1.0	0.40	0.45
420	0	7.7	3.0	1.08	0.40
			2.0	0.72	0.41
			1.0	0.36	0.41
420	20	11.3	3.0	2.16	0.32
			2.0	1.44	0.35
			1.0	0.72	0.35
520	20	7.7	3.0	1.20	0.45
			2.0	0.80	0.45
			1.0	0.40	0.45

Table 3-3 Parameters of Empirical Fragility Curves based on Field Earthquake Performance Data for Bushings of Seven Types of Non-Isolated Transformers (program SERA, Kempner, 2016)

Type of Transformer	Bushing Voltage (kV)	Median PGA_F (g)	Dispersion Factor β
	230	0.50-0.85	0.30
	500	0.45-0.75	0.30
	230	0.50-0.85	0.30
	500	0.45-0.75	0.30
	230	0.50-0.85	0.30
	500	0.30-0.60	0.30
	230	0.50-0.85	0.30
	500	0.40-0.70	0.30
	230	0.50-0.85	0.30
	500	0.50-0.85	0.30
	230	0.50-0.85	0.30
	500	0.40-0.65	0.30

	230	0.50-0.95	0.30
	500	0.50-0.85	0.30

A comparison of the data in Tables 3-2 and 3-3 reveals that the analytically constructed fragility curves are in close agreement with the empirical field data when the limit of bushing transverse acceleration is between 1.0g and 2.0g. The 2.0g limit appears to be high for most cases of bushing failure but it is representative of other types of failures not attributed to bushing breakage. The analytically predicted dispersion factors were in the range of 0.35 to 0.45, which compares to the empirical value of 0.30. This indicates that the transformer model is reasonably valid, that the selection and scaling of earthquake motions for the analysis are appropriate and that the analysis procedure is appropriate.

We consider that the transformer failure model based on the peak bushing acceleration values at to the center of mass of the upper part to have been validated. Analyses are thus conducted with bushing acceleration limits to be 1.0g and 2.0g in the transverse direction and 5.0g in the longitudinal direction, with the understanding that the 1.0g limit results are representative of most transformer failures attributed to porcelain bushing breakage and that the 2.0g limit results are representative of a few transformers and in cases where failure is attributed to breakage of components other than bushings.

3.3 Modeling the Transformer

The model of the transformer is based on Oikonomou et al (2016). The representation of the transformer is two-dimensional with horizontal and vertical degrees of freedom. Figure 3-11 illustrates the three transformer models considered: (a) fixed-base or non-isolated, (b) isolated only in the horizontal direction and (c) isolated in the horizontal and vertical directions. The elastic beam elements representing the transformer frame are designated rigid. Only flexible elements are those representing the bushing (see Figure 3-2).

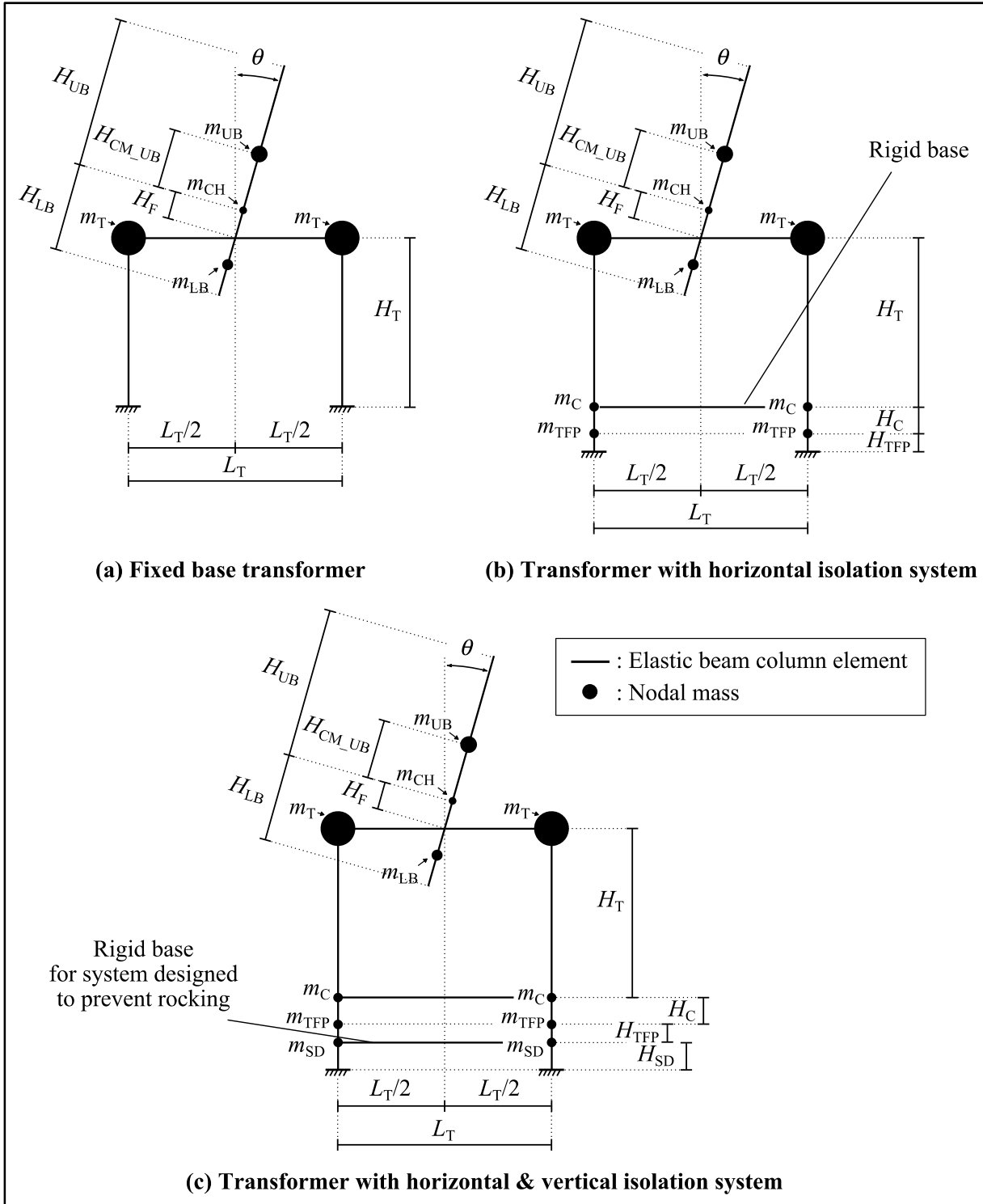


Figure 3-11 Two-Dimensional Transformer Models

The models depicted in Figure 3-11 are skeletal with lumped masses. Each model represents half of a transformer. It consists of one bushing modelled using the representation of Figure 3-2(b) with an angle of inclination θ equal to zero (vertical bushing) or 20 degrees (inclined bushing). The height and length (or width) of the transformer are denoted as H_T and L_T , respectively. The mass of the body of the transformer (excluding the bushings) is $2m_T$ and is considered lumped at two locations as shown in Figure 3-11. For the isolated transformer there is additional mass representing the concrete slab supporting the transformer on top of the isolators. This mass is $2m_C$ and is lumped at two locations on top of the supports. Small masses to represent the triple FP isolators and the spring-damper units are added at the isolator locations. The weight of each triple FP bearing is 700lb and the weight of each spring-damper unit is 500lb (these values include the weight of added beams to simulate the isolation system bases). Accordingly, the masses for the isolators, which represent one unit each, are given by $m_{TFP}=0.7\text{kip}/g$ and $m_{SD}=0.5\text{kip}/g$, where g is the gravity acceleration ($=386\text{ inch}/\text{sec}^2$).

The isolated model shown in Figure 3-11(c) with the combined horizontal-vertical isolation system distinguishes between the cases of allowing for or preventing rocking. As depicted in Figure 3-11(c), there is a rigid base placed below the triple FP isolators and connecting the top of the spring-damper units. This arrangement prevents rocking of the isolated structure but allows for vertical motion that is equal at each support. When the rigid base is removed, the structure is free to undergo rocking. In reality, the beam has to be of finite stiffness which will allow for some limited rocking to occur. In this work only results for the two bounding cases of zero and infinite base stiffness are presented, which correspond to the cases of allowing for free rocking and for completely restraining rocking, respectively. Some more details of how this is achieved in practice are presented in Section 4.

Specific values of properties used in the study are based on the isolated transformer described in Oikonomou et al (2016). This transformer is denoted as the 420kip transformer. The weight of the transformer is $W_T=380\text{kip}$ and the weight of the concrete slab is $W_C=40\text{kip}$, so that masses m_T each represent weight of 95kip and masses m_C each represent weight of 10 kip. Geometric parameters for the transformer described in Oikonomou et al (2016) are: $H_T=81\text{in}$, $L_T=110\text{in}$, $H_C=6.0\text{in}$, $H_{TFP}=4.75\text{in}$, $H_{SD}=3.0\text{in}$. Note that the L_T is the width in north-south direction of the transformer used in Oikonomou et al (2016). Also note that H_T is the height to the center of mass of the transformer body. Similarly, H_C , H_{TFP} and H_{SD} are the heights to the center of mass of each component, which are taken as half of the actual height.

Other weights of transformer model are also analyzed using the same basic dimensions as the 420kip transformer model but with the total weight adjusted to 320kip and to 520kip to represent a range of transformers likely to be seismically isolated. Also, the properties of bushings are varied by considering four different bushings, No. 3, 6, 7 and 8 per the data in Table 3-1. The dimensional, weight and frequency data for these bushings are as follows: (a) No.3: $H_{UB}=194.8$ in, $H_{LB}=50.0$ in, $H_{CM_UB}=87.6$ in, $H_{CM_LB}=59.2$ in, $H_F=11.5$ in, $m_{UB}=2156$ lb/g, $m_{CH}=100$ lb/g, $m_{LB}=554$ lb/g, $f_{Fix}=9.36$ Hz, $f_{AI}=4.25$ Hz; No. 6: $H_{UB}=91.4$ in, $H_{LB}=60.0$ in, $H_{CM_UB}=34.0$ in, $H_{CM_LB}=28.0$ in, $H_F=13.4$ in, $m_{UB}=447$ lb/g, $m_{CH}=100$ lb/g, $m_{LB}=293$ lb/g, $f_{Fix}=21.0$ Hz, $f_{AI}=11.25$ Hz; No. 7: $H_{UB}=208.3$ in, $H_{LB}=86.7$ in, $H_{CM_UB}=90.0$ in, $H_{CM_LB}=59.0$ in, $H_F=13.6$ in, $m_{UB}=3012$ lb/g, $m_{CH}=100$ lb/g, $m_{LB}=1218$ lb/g, $f_{Fix}=9.37$ Hz, $f_{AI}=2.57$ Hz; No. 8: $H_{UB}=190.2$ in, $H_{LB}=65.0$ in, $H_{CM_UB}=85.2$ in, $H_{CM_LB}=39.0$ in, $H_F=11.5$ in, $m_{UB}=1570$ lb/g, $m_{CH}=100$ lb/g, $m_{LB}=510$ lb/g, $f_{Fix}=9.35$ Hz, $f_{AI}=7.70$ Hz. (In the presented analysis results, the four bushings will be identified as the 4.3Hz, 17.3, 2.6Hz and 7.7Hz bushings, respectively). The vertical frequency is assumed to be 15Hz for all cases of bushings. Note that bushings with an as-installed frequency of 2.57Hz, as considered in this study, are atypical. Realistically, frequencies of about 4Hz represent the lowest bound for most installations (Kempner, 2016).

The seismically isolated transformers in the combined horizontal-vertical isolation system that is freely allowed to undergo rocking has a rocking frequency (actually the mode of vibration is dominated by rocking with some lateral deformation in the FP isolators) in the range of about 2.4 to 2.8Hz, depending on the supported weight (range of 520kip to 320kip). The calculation of the frequency is based on the assumption of rigid body for the entire transformer, the triple FP isolators represented as horizontal springs having a stiffness equal to the carried weight divided by the effective radius, the vertical springs being at a distance of $L_T=110$ inch (see Figure 3-11) and with a bushing inclined at 20 degrees and having the weight and dimensional characteristics of bushing No. 7 in Table 3-1.

The rocking frequency is very close to the as-installed frequency of one of the considered bushings (No. 7, frequency of 2.57Hz) so that the response is expected to be affected. Indeed, the results to be presented for the case of the transformer with the bushing having an as-installed frequency of 2.57Hz and the isolation system that is allowed to rock has the highest probabilities of failure. The case is regarded as a very special case that is atypical of transformers but it is used to demonstrate when an isolation system with restrained rocking is needed.

SECTION 4 DESCRIPTION OF SEISMIC ISOLATION SYSTEM

4.1 Triple Friction Pendulum Bearings

The seismic isolation system consists of triple Friction Pendulum (FP) bearings for providing isolation in the horizontal direction. When a three-dimensional isolation system is used, the triple FP isolators are supported by spring-damper devices to provide for some degree of vertical isolation. The spring-damper devices are designed to move only vertically and to resist rotation and lateral deformation due to the shear force and overturning moment transferred by the bearing above. Also they are designed to resist torsion and prevent instability due to the “negative stiffness” generated by the compressed springs in case they are accidentally twisted either by rotational ground motion or random torque transferred from the FP isolators above.

Figure 4-1 shows the section and plan of the smallest size triple FP isolator considered in this study for transformers of weight in the range of 320 to 520 kip. The isolator has capacity to accommodate larger loads but friction will be less than what is considered in this study. It has been used in a transformer described in Oikonomou et al (2016). The isolator is shown to have an inner restrainer ring, which does not offer any advantage and could be removed.

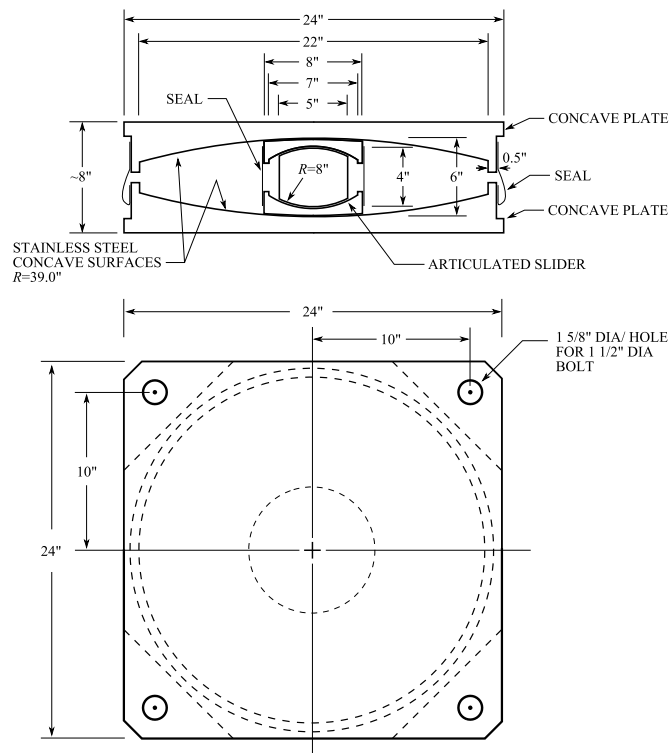


Figure 4-1 Section and Plan of Smallest Size Triple FP Bearing with Inner Restrainer

Figure 4-2 shows the internal construction of a modification of the isolator of Figure 4-1 to be without an inner restrainer ring. Both the isolators of Figures 4-1 and 4-2 have been tested and their frictional properties are identical and known. The latter type of isolator without the inner restrainer ring is considered in this study with only sample results provided for the one with the restrainer ring.

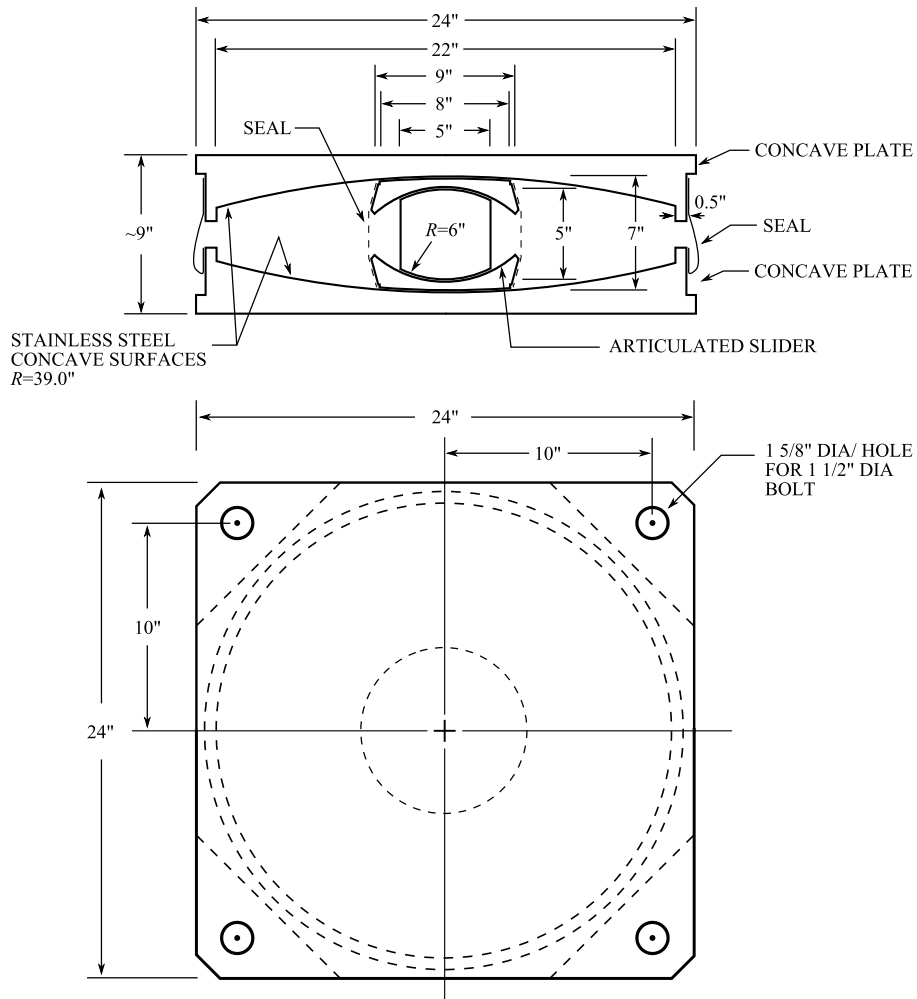


Figure 4-2 Section and Plan of Smallest Size Triple FP Bearing without Inner Restrainer

Two more isolator sizes are considered for this study. The isolators have the same internal construction as the bearing of Figure 4-2 but with increasingly larger concave plate diameter in standard size plates that are readily available (22inch, 33inch and 36inch). The 36inch diameter concave plate requires a larger radius of curvature for economy so that its radius of curvature is

61inch. Figure 4-3 shows sections of the two larger size bearings. The three isolators shown in Figures 4-2 and 4-3 have ultimate displacement capacities of 17.7in, 27.7in and 31.3in.

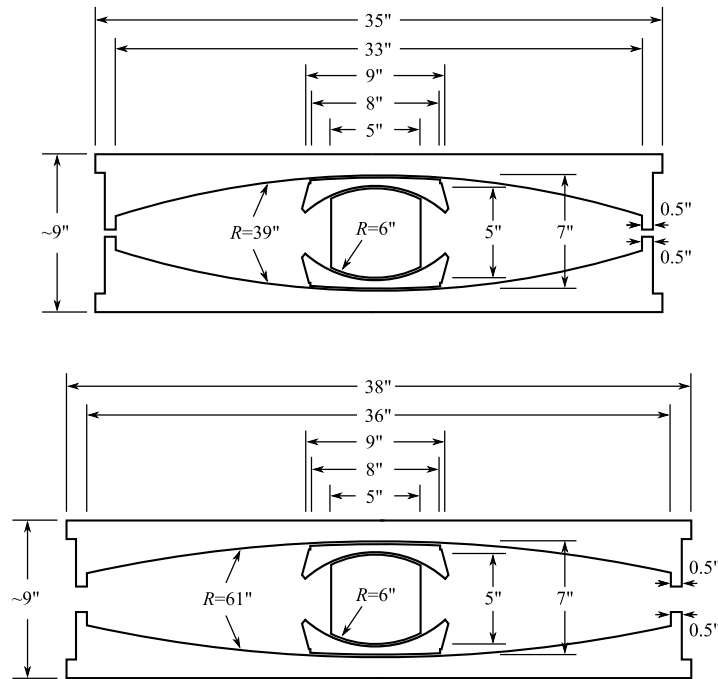


Figure 4-3 Sections of Larger Size Triple FP Bearings without Internal Restrainer

4.2 Behavior of Triple Friction Pendulum Bearings

The behavior of the triple FP bearings has been described in Fenz and Constantinou (2008) and in a more advanced form, including their ultimate characteristics in Sarlis and Constantinou (2013). Section 5 in this report presents a model for this bearing valid to collapse that has been implemented in program OpenSees (McKenna, 1997). The model is a modification of the series model of Fenz and Constantinou (2008) and includes the effect of the inner restrainer (when is used) based on the theory of Sarlis and Constantinou (2013) and the effect of fluctuating instantaneous axial load.

The lower bound frictional properties of the bearings of Figures 4-1 to 4-3 are as follows for high speed conditions. The upper bound properties, excluding effects of low temperature as those are

dependent on location, have been calculated based on the procedures described in McVitty and Constantinou (2015) using the following system property modification factors: $\lambda_{test, max}=1.10$, $\lambda_{ae, max}=1.12$, $\lambda_{spec, max}=1.00$, $\lambda_{max}=1.23$. Upper bound values should be obtained from the lower bound values of Table 4-1 by multiplying by factor of 1.23. Note that the system property modification factors used for uncertainties in properties when only prototype test data are available (λ_{spec}) are set equal to unity because test data on all isolators are presumed available.

Table 4-1 Lower Bound Frictional Properties of Triple Friction Pendulum Bearings

Load (kip)	$\mu_1=\mu_4$	$\mu_2=\mu_3$	Comments
80	0.130	0.095	For 320kip transformer. Adjusted from test data at 110kip load
110	0.120	0.080	For 420kip transformer. Based on test data
130	0.110	0.065	For 520kip transformer. Adjusted from test data at 110kip load
Test data are reported in Oikonomou et al (2016)			
For upper bound properties (excluding low temperature effects), multiply values by 1.23			

4.3 Description of Spring-Damper Device

The spring-damper device is designed for electrical transformers with total weight, including the triple FP isolators and any slab supporting the transformer on top of the isolators, in the range of 320kip to 520kip. Maximum static load per isolator is assumed to be 130kip. The basic function of the vertical isolator unit is to support the weight and provide a frequency in the vertical direction of 2.0Hz with a corresponding damping ratio of 0.50 of critical when the total supported load is 420kip. For the range of weights of 320 to 520kip, the frequency and damping ratio will be 2.3Hz and 0.56 when the weight is 320kip, and will be 1.8Hz and 0.44, respectively, when the weight is 520kip. The springs have linear elastic behavior and the damper has linear viscous behavior. Table 4-2 presents the parameters of one of these devices. The device has substantial margin of safety (factor of over 2) for the listed limits of force and moment.

Figure 4-4 shows a schematic of the device. Scaled versions of the device were used in testing of a 70kip model of isolated transformer at the University at Buffalo. Section 6 of this report describes a model of ultimate behavior of this device. The ultimate behavior of the device is summarized as follows.

Table 4-2 Parameters of Spring-Damper Device

Static load (per unit)	130kip
Static deflection	3.0inch
Stiffness per unit	44kip/inch
Damping constant per unit (linear viscous damping)	3.4kip-sec/inch
Dynamic deflection	±1.75inch
Total deflection	4.75inch
Stroke capacity	5.0inch
Displacement capacity (from position of -3inch static deflection; + is tension; - compression). Displacement limits change when static load changes.	+3.0inch -2.0inch
Peak rotation allowed for top plate with respect to bottom	0.1 degrees
Torsional rotation allowed	Zero

In compression, the displacement capacity is consumed when it reaches the limit of 5.0inch stroke and then the device exhibits very high stiffness with practically unlimited force capacity. The 5.0inch limit is controlled by the design of the damper, whereas the springs have additional displacement capacity which cannot be utilized.

In tension, the device reaches the limit of 5.0inch stroke which is the displacement capacity of the damper (the springs have additional displacement capacity which cannot be utilized). Thereafter, the device exhibits high stiffness until the ultimate force capacity of the damper in tension is reached. This limit of force depends on the design of the damper and typically exceeds twice the peak damping force. For this device the tensile limit is about 200kip. However, the triple FP isolators on top of the spring-viscous damper units do not have any tensile capacity so that the spring-damper units cannot fail in tension.

Note that the device features a telescopic sleeve system to act as a shear pin and to also prevent (limit) rotation (rocking of the top plate with respect to the bottom). Realistically, some small angle of rotation is possible, specified to be 0.1 degrees. Also, the coil springs of the device have

internal pins that limit the spring length available for shear deformation so that the shear and torsional stiffness are increased. This is needed as torsional ground motion and random transfer of torque from the FP isolator above will cause twisting of the springs and magnification of the angle of twist due to the large compressive forces in the springs (the system without torsional restraint at individual supports has negative torsional stiffness and is unstable).

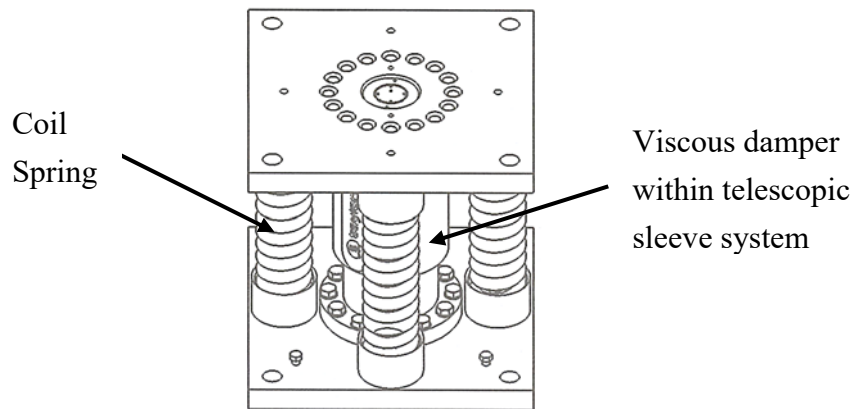


Figure 4-4 Schematic of Spring-Viscous Damper Device

Figures 4-5 and 4-6 illustrate the behavior of the two possible installation methods that either allow free rocking (Fig. 4-5) or restrain rocking (Fig. 4-6) of the isolated structure. In Figure 4-5 the isolated structure is supported by four triple FP isolators, which in turn are supported by four vertical spring-damper devices. The bottom concave plate of the triple FP isolators is allowed to rotate by an angle of rotation β that is limited by the telescopic sleeve system of the spring-damper unit. In general, angle β is small and limited to 0.1 degrees. The top plate of the triple FP isolators is free to rotate as the FP isolators have no resistance to rocking. This is possible because the spring-damper system allows for relative vertical motion at each support. The rocking angle α is limited by the ability of the spring-damper system to move vertically. Based on the limitations listed in Table 4-2, the vertical displacement capacity is 3inch downwards and 2inch upwards (for static load of 130kip). Most of the displacement capacity will be consumed by the average vertical motion of the four supports. Realistically, the relative vertical displacement between any two supports will be less than 2inch. For the shortest distance between supports of $L_T=110$ inch (see Fig. 3-6), the angle of rocking α is about equal to or less than 1 degree. The total angle of rotation $\alpha+\beta$ is thus less than about 1.1 degrees. This will result in additional displacements and acceleration at parts of the transformer furthest away from the isolation system.

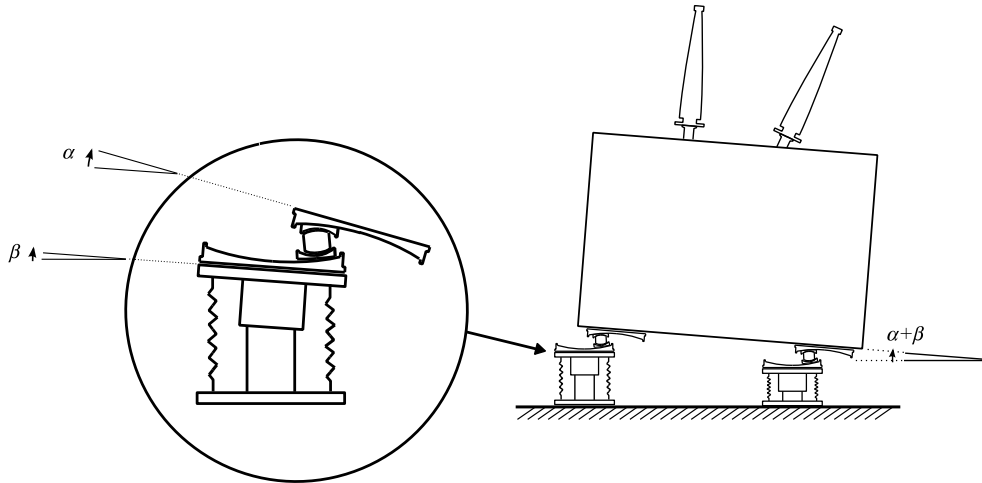


Figure 4-5 Installation Method that Freely Allows Rocking

When a stiff system is installed to span between supports (say a stiffened plate placed between the bottom FP concave plate and the top plate of the vertical spring-damper system) as shown in Figure 4-6, rocking of the superstructure is restrained so that angle α is essentially nil. The vertical isolators move in unison with essentially the same displacement. The total rotation $\alpha + \beta$ is now small and dependent on the stiffness of the connecting system. Effectively, it can be reduced to about 0.1 degrees but that requires an exceptionally stiff base.

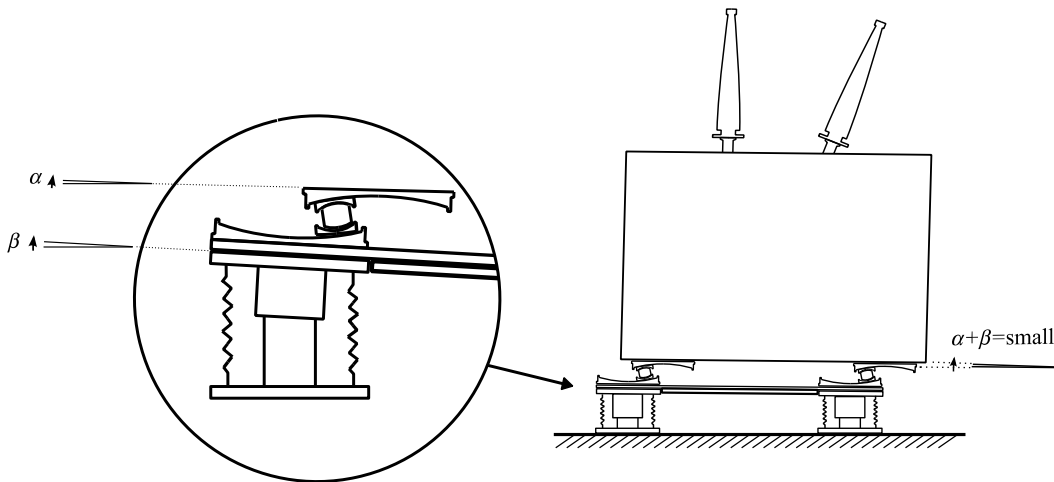


Figure 4-6 Installation Method that Restrains Rocking

Figures 4-7 and 4-8 show views of the two installation methods described above during testing on the seismic simulator at the University at Buffalo.

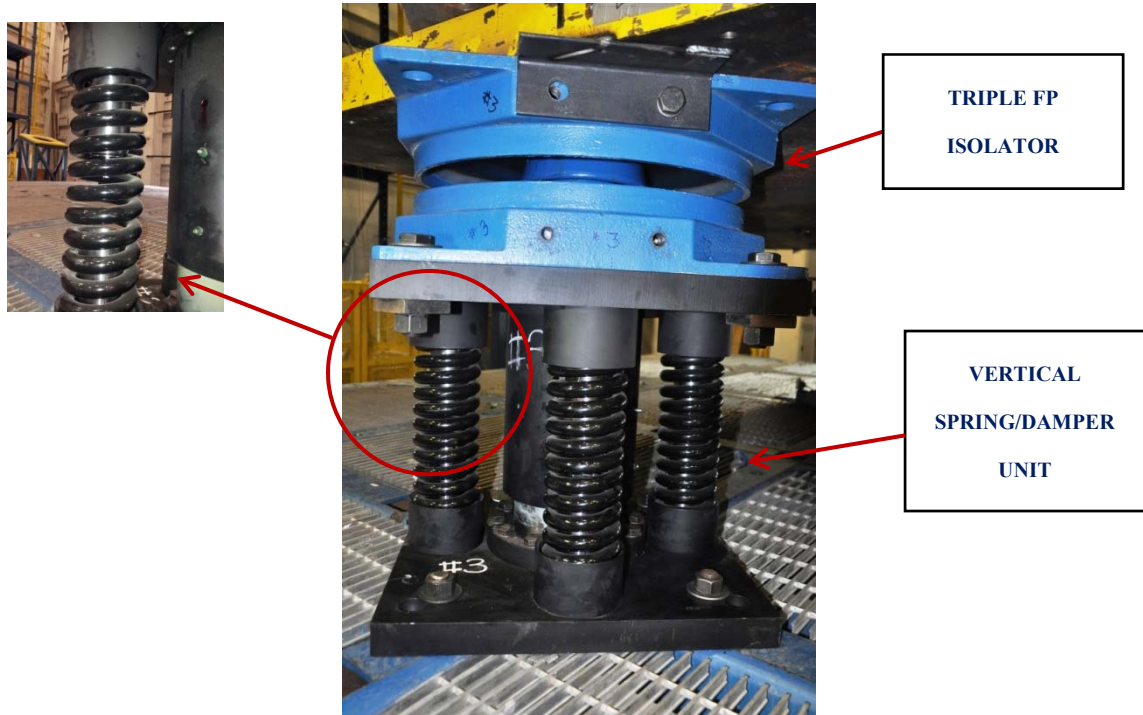


Figure 4-7 View of Isolation System with Installation Method that Allows Free Rocking



Figure 4-8 View of Isolation System with Installation Method that Restrains Rocking

SECTION 5

MODEL FOR SIMULATING THE ULTIMATE BEHAVIOR OF TRIPLE FRICTION PENDULUM BEARINGS

5.1 Introduction

This section describes a modified series model for simulating the ultimate behavior of triple Friction Pendulum (TFP) bearings that has been implemented in program OpenSees (McKenna, 1997). The model is capable of accounting for the stiffening behavior of the isolator, for the effect of the fluctuating axial force on the instantaneous stiffness and friction force, for uplift, for the effect of fracture of the inner restrainer ring and for motion until collapse of the slider assembly. Currently, the only available model of TFP capable of simulating its ultimate behavior is the one described in Sarlis and Constantinou (2013) and implemented in program 3pleANI. However, this model is complex, is difficult to implement in program OpenSees and is computationally intensive to be useful in the large number of analyses required for fragility analysis. Other models implemented in program OpenSees include the Becker and Mahin (2011) and Dao et al. (2013) models could not be used as they did not simulate behavior to collapse and they would have required modification. Also, the Becker and Mahin OpenSees model was dysfunctional when tested (last attempt was on 06/14/2016 using OpenSees Versions 2.3.0, 2.3.1, 2.4.2, 2.4.3, 2.4.4, 2.4.5, 2.4.6 and 2.5.0) and would have required complete reprogramming based on the original formulation in Becker and Mahin (2011). The model by Dao et al. (2013) could be modified but it was developed for bi-directional motion so again it would have required reprogramming to reduce to the one-directional motion and enhanced to include failure characteristics to be useful for the fragility analysis.

The approach followed herein is to modify the series model in Fenz and Constantinou (2008) in order to simulate the ultimate behavior of the TFP as predicted by the theory of Sarlis and Constantinou (2013). Advantages of the modified series model are its simplicity and the ease of implementation in programs like OpenSees and SAP2000 (Computers and Structures, 2015).

5.2 Description of Element

The modified series model has three units as shown in Figure 5-1. Each unit (FP1 to FP3) contains the following OpenSees elements: (a) a single FP bearing element (element *FPBearing* developed by Kumar et al., 2014), (b) a MinMax material (similar to the hook element in program SAP2000) and (c) an elastic-perfectly plastic gap material with two node link element.

The single FP bearing element can account for the effect of the varying axial load on the instantaneous stiffness and friction force (termed axial-shear force interaction in this document). A simplified version of the model that neglects this interaction replaces the single FP element with axial, rotational and horizontal springs in parallel as shown in Figure 5-2. Note this simplified model is computationally more stable. Examples will be provided to demonstrate the differences in the two models.

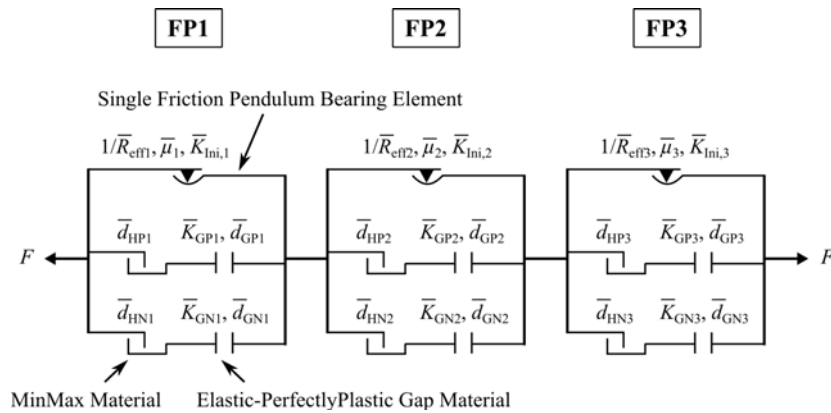


Figure 5-1 Organization of Elements of Modified Series Model in OpenSees

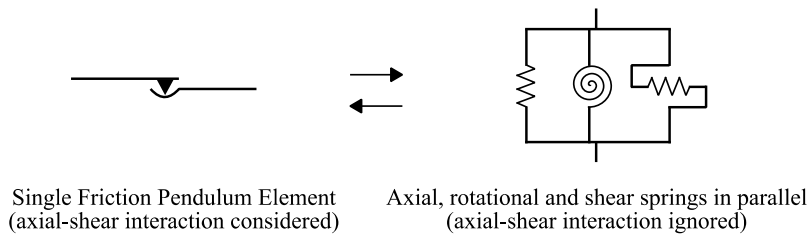


Figure 5-2 Three Springs in Parallel Element to Replace Single FP Element when Axial-Shear Force Interaction is Neglected

The axial spring shown in Figure 5-2 in the vertical direction for the model that ignores the axial-shear force interaction has bi-linear elastic behavior as shown in Figure 5-3 in order to simulate rigidity when in compression and allow for uplift when in tension. The compressive stiffness $K_{v,Compressed,i}$ is approximated by $3AE/h$, where A is the area of the rigid slider of the Triple FP bearing, E is a representative modulus (typically assumed about half of that of steel to account for flexibilities in the bearing assembly, herein 14500ksi) and h is the height of bearing, per Sarlis and Constantinou (2010). Note that the factor of 3 on the compressive stiffness accounts for the series arrangement of the three elements so that the collective stiffness is the correct AE/h .

When in uplift, the vertical stiffness of the isolator $K_{v,Uplift,i}$ is zero unless the contribution of the rubber seal is considered, which can be calculated from geometry of the rubber seal as described in Sarlis and Constantinou (2013). In this study, some arbitrary small stiffness (0.1 kip/inch) is used in each of the three elements (total is 0.1/3 kip/in) which allows for essentially unrestricted uplift and avoids numerical instabilities. Moreover, a linear viscous damper having a constant $C=4 \times 10^{-3}$ kip-sec/in is used spanning the three elements and connected to the two end nodes. When considering the transformer weight of 420kip, these values of tension stiffness (0.1/3 kip/in per supported weight of 105kip) and damping ($C=4 \times 10^{-3}$ kip-sec/in per supported weight of 105kip) correspond to a period of 18sec and damping ratio of 0.02. These values have insignificant impact on restraining uplift but may assist in providing stability in the numerical solution.

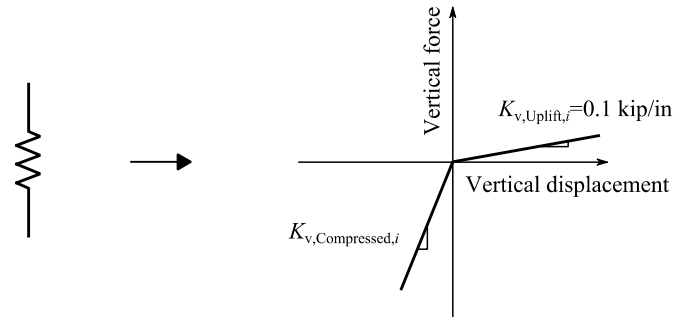


Figure 5-3 Bi-Linear Elastic Spring for Simulating Vertical Behavior

The rotational spring parameters in the model that neglects the axial-shear force interaction are selected on the basis of the recommendations of Sarlis and Constantinou (2010): (a) for element FP1, the rotational stiffness is zero (actually 10^{-9} kip-in/rad), and (b) for elements FP2 and FP3 the rotational stiffness is infinite (actually 10^9 kip-in/rad).

The single FP element in OpenSees (*FPBearingPTV* in OpenSees Version 2.5.0 – rev. 6248) is structured similarly to the description of the element depicted in Figure 5-3 but (a) an arbitrarily small value of tensile force is used by the program when the isolator is in uplift, and (b) the user is allowed to specify the vertical compressive stiffness. In general, a very small value of tensile stiffness produces acceptable results but there are occasional numerical instability problems. This problem may be mitigated by introducing viscous damping as described above for the case of the element where the axial-shear force interaction is neglected.

The parameters of the various components in Figure 5-1 are given by the following equations (note that index i takes values of 1 for element FP1, 2 for element FP2 and 3 for element FP3)

with reference to the parameter definition for the triple FP bearing in Figure 5-4. Also W is the weight on each isolator and P is the instantaneous axial load on each isolator (at time zero, $P=W$). When the axial-shear force interaction is neglected, $P=W$.

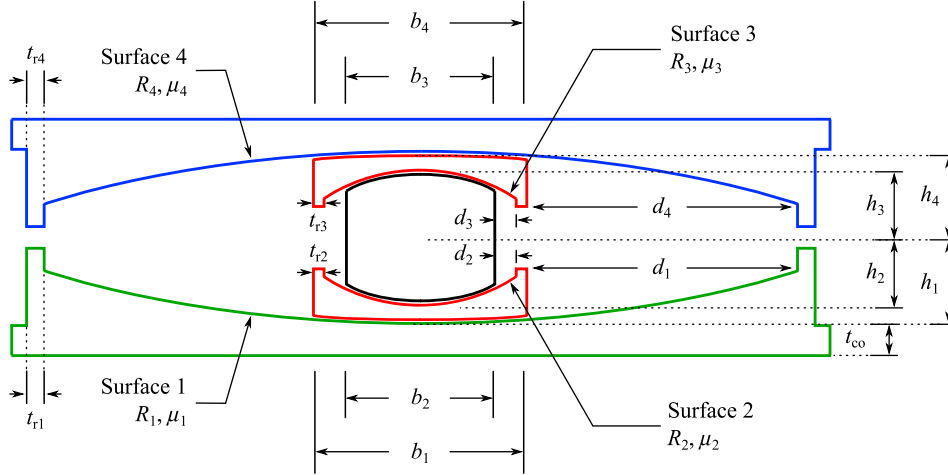


Figure 5-4 Definition of Parameters of Triple FP Bearing

$$\bar{R}_{\text{eff}1} = R_{\text{eff}2} + R_{\text{eff}3}, \quad \bar{R}_{\text{eff}2} = R_{\text{eff}1} - R_{\text{eff}2}, \quad \bar{R}_{\text{eff}3} = R_{\text{eff}4} - R_{\text{eff}3} \quad (5-1)$$

$$R_{\text{eff}i} = R_i - h_i \quad (5-2)$$

$$\bar{K}_{\text{ini},i} = \frac{\mu_n W}{2Y} \quad (5-3)$$

$$\bar{\mu}_1 = \mu_2 = \mu_3, \quad \bar{\mu}_2 = \mu_1, \quad \bar{\mu}_3 = \mu_4 \quad (5-4)$$

Index n takes values of 2 for element FP1, 1 for element FP2 and 4 for element FP3. Quantity Y is a yield displacement in the visco-plastic representation of friction which is typically assigned small values (of the order of 0.01 to 0.1inch).

$$\bar{d}_{\text{GP},1} = D_{\text{Capacity}} - \bar{d}_{\text{GP},2} - \bar{d}_{\text{GP},3}, \quad \bar{d}_{\text{GP},2} = \frac{R_{\text{eff}1} - R_{\text{eff}2}}{R_{\text{eff}1}} \cdot d_1^*, \quad \bar{d}_{\text{GP},3} = \frac{R_{\text{eff}4} - R_{\text{eff}3}}{R_{\text{eff}4}} \cdot d_4^* \quad (5-5)$$

Quantity D_{Capacity} is the displacement capacity when the outer and inner restrainers are reached, given by:

$$D_{\text{Capacity}} = d_1^* + d_2^* + d_3^* + d_4^* \quad (5-6)$$

$$d_i^* = d_i \cdot \frac{R_{\text{eff}i}}{R_i} \quad (5-7)$$

Also, the gap element displacements (Elastic-Perfectly Plastic Gap Material in Figure 5-1) capacities $\bar{d}_{GP,3}$ and $\bar{d}_{GN,3}$ are assigned arbitrarily large values when there is no restrainer for surfaces 2 and 3.

The stiffness of each restrainer is given by the following expressions. Note that the stiffness is defined as the strength of the restrainer (per Sarlis and Constantinou, 2013) divided by a yield displacement Y_r . Quantity F_{ry} is the shear yield stress of the material. Also, the stiffness of gap element GP1 is half that of each restrainer on surfaces 2 and 3 due to the fact that two identical restrainers are simultaneously engaged (one on surface 2 and one on surface 3) and that the two act as if they are connected in series.

$$\bar{K}_{GP1} = \bar{K}_{GN1} = \frac{1}{2} \cdot \left\{ \frac{1}{4} \cdot \frac{\pi (b_1^2 - s_2^2) F_{ry}}{6Y_r} \right\} \quad (5-8)$$

$$\bar{K}_{GP2} = \bar{K}_{GN2} = \frac{\pi t_{r1} (t_{r1} + s_1) F_{ry}}{6Y_r} \quad (5-9)$$

$$\bar{K}_{GP3} = \bar{K}_{GN3} = \frac{\pi t_{r4} (t_{r4} + s_4) F_{ry}}{6Y_r} \quad (5-10)$$

In these equations s_i is the diameter of the sliding surface i and $\bar{d}_{HP,i}$ is i^{th} hook element displacement capacity given by the following equations, where $i=1, 2$ or 3 :

$$s_i = b_i + 2d_i \quad (5-11)$$

$$\bar{d}_{HP,1} = -\bar{d}_{HN,1} = \bar{d}_{GP,1} + (t_{r2} + t_{r3}) \quad (5-12)$$

$$\bar{d}_{HP,2} = -\bar{d}_{HN,2} = \bar{d}_{GP,2} + t_{r1} \quad (5-13)$$

$$\bar{d}_{HP,3} = -\bar{d}_{HN,3} = \bar{d}_{GP,3} + t_{r3} \quad (5-14)$$

Note that Equations (5-8) to (5-10) are based on a simple model for predicting estimates of the restrainer stiffness and strength. The user may control the values of strength and stiffness by selecting values of the shear yield stress F_{ry} and the yield displacement Y_r .

The model described above is assumed valid until the displacement reaches a critical value which results in collapse or overturning of the bearing. This is considered to be at a displacement $D_{Ultimate}$ equal to the displacement capacity given by Equation (5-6) plus about half of the diameter of the rigid slider b_2 :

$$D_{Ultimate} = D_{Capacity} + \frac{b_2}{2} \quad (5-15)$$

Note that the model does not explicitly simulate collapse. Simply when this limit of displacement is exceeded, the isolator is considered failed and execution of the program should be terminated.

This is often called “non-simulated collapse”. Given that collapse is not directly simulated, the user may opt to use a different limit for the ultimate displacement as for example one calculated by the more advanced model in Sarlis and Constantinou (2013).

5.3 Example of Application and Investigation of Axial-Shear Force Interaction

Analysis was performed for a transformer model without and with a horizontal only seismic isolation system and a combined horizontal-vertical seismic isolation system. The horizontal isolation system consisted of the triple FP isolators shown in Figure 4-2 and having the parameters of Table 5-1 with reference to Figure 5-4 for definitions. The friction values in the table are those obtained in testing of the bearings, so they should be considered as the lower bound values of friction. Note that Table 5-1 also include the parameters for the triple FP isolator of Figure 4-1 (which has an inner restrainer ring) as analyses will also be performed for this case later in this report.

Tables 5-2 and 5-3 present values of the parameters used for input in program OpenSees for the two cases of the model where the axial-shear force interaction is considered and then neglected, respectively. Appendix A presents details of the calculations.

Table 5-1 Properties of Triple FP Bearings
(Values in Parenthesis are for Bearing without Inner Restrainer Ring)

Parameter	Value	Unit	Parameter	Value	Unit
$R_1 = R_4$	39	inch	d_1	7	inch
$R_2 = R_3$	8 (6)		d_2	1 (2)	
$R_{eff1} = R_{eff4}$	36 (35.5)		d_3	1 (2)	
$R_{eff2} = R_{eff3}$	6 (3.5)		d_4	7	
h_1	3 (3.5)		d_1^*	6.46 (6.37)	
h_2	2 (2.5)		d_2^*	0.75 (1.17)	
h_3	2 (2.5)		d_3^*	0.75 (1.17)	
h_4	3 (3.5)		d_4^*	6.46 (6.37)	
b_1	8		t_{r1}	0.5	
b_2	5		t_{r2}	0.5 (0)	
b_3	5		t_{r3}	0.5 (0)	
b_4	8		t_{r4}	0.5	

Y_r	0.5		F_{ry}	25	Ksi
Y	0.05		W	105	kip
μ_1	0.12	-	μ_3	0.08	-
μ_2	0.08	-	μ_4	0.12	-

Table 5-2 Material/Element Parameter Values in Program OpenSees for Model
Considering Axial-Shear Force Interaction
(Values in Parenthesis are for Bearing without Inner Restrainer Ring)

Parameter		FP1 ($i=1$)	FP2 ($i=2$)	FP3 ($i=3$)
Single FP Element	$\bar{K}_{ln,i}$	85.0 kip/in	126.0 kip/in	126.0 kip/in
	$\bar{\mu}_i$	0.08	0.12	0.12
	$\bar{R}_{eff,i}$	12.0 in (7.0 in)	30.0 in (32.0 in)	30.0 in (32.0 in)
	$K_{v,Compressed,i}$	92839.2 kip/in	92839.2 kip/in	92839.2 kip/in
	Rotational stiffness	1.0×10^{-9} kip-in/rad	1.0×10^9 kip-in/rad	1.0×10^9 kip-in/rad
Elastic-Perfectly Plastic Gap Material	$\bar{d}_{GP,i}$	3.66 in (100 in)	5.38 in (5.74 in)	5.38 in (5.74 in)
	$\bar{K}_{GP,i}$	49.1 kip/in (0.0 kip/in)	294.5 kip/in	294.5 kip/in
	$\bar{d}_{GN,i}$	-3.66 in (-100 in)	-5.38 in (-5.74 in)	-5.38 in (-5.74 in)
	$\bar{K}_{GN,i}$	49.1 kip/in (0.0 kip/in)	294.5 kip/in	294.5 kip/in
MinMax Material	$\bar{d}_{HP,i}$	4.66 in (101 in)	5.88 in (6.24 in)	5.88 in (6.24 in)
	$\bar{d}_{HN,i}$	-4.66 in (-101 in)	-5.88 in (-6.24 in)	-5.88 in (-6.24 in)
Global vertical linear viscous damping element (per isolator location)	C	4×10^{-3} kip-sec/in		

Analyses were conducted for a 420kip transformer configured as shown in Figure 3-6 and with the 7.7Hz bushing at inclination of 20 degrees. The cases analyzed are: (a) horizontally isolated only, (b) combined horizontal and vertical isolation system without rocking (double rigid base per Figure 3-6(c)), and (c) combined horizontal and vertical isolation system with free rocking (lower rigid base in Figure 3-6(c) removed). The vertical isolation system had the characteristics in Table 4-2 and was modelled using the procedures described in Section 6. One motion from the assembly of motions used in the fragility analysis was selected and utilized. It was the strongest horizontal component of the motion recorded at station Beverly Hills - Mulhol in the 1994

Northridge earthquake, scaled to a horizontal PGA of 0.6g and with the vertical component also scaled so that the vertical to horizontal peak acceleration ratio remained the same as in the originally recorded motions (see Table 7-1 for more details). Analyses were conducted using the two models that respectively consider and neglect axial-shear force interaction, and with and without the vertical earthquake component.

Table 5-3 Input Material/Element Parameter Values in Program OpenSees for Model
Neglecting Axial-Shear Force Interaction
(Values in Parenthesis are for Bearing without Inner Restrainer Ring)

Parameter		FP1 ($i=1$)	FP2 ($i=2$)	FP3 ($i=3$)
Elastic Uniaxial Material (axial)	$K_{v,Compressed,i}$	92839.2 kip/in	92839.2 kip/in	92839.2 kip/in
	$K_{v,Uplift,i}$	0.01 kip/in	0.01 kip/in	0.01 kip/in
Elastic Uniaxial Material (rotational)		1.0×10^{-9} kip-in/rad	1.0×10^9 kip-in/rad	1.0×10^9 kip-in/rad
Steel01 Material (shear)	$\bar{K}_{ln,i}$	85.0 kip/in	126.0 kip/in	126.0 kip/in
	$\bar{\mu}_i$	0.08	0.12	0.12
	W	105 kip	105 kip	105 kip
	$\bar{R}_{eff,i}$	12.0 in (7.0 in)	30.0 in (32.0 in)	30.0 in (32.0 in)
Elastic-Perfectly Plastic Gap Material	$\bar{d}_{GP,i}$	3.66 in (100 in)	5.38 in (5.74 in)	5.38 in (5.74 in)
	$\bar{K}_{GP,i}$	49.1 kip/in (0.0 kip/in)	294.5 kip/in	294.5 kip/in
	$\bar{d}_{GN,i}$	-3.66 in (-100 in)	-5.38 in (-5.74 in)	-5.38 in (-5.74 in)
	$\bar{K}_{GN,i}$	49.1 kip/in (0.0 kip/in)	294.5 kip/in	294.5 kip/in
MinMax Material	$\bar{d}_{HP,i}$	4.66 in (101 in)	5.88 in (6.24 in)	5.88 in (6.24 in)
	$\bar{d}_{HN,i}$	-4.66 in (-101 in)	-5.88 in (-6.24 in)	-5.88 in (-6.24 in)
Global vertical linear viscous damping element (per isolator location)	C	4×10^{-3} kip-sec/in		

Results are presented in Figures 5-5 to 5-10 for the three cases with horizontal only seismic excitation. The results demonstrate that the two models that respectively consider and neglect the axial-shear force interaction produce essentially the same results so that the simpler and computationally more stable model that neglects the interaction is preferred.

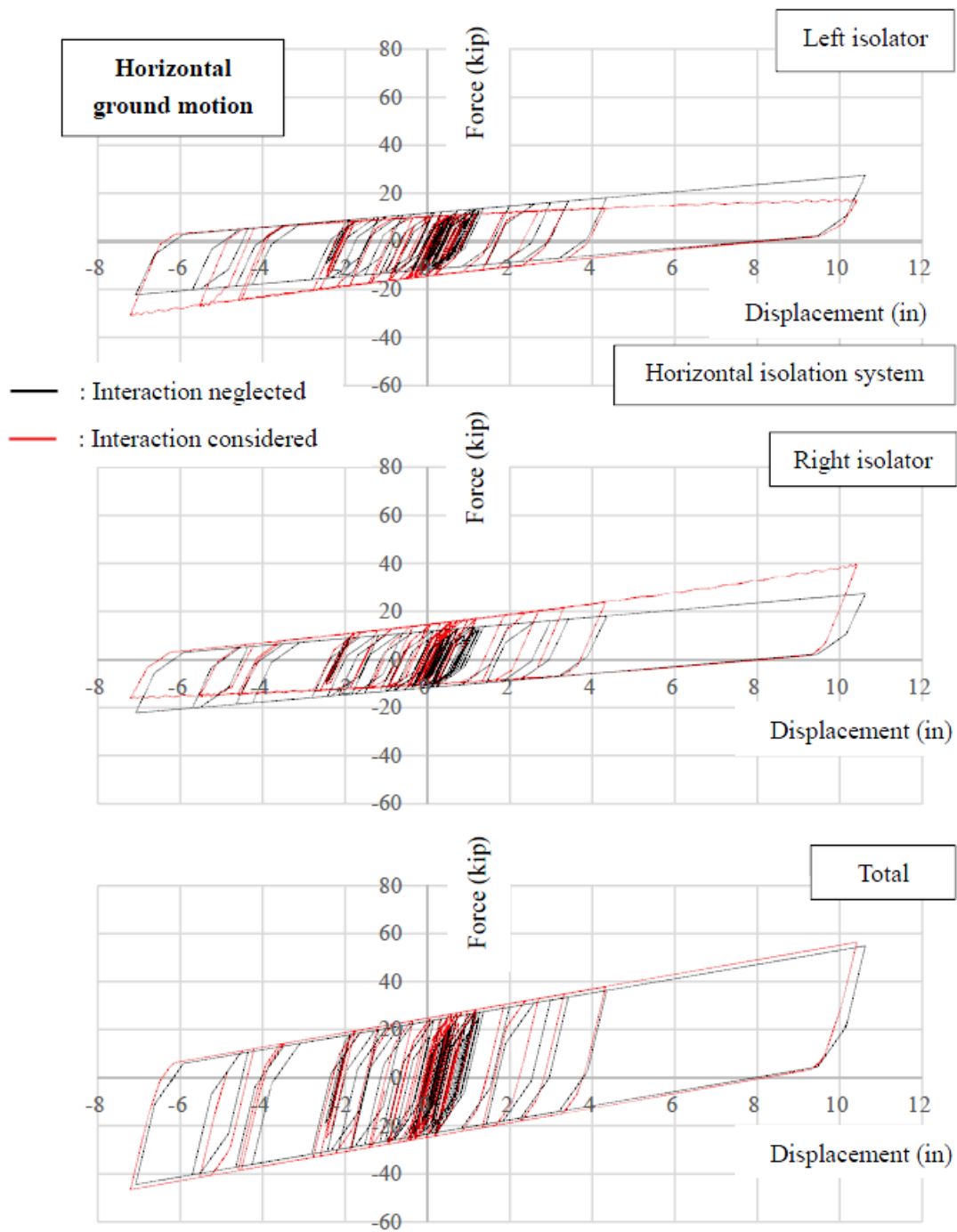


Figure 5-5 Force-Displacement Loops of Individual Isolators and Total Base Shear-Displacement Loop of Transformer with Horizontal Isolation System in Horizontal Only Ground Motion

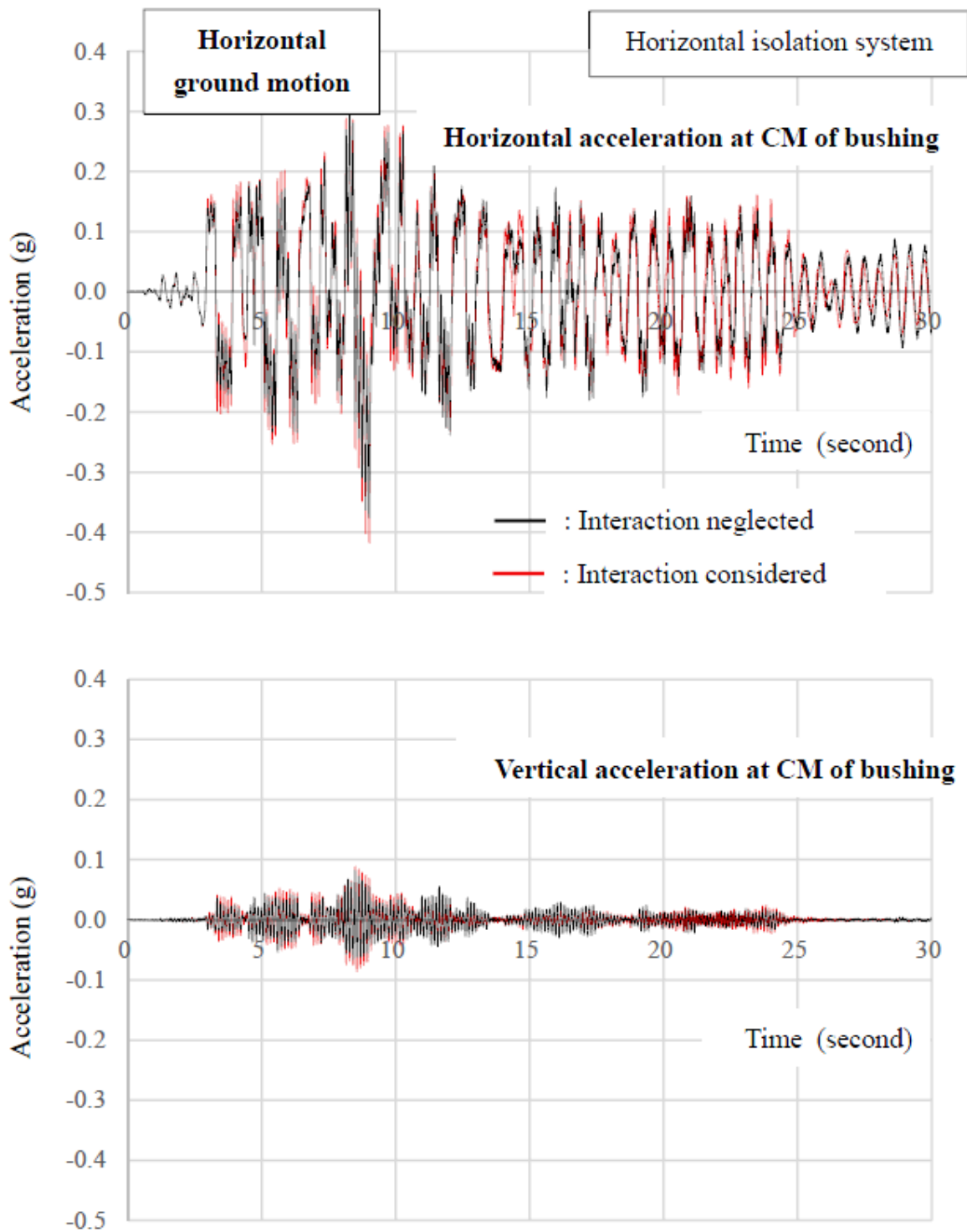


Figure 5-6 Acceleration Histories at Bushing Center of Mass of Transformer with Horizontal Isolation System in Horizontal Only Ground Motion

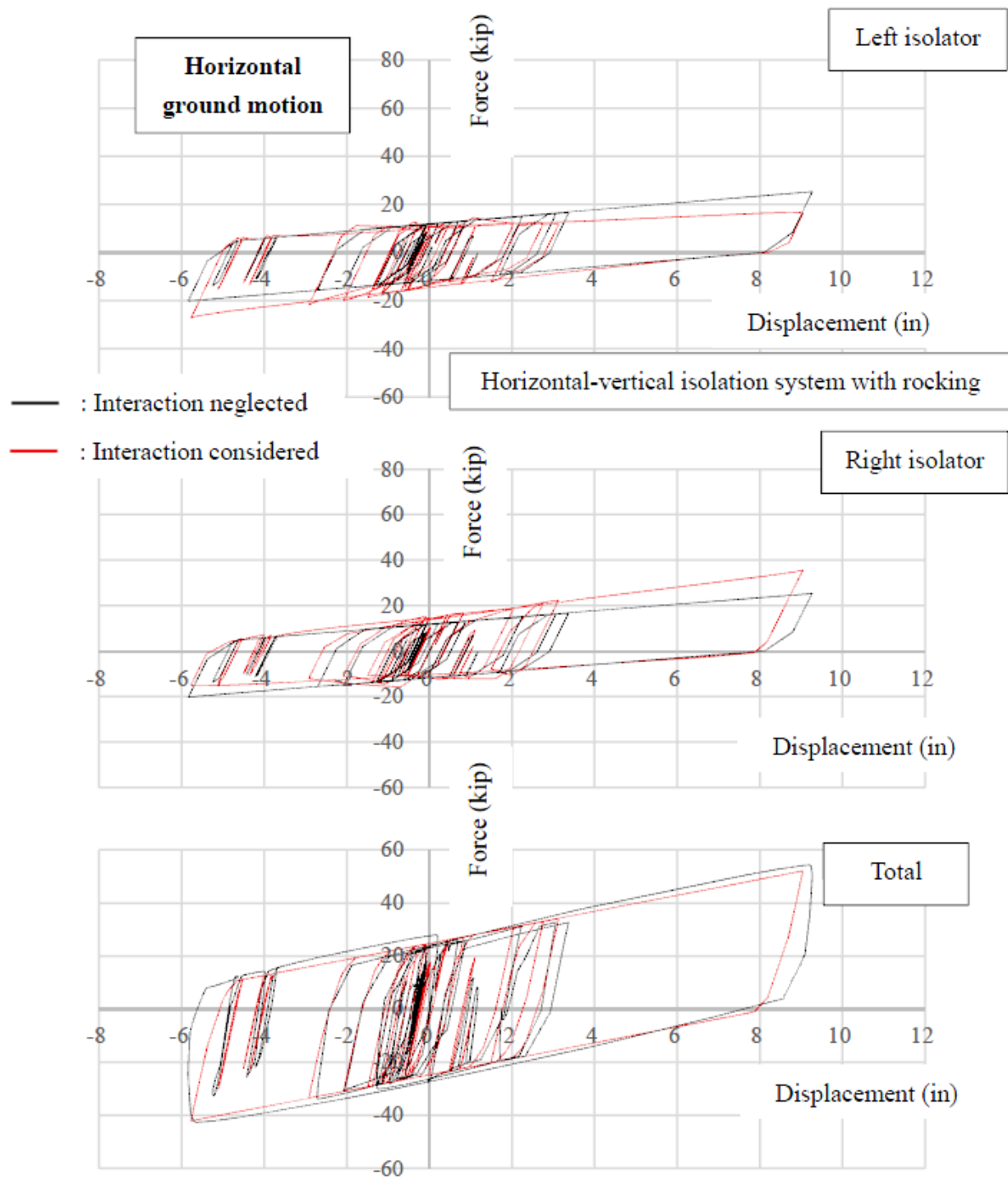


Figure 5-7 Force-Displacement Loops of Individual Isolators and Total Base Shear-Displacement Loop of Transformer with Horizontal-Vertical Isolation System with Rocking in Horizontal only Ground Motion

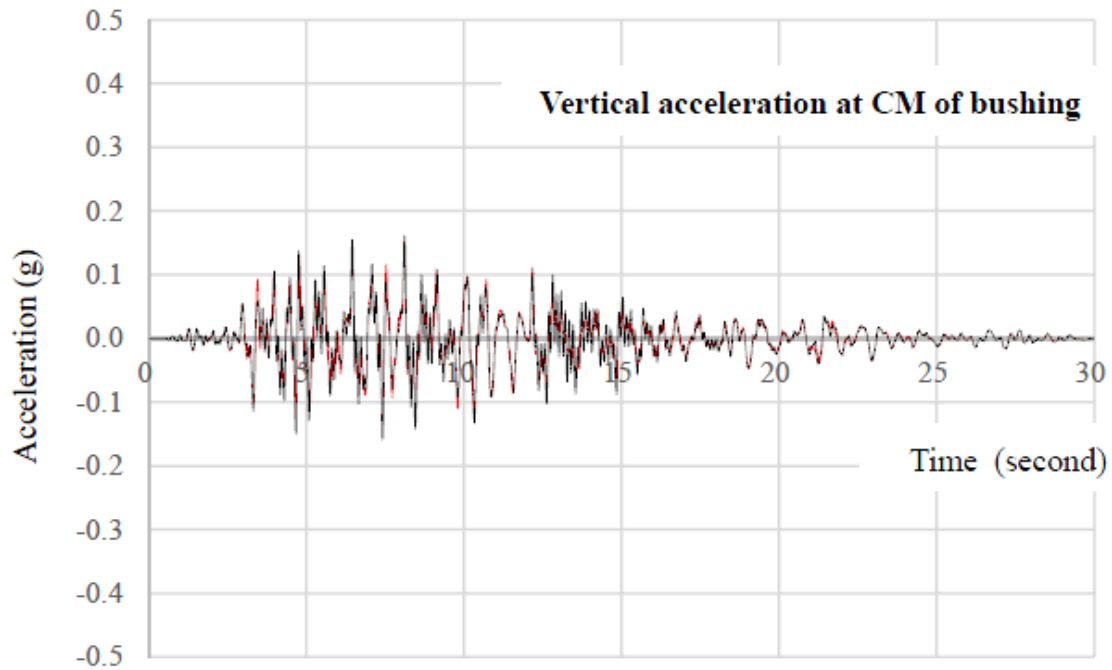
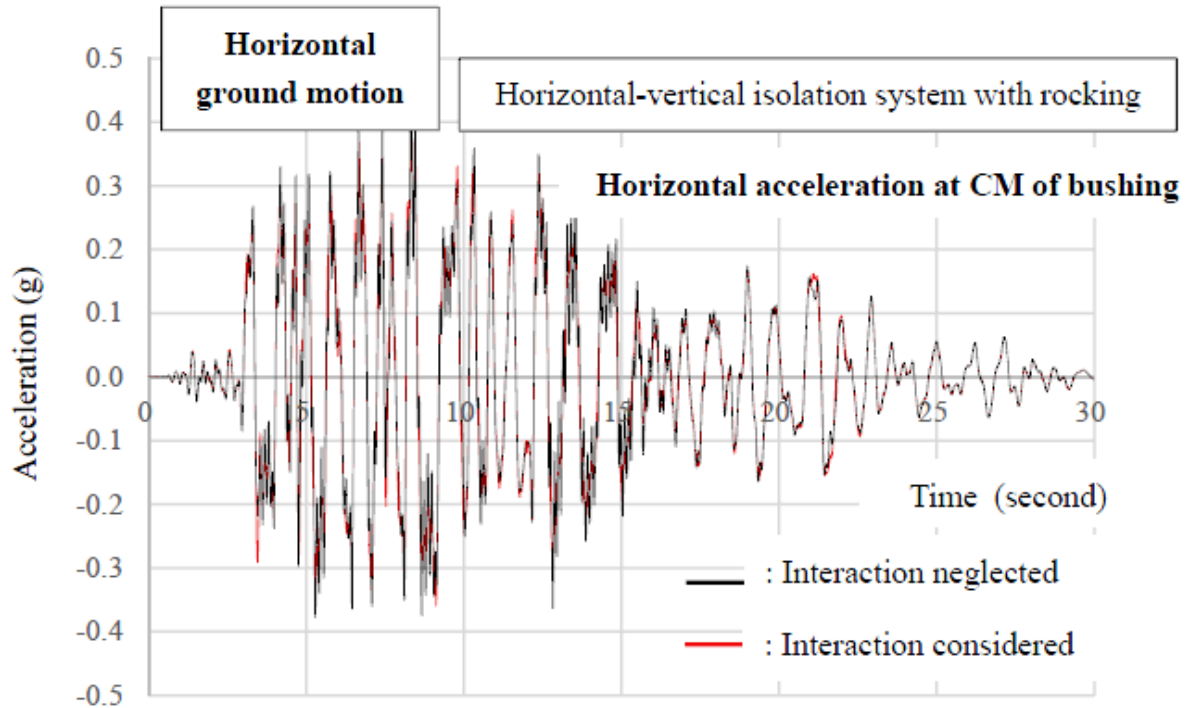


Figure 5-8 Acceleration Histories at Bushing Center of Mass of Transformer with Horizontal-Vertical Isolation System with Rocking in Horizontal Only Ground Motion

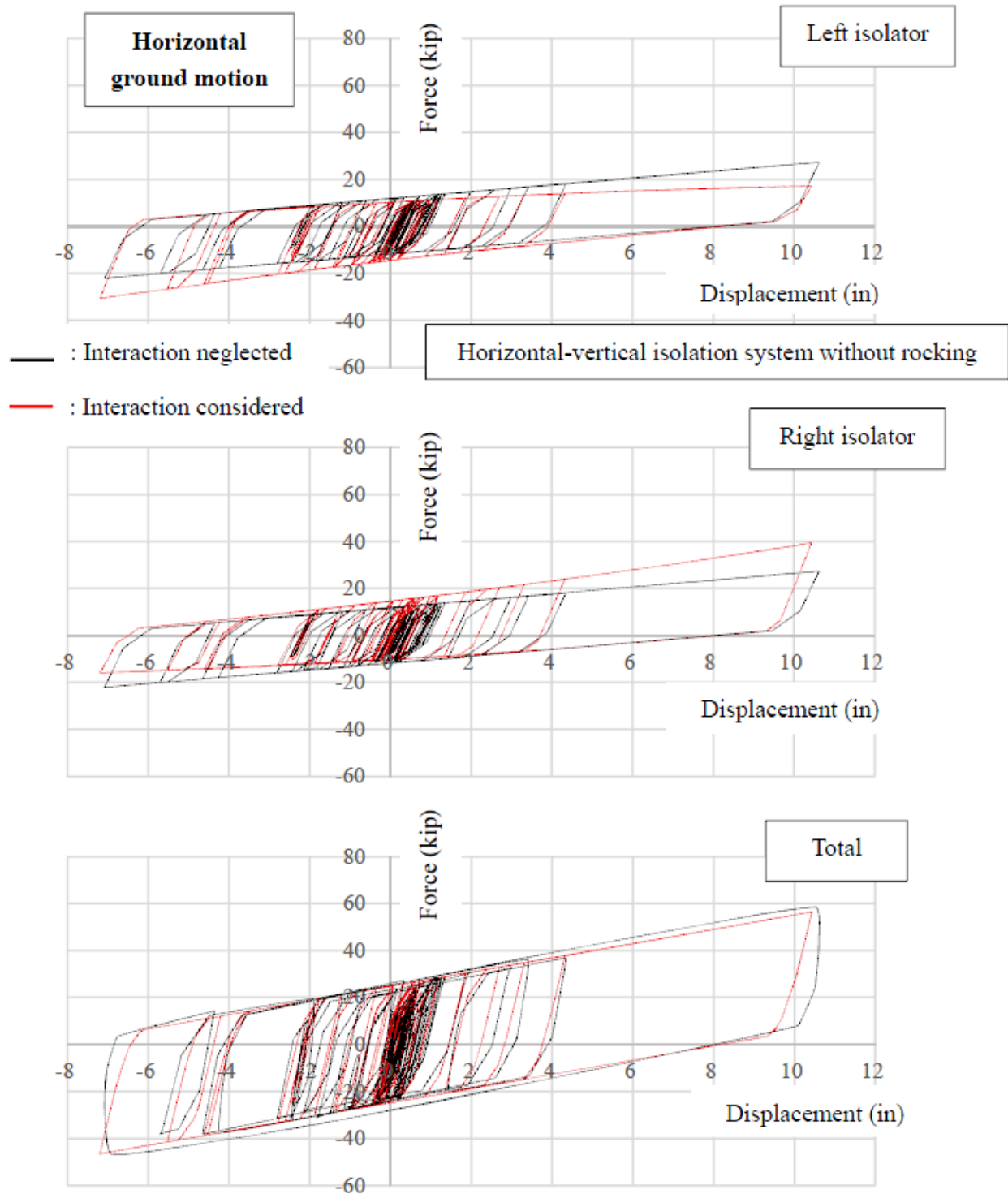


Figure 5-9 Force-Displacement Loops of Individual Isolators and Total Base Shear-Displacement Loop of Transformer with Horizontal-Vertical Isolation System without Rocking in Horizontal Only Ground Motion

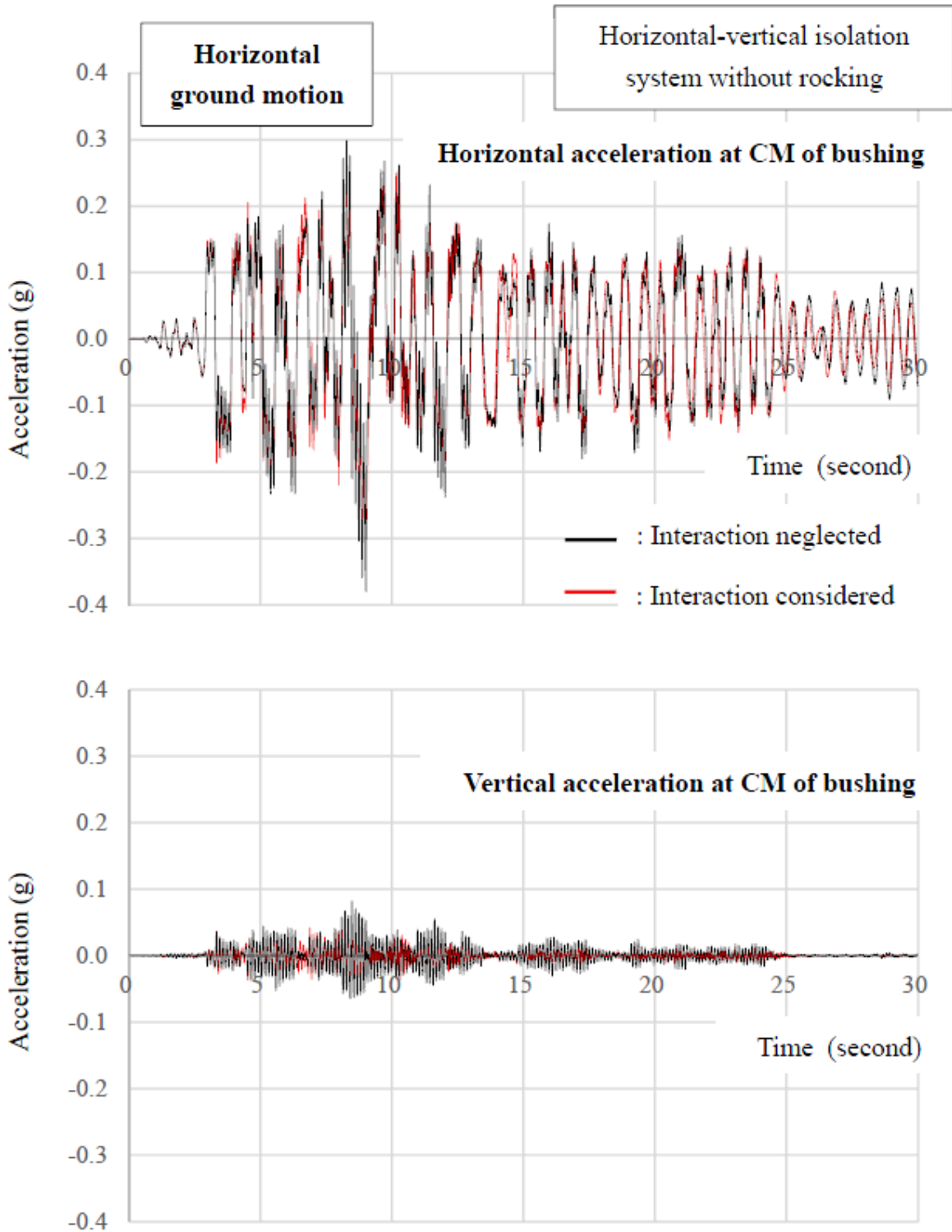


Figure 5-10 Acceleration Histories at Bushing Center of Mass of Transformer with Horizontal-Vertical Isolation System without Rocking in Horizontal Only Ground Motion

Figures 5-11 to 5-16 present results for the three isolated cases where combined horizontal and vertical seismic excitation was used. The results demonstrate that the model which considers the axial-shear force interaction results in about the same displacement demands but produces higher acceleration values than the model that neglects interaction, which is consistent with test observations (e.g., Sarlis et al, 2013, Oikonomou et al, 2016).

The results shown in these figures portray a behavior in which the FP isolators have large displacements but barely enter their stiffening regime. Also, there is no uplift in the isolators, a phenomenon that is difficult to numerically simulate given that it leads to global rocking and bouncing of the transformer on its two supports. Both models are capable of simulating global rocking and bouncing behavior but the model which neglects the axial-shear force interaction always results in numerically stable solutions whereas the model that accounts for the interaction does not.

Figures 5-17 and 5-18 compare results obtained by the two models in a set of analyses where a different excitation was used so that there is isolator uplift. The motion used was the strongest horizontal component of the motion recorded at station Canyon Country - WCL in the 1994 Northridge earthquake, scaled to a horizontal PGA of 1.0g and with the vertical component also scaled so that the vertical to horizontal peak acceleration ratio remained the same as in the originally recorded motions (see Table 7-1 for more details). The results in these figures are for the case of the combined horizontal-vertical isolation system. The analysis resulted in clearly erroneous results for the case of the model with axial-shear force interaction (predicted accelerations reached 30g). Even the results in Figures 5-17 and 5-18 were obtained in the case of the model with axial-shear force interaction at enormous computational cost and after several trials using progressively smaller time step of integration and by increasing the convergence tolerance. Yet both models resulted in essentially the same peak accelerations and isolator displacement (and actually both models predicted failure of the isolators).

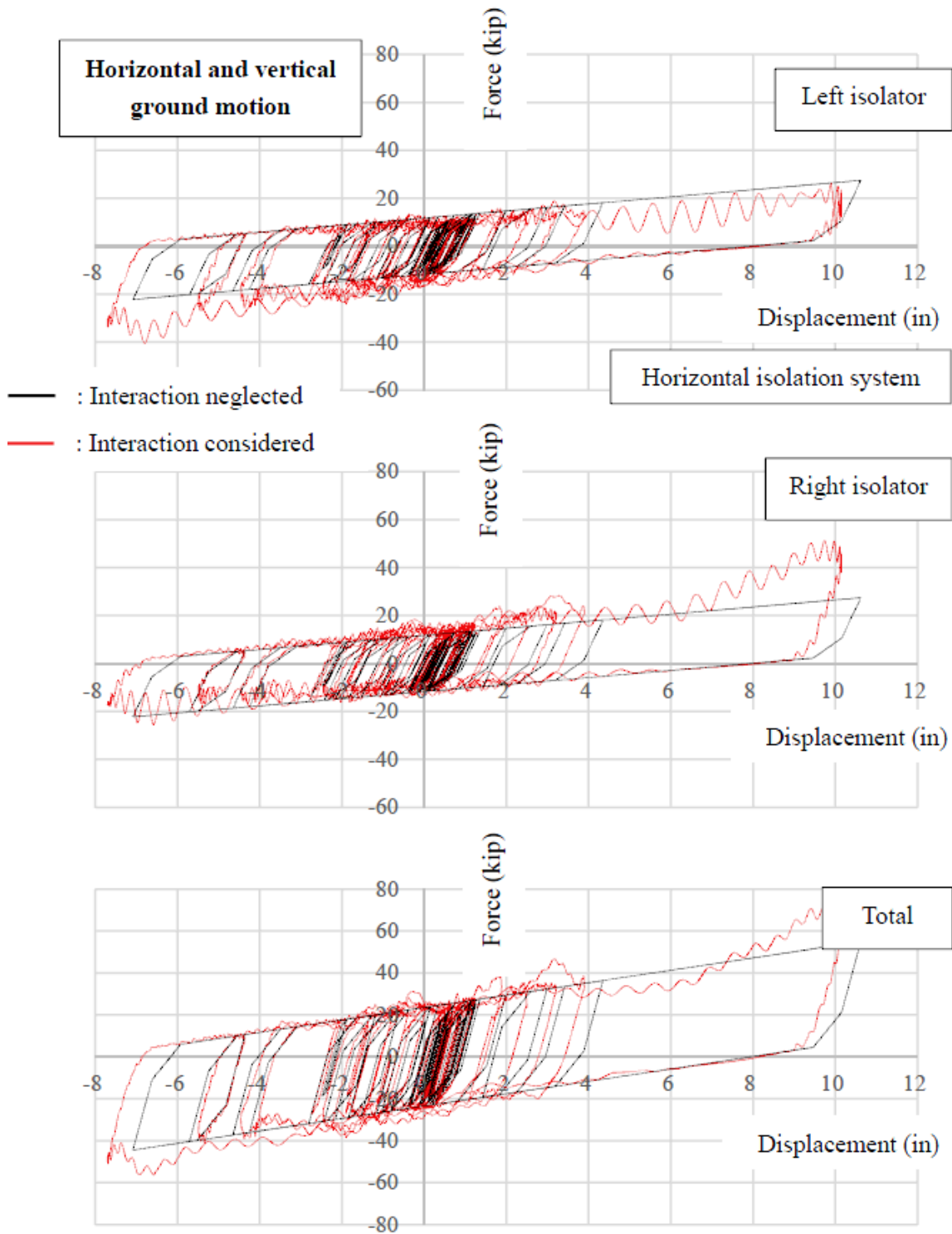


Figure 5-11 Force-Displacement Loops of Individual Isolators and Total Base Shear-Displacement Loop of Transformer with Horizontal Isolation System in Horizontal-Vertical Ground Motion

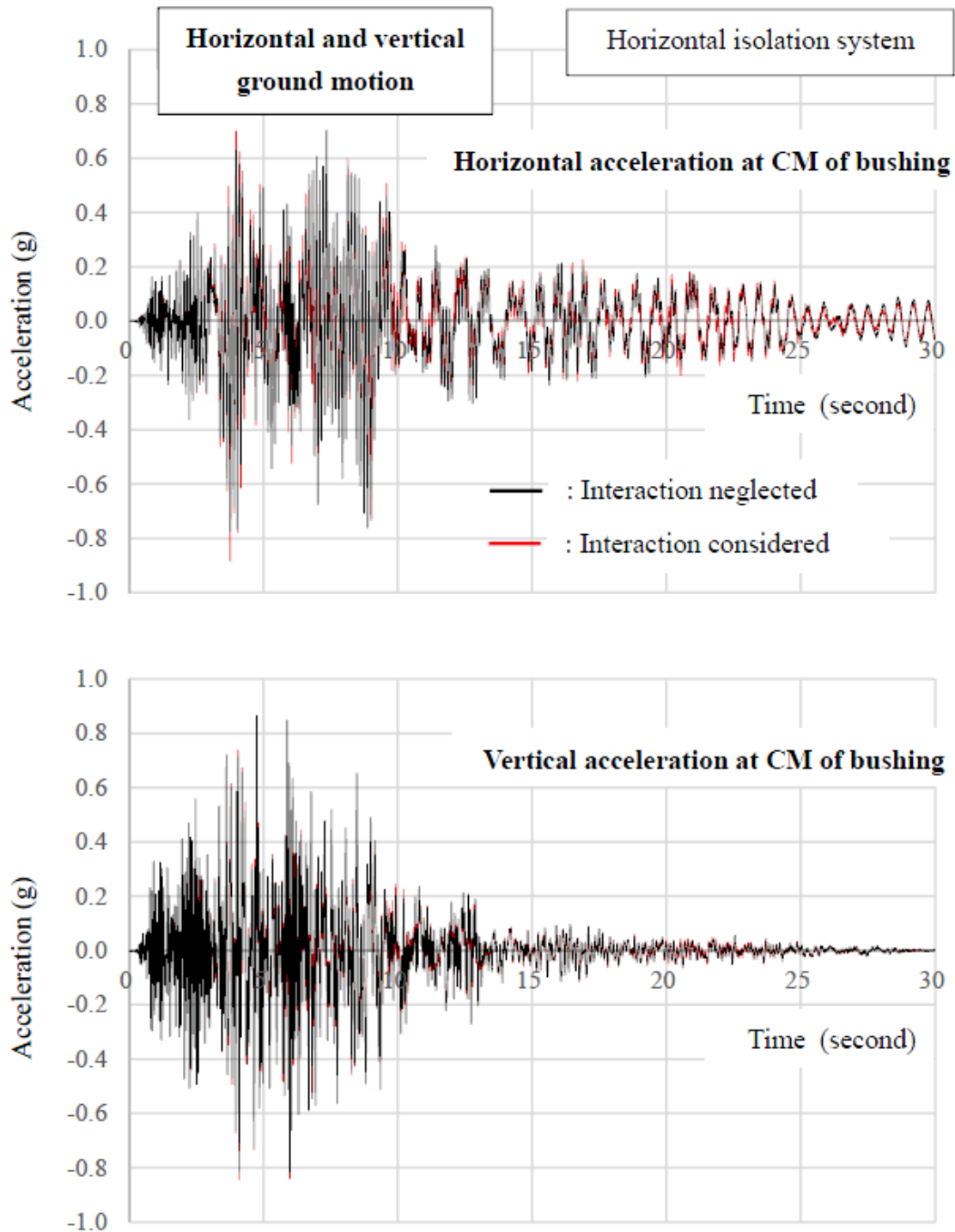


Figure 5-12 Acceleration Histories at Bushing Center of Mass of Transformer with Horizontal Isolation System in Horizontal-Vertical Ground Motion

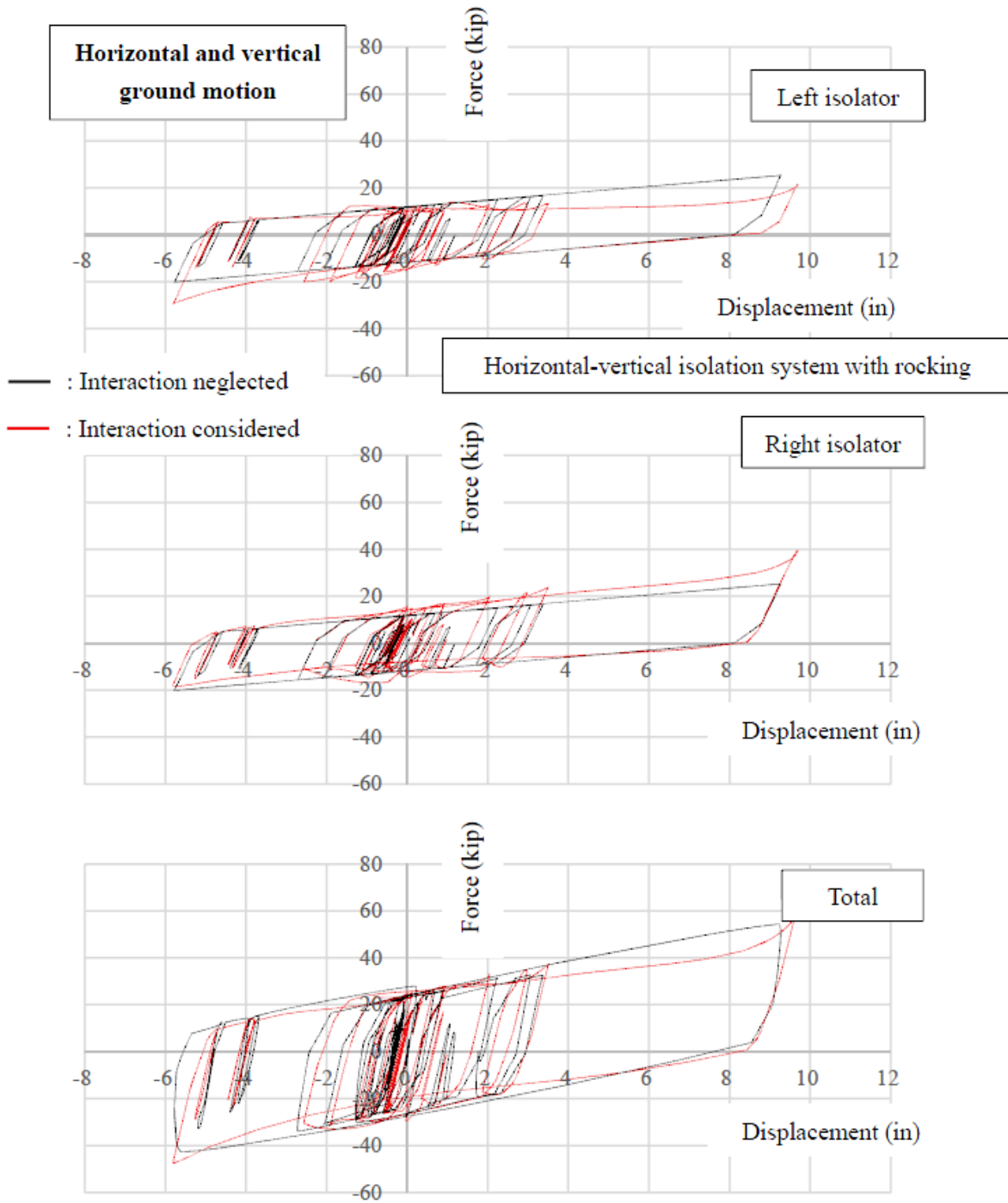


Figure 5-13 Force-Displacement Loops of Individual Isolators and Total Base Shear-Displacement Loop of Transformer with Horizontal-Vertical Isolation System with Rocking in Horizontal-Vertical Ground Motion

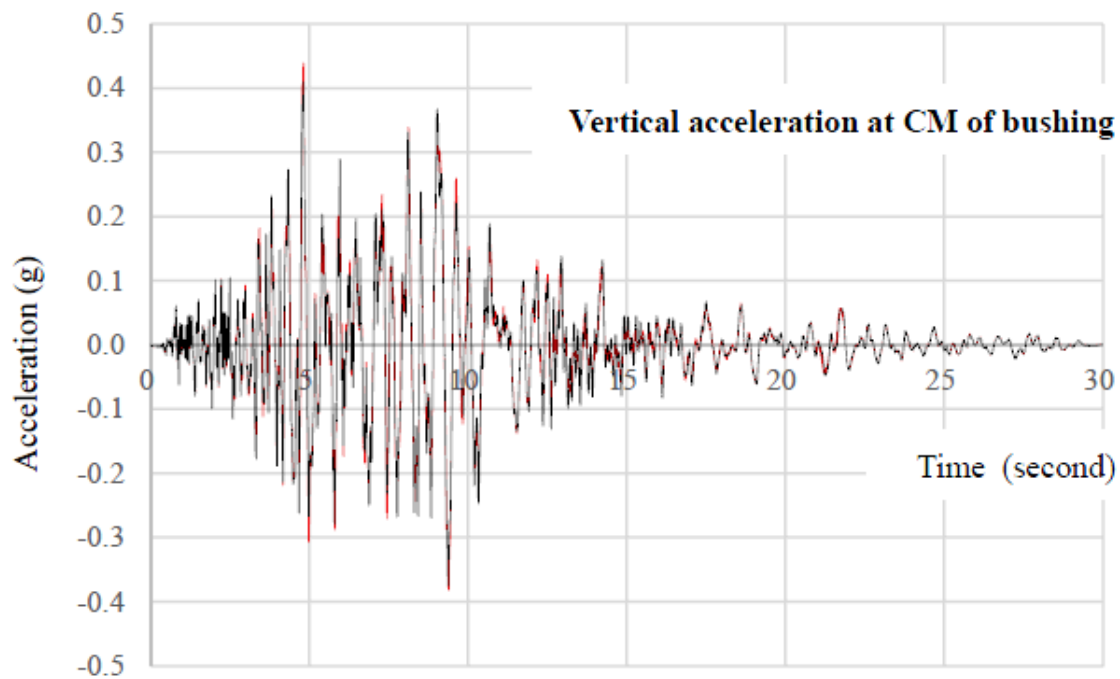
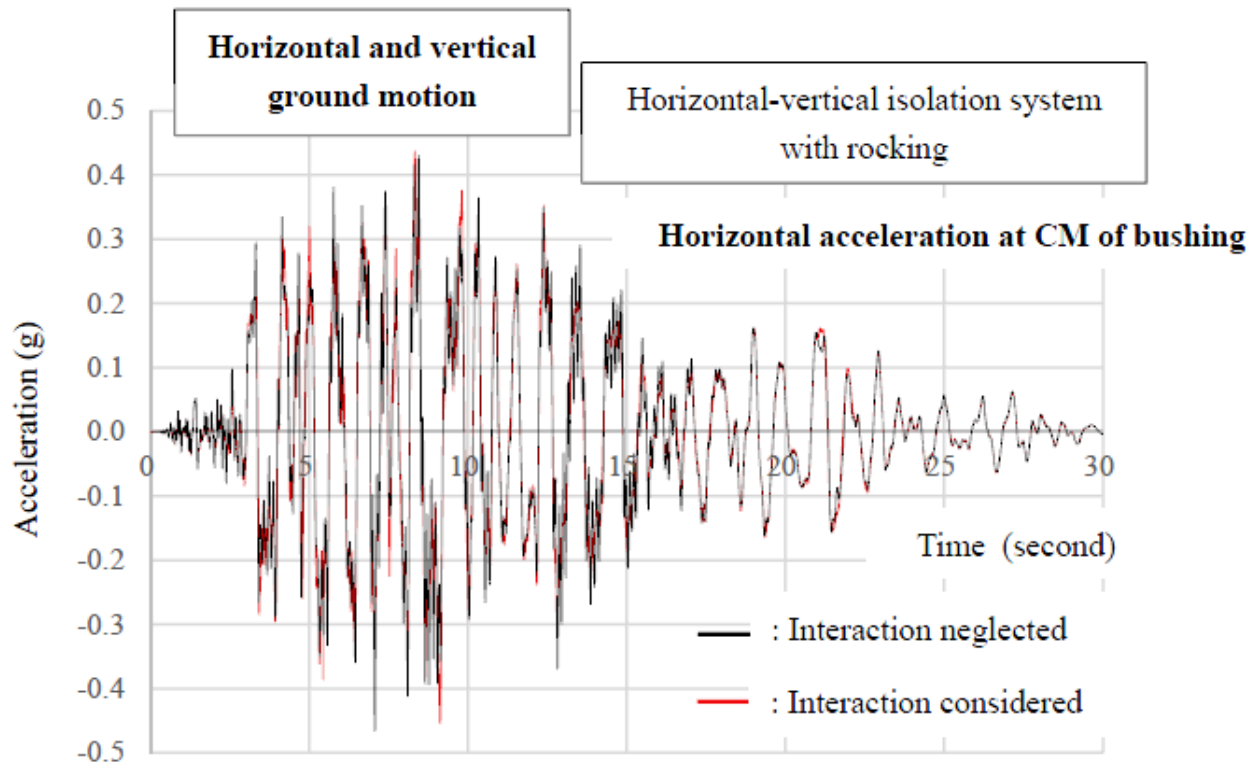


Figure 5-14 Acceleration Histories at Bushing Center of Mass of Transformer with Horizontal-Vertical Isolation System with Rocking in Horizontal-Vertical Ground Motion

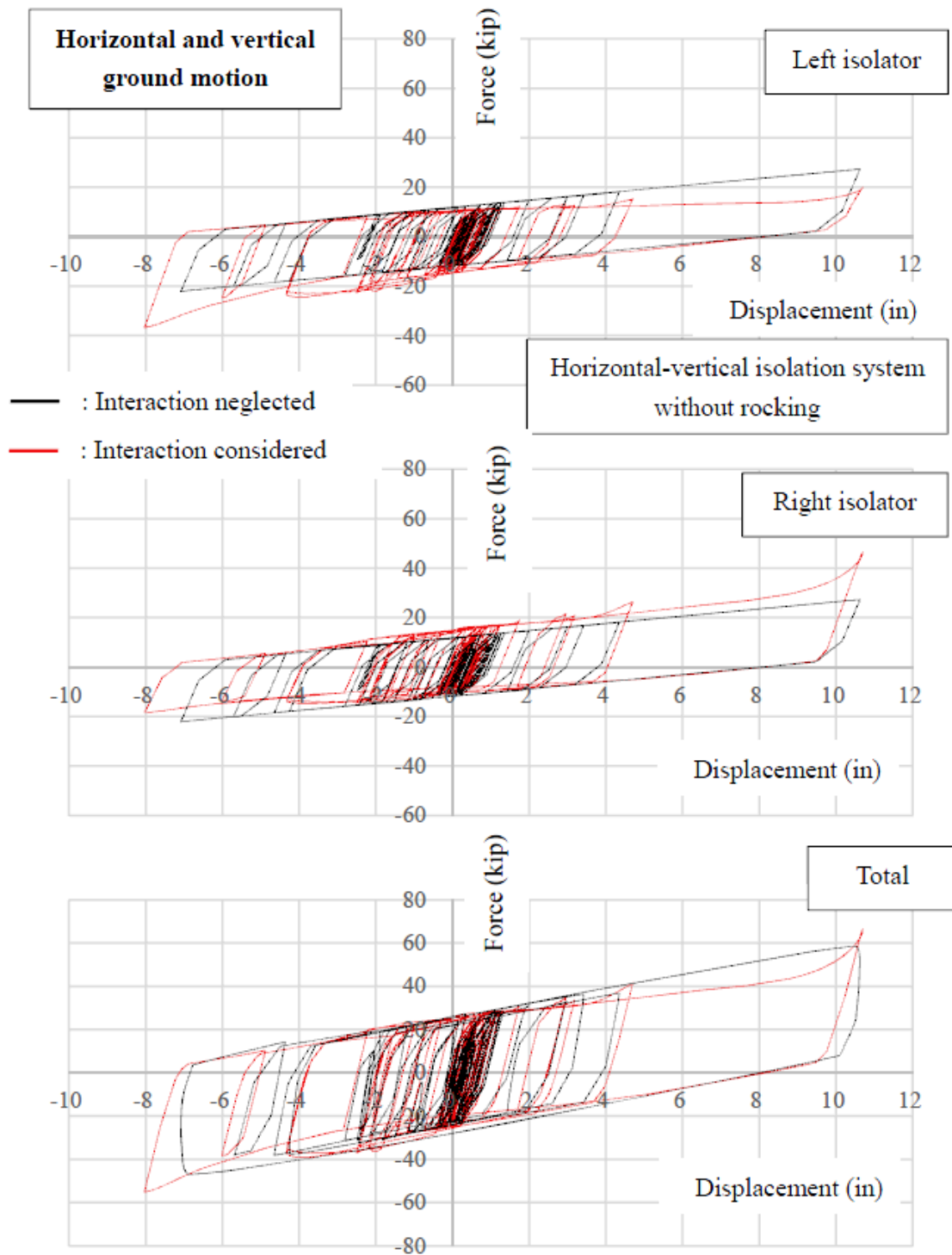


Figure 5-15 Force-Displacement Loops of Individual Isolators and Total Base Shear-Displacement Loop of Transformer with Horizontal-Vertical Isolation System without Rocking in Horizontal-Vertical Ground Motion

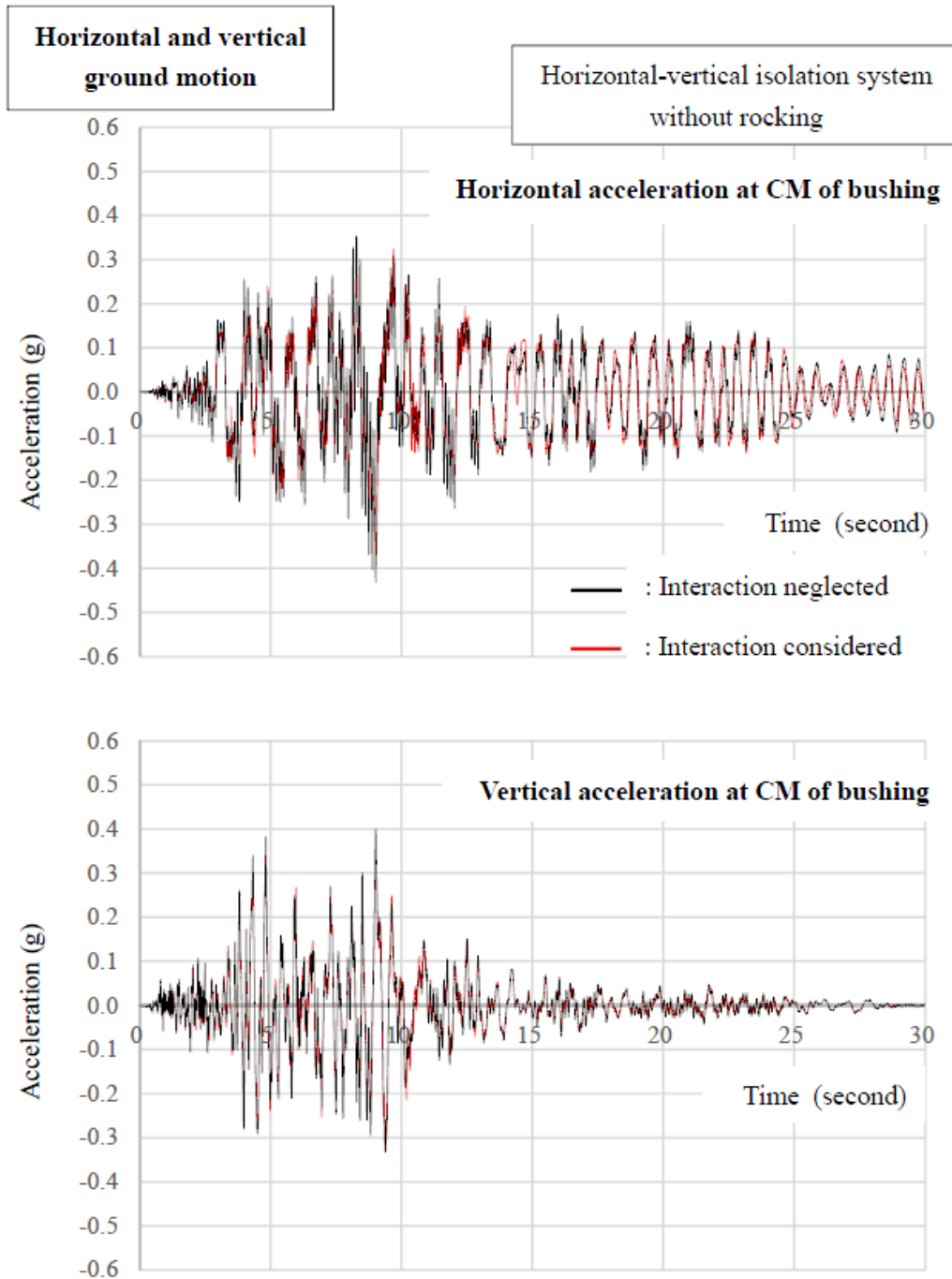


Figure 5-16 Acceleration Histories at Bushing Center of Mass of Transformer with Horizontal-Vertical Isolation System without Rocking in Horizontal-Vertical Ground Motion

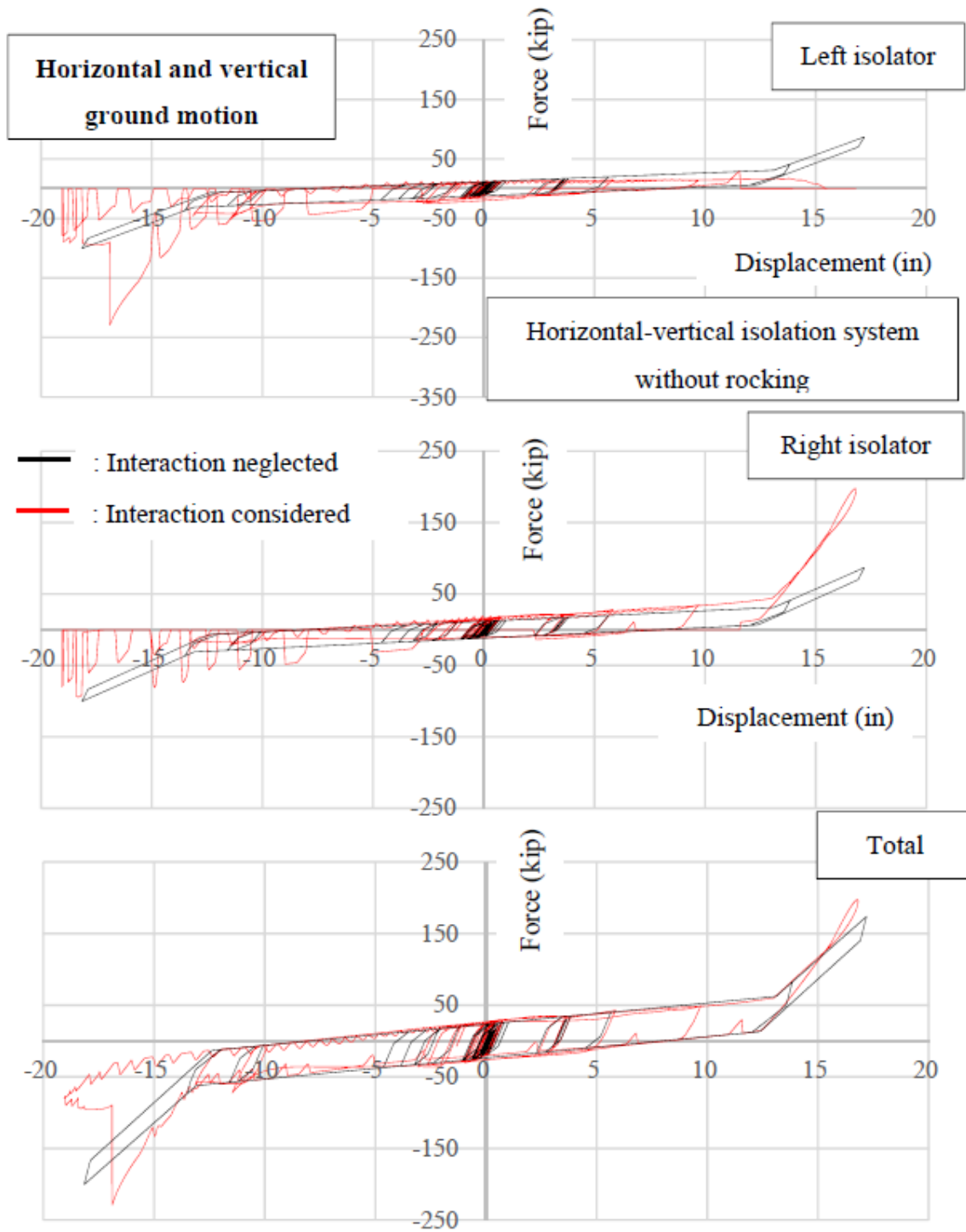


Figure 5-17 Force-Displacement Loops of Individual Isolators and Total Base Shear-Displacement Loop of Transformer with Horizontal-Vertical Isolation System without Rocking in Another Horizontal-Vertical Ground Motion Scaled to $PGA=1.0g$ so that there is Uplift

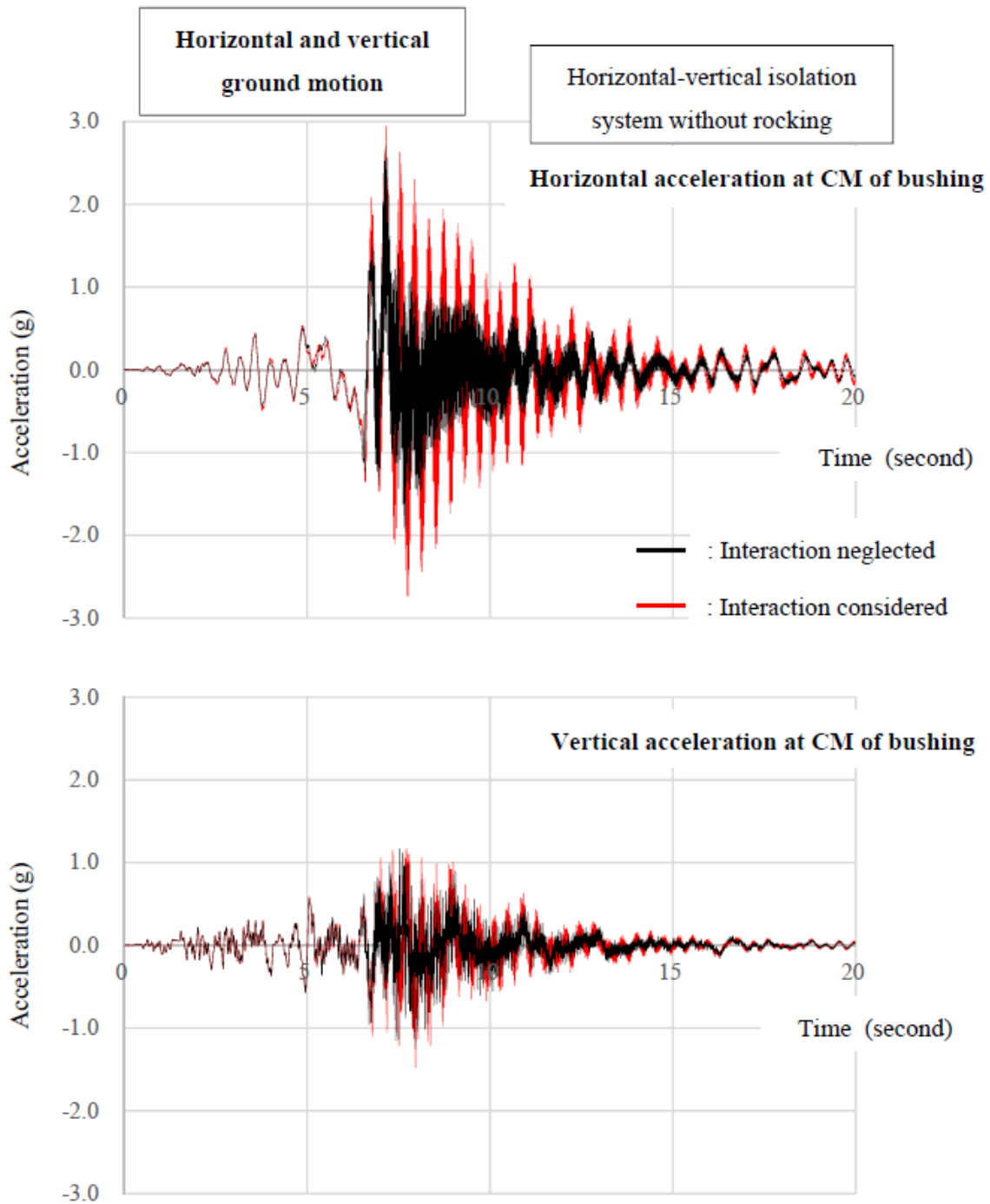


Figure 5-18 Acceleration Histories at Bushing Center of Mass of Transformer with Horizontal-Vertical Isolation System without Rocking in Another Horizontal-Vertical Ground Motion Scaled to PGA=1.0g so that there is Uplift

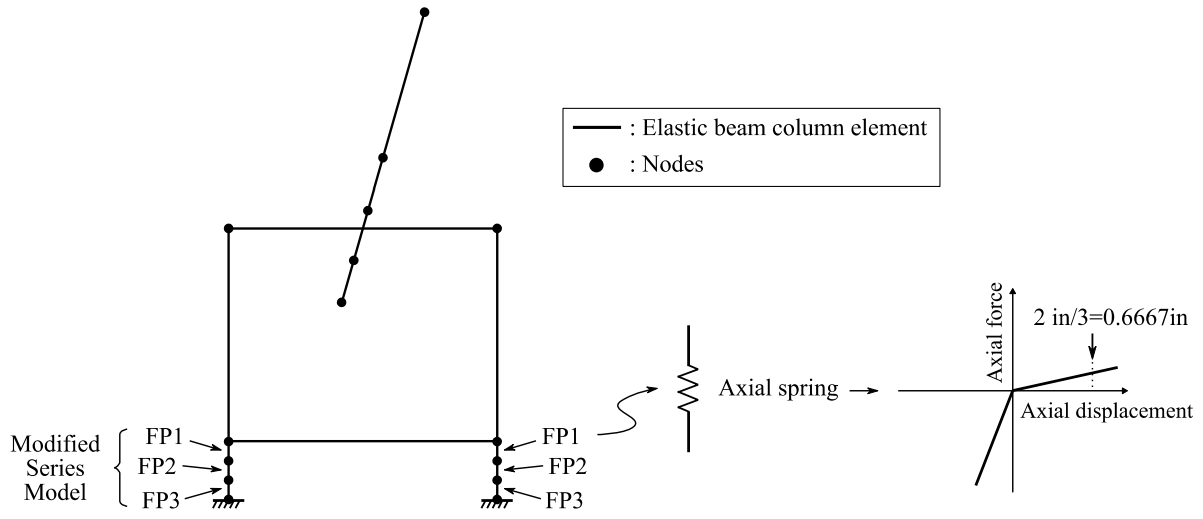
On the basis of the presented results it was concluded that the model that accounts for the axial-shear force interaction produces essentially the same results as the simpler model that neglects the interaction under extreme conditions that involve stiffening of the isolators, uplift and bouncing. Yet the model that accounts for axial-shear force interaction was computationally very costly, required adjustment of time step and convergence tolerance and often failed numerically. It was clear that the model could not be used in fragility analysis where a very large number of analyses are required.

When uplift did not occur, the model that accounts for axial-shear force interaction produced results that were consistent with test observations that included about the same isolator displacement demands but higher accelerations than those produced by the simpler model that neglected the interaction.

Accordingly, it was deemed to be appropriate to use the model that neglects axial-shear force interaction in the fragility analysis. The model will result in realistic probabilities of failures in cases where isolator stiffening, uplift and bouncing occur. However, the model will likely underestimate the probabilities of failure when these phenomena do not occur.

5.4 Calculation of Uplift Displacement

In the fragility analysis presented in this report, the isolators are considered failed when the uplift displacement exceeds 2inch. This 2inch limit was determined based on the geometry of the triple FP bearings shown in Figures 4-1 to 4-3 so that the lifted upper concave plate returns on the inner slider after an uplift episode without instability (also see Section 8). The uplift displacement is calculated by monitoring the axial deformation of element FP1 in the modified series model. In the model, uplift of 2inch occurs when the axial deformation of each of the three elements (FP1, FP2 and FP3) in series in the model exceeds one third of the limit or 0.667inch as depicted in Figure 5-19. Note that this is true as the three elements are assigned equal axial stiffness. Figure 5-20 presents an example of uplift displacement history of a FP isolator in analysis of a horizontal-only isolated transformer model with the 7.7Hz (No. 8) bushing inclined at 20 degrees in the 1994 Northridge earthquake (Beverly Hills - Mulhol; site class D) with PGA scaled to 0.9 g.



Transformer with horizontal isolation system

Figure 5-19 Measurement of Uplift Displacement

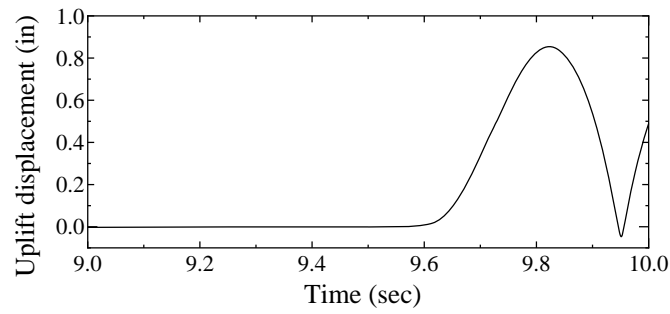


Figure 5-20 Example Uplift Displacement History of Triple FP Bearing

SECTION 6
MODEL FOR SIMULATING THE ULTIMATE BEHAVIOR OF SPRING-DAMPER
UNIT IN THREE-DIMENSIONAL SEISMIC ISOLATION SYSTEM

The model of the spring-damper unit in program OpenSees (McKenna, 1997) consists of two elements in parallel, one representing the springs and one representing the viscous damper. The element only represents the behavior of the unit in the vertical direction. It is presumed that the unit has unlimited capacity to resist shear force and overturning moment without any deformation.

Three uniaxial elements are used to represent the spring in program OpenSees: i) Elastic Uniaxial Material, ii) Elastic-Perfectly Plastic Material and iii) Elastic-Perfectly Plastic Gap Material. These are illustrated in Figure 6-1 and a force-displacement relation is for the entire element shown in Figure 6-2. Note that the springs are assumed to have a very low tensile stiffness when the displacement limit of 5.0inch is exceeded (α times the actual stiffness where $\alpha=0.001$). The model depicted in Figure 6-2 presents the behavior of the springs alone. Within the spring-damper assembly the springs can only deform in compression up to a maximum of 5.0inch from the unloaded position (as shown in Figure 6-2). In tension and without considering the damper, the springs can deform as shown in Figure 6-2. In reality however, the springs will be restrained by the damper which has a stroke capacity of 5.0inch. Therefore, the springs cannot be stretched in tension as the force will then be transferred to the damper which has reached its displacement capacity and resists deformation with very high stiffness. Nevertheless, the springs are represented by the model of Figures 6-1 and 6-2 and the tension stroke limit is utilized in the damper model as it is physically valid.

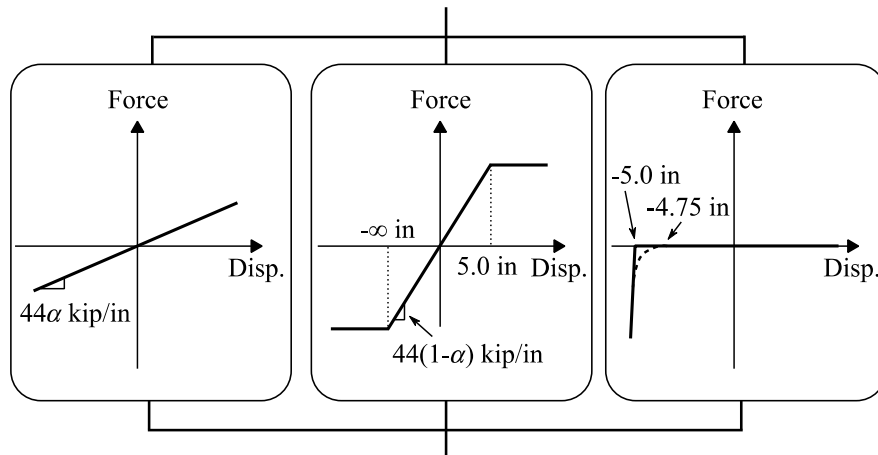


Figure 6-1 Elements Connected in Parallel to Represent the Ultimate Behavior of Springs

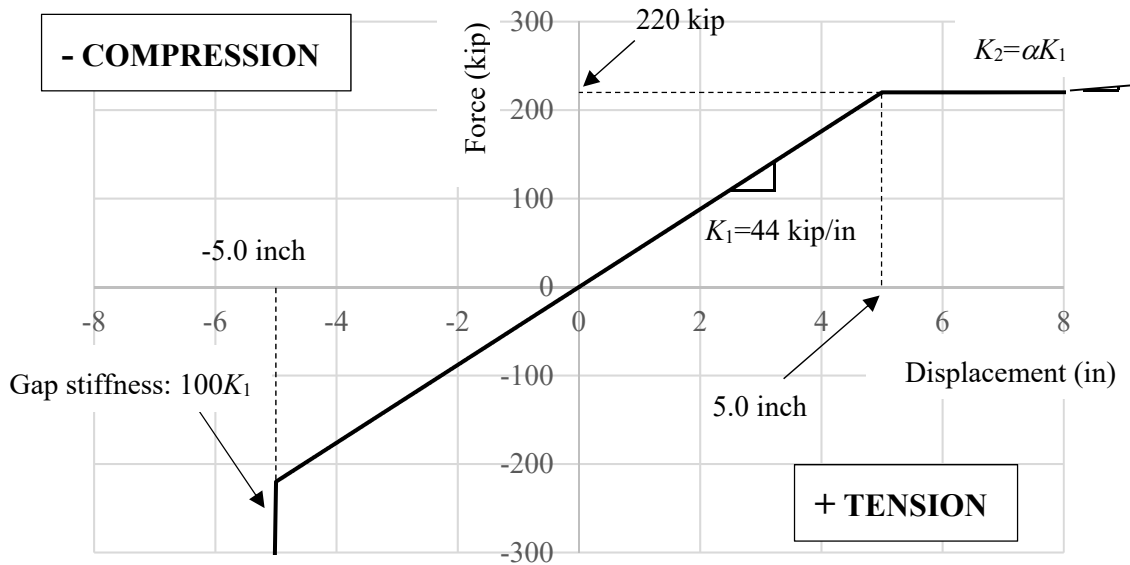


Figure 6-2 Force-Displacement Relation Produced by Spring Element

The viscous damper is represented in program OpenSees with a newly developed uniaxial material element called *ULTdamper*. The hysteretic rule for this element is presented in Figure 6-3. The viscous force is not shown for clarity. This force is simply linearly related to the velocity through the damping constant C ($=3.4\text{kip-sec/inch}$). Other parameters for this model are shown in Figure 6-3 and values of parameters are presented in Table 6-1. The tensile post-failure behavior of the device was defined in a manner that: (a) is physically meaningful and (b) is such that numerical instability in the analysis program is avoided. The failure behavior of the device was modeled so that when the device force reaches the ultimate value (“Ultimate F_{Tension} ” in Figure 6-3) the force is not abruptly removed but rather is gradually reduced at each time step by an amount equal to 10% of the value at the previous step. Note that when the damper element fails in tension and is removed from the spring-damper combined element, the element is still functional but with only the spring being effective.

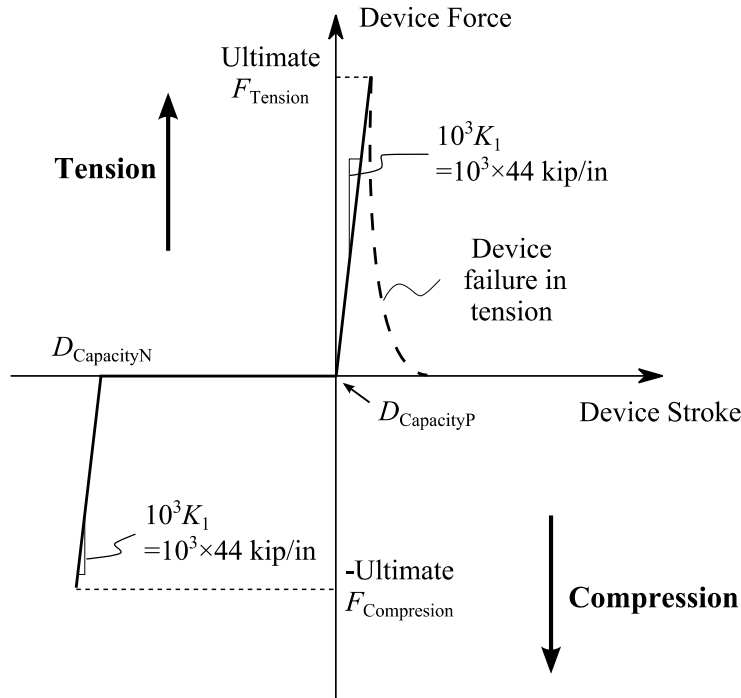


Figure 6-3 Ultimate Behavior of Viscous Damper Element (Viscous Force not Depicted)

Table 6-1 Parameters for Viscous Damper

$D_{CapacityP}$	0.0 inch
$D_{CapacityN}$	-5.0inch
Ultimate $F_{Compression}$	unlimited
Ultimate $F_{Tension}$	200kip

Representative force-displacement relations produced by the damper element are presented in Figure 6-4. Three different force-displacement hysteresis loops are shown in Figure 6-4. All loops were produced by imposing motion from a specified static position (starting point) and amplitude of 2.3inch at frequency of 2Hz. The latter two loops result either in failure in tension or reaching the bottom of the damper and thus generating very high compressive force. It should be noted that when a triple FP isolator is placed on top of the spring-damper unit, failure in tension is not possible as uplift will occur at the isolator prior to initiating tension in the damper.

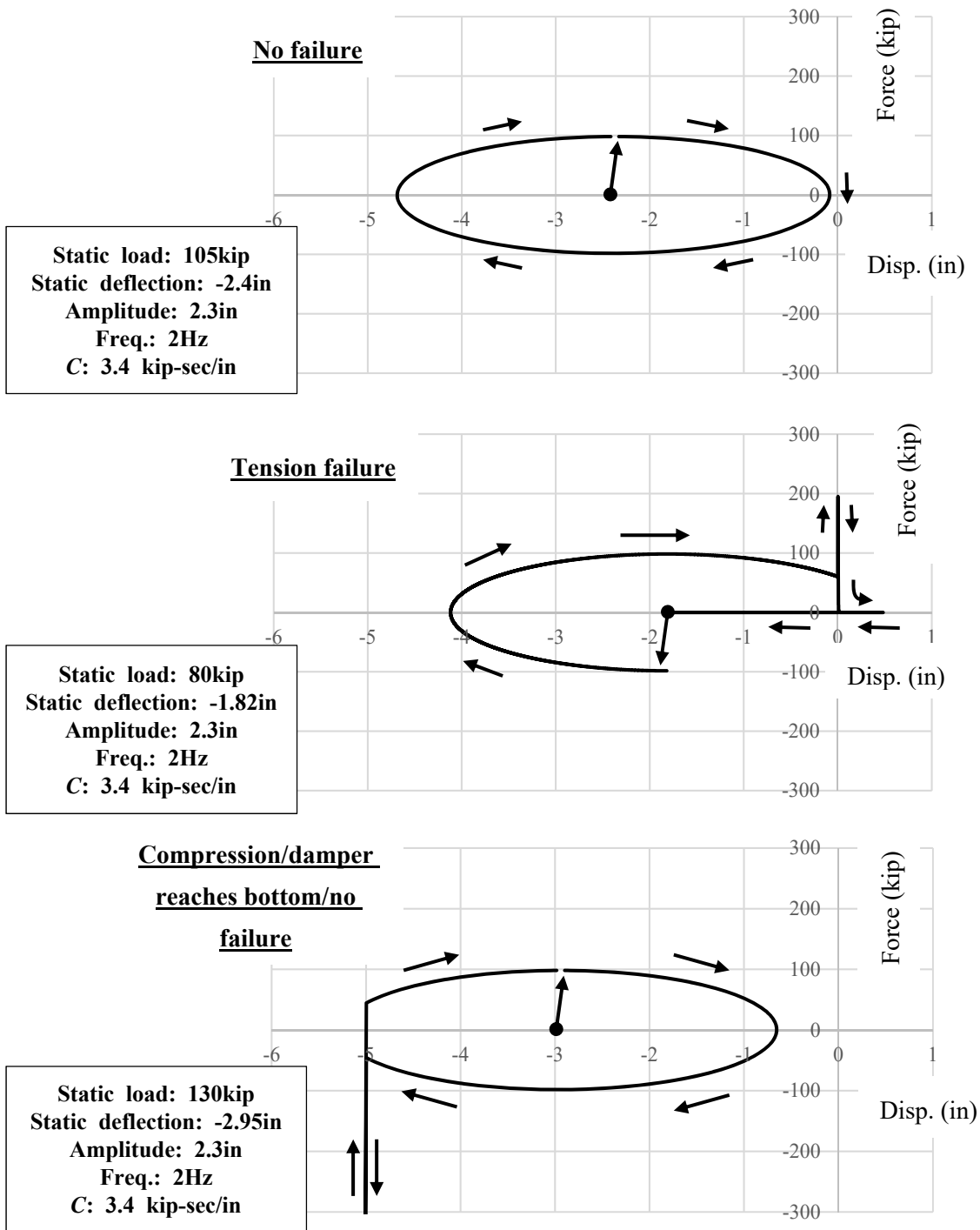


Figure 6-4 Force-Displacement Loops Produced by Damper Element

Figure 6-5 presents force-displacement loops produced by the combined spring-damper element for the three cases of loading of Figure 6-4. Note that in these figure the spring-damper units are assumed capable of transferring force in tension. When a triple FP isolator is placed on top of the

spring-damper unit, there is no transfer of tensile force so that the force-displacement loops are as shown in Figure 6-6.

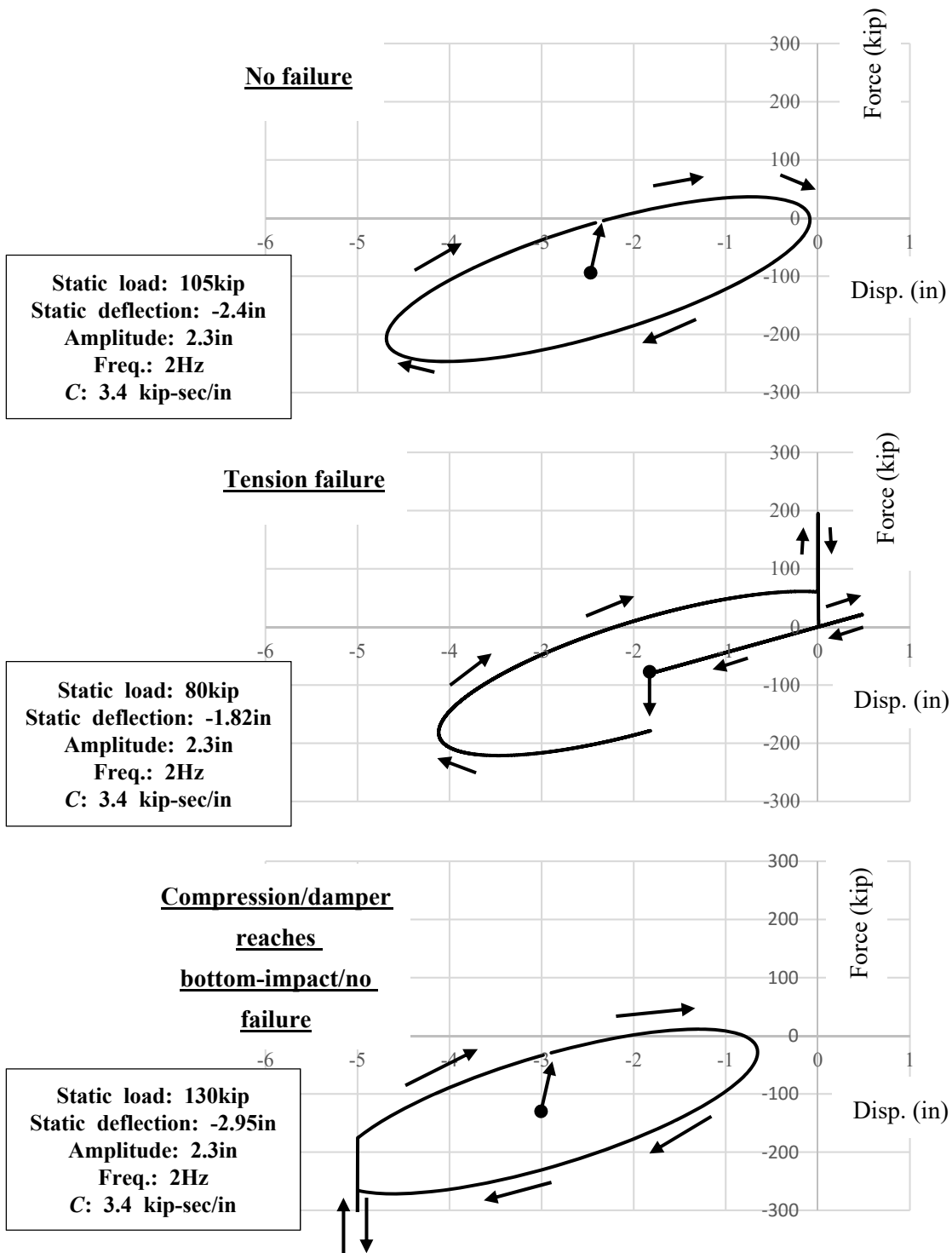


Figure 6-5 Force-Displacement Loops Produced by Combined Spring-Damper Element

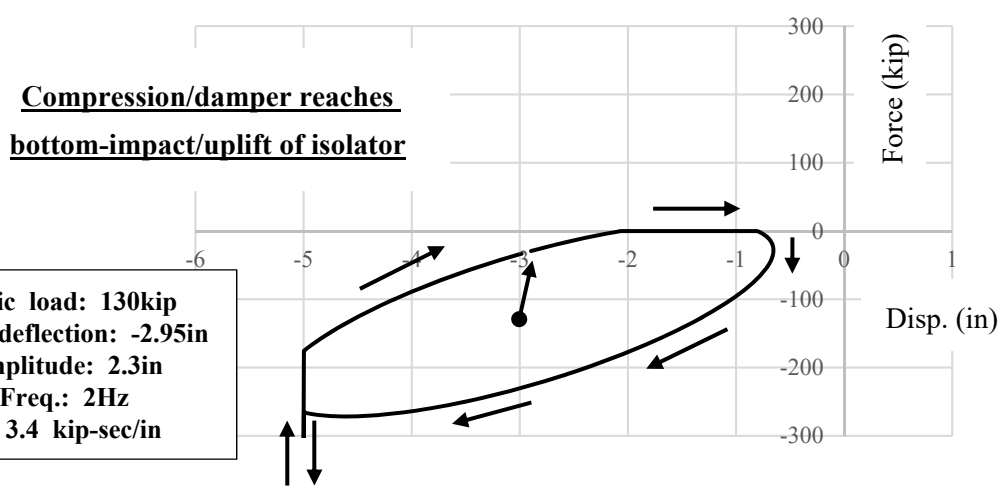
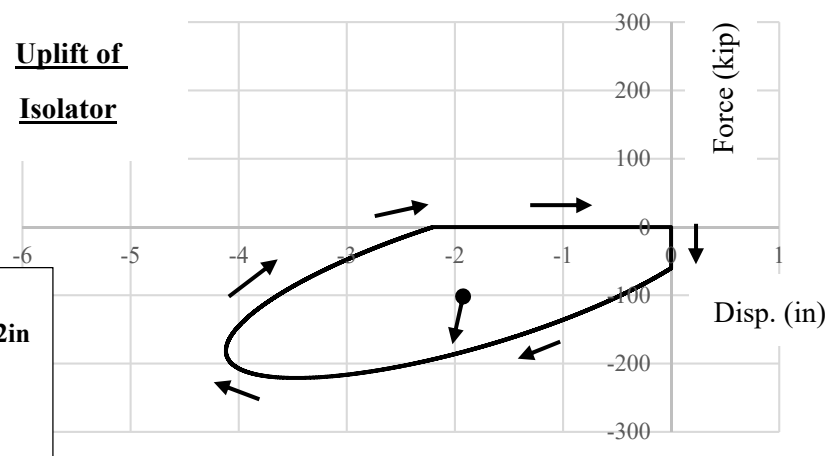
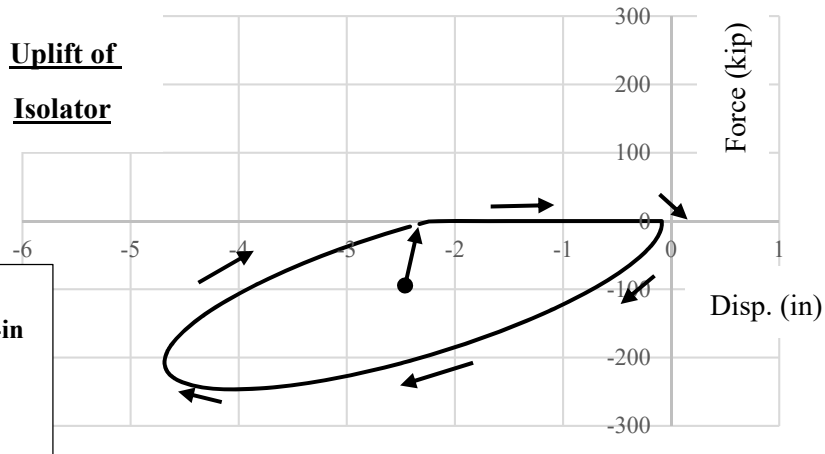


Figure 6-6 Force-Displacement Loops Produced by Combined Spring-Damper Element Supporting a Triple FP Isolator

SECTION 7

SELECTION AND SCALING OF GROUND MOTIONS

Failure resistance assessment requires performing Incremental Dynamic Analysis (Vamvatsikos and Cornell, 2002), which is used to assess the probability of failure for a particular set of motions per procedures of FEMA P695 (2009). While the procedures in FEMA P695 only include the horizontal components of ground motions, the analysis employed in this work requires that vertical components are also included. This is essential in assessing the performance of the combined horizontal-vertical isolation systems.

Far-field horizontal ground motions were selected from the suite of motions used in FEMA P695 (2009) and the corresponding vertical components were obtained from the PEER website (PEER, accessed 9th. Nov. 2015). The vertical components of two ground motion sets (Superstition Hills in Poe Road Station; and Cape Mendocino in Rio Dell Overpass Station) were not available. Accordingly, these two motions were removed from the suite and a total of 20 ground motion sets were used. These resulted in a total of 40 pairs of combined horizontal and vertical ground motion histories for use in the analysis (20 fault normal plus 20 fault parallel components, paired with the same 20 vertical components).

Table 7-1 presents information of ground motions used in this study. The magnitude of the motions is in the range of 6.5 to 7.6 with an average magnitude of 7.0. The table also shows the site class and the shear velocity for the site of each earthquake recording. The majority of the sites are class D. Figures 7-1 and 7-2 present the 5%-damped acceleration response spectra for the horizontal and vertical ground motions, respectively. The horizontal spectra consist of the 40 spectra of fault normal and fault parallel components, and the vertical spectra consist of the 20 spectra of the vertical components. The mean spectra are also shown for each direction.

Table 7-1 Ground Motions Used in Dynamic Analysis

PEER-NGA Record Number	Earthquake			Recording Station Name	Site Data	
	M	Year	Name		Site Class	Vs_30 (m/sec)
953	6.7	1994	Northridge	Beverly Hills - Mulhol	D	356
960	6.7	1994	Northridge	Canyon Country-WLC	D	309
1602	7.1	1999	Duzce, Turkey	Bolu	D	326
1787	7.1	1999	Hector Mine	Hector	C	685
169	6.5	1979	Imperial Valley	Delta	D	275
174	6.5	1979	Imperial Valley	El Centro Array #11	D	196
1111	6.9	1995	Kobe, Japan	Nishi-Akashi	C	609
1116	6.9	1995	Kobe, Japan	Shin-Osaka	D	256
1158	7.5	1999	Kocaeli, Turkey	Duzce	D	276
1148	7.5	1999	Kocaeli, Turkey	Arcelik	C	523
900	7.3	1992	Landers	Yermo Fire Station	D	354
848	7.3	1992	Landers	Coolwater	D	271
752	6.9	1989	Loma Prieta	Capitola	D	289
767	6.9	1989	Loma Prieta	Gilroy Array #3	D	350
1633	7.4	1990	Manjil, Iran	Abbar	C	724
721	6.5	1987	Superstition Hills	El Centro Imp. Co.	D	192
1244	7.6	1999	Chi-Chi, Taiwan	CHY101	D	259
1485	7.6	1999	Chi-Chi, Taiwan	TCU045	C	705
68	6.6	1971	San Fernando	LA - Hollywood Stor	D	316
125	6.5	1976	Friuli, Italy	Tolmezzo	C	425

Table 7-1 (Continued)

Earthquake Name	Recording Station Name	Values shown are in two horizontal directions, then vertical; units g, in/sec, inch		
		PGA	PGV	PGD
Northridge	Beverly Hills - Mulhol	0.42, 0.52, 0.32	23.2, 24.7, 8.0	5.2, 4.4, 1.1
Northridge	Canyon Country-WLC	0.41, 0.48, 0.30	16.9, 17.7, 7.3	4.6, 4.9, 2.1
Duzce, Turkey	Bolu	0.73, 0.82, 0.20	22.2, 24.4, 9.2	9.1, 5.3, 5.5
Hector Mine	Hector	0.27, 0.34, 0.15	11.2, 16.4, 4.7	8.9, 5.5, 3.0
Imperial Valley	Delta	0.24, 0.35, 0.14	10.2, 13.0, 6.0	4.7, 7.5, 3.6
Imperial Valley	El Centro Array #11	0.36, 0.38, 0.38	13.6, 16.6, 17.6	6.3, 7.3, 8.4
Kobe, Japan	Nishi-Akashi	0.51, 0.50, 0.39	14.7, 14.4, 9.7	3.8, 4.4, 2.0
Kobe, Japan	Shin-Osaka	0.24, 0.21, 0.06	14.9, 11.0, 2.4	3.4, 3.0, 0.7
Kocaeli, Turkey	Duzce	0.31, 0.36, 0.21	23.2, 18.3, 8.3	17.4, 6.9, 5.5
Kocaeli, Turkey	Arcelik	0.22, 0.15, 0.08	7.0, 15.6, 3.1	5.4, 14.0, 2.9
Landers	Yermo Fire Station	0.24, 0.15, 0.14	20.2, 11.7, 5.1	17.3, 9.7, 1.9
Landers	Coolwater	0.28, 0.42, 0.18	15.8, 26.0, 3.9	13.1, 13.2, 1.5
Loma Prieta	Capitola	0.53, 0.44, 0.56	13.8, 11.5, 7.4	3.6, 2.2, 1.0
Loma Prieta	Gilroy Array #3	0.56, 0.34, 0.34	14.0, 17.6, 17.9	3.3, 7.6, 9.5
Manjil, Iran	Abbar	0.51, 0.50, 0.54	16.7, 20.5, 16.7	5.9, 8.2, 10.3
Superstition Hills	El Centro Imp. Co.	0.36, 0.26, 0.13	18.3, 16.1, 3.2	6.9, 7.9, 1.9
Chi-Chi, Taiwan	CHY101	0.35, 0.44, 0.17	27.8, 45.3, 10.7	17.8, 27.1, 8.4
Chi-Chi, Taiwan	TCU045	0.47, 0.51, 0.36	14.4, 15.4, 8.1	20.0, 5.6, 8.3
San Fernando	LA - Hollywood Stor	0.21, 0.17, 0.16	7.4, 5.8, 2.0	4.9, 2.5, 1.6
Friuli, Italy	Tolmezzo	0.35, 0.31, 0.28	8.7, 12.1, 4.1	1.6, 2.0, 1.2

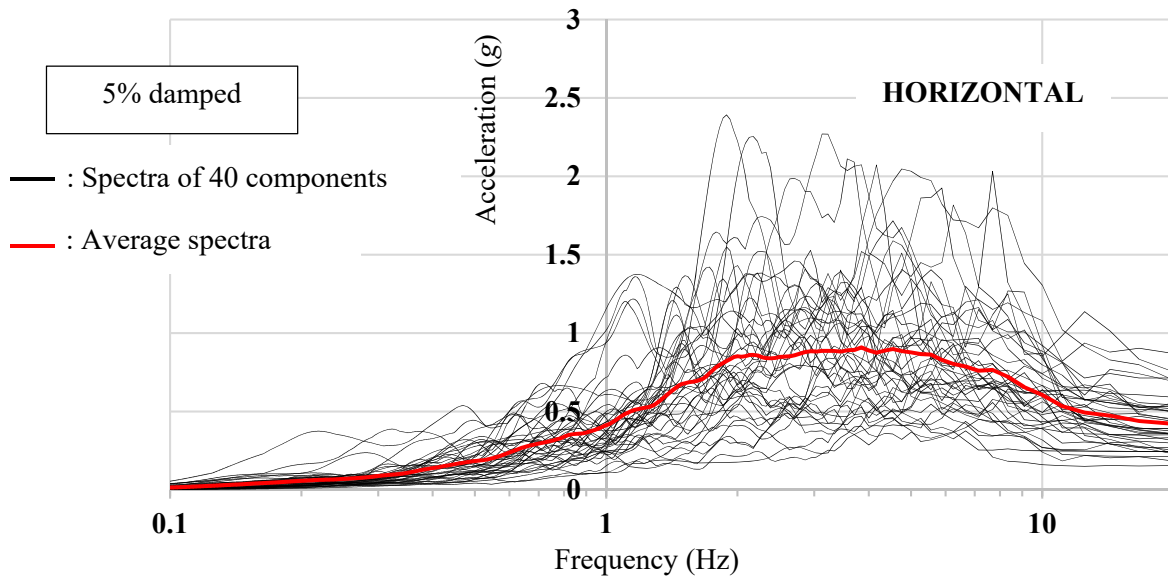


Figure 7-1 Horizontal Acceleration Response Spectra of Selected 20 Ground Motions (Total of 40 Components)

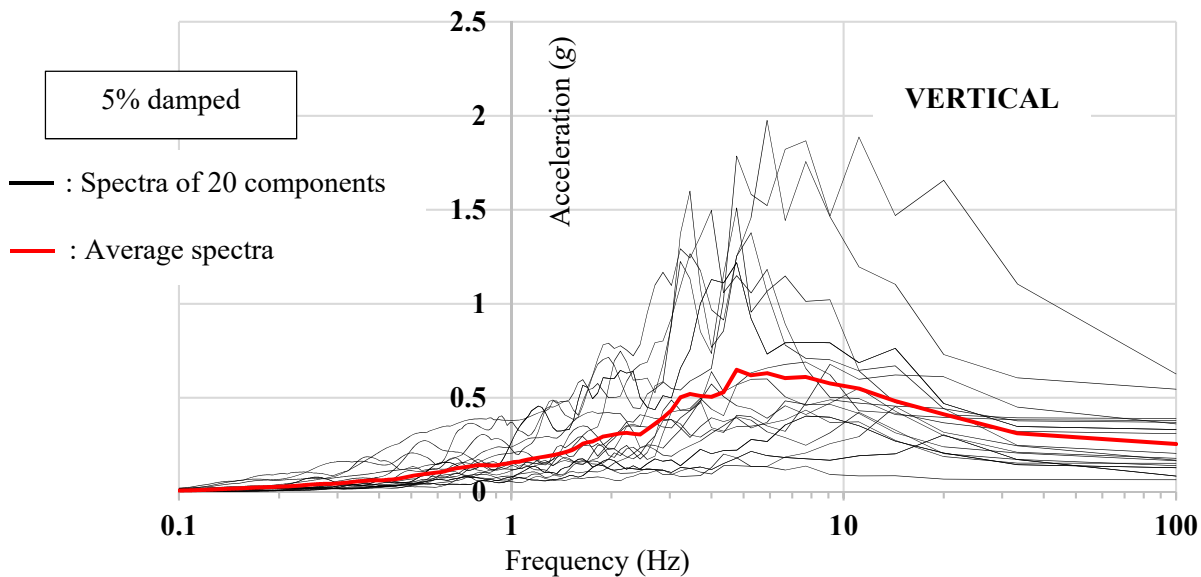


Figure 7-2 Vertical Acceleration Response Spectra of Selected 20 Ground Motions (Total of 20 Components)

Figure 7-3 presents the average ratio of the vertical to horizontal (geometric mean of two horizontal components) spectral acceleration of the selected 40 motions and compares it to one of the curves recommended in Bozorgnia and Campbell, 2004. Note that this ratio is dependent on the distance to the fault, the shear wave velocity of the soil and the source mechanism (Bozorgnia and Campbell, 2004; Bozorgnia and Campbell, 2016; Gulerce and Abrahamson, 2011). The graph is provided to demonstrate that the V/H ratio of the selected motions is appropriate.

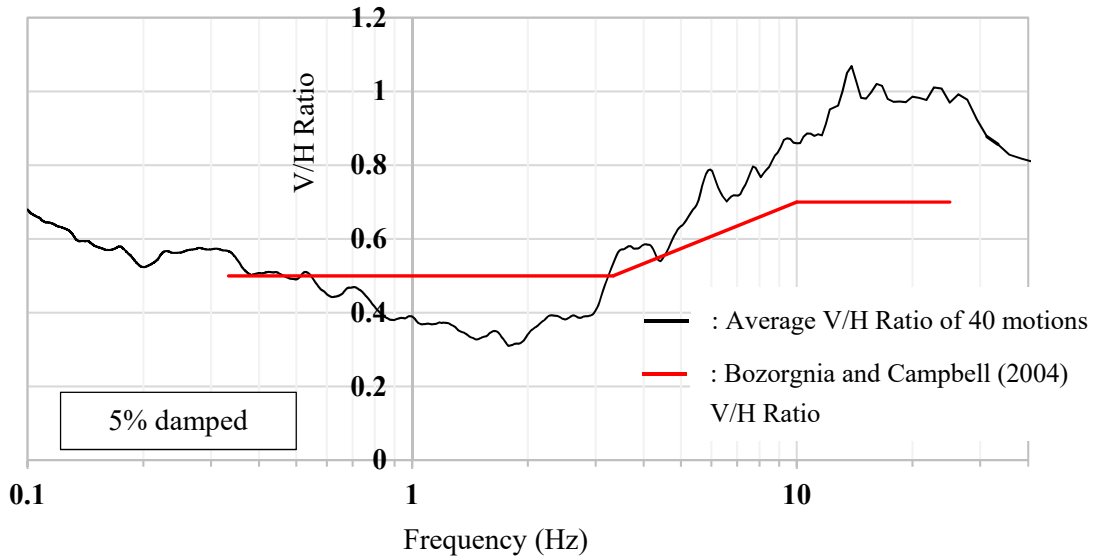


Figure 7-3 Average Vertical to Horizontal (V/H) Ratio of Spectral Accelerations of 40 Sets of Motions

Figure 7-4 compares the average spectra of the selected motions when scaled to a PGA of 0.5g in the horizontal direction and a PGA of 0.4g in the vertical direction to the IEEE high required response spectra (Figure 2-1). It may be seen that the horizontal average spectrum falls below the IEEE spectrum but has a wide frequency range consistent with the IEEE spectrum, whereas the vertical average spectrum deviates from the IEEE vertical spectrum. The average vertical spectrum correctly displays a narrower range and higher values of frequencies than the horizontal spectrum, which is not properly reflected in the IEEE spectrum. Figure 7-4 also includes the average spectra of the scaled motions so that the PGA is 0.6g rather than 0.5g (horizontal PGA is 0.6g, vertical GPA is 0.48g). The horizontal scaled motions now better represent the IEEE spectrum for frequencies larger than about 2Hz Thus, use of the results of the fragility studies in this report for a PGA of 0.6g may be an appropriate descriptor of behavior for the IEEE PGA 0.5g seismic motions.

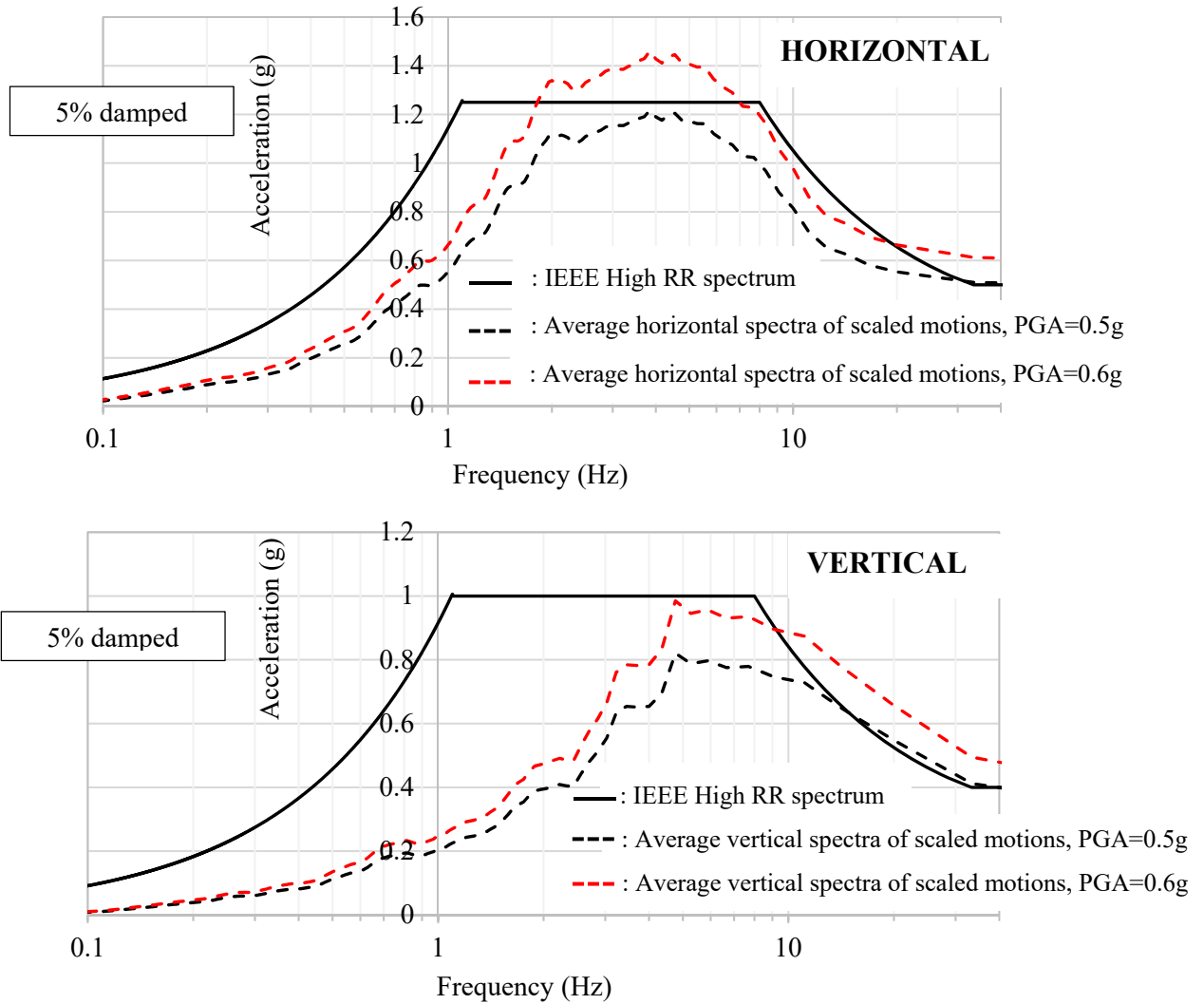


Figure 7-4 Comparison of Horizontal and Vertical Average Spectra to IEEE High Required Response Spectra

To conduct incremental dynamic analysis (IDA), the selected ground motions need to be progressively increased in intensity. The approach followed is to increase the acceleration of the horizontal component of each pair of horizontal-vertical motions while keeping the vertical to horizontal peak acceleration ratio the same as in the original, as-recorded, motion. The scaling approach for the horizontal component is similar to the S_a -Component Scaling approach in FEMA P695 (2009).

The scaled motions are used to repeatedly analyze the transformer model by increasing the intensity so that the peak acceleration of the horizontal component of each pair increases by increments of 0.05g until there is failure of either the bushings or the isolators. The vertical component of each pair of ground motions is increased by an amount different than 0.05g so that the final scaled pair maintains the peak vertical to peak horizontal acceleration ratio as in the originally recorded ground motion.

SECTION 8
FRAGILITY ANALYSIS RESULTS

Fragility analysis has been conducted and results are presented in terms of curves of probability of failure versus PGA for the cases in Table 8-1.

Table 8-1 Analyzed Cases of Non-Isolated and Isolated Transformers

Case	Parameters
Transformer (by weight in kip)	320; 420; 520
Bushing (by No. and frequency per Table 3-1)	7 ($f=2.57\text{Hz}$); 6 ($f=11.3\text{Hz}$); 8 ($f=7.7\text{Hz}$); 3 ($f=4.3\text{Hz}$)
Bushing Inclination (degrees)	0; 20
Bushing acceleration limit (g)	1 or 2g for transverse direction 5g for longitudinal direction
Isolation system type	Non-isolated; isolated in horizontal direction; isolated in horizontal-vertical direction without rocking; isolated in horizontal-vertical direction with rocking
Horizontal isolation system ultimate displacement capacity (inch)	17.7; 27.7; 31.3 (without inner restrainer) 17.0 (with inner restrainer)
Horizontal isolation system friction properties (per Table 4-1)	Lower bound; Upper bound
Vertical isolation system (vertical stiffness and damping constant per isolator, stroke)	$K=44\text{kip/in}$ $C=3.4\text{kip-s/in}$ Stroke 5in

Failure is defined when any of the following criteria is met, whichever occurs first:

- 1) The acceleration at the center of mass of the bushing in the longitudinal bushing direction exceeds 5g, or
- 2) The acceleration at the center of mass of the bushing in the direction perpendicular to the longitudinal bushing direction exceeds 1g or 2g (two different cases), or

- 3) The triple FP isolator horizontal displacement exceeds the ultimate capacity limit of 17.7, 27.7 and 31.3inch (three different cases), or
- 4) The net uplift FP isolator displacement exceeds 2inch, or
- 5) The analysis terminates due to numerical instability problems. (However, all analyses reported herein did not have any numerical instability problems).

The limit of 2-inch net uplift displacement is based on the geometry of the bearings shown in Figures 4-1 to 4-3. Any of these bearings can have a net uplift of up to 2inch without the possibility of collapse of its internal parts regardless of the position of the top concave plate. It is possible to have stable behavior for larger uplift but that is dependent on details of the motion that are difficult to analyze (Sarlis and Constantinou, 2013) and are highly dependent on the isolator and structural system properties and the details of the seismic excitation.

Note that there are no indirect failure criteria for the spring-damper units. Rather, when the displacement capacity of the spring-damper units is consumed in compression there is impact which is simulated and which in turn affects the bushing accelerations. Also, while the damper limited tension capacity is included in the model, and the damper may be removed from the model when considered failed, the option is never realized as the Triple FP isolator is incapable of developing tension and thus no tensile force is transferred to the damper.

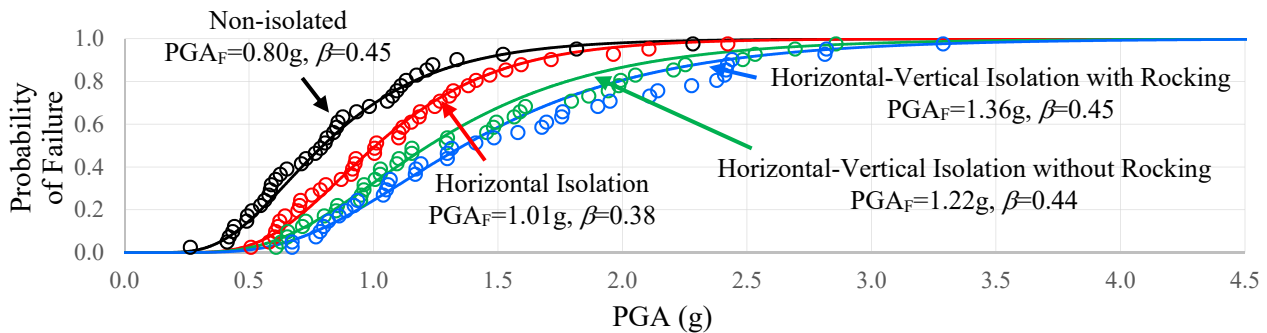
Analysis was conducted with the model that neglects the axial-shear force interaction.

Figure 8-1 presents fragility curves for the 420kip transformer with the 7.7Hz (No. 8) bushing inclined at 20 degrees and with the triple FP isolators having 17.7inch displacement capacity in the lower bound friction case and without an inner restrainer. To better understand the results in the fragility curves of Figure 8-1, Tables 8-2 and 8-3 have been prepared to present information on what mechanism causes failure in selected cases.

Specifically, Tables 8-2 and 8-3 present the number of failures attributed to bushing failure (transverse or longitudinal acceleration exceeding the specified limits), to the isolator horizontal displacement exceeding the ultimate limit or the vertical isolator failing in tension (also the number of cases where the vertical isolator reaches bottom and results in impact but no failure of the isolator) for four cases of PGA: the one in which the empirical probability of failure is 100% (40 failures), the one in which the empirical probability of failure is 50% (20 failures), the one in

which the empirical probability of failure is 25% (10 failures) and the one in which the empirical probability of failure is 10% (4 failures).

Inclined bushing, bushing lateral acceleration limit=2g, Isolator ultimate displacement=17.7inch, No inner restrainer, Lower bound friction



Inclined bushing, bushing lateral acceleration limit=1g, Isolator ultimate displacement=17.7inch, No inner restrainer, Lower bound friction

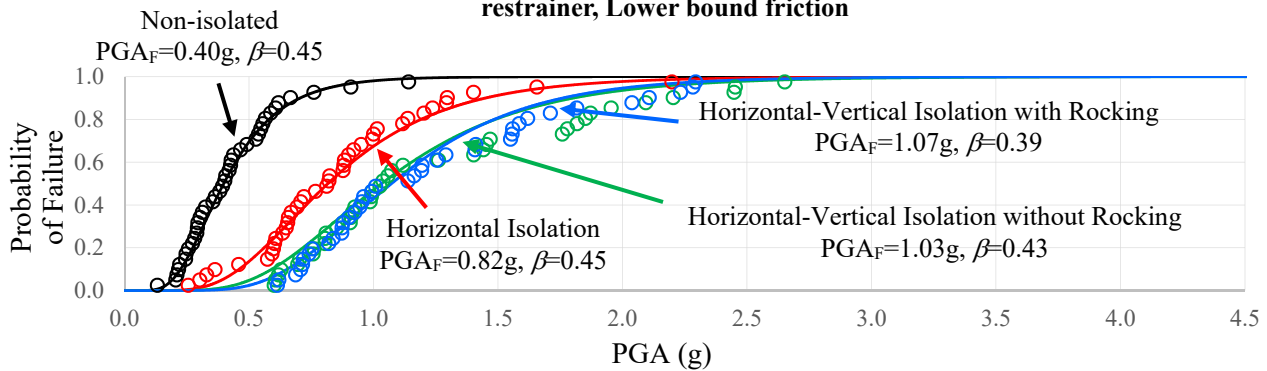


Figure 8-1 Fragility Curves for 420kip Transformer with 7.7Hz Bushing (No. 8) Inclined at 20 Degrees, Triple FP Bearings without Inner Restrainer, Lower Bound Friction Properties and Isolator Ultimate Displacement Capacity of 17.7inch

The results in Tables 8-2 and 8-3 and in Figure 8-1 demonstrate the following:

- 1) For all cases of analyzed transformers and for all levels of seismic intensity, failure due to exceeding the transverse bushing acceleration limit dominates when this limit is 1.0g. As the transverse bushing acceleration limit is increased to 2.0g, failures due to exceeding the bushing longitudinal acceleration limit (5.0g) begin to occur in the horizontally-only isolated transformers. This may appear as odd given that the horizontally-only isolated transformer behaves as non-isolated in the vertical direction. There is, however, a difference as the isolated transformer may experience uplift which

results in impact and increased acceleration in the longitudinal (nearly vertical) bushing direction.

- 2) For the combined horizontal-vertical isolation systems there are no failures due to exceeding the bushing longitudinal acceleration limit for all seismic intensities. Rather, failures are due to exceeding the bushing transverse acceleration limit for all cases when the bushing transverse acceleration limit is 1g. When the bushing transverse acceleration limit is 2g, most failures are due to exceeding the bushing transverse acceleration limit with a few failures due to exceeding the isolator horizontal displacement capacity when rocking is restrained and due to excessive isolator uplift displacement when rocking is allowed.

Table 8-2 Number of Failures for Case of 1g Transverse and 5g Longitudinal Bushing Acceleration Limits for 420kip Transformer with 7.7Hz Inclined Bushing (No. 8), Triple FP Bearings without Inner Restrainer, Lower Bound Friction Properties and Isolator Ultimate Displacement Capacity of 17.7inch

		Number of Ground Motions Causing Failure			
		Non-isolated	Horizontal Isolation	Horizontal-Vertical Isolation (without rocking)	Horizontal-Vertical Isolation (with rocking)
PGA (g) corresponding to 100% probability of failure		1.14	2.20	2.65	2.29
Bushing lateral acceleration exceeding 1g	Bushing – lateral direction acceleration-1g	40	40	40	40
	Bushing – Longitudinal direction acceleration-5g	0	0	0	0
Horizontal isolator displacement exceeding 17.7inch		-	0	0	0
Horizontal isolator net uplift displacement exceeding 2.0inch (exceeding 0 inch)		-	0 (18)	0 (27)	0 (14)
Vertical isolation system	Compression impact	-	-	0	0

		Number of Ground Motions Causing Failure			
		Non-isolated	Horizontal Isolation	Horizontal-Vertical Isolation (without rocking)	Horizontal-Vertical Isolation (with rocking)
PGA (g) corresponding to 50% probability of failure		0.40	0.82	1.03	1.07
Bushing lateral acceleration exceeding 1g	Bushing – lateral direction acceleration-1g	20	20	20	20
	Bushing – Longitudinal direction acceleration-5g	0	0	0	0
Horizontal isolator displacement exceeding 17.7inch		-	0	0	0
Horizontal isolator net uplift displacement exceeding 2.0inch (exceeding 0 inch)		-	0 (7)	0 (13)	0 (6)
Vertical isolation system	Compression impact	-	-	0	0

Table 8-2 Continued

		Number of Ground Motions Causing Failure			
		Non-isolated	Horizontal Isolation	Horizontal-Vertical Isolation (without rocking)	Horizontal-Vertical Isolation (with rocking)
PGA (g) corresponding to 25% probability of failure		0.28	0.61	0.81	0.84
Bushing lateral acceleration exceeding 1g	Bushing – lateral direction acceleration-1g	10	10	10	10
	Bushing – Longitudinal direction acceleration-5g	0	0	0	0
Horizontal isolator displacement exceeding 17.7inch		-	0	0	0
Horizontal isolator net uplift displacement exceeding 2.0inch (exceeding 0 inch)		-	0 (3)	0 (8)	0 (5)
Vertical isolation system	Compression impact	-	-	0	0

		Number of Ground Motions Causing Failure			
		Non-isolated	Horizontal Isolation	Horizontal-Vertical Isolation (without rocking)	Horizontal-Vertical Isolation (with rocking)
PGA (g) corresponding to 10% probability of failure		0.22	0.36	0.63	0.71
Bushing lateral acceleration exceeding 1g	Bushing – lateral direction acceleration-1g	4	4	4	4
	Bushing – Longitudinal direction acceleration-5g	0	0	0	0
Horizontal isolator displacement exceeding 17.7inch		-	0	0	0
Horizontal isolator net uplift displacement exceeding 2.0inch (exceeding 0 inch)		-	0 (1)	0 (4)	0 (1)
Vertical isolation system	Compression impact	-	-	0	0

Table 8-3 Number of Failures for Case of 2g Transverse and 5g Longitudinal Bushing Acceleration Limits for 420kip Transformer with 7.7Hz Inclined Bushing (No. 8), Triple FP Bearings without Inner Restrainer, Lower Bound Friction Properties and Isolator Ultimate Displacement Capacity of 17.7inch

		Number of Ground Motions Causing Failure			
		Non-isolated	Horizontal Isolation	Horizontal-Vertical Isolation (without rocking)	Horizontal-Vertical Isolation (with rocking)
PGA (g) corresponding to 100% probability of failure		2.28	2.42	2.86	3.29
Bushings lateral acceleration exceeding 2g	Bushing – lateral direction acceleration-2g	40	27	37	33
	Bushing – Longitudinal direction acceleration-5g	0	13	0	0
Horizontal isolator displacement exceeding 17.7inch		-	0	3	0
Horizontal isolator net uplift displacement exceeding 2.0inch (exceeding 0 inch)		-	0 (33)	0 (40)	7 (35)
Vertical isolation system	Compression impact	-	-	0	14

		Number of Ground Motions Causing Failure			
		Non-isolated	Horizontal Isolation	Horizontal-Vertical Isolation (without rocking)	Horizontal-Vertical Isolation (with rocking)
PGA (g) corresponding to 50% probability of failure		0.80	1.01	1.22	1.36
Bushings lateral acceleration exceeding 2g	Bushing – lateral direction acceleration-2g	20	14	18	16
	Bushing – Longitudinal direction acceleration-5g	0	6	0	0
Horizontal isolator displacement exceeding 17.7inch		-	0	2	0
Horizontal isolator net uplift displacement exceeding 2.0inch (exceeding 0 inch)		-	0 (16)	0 (20)	4 (17)
Vertical isolation system	Compression impact	-	-	0	7

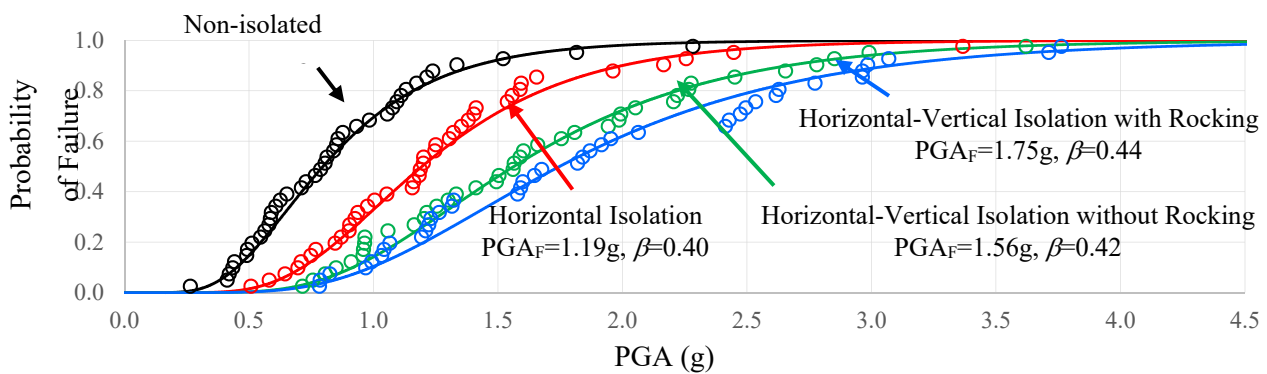
Table 8-3 Continued

		Number of Ground Motions Causing Failure			
		Non-isolated	Horizontal Isolation	Horizontal-Vertical Isolation (without rocking)	Horizontal-Vertical Isolation (with rocking)
PGA (g) corresponding to 25% probability of failure		0.56	0.71	0.95	0.94
Bushings lateral acceleration exceeding 2g	Bushing – lateral direction acceleration-2g	10	8	9	7
	Bushing – Longitudinal direction acceleration-5g	0	2	0	0
Horizontal isolator displacement exceeding 17.7inch		-	0	1	0
Horizontal isolator net uplift displacement exceeding 2.0inch (exceeding 0 inch)		-	0 (7)	0 (10)	3 (8)
Vertical isolation system	Compression impact	-	-	0	2

		Number of Ground Motions Causing Failure			
		Non-isolated	Horizontal Isolation	Horizontal-Vertical Isolation (without rocking)	Horizontal-Vertical Isolation (with rocking)
PGA (g) corresponding to 10% probability of failure		0.43	0.61	0.66	0.79
Bushings lateral acceleration exceeding 2g	Bushing – lateral direction acceleration-2g	4	3	4	2
	Bushing – Longitudinal direction acceleration-5g	0	1	0	0
Horizontal isolator displacement exceeding 17.7inch		-	0	0	0
Horizontal isolator net uplift displacement exceeding 2.0inch (exceeding 0 inch)		-	0 (4)	0 (4)	2 (3)
Vertical isolation system	Compression impact	-	-	0	1

The effect of increasing the displacement capacity of the FP isolators is seen in the fragility curves of Figures 8-2 and 8-3. It is evident that increasing the isolator displacement capacity has some improvement in the probability of failure for the case of the horizontal-only isolated transformer when the bushing transverse acceleration limit is 2g but not in the case of the limit of 1g. The reason is that failures for the low acceleration limit occur in the bushing prior to consuming the displacement capacity of the isolators. The effect of the increased FP isolator displacement capacity in reducing the probability of failure for the combined horizontal-vertical isolation system of either the restrained or the free to rock type is much more pronounced. The reason is that some failures for the combined horizontal-vertical isolation systems are due to excessive isolator displacement or uplift. Note that uplift typically occurred when the displacement capacity was consumed and the outer isolator ring was impacted.

Inclined bushing, bushing lateral acceleration limit=2g, Isolator ultimate displacement=27.7inch, No inner restrainer, Lower bound friction



Inclined bushing, bushing lateral acceleration limit=1g, Isolator ultimate displacement=27.7inch, No inner restrainer, Lower bound friction

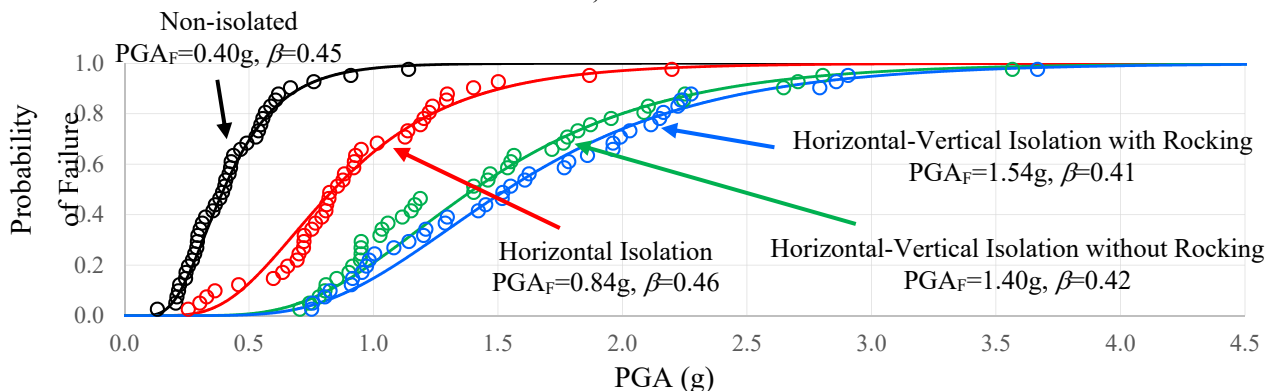
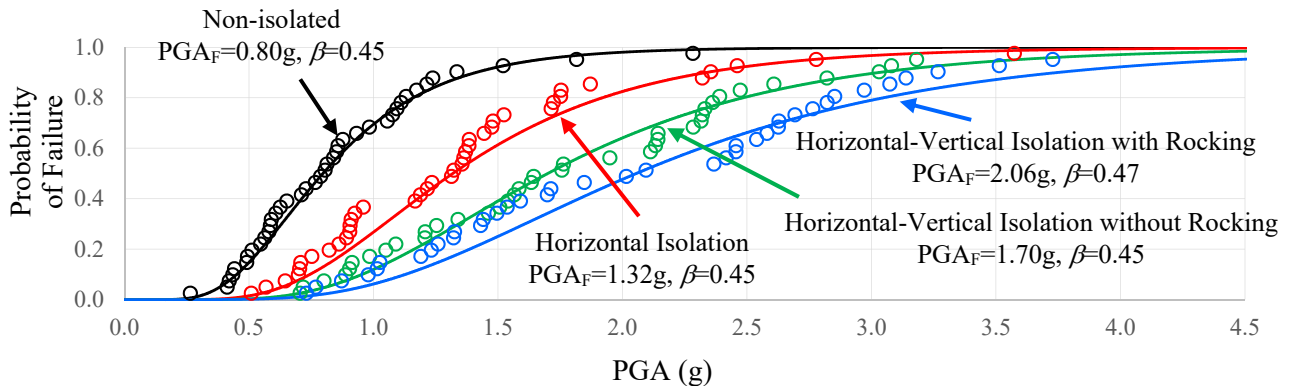


Figure 8-2 Fragility Curves for 420kip Transformer with 7.7Hz Bushing (No. 8) Inclined at 20 Degrees, Triple FP Bearings without Inner Restrainer, Lower Bound Friction Properties and Isolator Ultimate Displacement Capacity of 27.7inch

Inclined bushing, bushing lateral acceleration limit=2g, Isolator ultimate displacement=31.3inch, No inner restrainer, Lower bound friction



Inclined bushing, bushing lateral acceleration limit=1g, Isolator ultimate displacement=31.3inch, No inner restrainer, Lower bound friction

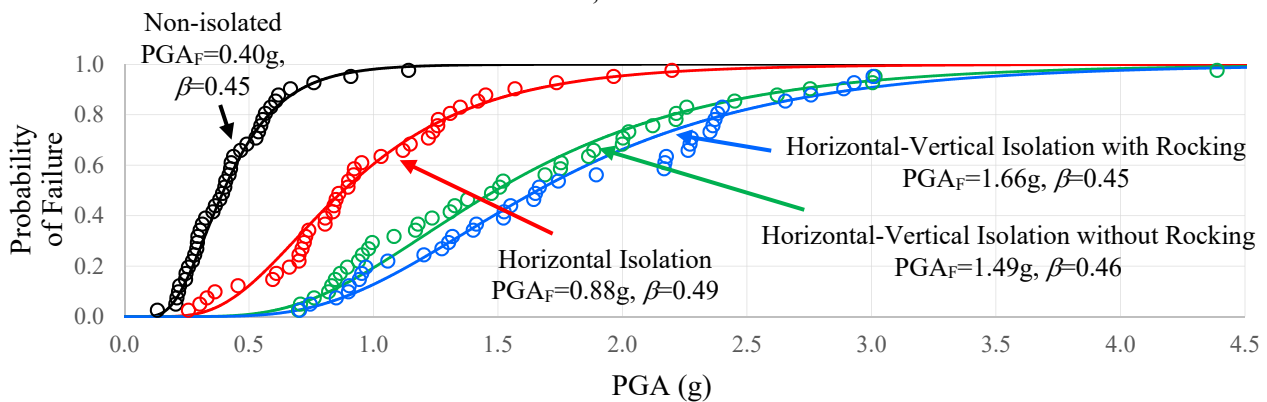
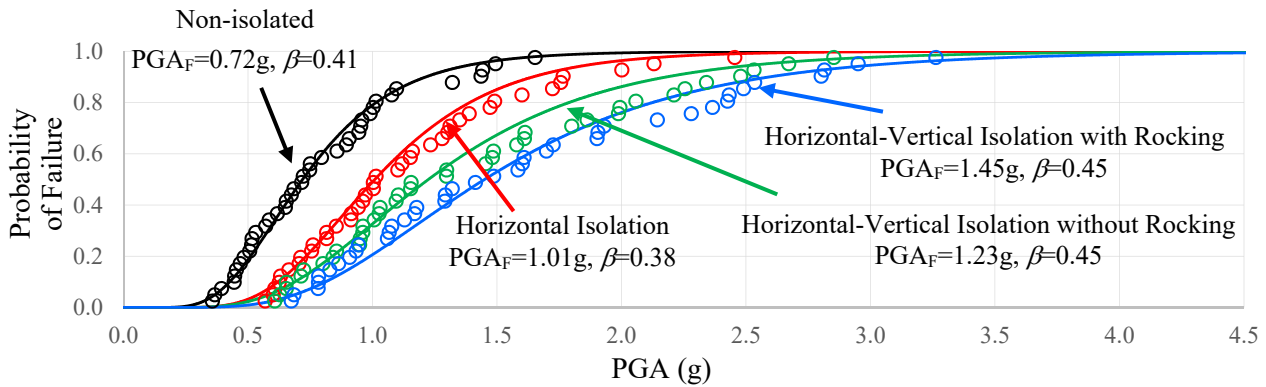


Figure 8-3 Fragility Curves for 420kip Transformer with 7.7Hz Bushing (No. 8) Inclined at 20 Degrees, Triple FP Bearings without Inner Restrainer, Lower Bound Friction Properties and Isolator Ultimate Displacement Capacity of 31.3inch

Figures 8-4 to 8-6 present fragility curves for the same systems as those for which fragility curves are shown in Figures 8-1 to 8-3 but for the bushings that are vertically placed instead of inclined at 20 degrees. Evidently, there are small differences between the two cases, apparently due to the small angle of inclination, with the exception of the horizontal-only isolated transformer when the transverse acceleration limit is 1g. Then there is a noted reduction in the probability of failure when the bushing is vertical particularly for the two cases of large displacement capacity isolators (27.7 and 31.3inch). This is likely due to a small contribution of the vertical component of the earthquake in magnifying the transverse acceleration of inclined bushings. This is more pronounced in the horizontal-only isolated transformer due to the lack of vertical isolation that mitigates the vertical earthquake effect.

Vertical bushing, bushing lateral acceleration limit=2g, Isolator ultimate displacement=17.7inch, No inner restrainer, Lower bound friction



Vertical bushing, bushing lateral acceleration limit=1g, Isolator ultimate displacement=17.7inch, No inner restrainer, Lower bound friction

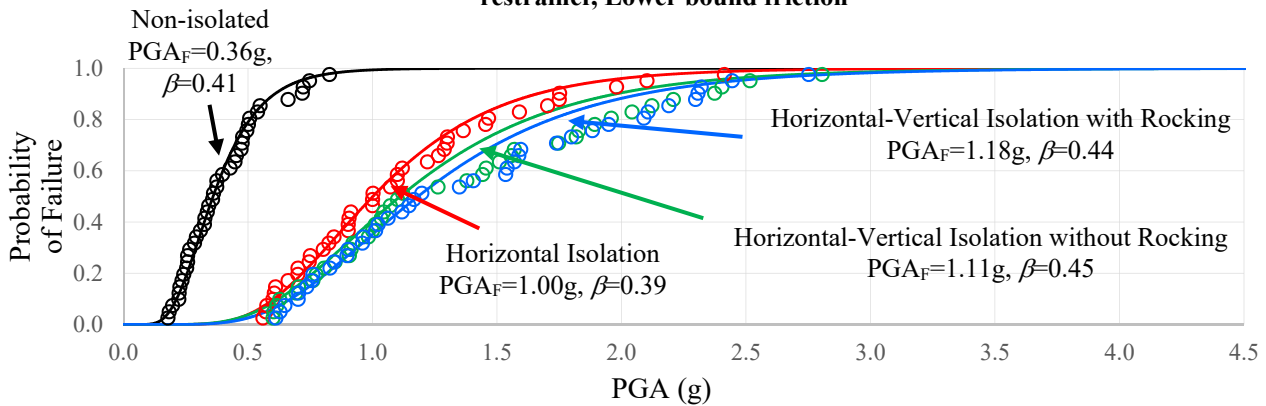
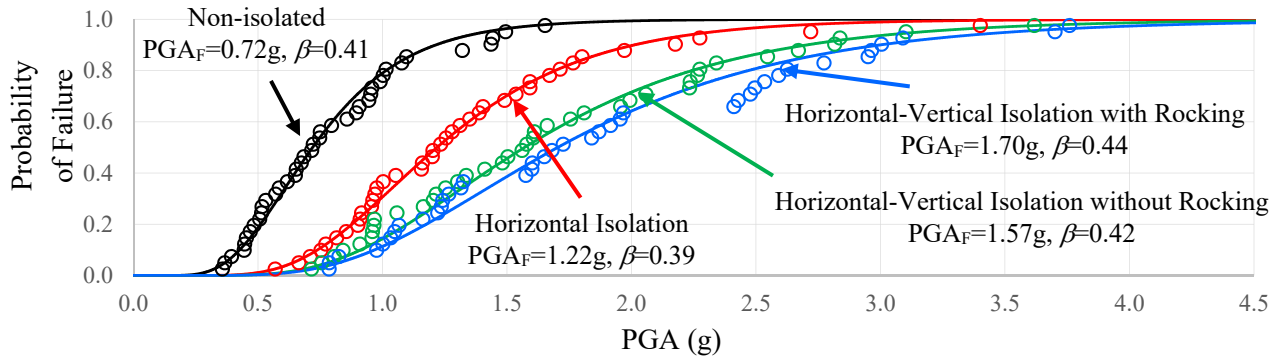


Figure 8-4 Fragility Curves for 420kip Transformer with Vertically Placed 7.7Hz Bushing (No. 8), Triple FP Bearings without Inner Restrainer, Lower Bound Friction Properties and Isolator Ultimate Displacement Capacity of 17.7inch

Vertical bushing, bushing lateral acceleration limit=2g, Isolator ultimate displacement=27.7inch, No inner restrainer, Lower bound friction



Vertical bushing, bushing lateral acceleration limit=1g, Isolator ultimate displacement=27.7inch, No inner restrainer, Lower bound friction

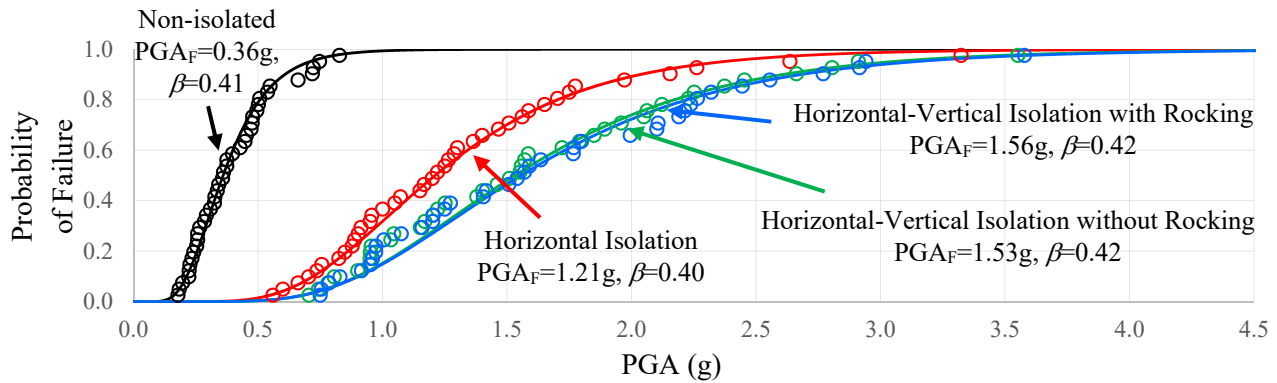
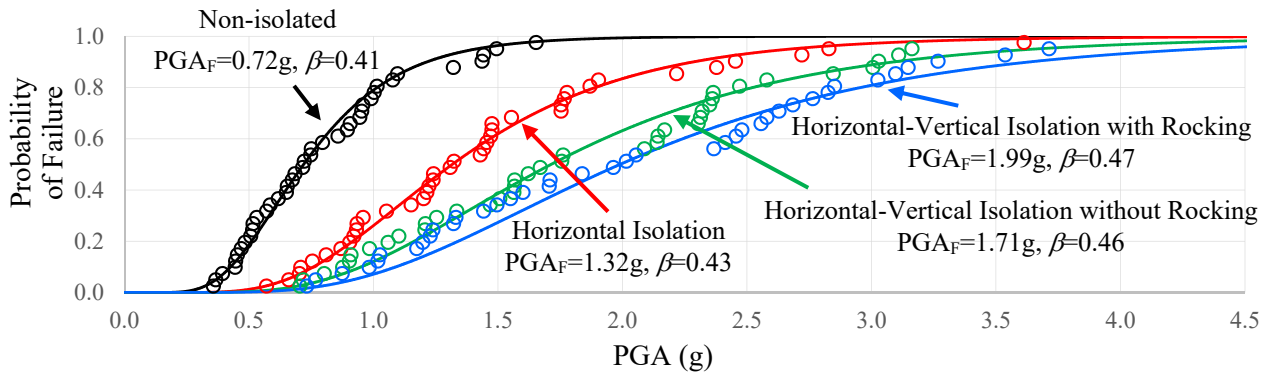


Figure 8-5 Fragility Curves for 420kip Transformer with Vertically Placed 7.7Hz Bushing (No. 8), Triple FP Bearings without Inner Restrainer, Lower Bound Friction Properties and Isolator Ultimate Displacement Capacity of 27.7inch

Vertical bushing, bushing lateral acceleration limit=2g, Isolator ultimate displacement=31.3inch, No inner restrainer, Lower bound friction



Vertical bushing, bushing lateral acceleration limit=1g, Isolator ultimate displacement=31.3inch, No inner restrainer, Lower bound friction

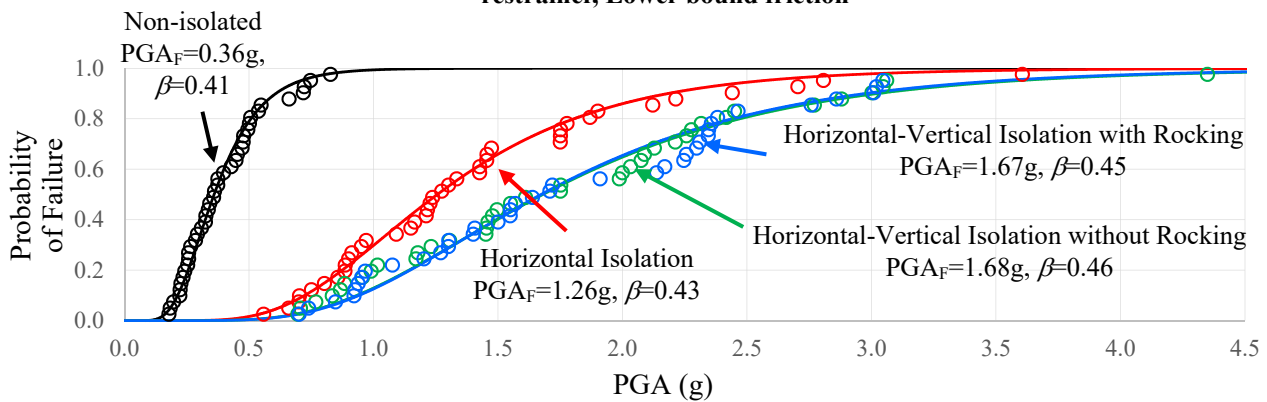


Figure 8-6 Fragility Curves for 420kip Transformer with Vertically Placed 7.7Hz Bushing (No. 8), Triple FP Bearings without Inner Restrainer, Lower Bound Friction Properties and Isolator Ultimate Displacement Capacity of 31.3inch

The effect of the transformer weight is investigated in Figure 8-7 which presents fragility curves for the transformers of 320, 420 and 520kip weight in the case of the inclined bushing of 7.7Hz frequency and bushing lateral acceleration limit of 1g. For the isolated cases, the triple FP isolators have the lower bound friction properties and the least displacement capacity of 17.7inch. Evidently, there is insignificant effect of the transformer weight within the range of 320 to 520kip on the probability of failure for all levels of seismic intensity.

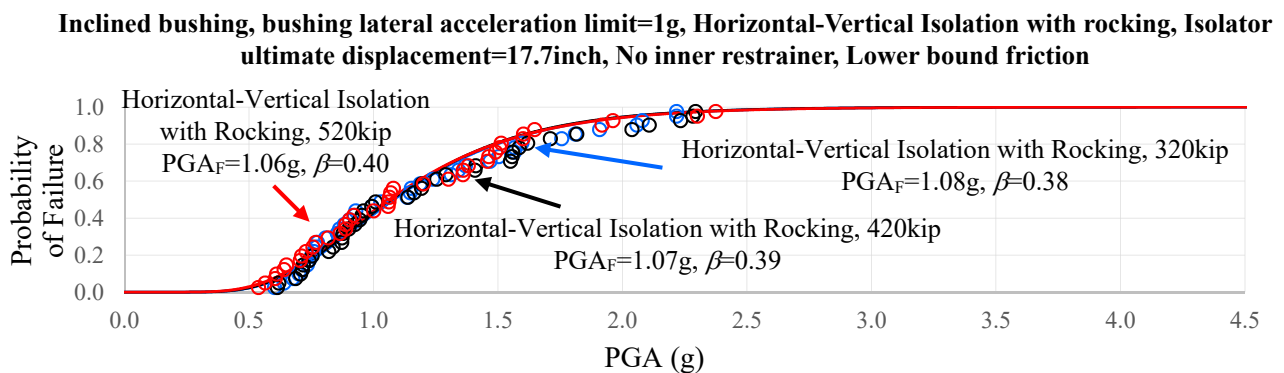
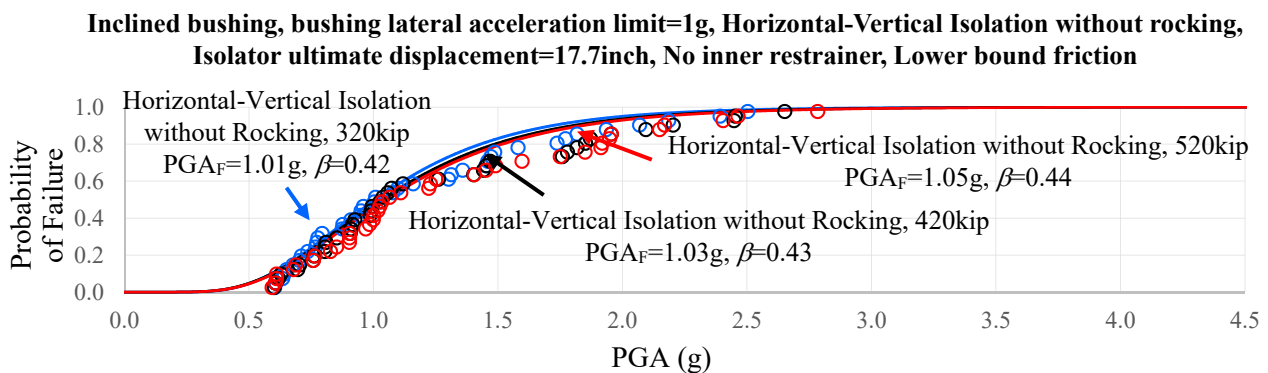
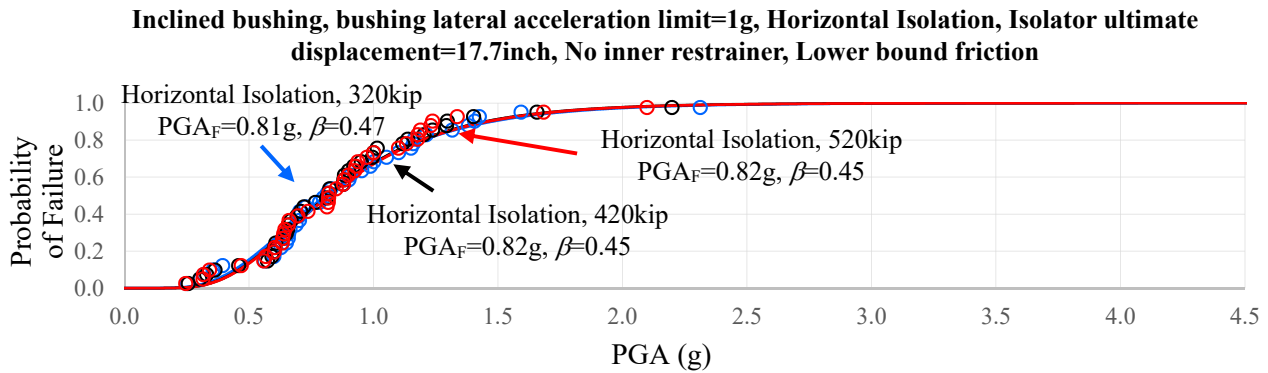
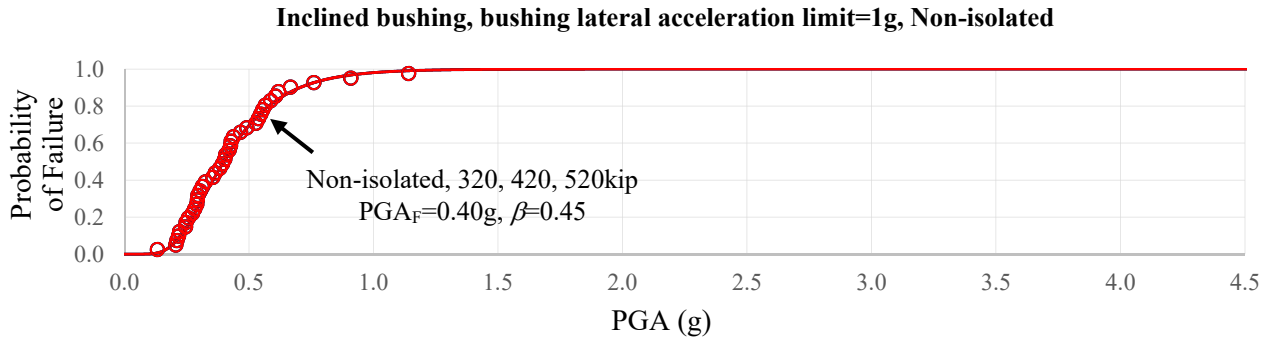


Figure 8-7 Fragility Curves for 320, 420, 520kip Transformer with 7.7Hz Bushing (No. 8) Inclined at 20 Degrees, Triple FP Bearings without Inner Restrainer, Lower Bound Friction Properties and Isolator Ultimate Displacement Capacity of 17.7inch, Bushing Lateral Acceleration limit=1g

The effect of the bushing as-installed frequency is demonstrated in the results of Figures 8-8 and 8-9 where fragility curves for four cases of bushings are presented. The four bushings are inclined at 20 degrees and have frequencies of 2.6, 4.3, 7.7 and 11.3Hz (No. 7, 3, 8 and 6, respectively, in Table 3-1). The bushing lateral acceleration limit is either 1g or 2g. When the transformer is isolated, the isolators have the lower bound frictional properties and their displacement capacity is 17.7inch. The effect of the bushing frequency is significant for the non-isolated transformer. For the isolated transformer, the bushing frequency has minor effects except for the case of the lower frequency bushings (2.6 and 4.3Hz) for the horizontal-vertical isolation system with rocking and when the bushing transverse acceleration limit is 1g. This is due to magnification of the bushing response as a result of the proximity of the bushing as-installed frequency to the frequency of rocking of the transformer (range of 2.4 to 2.8Hz). As discussed in Section 3, the case of the 2.6Hz bushing is atypical. Nevertheless, the case may be considered as an upper case of what is possible, although highly unlikely to have such a case of bushing implemented in a new transformer.

Figure 8-10 presents fragility curves of the 420kip transformer when upper and lower bound properties of the isolators are considered. The bushing is inclined, has 7.7Hz frequency and its lateral acceleration limit is 1g. The isolation system displacement capacity is 17.7inch. Consideration the two bounds of frictional properties has an insignificant effect on the probability of failure.

The effect of the displacement capacity of the FP isolators is presented in the fragility curves of Figures 8-11 and 8-12 constructed for the 420kip transformer with an inclined bushing of 7.7Hz frequency and transverse acceleration limit of either 2g or 1g. The displacement capacity of the isolators is in the range of 17.7inch to 31.3inch. All isolators lack an inner restrainer ring and friction has the lower bound values. Note that the results are the same as those in Figures 8-1 to 8-3 but presented in a different way to directly compare the isolator displacement capacity effect. As discussed earlier, increasing the isolator displacement capacity has some improvement in the probability of failure for the case of the horizontal-only isolated transformer when the bushing transverse acceleration limit is 2g but not in the case of the limit of 1g. Also, increasing the isolator displacement capacity has a much more pronounced effect in reducing the probability of failure for the combined horizontal-vertical isolation system of either the restrained or the free to rock type.

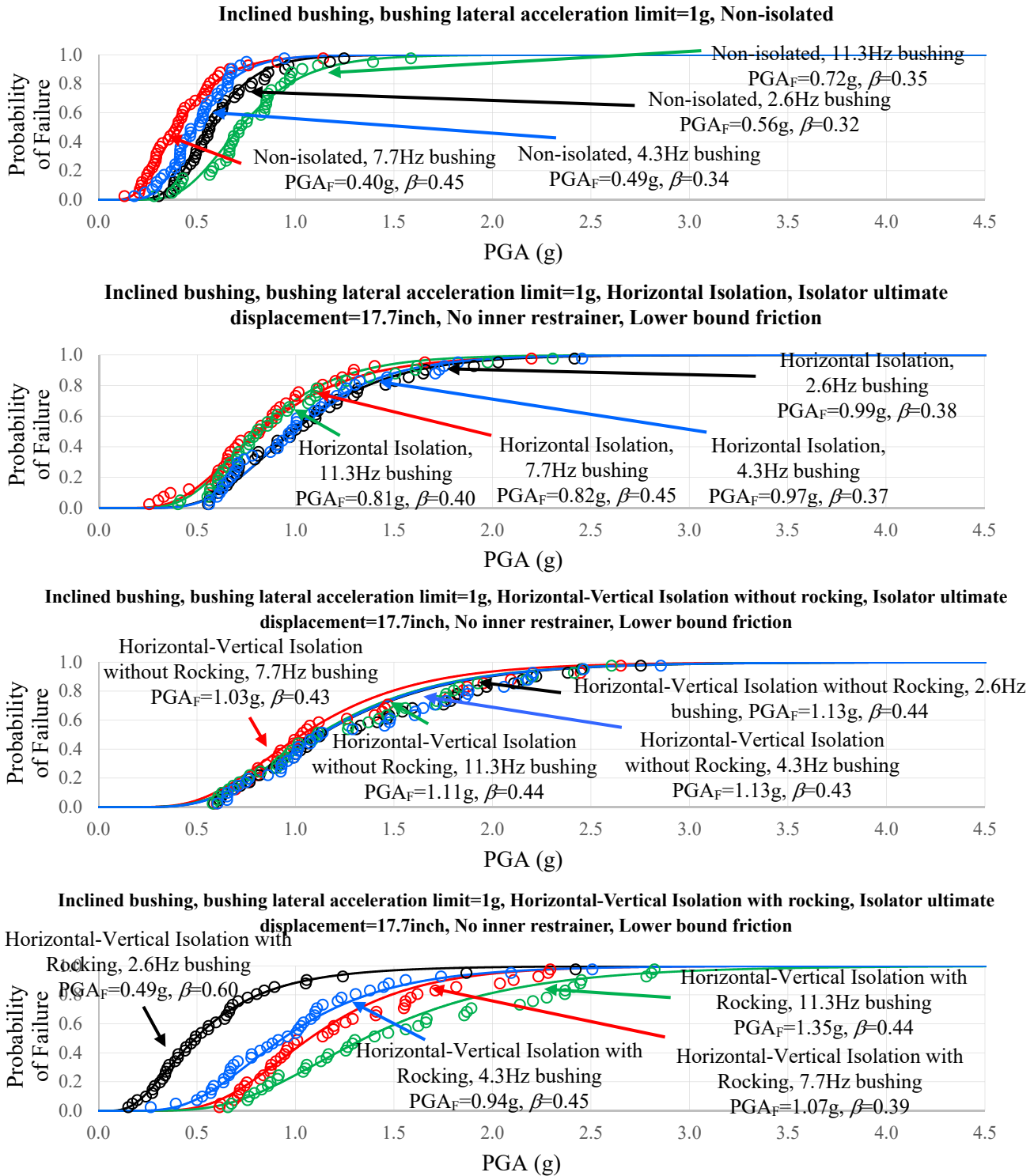


Figure 8-8 Fragility Curves for 420kip Transformer with 2.6Hz, 4.3Hz, 7.7Hz and 11.3Hz Bushings (No. 7, 3, 8 and 6) Inclined at 20 Degrees, Triple FP Bearings without Inner Restrainer, Lower Bound Friction Properties and Isolator Ultimate Displacement Capacity of 17.7inch, Bushing Lateral Acceleration Limit=1g

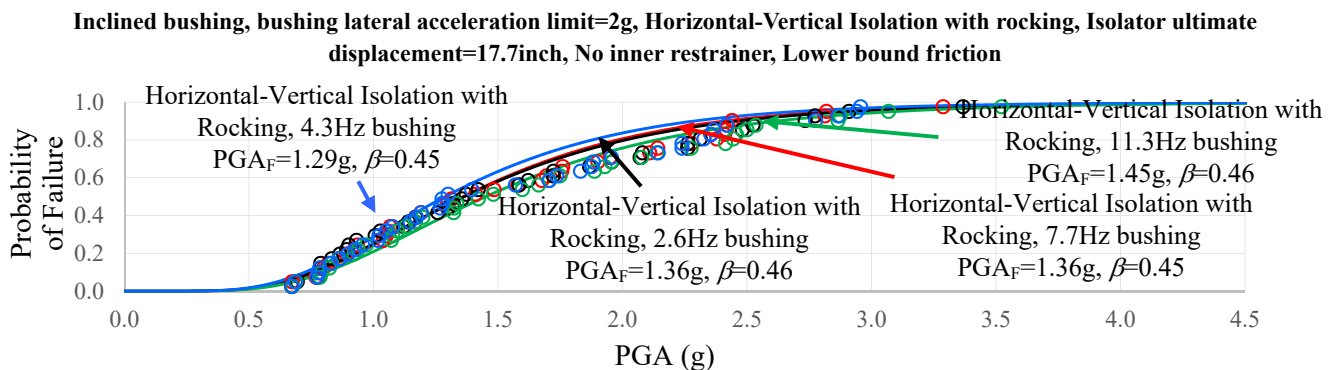
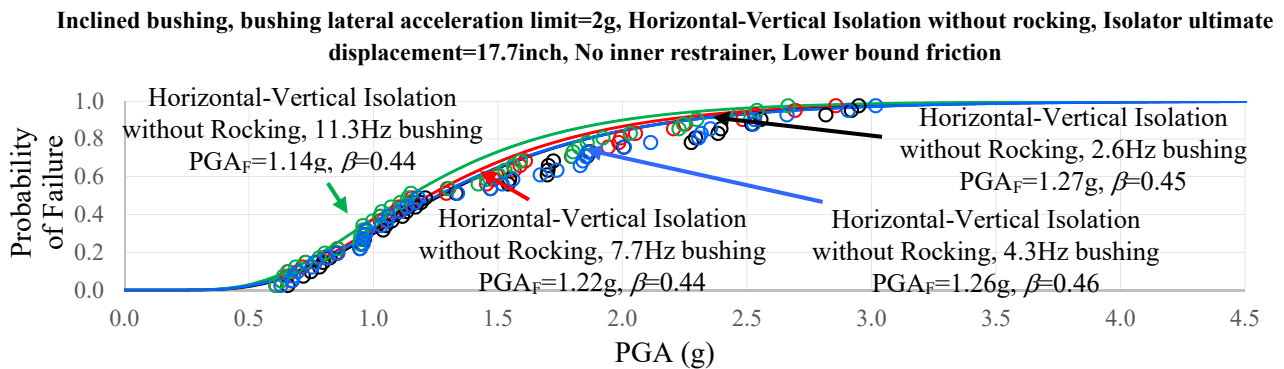
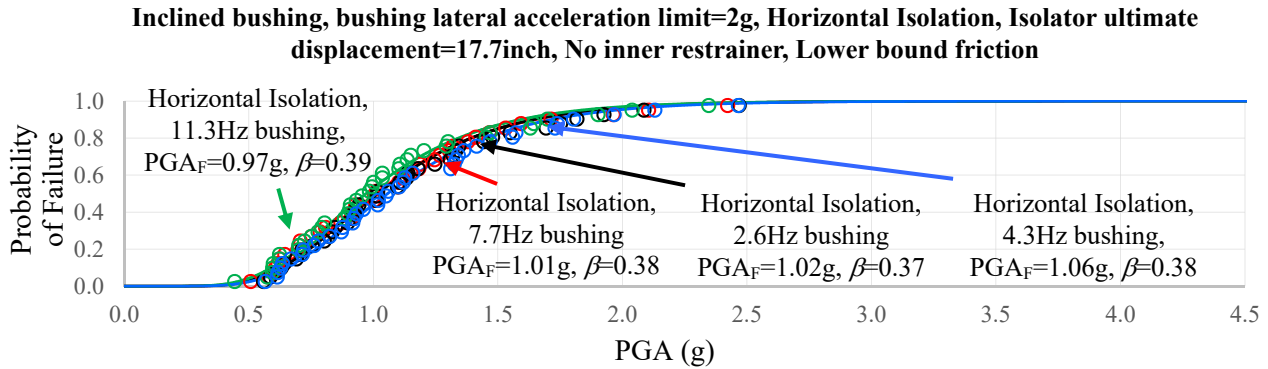
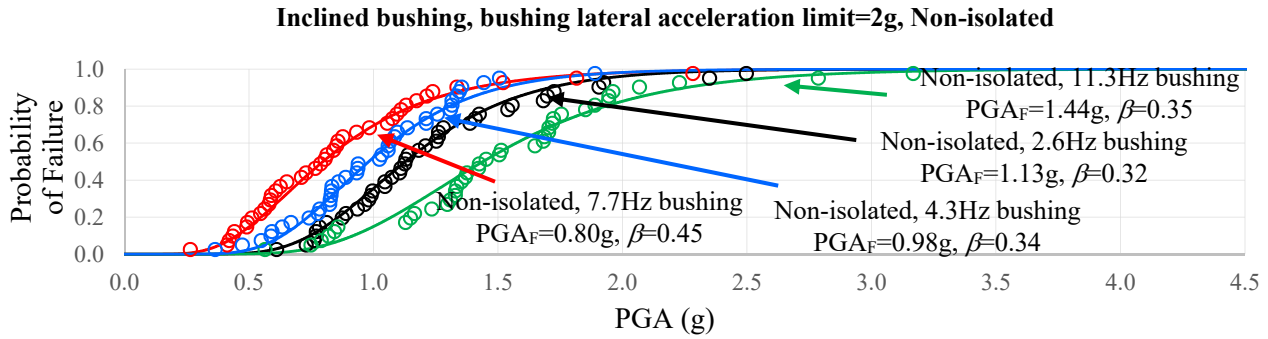
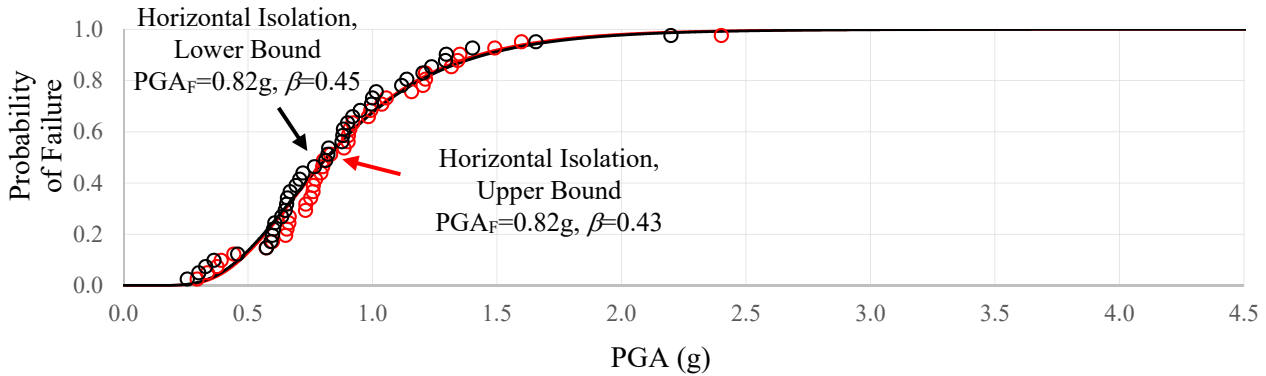
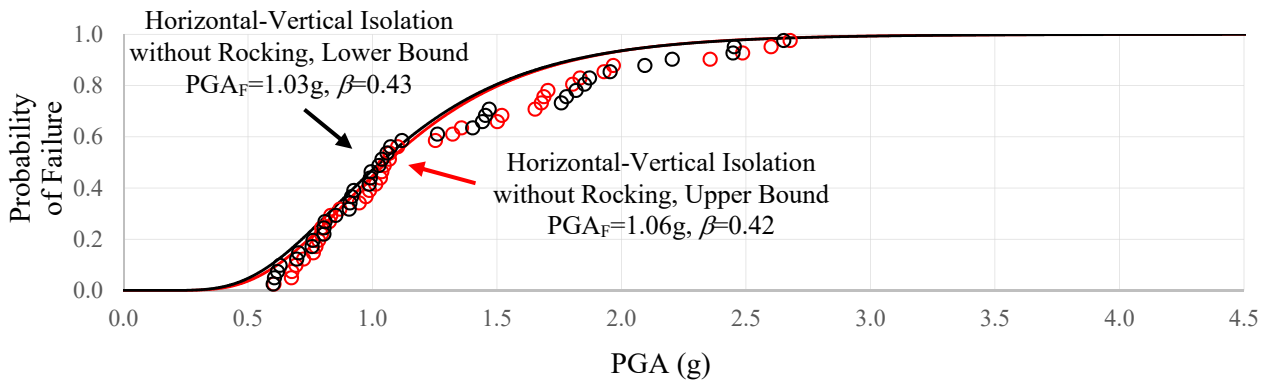


Figure 8-9 Fragility Curves for 420kip Transformer with 2.6Hz, 4.3Hz, 7.7Hz and 11.3Hz Bushings (No. 7, 3, 8 and 6) Inclined at 20 Degrees, Triple FP Bearings without Inner Restrainer, Lower Bound Friction Properties and Isolator Ultimate Displacement Capacity of 17.7inch, Bushing Lateral Acceleration Limit=2g

Inclined bushing, bushing lateral acceleration limit=1g, Horizontal Isolation, Isolator ultimate displacement=17.7inch, No inner restrainer, Lower and Upper bound friction



Inclined bushing, bushing lateral acceleration limit=1g, Horizontal-Vertical Isolation without rocking, Isolator ultimate displacement=17.7inch, No inner restrainer, Lower and Upper bound friction



Inclined bushing, bushing lateral acceleration limit=1g, Horizontal-Vertical Isolation with rocking, Isolator ultimate displacement=17.7inch, No inner restrainer, Lower and Upper bound friction

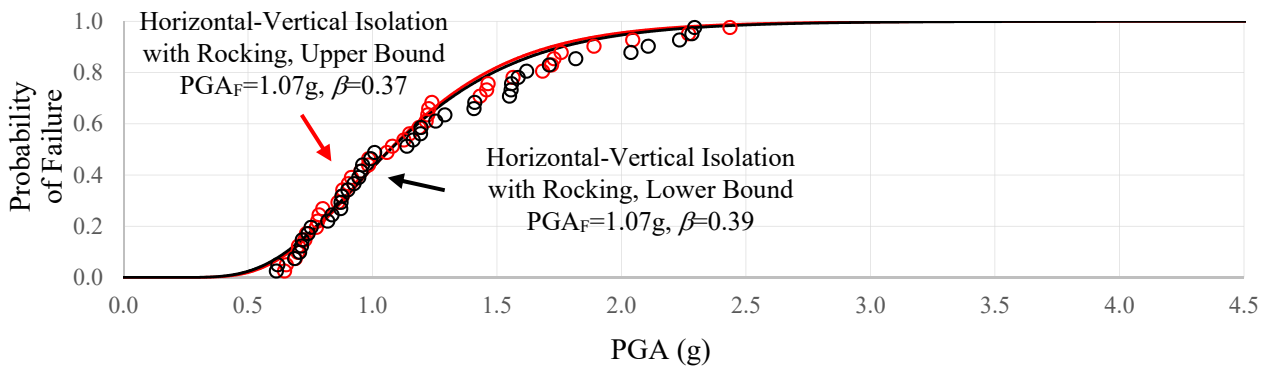
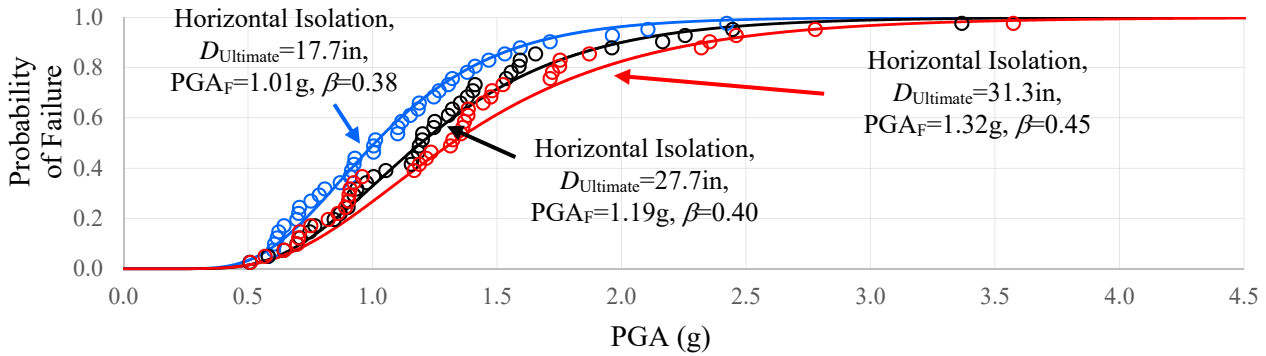
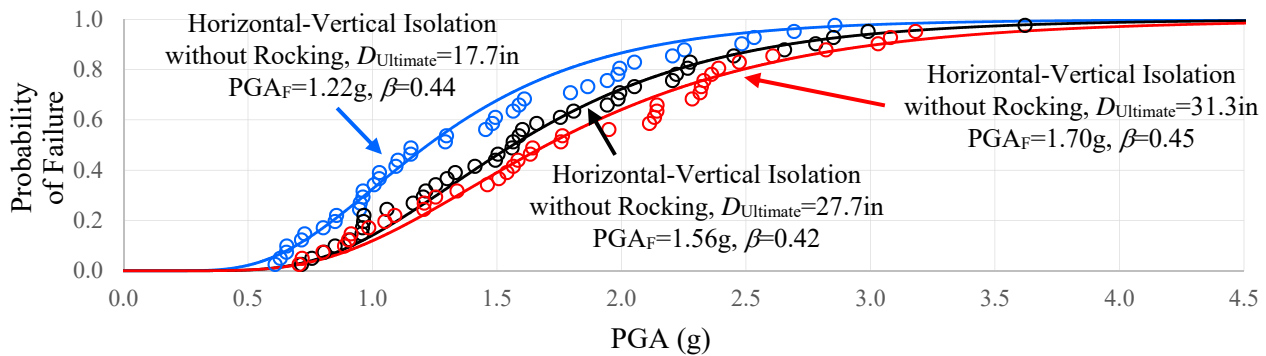


Figure 8-10 Fragility Curves for 420kip Transformer with 7.7Hz Bushing (No. 8) Inclined at 20 Degrees, Triple FP Bearings without Inner Restrainer, Lower and Upper Bound Friction Properties and Isolator Ultimate Displacement Capacity of 17.7inch, Bushing Lateral Acceleration Limit=1g

Inclined bushing, bushing lateral acceleration limit=2g, Horizontal Isolation, Isolator ultimate displacement of 17.7, 27.7 or 31.3inch, No inner restrainer, Lower bound friction



Inclined bushing, bushing lateral acceleration limit=2g, Horizontal-Vertical Isolation without rocking, Isolator ultimate displacement of 17.7, 27.7 or 31.3inch, No inner restrainer, Lower bound friction



Inclined bushing, bushing lateral acceleration limit=2g, Horizontal-Vertical Isolation with rocking, Isolator ultimate displacement of 17.7, 27.7 or 31.3inch, No inner restrainer, Lower bound friction

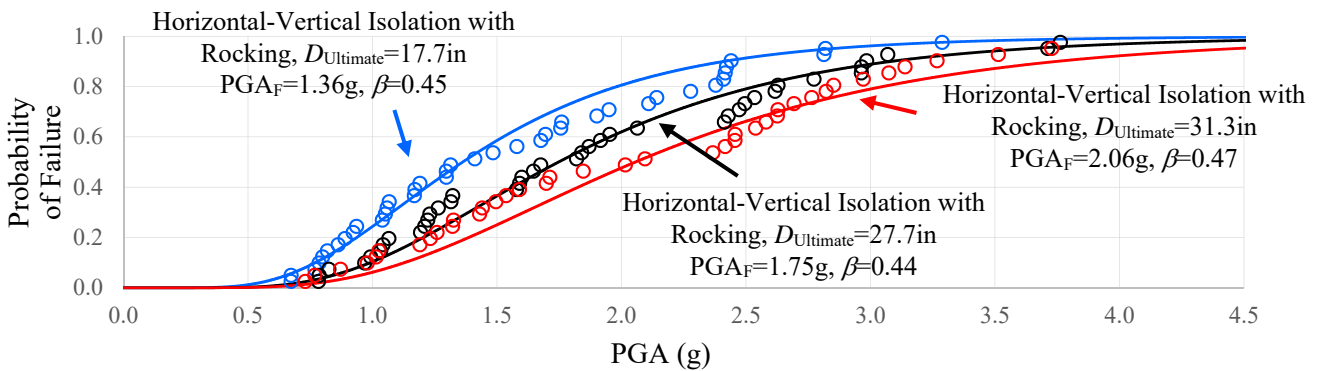
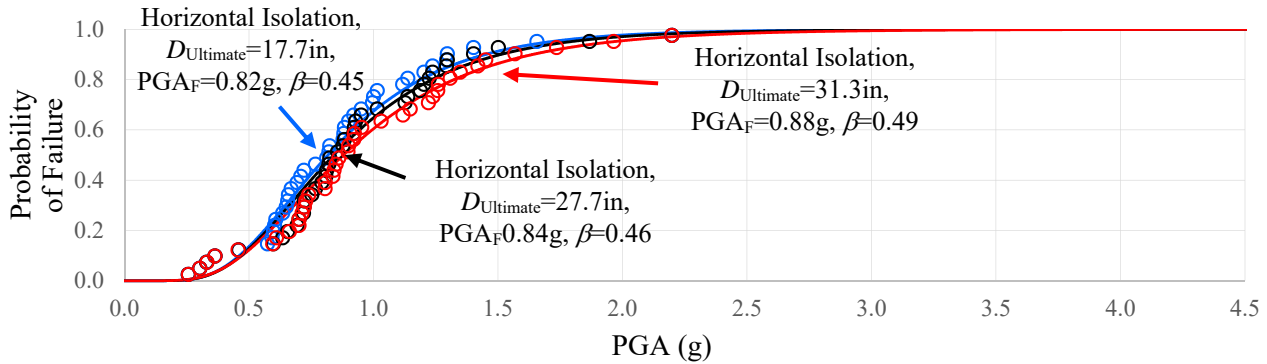
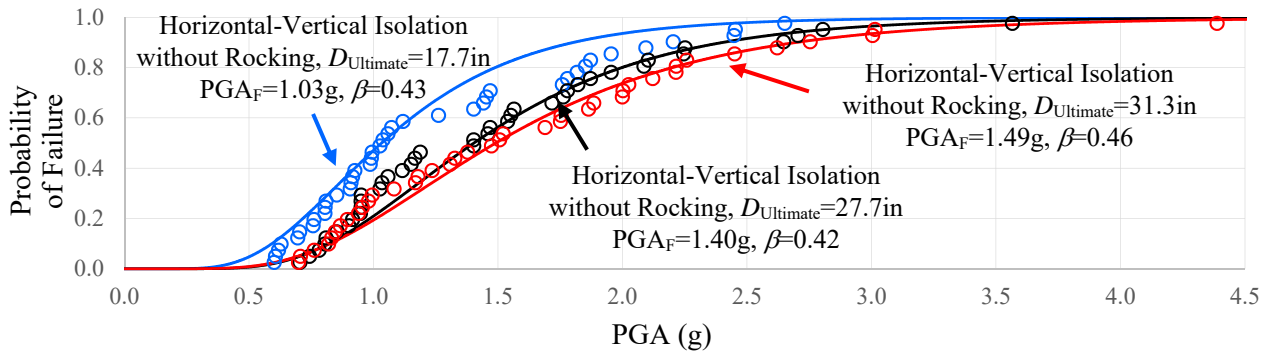


Figure 8-11 Fragility Curves, for 420kip Transformer with 7.7Hz Bushing (No. 8) Inclined at 20 Degrees, Triple FP Bearings without Inner Restrainer, Lower Bound Friction Properties and Isolator Ultimate Displacement Capacity of 17.7, 27.7 or 31.3inch, Bushing Lateral Acceleration Limit=2g

Inclined bushing, bushing lateral acceleration limit=1g, Horizontal Isolation, Isolator ultimate displacement 17.7, 27.7 or 31.3inch, No inner restrainer, Lower bound friction



Inclined bushing, bushing lateral acceleration limit=1g, Horizontal-Vertical Isolation without rocking, Isolator ultimate displacement of 17.7, 27.7 or 31.3inch, No inner restrainer, Lower bound friction



Inclined bushing, bushing lateral acceleration limit=1g, Horizontal-Vertical Isolation with rocking, Isolator ultimate displacement 17.7, 27.7 or 31.3inch, No inner restrainer, Lower bound friction

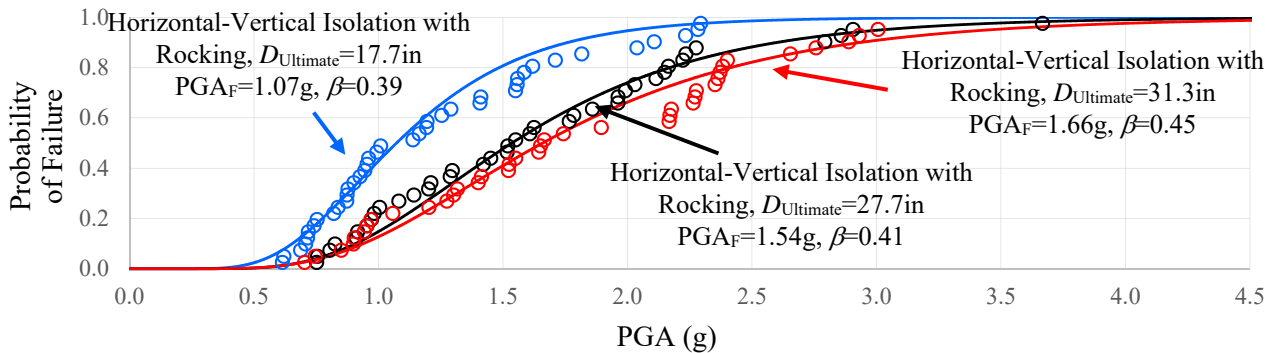
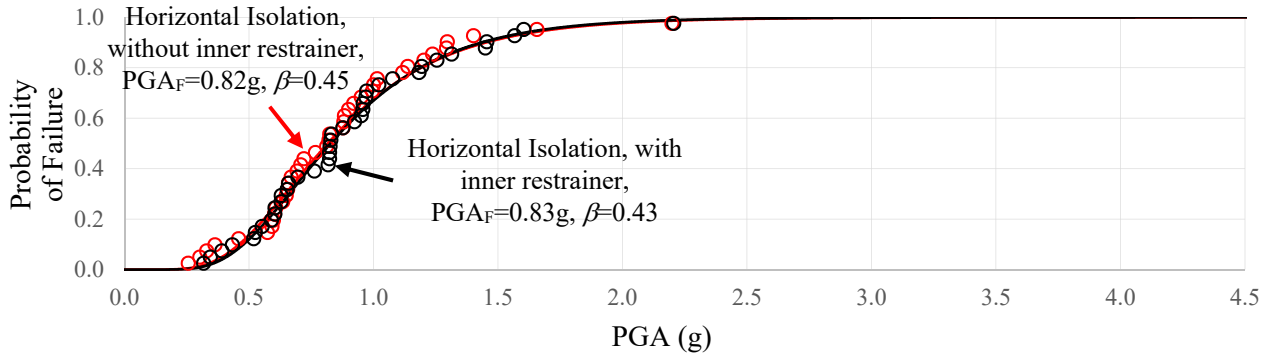


Figure 8-12 Fragility Curves for 420kip Transformer with 7.7Hz Bushing (No. 8) Inclined at 20 Degrees, Triple FP Bearings without Inner Restrainer, Lower Bound Friction Properties and Isolator Ultimate Displacement Capacity of 17.7, 27.7 or 31.3inch, Bushing Lateral Acceleration Limit=1g

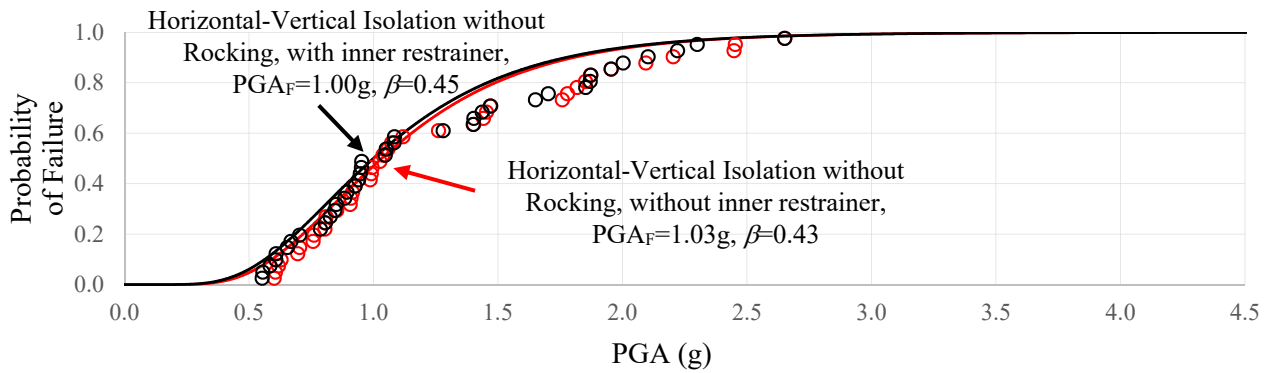
Finally, Figure 8-13 compares fragility curves of the 420kip transformer with the 7.7Hz inclined bushing having 1g lateral acceleration limit when the FP isolators are with or without an inner restrainer ring. The isolators have lower bound properties and a displacement capacity of 17.7inch. Evidently, the inner restrainer has an insignificant effect on the probability of failure.

It should be noted that the discussion on the effects of various parameters on the probability of failure is only based on inspection of the fragility curves. Therefore, the observations apply on the probability of failure given the occurrence of a particular intensity earthquake as measured by the PGA of the horizontal component. Truly what is important is the probability of failure given the lifetime of the equipment at a particular site, which will be investigated in the next section. The calculation of the probability of failure given the lifetime of the equipment considers the complete shape of the fragility curve and the shape of the seismic hazard curve.

Inclined bushing, bushing lateral acceleration limit=1g, Horizontal Isolation, Isolator ultimate displacement=17.7inch, with and without inner restrainer, Lower bound friction



Inclined bushing, bushing lateral acceleration limit=1g, Horizontal-Vertical Isolation without rocking, Isolator ultimate displacement=17.7inch, with and without inner restrainer, Lower bound friction



Inclined bushing, bushing lateral acceleration limit=1g, Horizontal-Vertical Isolation with rocking, Isolator ultimate displacement=17.7inch, with and without inner restrainer, Lower bound friction

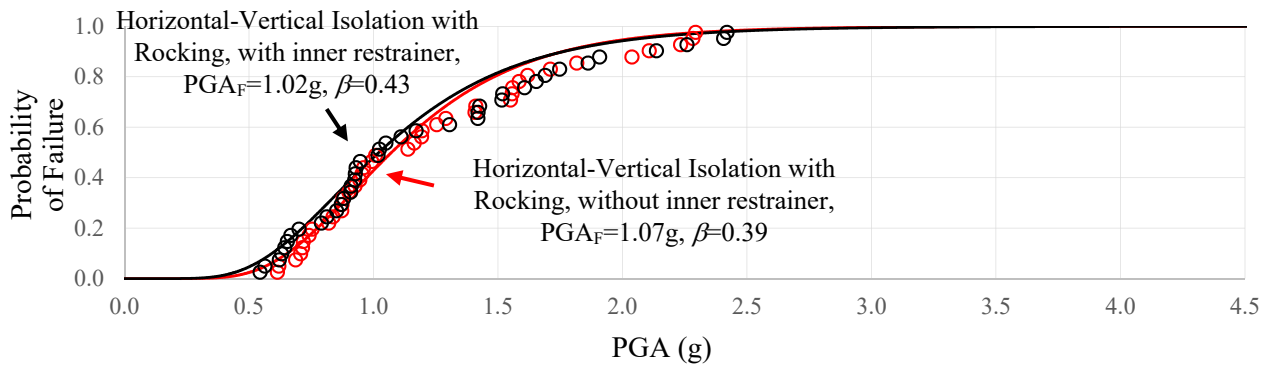


Figure 8-13 Fragility Curves for 420kip Transformer with 7.7Hz Bushing (No. 8) Inclined at 20 Degrees, Triple FP Bearings with and without Inner Restrainer, Lower Bound Friction Properties and Isolator Ultimate Displacement Capacity of 17.7inch, Bushing Lateral Acceleration Limit=1g

SECTION 9
SUMMARY OF RESULTS AND SAMPLE PROBABILITY OF FAILURE LIFETIME
RISK CALCULATIONS

Tables 9-1 to 9-4 present a summary of the fragility analysis results. The tables include the transformer conditions in each analyzed case and the resulting values of PGA_F (PGA value of horizontal seismic motion for which the probability of failure is 50%) and dispersion factor β . The best fit fragility curves for the empirical data of each analyzed case can then be constructed using Equation (2-1).

Table 9-1 Fragility Data for Analyzed Transformers in Case of Lower Bound Friction, Bushing Inclined at 20 Degrees and FP Isolators without Inner Restrainer

Transformer Weight (kip)	Bushing Freq. (Hz)	Isolator Displ. Capacity (inch)	Bushing Accel. Limit (g)	Non Isolated		Horizontal Isolation Only		Horizontal-Vertical Isolation Rocking Restrained		Horizontal-Vertical Isolation Rocking Allowed	
				PGA_F (g)	β	PGA_F (g)	β	PGA_F (g)	β	PGA_F (g)	β
320	7.7	17.7	2.0	0.80	0.45	1.06	0.39	1.17	0.42	1.38	0.43
			1.0	0.40	0.45	0.81	0.47	1.01	0.42	1.08	0.38
420	2.6	17.7	2.0	1.13	0.32	1.02	0.37	1.27	0.45	1.36	0.46
			1.0	0.56	0.32	0.99	0.38	1.13	0.44	0.49	0.60
	4.3	17.7	2.0	0.98	0.34	1.06	0.38	1.26	0.46	1.29	0.45
			1.0	0.49	0.34	0.97	0.37	1.13	0.43	0.94	0.45
	7.7	17.7	2.0	0.80	0.45	1.01	0.38	1.22	0.44	1.36	0.45
			1.0	0.40	0.45	0.82	0.45	1.03	0.43	1.07	0.39
		27.7	2.0	0.80	0.45	1.19	0.40	1.56	0.42	1.75	0.44
			1.0	0.40	0.45	0.84	0.46	1.40	0.42	1.54	0.41
		31.3	2.0	0.80	0.45	1.32	0.45	1.70	0.45	2.06	0.47
			1.0	0.40	0.45	0.88	0.49	1.49	0.46	1.66	0.45
	11.3	17.7	2.0	1.44	0.35	0.97	0.39	1.14	0.44	1.45	0.46
			1.0	0.72	0.35	0.81	0.40	1.11	0.44	1.35	0.44
		27.7	2.0	1.44	0.35	1.10	0.42	1.55	0.41	1.83	0.45
			1.0	0.72	0.35	0.86	0.43	1.48	0.40	1.66	0.43
520	7.7	17.7	2.0	0.80	0.45	0.99	0.40	1.21	0.46	1.15	0.43
			1.0	0.40	0.45	0.82	0.45	1.05	0.44	1.06	0.40

Table 9-2 Fragility Data for Analyzed Transformers in Case of Lower Bound Friction, Vertical Bushing and FP Isolators without Inner Restrainer

Transformer Weight (kip)	Bushing Freq. (Hz)	Isolator Displ. Capacity (inch)	Bushing Accel. Limit (g)	Non Isolated		Horizontal Isolation Only		Horizontal-Vertical Isolation Rocking Restrained		Horizontal-Vertical Isolation Rocking Allowed	
				PGA_F (g)	β	PGA_F (g)	β	PGA_F (g)	β	PGA_F (g)	β
420	7.7	17.7	2.0	0.72	0.41	1.01	0.38	1.23	0.45	1.45	0.45
			1.0	0.36	0.41	1.00	0.39	1.11	0.45	1.18	0.44
		27.7	2.0	0.72	0.41	1.22	0.39	1.57	0.42	1.70	0.44
			1.0	0.36	0.41	1.21	0.40	1.53	0.42	1.56	0.42
		31.3	2.0	0.72	0.41	1.32	0.43	1.71	0.46	1.99	0.47
			1.0	0.36	0.41	1.26	0.43	1.68	0.46	1.67	0.45

Table 9-3 Fragility Data for Analyzed Transformers in Case of Upper Bound Friction, Bushing Inclined at 20 Degrees and FP Isolators without Inner Restrainer

Transformer Weight (kip)	Bushing Freq. (Hz)	Isolator Displ. Capacity (inch)	Bushing Accel. Limit (g)	Non Isolated		Horizontal Isolation Only		Horizontal-Vertical Isolation Rocking Restrained		Horizontal-Vertical Isolation Rocking Allowed	
				PGA_F (g)	β	PGA_F (g)	β	PGA_F (g)	β	PGA_F (g)	β
420	7.7	17.7	2.0	0.80	0.45	1.04	0.37	1.23	0.43	1.46	0.43
			1.0	0.40	0.45	0.82	0.43	1.06	0.42	1.07	0.37

Table 9-4 Fragility Data for Analyzed Transformers in Case of Lower Bound Friction, Bushing Inclined at 20 Degrees and FP Isolators with Inner Restrainer

Transformer Weight (kip)	Bushing Freq. (Hz)	Isolator Displ. Capacity (inch)	Bushing Accel. Limit (g)	Non Isolated		Horizontal Isolation Only		Horizontal-Vertical Isolation Rocking Restrained		Horizontal-Vertical Isolation Rocking Allowed	
				PGA_F (g)	β	PGA_F (g)	β	PGA_F (g)	β	PGA_F (g)	β
420	7.7	17.7	2.0	0.80	0.45	0.96	0.39	1.23	0.47	1.24	0.44
			1.0	0.40	0.45	0.83	0.43	1.00	0.45	1.02	0.43

Based on the results in Tables 9-1 to 9-4, calculations for the probability of failure given the PGA value of 0.6g were performed by use of Equation (2-1) for $x=0.6g$ and the values of PGA_F and β calculated in the fragility analysis. Note that based on the discussion in Section 7 on the selection and scaling of motions for the analysis and the results shown in Figure 7-3, a $PGA=0.6g$ is representative of the IEEE High Required Response Spectra (rather than a $PGA=0.5g$). The results are presented in Table 9-5.

Table 9-5 Values of Probability of Failure of Transformer with Bushing Inclined at 20 Degrees, FP Isolators without Inner Restrainer in Lower Bound Conditions for Seismic Intensity with PGA=0.6g, $P_F/PGA=0.6g$

Weight (kip)	Bushing Freq. (Hz)	Isolator Displ. Capacity (inch)	Bushing Accel. Limit (g)	Non Isolated	Horizontal Isolation Only	Horizontal-Vertical Isolation Rocking Restrained	Horizontal-Vertical Isolation Rocking Allowed
				$P_F/PGA=0.6g$ (%)	$P_F/PGA=0.6g$ (%)	$P_F/PGA=0.6g$ (%)	$P_F/PGA=0.6g$ (%)
420	2.6	17.7	2.0	2.58	7.91	4.82	3.75
			1.0	57.52	9.61	7.58	63.11
	4.3	17.7	2.0	54.33	9.22	5.29	3.47
			1.0	96.11	39.43	12.09	45.9
	7.7	17.7	2.0	26.24	8.74	5.46	3.29
			1.0	82.16	24.55	10.60	6.67
		27.7	2.0	26.24	4.33	1.07	0.79
			1.0	82.16	23.10	2.14	1.11
		31.3	2.0	26.24	3.88	1.04	0.43
			1.0	82.16	21.62	2.45	1.12
	11.3	17.7	2.0	0.63	10.65	6.94	2.75
			1.0	30.17	22.93	7.99	3.27

A number of interesting observations can be made on the basis of the results in Table 9-5:

- 1) The non-isolated transformer with the least (2.6Hz) and the highest (11.3Hz) bushing frequencies considered have low probabilities of failures when the transverse bushing acceleration limit is 2g. For the case of the stiff 11.3Hz bushing this is explained by the fact that the fundamental frequency is high enough so that there is little magnification of acceleration as seen in the average spectra of Figure 7-3. However, the low probability of failure for the case of the 2.6Hz bushing cannot be explained by the shape of the response spectrum. It likely is the result of the particular motions selected for the incremental dynamic analysis.
- 2) The probability of failure given the occurrence of the earthquake representative of the IEEE High Required Response Spectrum (PGA=0.6g) for the non-isolated transformers is high (with the exception of the cases discussed in item 1 above). For comparison, building standards define the acceptable probability of collapse given the maximum considered earthquake as 10% for regular structures and as 3% for important structures (ASCE, 2010). The horizontally-vertically isolated transformer has acceptable probability

of failure (with the exception of the two cases of low as-installed frequency in the bushing limit of 1g and for the system allowed to freely rock) whereas the horizontally-only isolated transformers have acceptable probability of failure provided the transverse bushing acceleration limit is 2g.

- 3) Excluding the case of the atypical 2.6Hz frequency bushing, where resonance phenomena affected the response of the combined horizontal-vertical seismic isolation system that was free to rock (but also for the more realistic lower bound bushing frequency of 4.3Hz), the probabilities of failure for the combined horizontal-vertical seismic isolation system are sufficiently low for either of the two systems (allowing or restraining rocking) so that the simpler system that allows for rocking may be preferable. For atypical cases like the 2.6Hz frequency bushing, where the proximity of this frequency to the rocking frequency of the transformer leads to amplification of response, the system with a stiff base is preferred as it can be designed to prevent or reduce rocking and avoid or reduce resonance.

The results in Table 9-5 and the preceding discussion apply for one earthquake intensity and they will differ as that intensity measure is changed. Consideration of the seismic hazard for a particular location over the lifetime of the equipment provides much more useful information.

Calculations for the mean annual frequency of failure, λ_F , as obtained by use of Equation (2-3) for the ten locations in Table 2-1, for which the seismic hazard curves are shown in Figure 2-3, were performed for several cases of the 420kip transformer with the inclined bushing when non-isolated and when isolated by the horizontal only isolation system and by the horizontal-vertical isolation system with and without restraint for rocking. When isolated, the triple FP isolators were without an inner restrainer. Based on these values of the mean annual frequency, calculations for the probability of failure in a lifetime of 50 years were performed using Equation (2-2). Results for the probability of failure are presented in Tables 9-6 to 9-13 for the three cases of bushing as-installed frequency and two values of bushing lateral acceleration limit. Note that the mean annual frequency may be back-calculated from the data in Tables 9-6 to 9-13 by use of Equation (2-3).

Table 9-6 Probability of Failure (in %) in 50 Years P_F of 420 kip Transformer with 2.6Hz Bushing for Locations in Western US with 1g Transverse Acceleration Limit

Location (per Table 2-1)	Isolator Displ. Capacity (in)	Non-Isolated	Horizontal Isolation Only	Horizontal-Vertical Isolation Rocking Restrained	Horizontal-Vertical Isolation Rocking Allowed
1	17.7	3.10	0.72	0.59	6.88
2	17.7	14.66	3.13	2.53	30.91
3	17.7	19.17	5.15	4.17	34.01
4	17.7	7.20	2.56	2.13	12.14
5	17.7	5.15	1.30	1.05	10.72
6	17.7	3.87	0.98	0.79	7.82
7	17.7	1.24	0.39	0.33	3.17
8	17.7	3.40	0.81	0.65	7.20
9	17.7	7.48	3.03	2.52	10.38
10	17.7	2.62	0.59	0.47	6.07

Table 9-7 Probability of Failure (in %) in 50 Years P_F of 420kip Transformer with 2.6Hz Bushing for Ten Locations in Western US with 2g Transverse Acceleration Limit

Location (per Table 2-1)	Isolator Displ. Capacity (in)	Non-Isolated	Horizontal Isolation Only	Horizontal-Vertical Isolation Rocking Restrained	Horizontal-Vertical Isolation Rocking Allowed
1	17.7	0.38	0.64	0.42	0.34
2	17.7	1.45	2.72	1.75	1.42
3	17.7	2.86	4.62	3.03	2.52
4	17.7	1.76	2.38	1.68	1.46
5	17.7	0.72	1.16	0.77	0.64
6	17.7	0.55	0.88	0.58	0.48
7	17.7	0.27	0.36	0.26	0.23
8	17.7	0.43	0.72	0.47	0.39
9	17.7	2.17	2.84	2.02	1.77
10	17.7	0.30	0.52	0.34	0.28

Table 9-8 Probability of Failure (in %) in 50 Years P_F of 420kip Transformer with 4.3 Hz Bushing for Ten Locations in Western US with 1g Transverse Acceleration Limit

Location (per Table 2-1)	Isolator Displ. Capacity (in)	Non Isolated	Horizontal Isolation Only	Horizontal-Vertical Isolation Rocking Restrained	Horizontal-Vertical Isolation Rocking Allowed
1	17.7	4.48	0.71	0.57	1.06
2		21.09	3.06	2.47	4.84
3		26.07	5.11	4.11	7.21
4		9.49	2.57	2.11	3.18
5		7.39	1.28	1.03	1.84
6		5.53	0.97	0.78	1.38
7		1.92	0.38	0.33	0.51
8		4.95	0.80	0.64	1.17
9		9.17	3.05	2.50	3.60
10		3.82	0.58	0.46	0.87

Table 9-9 Probability of Failure (in %) in 50 Years P_F of 420kip Transformer with 4.3 Hz Bushing for Ten Locations in Western US with 2g Transverse Acceleration Limit

Location (per Table 2-1)	Isolator Displ. Capacity (in)	Non Isolated	Horizontal Isolation Only	Horizontal-Vertical Isolation Rocking Restrained	Horizontal-Vertical Isolation Rocking Allowed
1	17.7	0.65	0.57	0.45	0.39
2		2.72	2.41	1.90	1.64
3		4.70	4.16	3.24	2.87
4		2.45	2.20	1.75	1.62
5		1.18	1.04	0.82	0.73
6		0.89	0.79	0.62	0.55
7		0.37	0.33	0.27	0.25
8		0.73	0.64	0.50	0.44
9		2.94	2.64	2.09	1.95
10		0.52	0.46	0.36	0.32

Table 9-10 Probability of Failure (in %) in 50 Years P_F of 420kip Transformer with 7.7 Hz Bushing for Ten Locations in Western US with 1g Transverse Acceleration Limit

Location (per Table 2-1)	Isolator Displ. Capacity (in)	Non Isolated	Horizontal Isolation Only	Horizontal-Vertical Isolation Rocking Restrained	Horizontal-Vertical Isolation Rocking Allowed
1	17.7	8.09	1.54	0.76	0.57
	27.7	8.09	1.47	0.26	0.18
	31.3	8.09	1.42	0.26	0.16
2	17.7	35.93	7.24	3.34	2.37
	27.7	35.93	6.89	1.00	0.65
	31.3	35.93	6.66	1.02	0.59
3	17.7	39.80	10.18	5.30	4.09
	27.7	39.80	9.72	1.94	1.36
	31.3	39.80	9.33	1.90	1.22
4	17.7	14.46	4.17	2.54	2.16
	27.7	14.46	4.01	1.26	1.00
	31.3	14.46	3.84	1.19	0.89
5	17.7	12.77	2.64	1.34	1.03
	27.7	12.77	2.52	0.49	0.35
	31.3	12.77	2.42	0.48	0.31
6	17.7	9.43	1.98	1.01	0.78
	27.7	9.43	1.89	0.37	0.26
	31.3	9.43	1.81	0.36	0.24
7	17.7	3.84	0.69	0.39	0.33
	27.7	3.84	0.67	0.20	0.16
	31.3	3.84	0.65	0.19	0.14
8	17.7	8.68	1.70	0.84	0.63
	27.7	8.68	1.62	0.29	0.21
	31.3	8.68	1.56	0.29	0.18
9	17.7	12.30	4.55	2.96	2.59
	27.7	12.30	4.38	1.56	1.26
	31.3	12.30	4.18	1.47	1.12
10	17.7	7.08	1.29	0.62	0.45
	27.7	7.08	1.23	0.20	0.14
	31.3	7.08	1.18	0.20	0.12

Table 9-11 Probability of Failure (in %) in 50 Years P_F of 420 kip Transformer with 7.7 Hz Bushing for Ten Locations in Western US with 2g Transverse Acceleration Limit

Location (per Table 2-1)	Isolator Displ. Capacity (in)	Non Isolated	Horizontal Isolation Only	Horizontal-Vertical Isolation Rocking Restrained	Horizontal-Vertical Isolation Rocking Allowed
1	17.7	1.64	0.68	0.46	0.32
	27.7	1.64	0.42	0.17	0.13
	31.3	1.64	0.36	0.15	0.08
2	17.7	7.72	2.91	1.94	1.31
	27.7	7.72	1.70	0.62	0.47
	31.3	7.72	1.48	0.55	0.28
3	17.7	10.76	4.85	3.32	2.38
	27.7	10.76	3.07	1.31	1.00
	31.3	10.76	2.64	1.15	0.63
4	17.7	4.36	2.45	1.80	1.42
	27.7	4.36	1.75	0.97	0.78
	31.3	4.36	1.53	0.85	0.55
5	17.7	2.80	1.22	0.84	0.60
	27.7	2.80	0.77	0.34	0.26
	31.3	2.80	0.67	0.30	0.17
6	17.7	2.10	0.92	0.63	0.45
	27.7	2.10	0.58	0.25	0.19
	31.3	2.10	0.50	0.22	0.12
7	17.7	0.73	0.37	0.28	0.22
	27.7	0.73	0.27	0.16	0.13
	31.3	0.73	0.24	0.14	0.09
8	17.7	1.81	0.76	0.52	0.36
	27.7	1.81	0.47	0.20	0.15
	31.3	1.81	0.41	0.17	0.09
9	17.7	4.73	2.91	2.16	1.73
	27.7	4.73	2.13	1.22	0.99
	31.3	4.73	1.85	1.07	0.71
10	17.7	1.37	0.55	0.37	0.26
	27.7	1.37	0.33	0.13	0.10
	31.3	1.37	0.29	0.12	0.06

Table 9-12 Probability of Failure (in %) in 50 Years P_F of 420 kip Transformer with 11.3 Hz Bushing for Ten Locations in Western US with 1g Transverse Acceleration Limit

Location (per Table 2-1)	Isolator Displ. Capacity (in)	Non Isolated	Horizontal Isolation Only	Horizontal-Vertical Isolation Rocking Restrained	Horizontal-Vertical Isolation Rocking Allowed
1	17.7	1.71	1.40	0.61	0.32
2		7.89	6.43	2.64	1.31
3		11.31	9.38	4.33	2.39
4		4.66	3.97	2.19	1.43
5		2.90	2.40	1.09	0.61
6		2.19	1.81	0.82	0.46
7		0.72	0.62	0.34	0.22
8		1.87	1.54	0.68	0.37
9		5.18	4.45	2.59	1.74
10		1.42	1.16	0.49	0.26

Table 9-13 Probability of Failure (in %) in 50 Years P_F of 420 kip Transformer with 11.3 Hz Bushing for Ten Locations in Western US with 2g Transverse Acceleration Limit

Location (per Table 2-1)	Isolator Displ. Capacity (in)	Non Isolated	Horizontal Isolation Only	Horizontal-Vertical Isolation Rocking Restrained	Horizontal-Vertical Isolation Rocking Allowed
1	17.7	0.17	0.78	0.55	0.28
2		0.58	3.38	2.36	1.12
3		1.32	5.49	3.94	2.06
4		1.04	2.67	2.05	1.26
5		0.34	1.38	0.99	0.52
6		0.26	1.04	0.75	0.39
7		0.17	0.40	0.32	0.20
8		0.20	0.86	0.62	0.32
9		1.32	3.15	2.43	1.55
10		0.13	0.63	0.44	0.22

Based on the results in these tables, the following are observed:

- 1) For the ten sites of Table 2-1 the calculated probabilities of failure in a 50-year lifespan are substantially less for the case of any of the isolated than for the non-isolated transformers. Only exceptions are
 - a. The case of the 2.6Hz frequency bushing when the transverse acceleration limit is 1g (Table 9-6) where the horizontally-vertically isolated transformer with allowance to rock has some high probabilities of failure due to the aforementioned amplification of response caused by the proximity of the bushing frequency to the rocking frequency of the transformer.
 - b. Some cases of the 2.6Hz frequency bushing when the transverse acceleration limit is 2g (Table 9-7) where the non-isolated transformer has smaller probability of failure than the isolated transformers. As discussed earlier this is an atypical case of bushing at the upper bound of bushing acceleration limit and with results that may have been affected by the selected motions for analysis.
 - c. Some cases of the 11.3Hz frequency bushing when the transverse acceleration limit is 2g (Table 9-13) where the non-isolated transformer has smaller probability of failure than the isolated transformers. This behavior was investigated and found that the probability of failure of the isolated transformers improved when the displacement capacity of the FP isolators was increased. Figures 9-1 and 9-2 present fragility curves for 420kip transformer with inclined bushing of 11.3Hz frequency and 2g transverse acceleration limit for two FP isolator displacement limits: 17.7 and 27.7inch.
- 2) Transformers with the combined horizontal-vertical isolation systems of either type have lower probabilities of failure in a 50-year lifespan than the horizontally-only isolated transformers except when the bushing frequency is low and the transverse bushing acceleration limit is 1g. Then the horizontal-vertical isolation system that allows for rocking has higher probabilities of failure due to excessive rocking. Excluding these cases, the system that allows for free rocking has the lowest probabilities of failure.
- 3) For the case of transformers with a 7.7Hz bushing and bushing acceleration limit of 1g, which a representative case for many transformers, the probability of failure is as follows:

(a) for the non-isolated transformers is as high as 39.8% (at location 3), for the horizontally isolated transformer is less than 10.2% (again location 3) and can be marginally improved by increasing the displacement capacity of the isolators, (c) for the combined horizontal-vertical isolation system that restrains rocking is less than 5.3% (location 3) and can be reduced at the same location to 1.9% by increasing the displacement capacity of the isolators, and (d) for the combined horizontal-vertical isolation system that allows for rocking is less than 4.1% (location 3) and can be reduced at the same location to 1.2% by increasing the displacement capacity of the isolators.

- 4) For locations other than locations 2 and 3 which are two of the most seismically hazardous sites in California, the probability of failure for the isolated transformer, whether only by horizontal or combined horizontal-vertical isolation system, is low. Important is that these low probabilities of failure are accomplished for the least displacement capacity of the isolators without the need to implement larger displacement capacity isolators. For example consider the case of the 7.7Hz bushing transformer with a transverse acceleration limit of 1g at location 1 in Vancouver, WA. The probability of failure in 50 years of lifetime for the horizontal-only isolation system is 1.54% when the least displacement isolator of 17.7inch is used and is 1.47% when the 27.7inch isolator is used. However, when for the same location the combined horizontal-vertical isolation system that is free to rock is used, the probability of failure in 50 years is 0.57% when the isolator displacement capacity is 17.7inch and is 0.18% when the 27.7inch capacity isolator is used.

The information presented in terms of probability of failure given the maximum earthquake and the probability of failure for particular locations within the lifetime of the equipment is important in making decision on the use and the form of seismic isolation depending on the particular equipment and its location. However, given that transformers are considered critical structures, acceptably low probabilities of failure can be achieved only with the use of a combined horizontal-vertical isolation system with FP isolators having some increased displacement capacity.

Inclined bushing, Bushing lateral acceleration limit=2g, Horizontal isolation, Isolator ultimate displacement of 17.7 or 27.7 inch, No inner restrainer, Lower bound friction

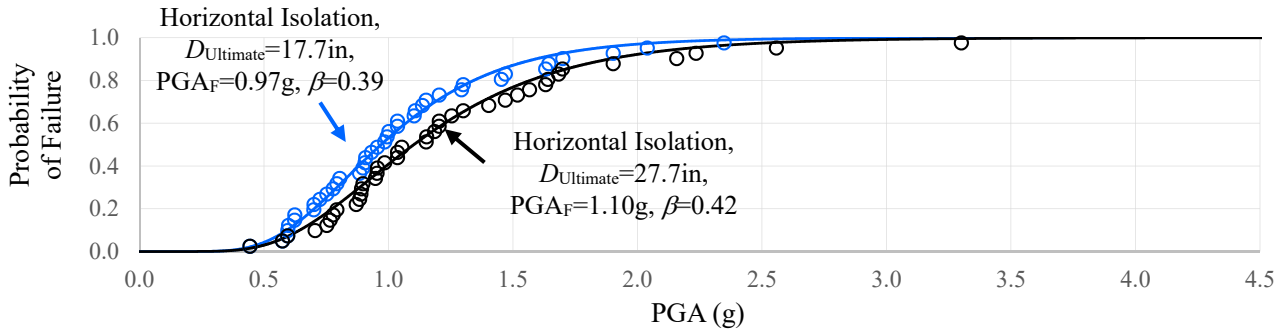


Figure 9-1 Fragility Curves for 420kip Transformer with 11.3Hz Bushing (No. 6) Inclined at 20 Degrees, Triple FP Bearings without Inner Restrainer, Lower Bound Friction Properties and Isolator Ultimate Displacement Capacity of 17.7 or 27.7 inch, Horizontal Isolation, Bushing Lateral Acceleration Limit=2g

Inclined bushing, Bushing lateral acceleration limit=2g, Horizontal-vertical isolation with rocking, Isolator ultimate displacement of 17.7 or 27.7 inch, No inner restrainer, Lower bound friction

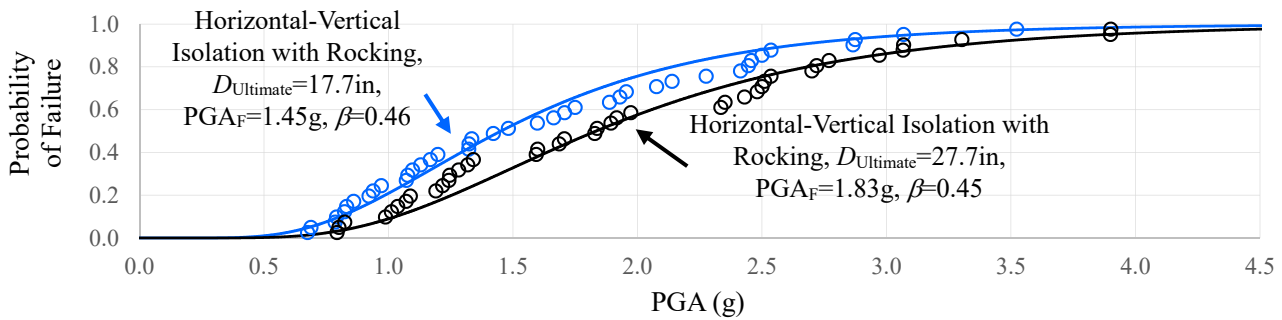


Figure 9-2 Fragility Curves for 420kip Transformer with 11.3Hz Bushing (No. 6) Inclined at 20 Degrees, Triple FP Bearings without Inner Restrainer, Lower Bound Friction Properties and Isolator Ultimate Displacement Capacity of 17.7 or 27.7 inch, Horizontal-Vertical Isolation with Rocking, Bushing Lateral Acceleration Limit=2g

SECTION 10

SUMMARY AND CONCLUSIONS

This report presented an analytical study of the response of seismically isolated electrical transformers for the purpose of comparing the performance of equipment that is non-isolated to equipment that is isolated only in the horizontal direction or is isolated by a three-dimensional isolation system. The isolation system consisted of triple FP isolators in the horizontal direction and spring and viscous dampers in the vertical direction. The performance was assessed by calculating the probability of failure as a function of the seismic intensity with due consideration of (a) horizontal and vertical ground seismic motion effects, (b) displacement capacity of the seismic isolation system, including uplift capacity (c) acceleration limits for failure of electrical bushings, (d) details of construction of the isolation system that allow or restrain rocking of the isolated structure, (e) weight of the isolated transformer in the range of 320 to 520kip, (f) bushings with as-installed frequencies of 2.6 to 11.3Hz, (g) inclined and vertical placed bushings and (h) various details of the isolators, including upper and lower bound properties and details of construction of the isolators. The acceleration failure limits for the transformer bushing were determined on the basis of a comparison of calculated fragility data in this study to empirical fragility data based on observations in past earthquakes for non-isolated transformers. Moreover, sample calculations of the probability of failure within a 50-year lifetime of isolated and non-isolated transformers at ten locations in the Western US were performed.

The results demonstrate the following:

- 1) Seismic isolation, whether horizontal-only or combined horizontal-vertical, results in substantial reduction of the probability of failure by comparison to non-isolated transformers. There are exceptions in the case of an atypically low frequency bushing (2.6Hz) when the transverse acceleration limit was 2g, which is an upper bound case of acceleration limit
- 2) Excluding the cases where the as-installed frequency of the bushings was close to the rocking frequency of the isolated transformer and the bushing acceleration limit was low (i.e., the atypical case of the 2.6Hz bushing transformer and bushing acceleration limit of 1g), the combined horizontal-vertical isolation systems that allows for rocking of the isolated transformer typically result in the lowest probabilities of failure. For the case of the combined horizontal-vertical isolation system that allows for rocking and with the 2.6Hz frequency bushing there was significant magnification of the rocking response of

the bushing so that the calculated probabilities of failure were for some cases unacceptable. This was particularly pronounced when the bushing transverse acceleration limit is low as rocking significantly magnified the response given the short distance between isolators (110inch, which is typically the shortest distance between isolators in transformers in the 320 to 520kip range). This phenomenon also occurred for the case of the 4.3Hz frequency bushing but to a lesser extent.

- 3) Given the occurrence of an earthquake representative of the IEEE High Required Response Spectra, defined herein to have a $PGA=0.6g$, the non-isolated transformers have unacceptably high probability of failure, whereas the horizontal-only isolated transformers have lower but still high probability of failure, which cannot be improved by increasing the displacement capacity of the isolators. Transformers with combined horizontal-vertical isolation systems, either restraining or allowing for rocking (but for cases of very low bushing frequencies), have acceptable probability of failure.
- 4) For the ten sites in the Western US considered in this study, the calculated probabilities of failure in a 50-year lifespan were notably lower for transformers with horizontal-only and horizontal-vertical isolation systems than non-isolated transformers for all analyzed cases barring a few cases that include the atypical case of the 2.6Hz frequency bushing with the 2g transverse acceleration limit and some others.

The performance assessment procedures described in this report (a) may be used to decide on the benefits offered by the seismic protective system depending on the limits of the protected equipment, location of the equipment (value of PGA) and configuration and properties of the seismic protective system, (b) may be used to calculate the mean annual frequency of functional failure and the corresponding probability of failure over the lifetime of the equipment and (c) the information may be used to assess the seismic performance of electric transmission networks under scenarios of component failures.

SECTION 11 REFERENCES

Anagnos, T. (1999). “Development of an Electrical Substation Equipment Performance Database for Evaluation of Equipment Fragilities.” *Report PEER Report 2001/06*, Pacific Earthquake Engineering Research Center, University of California, Berkeley, California.

ASCE/SEI 7 (2010). “Minimum Design Loads for Buildings and Other Structures.” American Society of Civil Engineers, Reston, VA.

Bozorgnia Y., Campbell K. W. (2004). “The Vertical-to-Horizontal Response Spectral Ratio and Tentative Procedures for Developing Simplified V/H and Vertical Design Spectra.” *Journal of Earthquake Engineering*, **8** (2), 175–207.

Bozorgnia Y., Campbell, K. W. (2016). “Ground Motion Model for the Vertical-to-Horizontal (V/H) Ratios of PGA, PGV, and Response Spectra.” *Earthquake Spectra*, **32** (2): 951-978.

Champion C., Liel A. (2012). “The Effect of Near-Fault Directivity on Building Seismic Collapse Risk.” *Earthquake Engineering and Structural Dynamics*, **41**(10): 1391-1409.

Computers and Structures, Inc. (2015). *SAP2000 Structural Analysis Program*, Berkeley, CA.

Eads L., Miranda E., Krawinkler H., Lignos D. G. (2013). “An Efficient Method for Estimating the Collapse Risk of Structures in Seismic Regions.” *Earthquake Engineering and Structural Dynamics*, **42**(1): 25-41.

Elkady A., Lignos D. G. (2014). “Modeling of the Composite Action in Fully Restrained Beam-to-Column Connections: Implications in the Seismic Design and Collapse Capacity of Steel Special Moment Frames.” *Earthquake Engineering and Structural Dynamics*, **43**(13): 1935–1954.

Ersoy S., Feizi B., Ashrafi A., Saadeghvaziri M. A. (2008) “Seismic Evaluation and Rehabilitation of Critical Components of Electrical Power Systems.” *Report MCEER-08-0011*, Multidisciplinary Center for Earthquake Engineering Research, University at Buffalo, Buffalo, NY.

Fahad M. (2013). "Seismic Evaluation and Qualification of Transformer Bushings." *Ph.D. Thesis*, University at Buffalo, State University of New York, Buffalo, NY.

FEMA (2009). "Quantification of Building Seismic Performance Factors" *Report FEMA P695*, Federal Emergency Management Agency, Washington, DC.

FEMA (2012). "Seismic Performance Assessment of Buildings" *Report FEMA P-58*, Federal Emergency Management Agency, Washington, DC.

Fenz D. M., Constantinou M. C. (2008a). "Spherical Sliding Isolation Bearings with Adaptive Behavior: Theory." *Earthquake Engineering and Structural Dynamics*, **37**(2): 163-183.

Fenz D. M., Constantinou M. C. (2008b). "Modeling Triple Friction Pendulum Bearings for Response-History Analysis." *Earthquake Spectra*, November, **24**(4): 1011-1028.

Gulerce Z., Abrahamson N. A. (2011). "Site-Specific Design Spectra for Vertical Ground Motion." *Earthquake Spectra*, **27** (4): 1023-1047.

Haselton C. B. (2006). "Assessing Seismic Collapse Safety of Modern Reinforced Concrete Moment Frame Buildings" *Ph.D. Thesis*, Department of Civil and Environmental Engineering, Stanford University, Palo Alto, CA.

Haselton C. B., Deierlein G. G. (2007). "Assessing Seismic Collapse Safety of Modern Reinforced Concrete Frame Buildings" *Blume Earthquake Engineering Research Center Technical Report No. 156*, Stanford University, Palo Alto, CA.

Haselton C. B., Mitrani-Reiser J., Goulet C. A., Deierlein G. G., Beck J. L., Porter K. A., Stewart J. P., Taciroglu E. (2008). "An Assessment to Benchmark the Seismic Performance of a Code-Conforming Reinforced-Concrete Moment-Frame Building". *Report PEER Report 2007/12*, Pacific Earthquake Engineering Research Center, University of California, Berkeley, CA.

Institute of Electrical and Electronics Engineers (IEEE) (2005). "IEEE Recommended Practice for Seismic Design of Substations, IEEE Standard 693." IEEE Power Engineering Society, The Institute of Electrical and Electronics Engineers, Inc., New York, NY.

Ibarra L. F., Krawinkler H. (2005). “Global Collapse of Frame Structures under Seismic Excitations.” *Report PEER Report 2005/06*; Pacific Earthquake Engineering Research Center, University of California, Berkeley, CA.

Kempner L. Jr., Eidinger J., Perez J., Schiff A. (2006). “Seismic Risk of High Voltage Electric Transmission Network.” *8th U.S. National Conference on Earthquake Engineering*, April 18-22, San Francisco, CA.

Kempner, L. Jr (2016). Personal communication on June 8, 2016, August 11, 2016, November 9, 2016 and November 28, 2016.

Kong D. (2010). “Evaluation and Protection of High Voltage Electrical Equipment against Severe Shock and Vibrations.” *Ph.D. Thesis*, University at Buffalo, State University of New York, Buffalo, NY.

Krawinkler H., Zarein F., Medina R. A., Ibarra L. F. (2006). “Decision Support for Conceptual Performance-Based Design.” *Earthquake Engineering and Structural Dynamics*, **35**(1): 115-133.

Kumar M., Whittaker A. S., Constantinou M. C. (2014). “Characterizing Friction in Sliding Isolation Bearings.” *Earthquake Engineering and Structural Dynamics*, **44** (9): 1409–1425.

Liel A. B., Haselton C. B., Deierlein G. G. (2011). “Seismic Collapse Safety of Reinforced Concrete Buildings: II. Comparative Assessment of Non-Ductile and Ductile Moment Frames.” *Journal of Structural Engineering* **134** (7): 492-502.

Lignos D., Krawinkler H. (2013). “Sidesway Collapse of Deteriorating Structural Systems under Seismic Excitations.” *Blume Earthquake Engineering Research Center Technical Report No. 177*, Stanford University, Palo Alto, CA.

McKenna F. T. (1997). “Object-Oriented Finite Element Programming: Frameworks for Analysis, Algorithms and Parallel Computing.” *Ph.D. Thesis*, Department of Civil and Environmental Engineering, University of California, Berkeley, CA.

McVitty W. J., Constantinou M. C. (2015). "Property Modification Factors for Seismic Isolators: Design Guidance for Buildings". *Report MCEER-15-0005*, Multidisciplinary Center for Earthquake Engineering Research, University at Buffalo, Buffalo, NY.

Medina R. A., Krawinkler H. (2004). "Seismic Demands for Nondeteriorating Structures and Their Dependence on Ground Motions." *Report MEER Report 2003/15*, Pacific Earthquake Engineering Research Center College of Engineering University of California, Berkeley, CA.

Murota N., Feng M. Q., Liu G. Y. (2005). "Experimental and Analytical Studies of Base Isolation Systems for Seismic Protection of Power Transformers." *Report MCEER-05-0008*, Multidisciplinary Center for Earthquake Engineering Research, University at Buffalo, Buffalo, NY.

Oikonomou K., Constantinou M. C., Reinhorn A. M., Kempner L. Jr. (2016). "Seismic Isolation of Electrical Transformers." *Report MCEER-16-0006*; Multidisciplinary Center for Earthquake Engineering Research, University at Buffalo, Buffalo, NY.

Sarlis A. A., Constantinou M. C. (2010). "Modeling Triple Friction Pendulum Isolators in Program SAP2000." *Personal Communication*. June 27.

Sarlis A. A., Constantinou M. C. (2013). "Model of Triple Friction Pendulum Bearing for General Geometric and Frictional Parameters and for Uplift Conditions." *MCEER-13-0010*; Multidisciplinary Center for Earthquake Engineering Research, University at Buffalo, Buffalo, NY.

Sarlis A. A., Constantinou M. C., Reinhorn A. M. (2013). "Shake Table Testing of Triple Friction Pendulum Isolators under Extreme Conditions." *MCEER-13-0011*; Multidisciplinary Center for Earthquake Engineering Research, University at Buffalo, Buffalo, NY.

Schiff A. J. (1997). "Guide to Post-Earthquake Investigation of Lifelines." *Technical Council on Lifeline Earthquake Engineering*, Monograph No.11, American Society of Civil Engineers, Washington, DC.

Shinozuka M., Dong X., Chen T. C., Jin X. (2007). "Seismic Performance of Electric Transmission Network under Component Failures." *Earthquake Engineering and Structural Dynamics*; **36**: 227-244.

Shumuta Y. (2007). “Practical Seismic Upgrade Strategy for Substation Equipment based on Performance Indices.” *Earthquake Engineering and Structural Dynamics*, **27**(2): 209-226.

US Geological Survey. <http://earthquake.usgs.gov/designmaps/us/application.php> [9 November 2015] (for response spectra).

US Geological Survey. <http://geohazards.usgs.gov/hazardtool/application.php> [11 November 2015] (for seismic hazard curves).

Vamvatsikos D., Cornell C. A. (2002). “Incremental Dynamic Analysis”. *Earthquake Engineering and Structural Dynamics*; **31** (3): 491-514.

APPENDIX A
MODIFIED SERIES MODEL PARAMETERS

This appendix presents details of the calculation for the model parameters of the triple FP bearings.

A.1 Case of Bearing without Inner Restrainer Ring (Figure 4-2)

A.1.1 Model with Axial-Shear Force Interaction

- Vertical Stiffness

The bearing vertical stiffness is approximately calculated as AE/h , where A is the area of the center slider (diameter $b_2=5$ inch), E is a representative modulus (typically assumed about half of steel to account for flexibilities in the bearing assembly, herein 14500ksi) and h is the height (herein $2t_{CO}+h_1+h_4=9.2$ inch). The vertical stiffness is thus equal to $\pi \times 2.5^2 \times 14500 / 9.2 = 30946.4$ kip/in.

Each of the three elements of the series model has vertical stiffness $K_{v,Compressive,i}$ so that the combined stiffness equals 54751.3kip/in. That is, $(1/K_{v,Compressive,i+1} + 1/K_{v,Compressive,i+1} + 1/K_{v,Compressive,i})^{-1} = 30946.4$ kip/in or $K_{v,Compressive,i} = 92839.2$ kip/in.

- Elastic Stiffness: $\bar{K}_{ini,i}$

Element FP1:
$$\bar{K}_{ini,1} = \frac{\mu_2 W}{2Y} = \frac{0.08 \times 105}{2 \times 0.05} = 84 \text{kip} / \text{in}$$

Element FP2:
$$\bar{K}_{ini,2} = \frac{\mu_4 W}{2Y} = \frac{0.12 \times 105}{2 \times 0.05} = 126 \text{kip} / \text{in}$$

Element FP3:
$$\bar{K}_{ini,3} = \frac{\mu_4 W}{2Y} = \frac{0.12 \times 105}{2 \times 0.05} = 126 \text{kip} / \text{in}$$

- Friction Coefficient: $\bar{\mu}_i$

Element FP1:
$$\bar{\mu}_1 = \mu_2 = \mu_3 = 0.08$$

Element FP2: $\bar{\mu}_2 = \mu_1 = 0.12$

Element FP3: $\bar{\mu}_3 = \mu_4 = 0.12$

- **Radius of Curvature:** $\bar{R}_{\text{eff},i}$

Element FP1: $\bar{R}_{\text{eff1}} = R_{\text{eff2}} + R_{\text{eff3}} = 3.5 + 3.5 = 7.0in$

Element FP2: $\bar{R}_{\text{eff2}} = R_{\text{eff1}} - R_{\text{eff2}} = 35.5 - 3.5 = 32.0in$

Element FP3: $\bar{R}_{\text{eff3}} = R_{\text{eff4}} - R_{\text{eff3}} = 35.5 - 3.5 = 32.0in$

- **Restrainer Gap Stiffness:** $\bar{K}_{\text{GP},i}$, $\bar{K}_{\text{GN},i}$

Element FP1:

$$\bar{K}_{\text{GP1}} = -\bar{K}_{\text{GN1}} = 0.0kip / in \quad (\text{no inner restrainer ring})$$

Element FP2:

$$\bar{K}_{\text{GP2}} = -\bar{K}_{\text{GN2}} = \frac{\pi t_{r1} (t_{r1} + s_1) F_{ry}}{6Y_r} = \frac{\pi \cdot 0.5 \cdot (0.5 + 22) \cdot 25}{6 \cdot 0.5} = 294.5kip / in$$

Element FP3:

$$\bar{K}_{\text{GP3}} = -\bar{K}_{\text{GN3}} = \frac{\pi t_{r4} (t_{r4} + s_4) F_{ry}}{6Y_r} = \frac{\pi \cdot 0.5 \cdot (0.5 + 22) \cdot 25}{6 \cdot 0.5} = 294.5kip / in$$

Diameter s_i , $i=1, 2$ (see Figure 5-1)

$$s_i = b_i + 2d_i$$

$$s_1 = s_4 = b_1 + 2d_1 = 8 + 2 \cdot 7 = 22in$$

$$s_2 = s_3 = b_2 + 2d_2 = 5 + 2 \cdot 2 = 9in$$

- **Restrainer Gap Displacement Capacity:** $\bar{d}_{GP,i}$, $\bar{d}_{GN,i}$

Element FP1: $\bar{d}_{GP1} = 100in$ (no restrainer)

Element FP2: $\bar{d}_{GP2} = \frac{(R_{eff1} - R_{eff2})}{R_{eff1}} d_1^* = \frac{(35.5 - 3.5)}{35.5} \cdot 6.37 = 5.74in$

Element FP3: $\bar{d}_{GP3} = \frac{(R_{eff4} - R_{eff3})}{R_{eff4}} d_4^* = \frac{(35.5 - 3.5)}{35.5} \cdot 6.37 = 5.74in$

Also,

$$\bar{d}_{GN1} = -\bar{d}_{GP1}, \bar{d}_{GN2} = -\bar{d}_{GP2}, \bar{d}_{GN3} = -\bar{d}_{GP3}$$

$D_{Capacity}$ is the displacement capacity of the triple FP bearing:

$$D_{Capacity} = d_1^* + d_2^* + d_3^* + d_4^* = 6.37 + 1.17 + 1.17 + 6.37 = 15.08in$$

- **Displacement at the fracture of restrainer:** $\bar{d}_{HP,i}$, $\bar{d}_{HN,i}$

Element FP1: $\bar{d}_{HP1} = -\bar{d}_{HN1} = \bar{d}_{GP1} + (t_{r2} + t_{r3}) = 100 + (0.5 + 0.5) = 101.0in$ (no inner restrainer ring)

Element FP2: $\bar{d}_{HP2} = -\bar{d}_{HN2} = \bar{d}_{GP2} + t_{r1} = 5.74 + 0.5 = 6.24in$

Element FP3: $\bar{d}_{HP3} = -\bar{d}_{HN3} = \bar{d}_{GP3} + t_{r3} = 5.74 + 0.5 = 6.24in$

A.1.2 Model without Axial-Shear Force Interaction

- Vertical Stiffness

The bearing vertical stiffness is approximately calculated as AE/h , where A is the area of the center slider (diameter $b_2=5$ inch), E is a representative modulus (typically assumed about half of steel to account for flexibilities in the bearing assembly, herein 14500ksi) and h is the height (herein $2t_{CO}+h_1+h_4=9.2$ inch). The vertical stiffness is thus equal to $\pi \times 2.5^2 \times 14500 / 9.2 = 30946.4$ kip/in.

Each of the three elements of the series model has vertical stiffness $K_{v,Compressive,i}$ so that the combined stiffness equals 54751.3kip/in. That is, $(1/K_{v,Compressive,i+1} + 1/K_{v,Compressive,i+1} + 1/K_{v,Compressive,i})^{-1} = 30946.4$ kip/in or $K_{v,Compressive,i} = 92839.2$ kip/in.

For uplift (tension) $K_{v,Uplift,i} = 0.1$ kip/in.

- Elastic Stiffness: $\bar{K}_{ini,i}$

Element FP1:
$$\bar{K}_{ini,1} = \frac{\mu_2 W}{2Y} = \frac{0.08 \times 105}{2 \times 0.05} = 84 \text{kip/in}$$

Element FP2:
$$\bar{K}_{ini,2} = \frac{\mu_4 W}{2Y} = \frac{0.12 \times 105}{2 \times 0.05} = 126 \text{kip/in}$$

Element FP3:
$$\bar{K}_{ini,3} = \frac{\mu_4 W}{2Y} = \frac{0.12 \times 105}{2 \times 0.05} = 126 \text{kip/in}$$

- Friction Coefficient: $\bar{\mu}_i$

Element FP1:
$$\bar{\mu}_1 = \mu_2 = \mu_3 = 0.08$$

Element FP2:
$$\bar{\mu}_2 = \mu_4 = 0.12$$

Element FP3:
$$\bar{\mu}_3 = \mu_4 = 0.12$$

- **Radius of Curvature:** $\bar{R}_{\text{eff},i}$

Element FP1: $\bar{R}_{\text{eff1}} = R_{\text{eff2}} + R_{\text{eff3}} = 3.5 + 3.5 = 7.0in$

Element FP2: $\bar{R}_{\text{eff2}} = R_{\text{eff1}} - R_{\text{eff2}} = 35.5 - 3.5 = 32.0in$

Element FP3: $\bar{R}_{\text{eff3}} = R_{\text{eff4}} - R_{\text{eff3}} = 35.5 - 3.5 = 32.0in$

- **Restrainer Gap Stiffness:** $\bar{K}_{\text{GP},i}$, $\bar{K}_{\text{GN},i}$

Element FP1:

$$\bar{K}_{\text{GP1}} = -\bar{K}_{\text{GN1}} = 0.0kip / in \quad (\text{no restrainer})$$

Element FP2:

$$\bar{K}_{\text{GP2}} = -\bar{K}_{\text{GN2}} = \frac{\pi t_{r1} (t_{r1} + s_1) F_{ry}}{6Y_r} = \frac{\pi \cdot 0.5 \cdot (0.5 + 22) \cdot 25}{6 \cdot 0.5} = 294.5kip / in$$

Element FP3:

$$\bar{K}_{\text{GP3}} = -\bar{K}_{\text{GN3}} = \frac{\pi t_{r4} (t_{r4} + s_4) F_{ry}}{6Y_r} = \frac{\pi \cdot 0.5 \cdot (0.5 + 22) \cdot 25}{6 \cdot 0.5} = 294.5kip / in$$

Diameter s_i , $i=1, 2$ (see Figure 5-1)

$$\begin{aligned} s_i &= b_i + 2d_i \\ s_1 = s_4 &= b_1 + 2d_1 = 8 + 2 \cdot 7 = 22in \\ s_2 = s_3 &= b_2 + 2d_2 = 5 + 2 \cdot 2 = 9in \end{aligned}$$

- **Restrainer Gap Displacement Capacity:** $\bar{d}_{\text{GP},i}$, $\bar{d}_{\text{GN},i}$

Element FP1: $\bar{d}_{\text{GP1}} = 100in$ (no inner restrainer ring)

Element FP2:
$$\bar{d}_{GP2} = \frac{(R_{\text{eff1}} - R_{\text{eff2}})}{R_{\text{eff1}}} d_1^* = \frac{(35.5 - 3.5)}{35.5} \cdot 6.37 = 5.74 \text{in}$$

Element FP3:
$$\bar{d}_{GP3} = \frac{(R_{\text{eff4}} - R_{\text{eff3}})}{R_{\text{eff4}}} d_4^* = \frac{(35.5 - 3.5)}{35.5} \cdot 6.37 = 5.74 \text{in}$$

Also,

$$\bar{d}_{GN1} = -\bar{d}_{GP1}, \quad \bar{d}_{GN2} = -\bar{d}_{GP2}, \quad \bar{d}_{GN3} = -\bar{d}_{GP3}$$

D_{Capacity} is the displacement capacity of the Triple FP bearing:

$$D_{\text{Capacity}} = d_1^* + d_2^* + d_3^* + d_4^* = 6.37 + 1.17 + 1.17 + 6.37 = 15.08 \text{in}$$

- **Displacement at the fracture of restrainer:** $\bar{d}_{HP,i}$, $\bar{d}_{HN,i}$

Element FP1:
$$\bar{d}_{HP1} = -\bar{d}_{HN1} = \bar{d}_{GP1} + (t_{r2} + t_{r3}) = 100 + (0.5 + 0.5) = 101.0 \text{in} \quad (\text{no inner restrainer ring})$$

Element FP2:
$$\bar{d}_{HP2} = -\bar{d}_{HN2} = \bar{d}_{GP2} + t_{r1} = 5.74 + 0.5 = 6.24 \text{in}$$

Element FP3:
$$\bar{d}_{HP3} = -\bar{d}_{HN3} = \bar{d}_{GP3} + t_{r3} = 5.74 + 0.5 = 6.24 \text{in}$$

A.2 Case of Bearing with Inner Restrainer Ring (Figure 4-1)

A.2.1 Model with Axial-Shear Force Interaction

- **Vertical Stiffness**

The bearing vertical stiffness is approximately calculated as AE/h , where A is the area of the center slider (diameter $b_2=5$ inch), E is a representative modulus (typically assumed about half of steel to account for flexibilities in the bearing assembly, herein 14500ksi) and h is the height

(herein $2t_{CO}+h_1+h_4=9.2$ inch). The vertical stiffness is thus equal to $\pi \times 2.5^2 \times 14500 / 9.2 = 30946.4 \text{ kip/in}$.

Each of the three elements of the series model has vertical stiffness $K_{v,Compressive,i}$ so that the combined stiffness equals 54751.3 kip/in . That is, $(1/K_{v,Compressive,i+1} + 1/K_{v,Compressive,i+1} + 1/K_{v,Compressive,i})^{-1} = 30946.4 \text{ kip/in}$ or $K_{v,Compressive,i} = 92839.2 \text{ kip/in}$.

- **Elastic Stiffness:** $\bar{K}_{lni,i}$

Element FP1:
$$\bar{K}_{lni,1} = \frac{\mu_2 W}{2Y} = \frac{0.08 \times 105}{2 \times 0.05} = 84 \text{ kip/in}$$

Element FP2:
$$\bar{K}_{lni,2} = \frac{\mu_1 W}{2Y} = \frac{0.12 \times 105}{2 \times 0.05} = 126 \text{ kip/in}$$

Element FP3:
$$\bar{K}_{lni,3} = \frac{\mu_4 W}{2Y} = \frac{0.12 \times 105}{2 \times 0.05} = 126 \text{ kip/in}$$

- **Friction Coefficient:** $\bar{\mu}_i$

Element FP1:
$$\bar{\mu}_1 = \mu_2 = \mu_3 = 0.08$$

Element FP2:
$$\bar{\mu}_2 = \mu_1 = 0.12$$

Element FP3:
$$\bar{\mu}_3 = \mu_4 = 0.12$$

- **Radius of Curvature:** $\bar{R}_{eff,i}$

Element FP1:
$$\bar{R}_{eff1} = R_{eff2} + R_{eff3} = 6 + 6 = 12 \text{ in}$$

Element FP2:
$$\bar{R}_{eff2} = R_{eff1} - R_{eff2} = 36 - 6 = 30 \text{ in}$$

Element FP3:
$$\bar{R}_{eff3} = R_{eff4} - R_{eff3} = 36 - 6 = 30 \text{ in}$$

- **Restrainer Gap Stiffness:** $\bar{K}_{GP,i}$, $\bar{K}_{GN,i}$

Element FP1:

$$\bar{K}_{GP1} = -\bar{K}_{GN1} = \frac{1}{2} \cdot \left\{ \frac{1}{4} \cdot \frac{\pi(b_1^2 - s_2^2)F_{ry}}{6Y_r} \right\} = \frac{1}{2} \cdot \left\{ \frac{1}{4} \cdot \frac{\pi(8^2 - 7^2) \cdot 25}{6 \cdot 0.5} \right\} = 49.1 \text{kip} / \text{in}$$

Element FP2:

$$\bar{K}_{GP2} = -\bar{K}_{GN2} = \frac{\pi t_{r1}(t_{r1} + s_1)F_{ry}}{6Y_r} = \frac{\pi \cdot 0.5 \cdot (0.5 + 22) \cdot 25}{6 \cdot 0.5} = 294.5 \text{kip} / \text{in}$$

Element FP3:

$$\bar{K}_{GP3} = -\bar{K}_{GN3} = \frac{\pi t_{r4}(t_{r4} + s_4)F_{ry}}{6Y_r} = \frac{\pi \cdot 0.5 \cdot (0.5 + 22) \cdot 25}{6 \cdot 0.5} = 294.5 \text{kip} / \text{in}$$

Diameter s_i , $i=1, 2$ (see Figure 5-1)

$$s_i = b_i + 2d_i$$

$$s_1 = s_4 = b_1 + 2d_1 = 8 + 2 \cdot 7 = 22 \text{in}$$

$$s_2 = s_3 = b_2 + 2d_2 = 5 + 2 \cdot 1 = 7 \text{in}$$

- **Restrainer Gap Displacement Capacity:** $\bar{d}_{GP,i}$, $\bar{d}_{GN,i}$

Element FP1: $\bar{d}_{GP1} = D_{\text{Capacity}} - \bar{d}_{GP2} - \bar{d}_{GP3} = 14.42 - 5.38 - 5.38 = 3.66 \text{in}$

Element FP2: $\bar{d}_{GP2} = \frac{(R_{\text{eff1}} - R_{\text{eff2}})}{R_{\text{eff1}}} d_1^* = \frac{(36.0 - 6.0)}{36.0} \cdot 6.46 = 5.38 \text{in}$

Element FP3: $\bar{d}_{GP3} = \frac{(R_{\text{eff4}} - R_{\text{eff3}})}{R_{\text{eff4}}} d_4^* = \frac{(36.0 - 6.0)}{36.0} \cdot 6.46 = 5.38 \text{in}$

Also,

$$\bar{d}_{GN1} = -\bar{d}_{GP1}, \quad \bar{d}_{GN2} = -\bar{d}_{GP2}, \quad \bar{d}_{GN3} = -\bar{d}_{GP3}$$

$D_{Capacity}$ is the displacement capacity of the triple FP bearing:

$$D_{Capacity} = d_1^* + d_2^* + d_3^* + d_4^* = 6.46 + 0.75 + 0.75 + 6.46 = 14.42in$$

- **Displacement at the fracture of restrainer:** $\bar{d}_{HP,i}$, $\bar{d}_{HN,i}$

$$\text{Element FP1:} \quad \bar{d}_{HP1} = -\bar{d}_{HN1} = \bar{d}_{GP1} + (t_{r2} + t_{r3}) = 3.66 + (0.5 + 0.5) = 4.66in$$

$$\text{Element FP2:} \quad \bar{d}_{HP2} = -\bar{d}_{HN2} = \bar{d}_{GP2} + t_{r1} = 5.38 + 0.5 = 5.88in$$

$$\text{Element FP3:} \quad \bar{d}_{HP3} = -\bar{d}_{HN3} = \bar{d}_{GP3} + t_{r3} = 5.38 + 0.5 = 5.88in$$

A.2.2 Model without Axial-Shear Force Interaction

- **Vertical Stiffness**

The bearing vertical stiffness is approximately calculated as AE/h , where A is the area of the center slider (diameter $b_2=5$ inch), E is a representative modulus (typically assumed about half of steel to account for flexibilities in the bearing assembly, herein 14500ksi) and h is the height (herein $2t_{CO}+h_1+h_4=9.2$ inch). The vertical stiffness is thus equal to $\pi \times 2.5^2 \times 14500 / 9.2 = 30946.4$ kip/in.

Each of the three elements of the series model has vertical stiffness $K_{v,Compressive,i}$ so that the combined stiffness equals 54751.3kip/in. That is, $(1/K_{v,Compressive,i} + 1/K_{v,Compressive,i} + 1/K_{v,Compressive,i})^{-1} = 30946.4$ kip/in or $K_{v,Compressive,i} = 92839.2$ kip/in.

For uplift (tension) $K_{v,Uplift,i} = 0.1$ kip/in.

- **Elastic Stiffness:** $\bar{K}_{\text{ini},i}$

Element FP1:
$$\bar{K}_{\text{ini},1} = \frac{\mu_2 W}{2Y} = \frac{0.08 \times 105}{2 \times 0.05} = 84 \text{kip} / \text{in}$$

Element FP2:
$$\bar{K}_{\text{ini},2} = \frac{\mu_1 W}{2Y} = \frac{0.12 \times 105}{2 \times 0.05} = 126 \text{kip} / \text{in}$$

Element FP3:
$$\bar{K}_{\text{ini},3} = \frac{\mu_4 W}{2Y} = \frac{0.12 \times 105}{2 \times 0.05} = 126 \text{kip} / \text{in}$$

- **Friction Coefficient:** $\bar{\mu}_i$

Element FP1:
$$\bar{\mu}_1 = \mu_2 = \mu_3 = 0.08$$

Element FP2:
$$\bar{\mu}_2 = \mu_1 = 0.12$$

Element FP3:
$$\bar{\mu}_3 = \mu_4 = 0.12$$

- **Radius of Curvature:** $\bar{R}_{\text{eff},i}$

Element FP1:
$$\bar{R}_{\text{eff}1} = R_{\text{eff}2} + R_{\text{eff}3} = 6.0 + 6.0 = 12 \text{in}$$

Element FP2:
$$\bar{R}_{\text{eff}2} = R_{\text{eff}1} - R_{\text{eff}2} = 36 - 6 = 30 \text{in}$$

Element FP3:
$$\bar{R}_{\text{eff}3} = R_{\text{eff}4} - R_{\text{eff}3} = 36 - 6 = 30 \text{in}$$

- **Restrainer Gap Stiffness:** $\bar{K}_{\text{GP},i}$, $\bar{K}_{\text{GN},i}$

Element FP1:

$$\bar{K}_{\text{GP}1} = -\bar{K}_{\text{GN}1} = \frac{1}{2} \cdot \left\{ \frac{1}{4} \cdot \frac{\pi(8^2 - 7^2)}{6 \cdot 0.5} \right\} = 49.1 \text{kip} / \text{in}$$

Element FP2:

$$\bar{K}_{GP2} = -\bar{K}_{GN2} = \frac{\pi t_{r1} (t_{r1} + s_1) F_{ry}}{6Y_r} = \frac{\pi \cdot 0.5 \cdot (0.5 + 22) \cdot 25}{6 \cdot 0.5} = 294.5 \text{ kip / in}$$

Element FP3:

$$\bar{K}_{GP3} = -\bar{K}_{GN3} = \frac{\pi t_{r4} (t_{r4} + s_4) F_{ry}}{6Y_r} = \frac{\pi \cdot 0.5 \cdot (0.5 + 22) \cdot 25}{6 \cdot 0.5} = 294.5 \text{ kip / in}$$

Diameter s_i , $i=1, 2$ (see Figure 5-1)

$$\begin{aligned} s_i &= b_i + 2d_i \\ s_1 = s_4 &= b_1 + 2d_1 = 8 + 2 \cdot 7 = 22 \text{ in} \\ s_2 = s_3 &= b_2 + 2d_2 = 5 + 2 \cdot 5 = 7 \text{ in} \end{aligned}$$

- **Restrainer Gap Displacement Capacity:** $\bar{d}_{GP,i}$, $\bar{d}_{GN,i}$

Element FP1: $\bar{d}_{GP1} = D_{\text{Capacity}} - \bar{d}_{GP2} - \bar{d}_{GP3} = 14.42 - 5.38 - 5.38 = 3.66 \text{ in}$

Element FP2: $\bar{d}_{GP2} = \frac{(R_{\text{eff}1} - R_{\text{eff}2})}{R_{\text{eff}1}} d_1^* = \frac{(36.0 - 6.0)}{36.0} \cdot 6.46 = 5.38 \text{ in}$

Element FP3: $\bar{d}_{GP3} = \frac{(R_{\text{eff}4} - R_{\text{eff}3})}{R_{\text{eff}4}} d_4^* = \frac{(36.0 - 6.0)}{36.0} \cdot 6.46 = 5.38 \text{ in}$

Also,

$$\bar{d}_{GN1} = -\bar{d}_{GP1}, \quad \bar{d}_{GN2} = -\bar{d}_{GP2}, \quad \bar{d}_{GN3} = -\bar{d}_{GP3}$$

D_{Capacity} is the displacement capacity of the triple FP bearing:

$$D_{\text{Capacity}} = d_1^* + d_2^* + d_3^* + d_4^* = 6.46 + 0.75 + 0.75 + 6.46 = 14.42 \text{ in}$$

- **Displacement at the fracture of restrainer:** $\bar{d}_{HP,i}$, $\bar{d}_{HN,i}$

Element FP1: $\bar{d}_{HP1} = -\bar{d}_{HN1} = \bar{d}_{GP1} + (t_{r2} + t_{r3}) = 3.66 + (0.5 + 0.5) = 4.66in$ (no restrainer)

Element FP2: $\bar{d}_{HP2} = -\bar{d}_{HN2} = \bar{d}_{GP2} + t_{r1} = 5.38 + 0.5 = 5.88in$

Element FP3: $\bar{d}_{HP3} = -\bar{d}_{HN3} = \bar{d}_{GP3} + t_{r3} = 5.38 + 0.5 = 5.88in$

MCEER Technical Reports

MCEER publishes technical reports on a variety of subjects written by authors funded through MCEER. These reports are available from both MCEER Publications and the National Technical Information Service (NTIS). Requests for reports should be directed to MCEER Publications, MCEER, University at Buffalo, State University of New York, 133A Ketter Hall, Buffalo, New York 14260. Reports can also be requested through NTIS, P.O. Box 1425, Springfield, Virginia 22151. NTIS accession numbers are shown in parenthesis, if available.

- NCEER-87-0001 "First-Year Program in Research, Education and Technology Transfer," 3/5/87, (PB88-134275, A04, MF-A01).
- NCEER-87-0002 "Experimental Evaluation of Instantaneous Optimal Algorithms for Structural Control," by R.C. Lin, T.T. Soong and A.M. Reinhorn, 4/20/87, (PB88-134341, A04, MF-A01).
- NCEER-87-0003 "Experimentation Using the Earthquake Simulation Facilities at University at Buffalo," by A.M. Reinhorn and R.L. Ketter, not available.
- NCEER-87-0004 "The System Characteristics and Performance of a Shaking Table," by J.S. Hwang, K.C. Chang and G.C. Lee, 6/1/87, (PB88-134259, A03, MF-A01). This report is available only through NTIS (see address given above).
- NCEER-87-0005 "A Finite Element Formulation for Nonlinear Viscoplastic Material Using a Q Model," by O. Gyebe and G. Dasgupta, 11/2/87, (PB88-213764, A08, MF-A01).
- NCEER-87-0006 "Symbolic Manipulation Program (SMP) - Algebraic Codes for Two and Three Dimensional Finite Element Formulations," by X. Lee and G. Dasgupta, 11/9/87, (PB88-218522, A05, MF-A01).
- NCEER-87-0007 "Instantaneous Optimal Control Laws for Tall Buildings Under Seismic Excitations," by J.N. Yang, A. Akbarpour and P. Ghaemmaghami, 6/10/87, (PB88-134333, A06, MF-A01). This report is only available through NTIS (see address given above).
- NCEER-87-0008 "IDARC: Inelastic Damage Analysis of Reinforced Concrete Frame - Shear-Wall Structures," by Y.J. Park, A.M. Reinhorn and S.K. Kunnath, 7/20/87, (PB88-134325, A09, MF-A01). This report is only available through NTIS (see address given above).
- NCEER-87-0009 "Liquefaction Potential for New York State: A Preliminary Report on Sites in Manhattan and Buffalo," by M. Budhu, V. Vijayakumar, R.F. Giese and L. Baumgras, 8/31/87, (PB88-163704, A03, MF-A01). This report is available only through NTIS (see address given above).
- NCEER-87-0010 "Vertical and Torsional Vibration of Foundations in Inhomogeneous Media," by A.S. Veletsos and K.W. Dotson, 6/1/87, (PB88-134291, A03, MF-A01). This report is only available through NTIS (see address given above).
- NCEER-87-0011 "Seismic Probabilistic Risk Assessment and Seismic Margins Studies for Nuclear Power Plants," by Howard H.M. Hwang, 6/15/87, (PB88-134267, A03, MF-A01). This report is only available through NTIS (see address given above).
- NCEER-87-0012 "Parametric Studies of Frequency Response of Secondary Systems Under Ground-Acceleration Excitations," by Y. Yong and Y.K. Lin, 6/10/87, (PB88-134309, A03, MF-A01). This report is only available through NTIS (see address given above).
- NCEER-87-0013 "Frequency Response of Secondary Systems Under Seismic Excitation," by J.A. HoLung, J. Cai and Y.K. Lin, 7/31/87, (PB88-134317, A05, MF-A01). This report is only available through NTIS (see address given above).
- NCEER-87-0014 "Modelling Earthquake Ground Motions in Seismically Active Regions Using Parametric Time Series Methods," by G.W. Ellis and A.S. Cakmak, 8/25/87, (PB88-134283, A08, MF-A01). This report is only available through NTIS (see address given above).

- NCEER-87-0015 "Detection and Assessment of Seismic Structural Damage," by E. DiPasquale and A.S. Cakmak, 8/25/87, (PB88-163712, A05, MF-A01). This report is only available through NTIS (see address given above).
- NCEER-87-0016 "Pipeline Experiment at Parkfield, California," by J. Isenberg and E. Richardson, 9/15/87, (PB88-163720, A03, MF-A01). This report is available only through NTIS (see address given above).
- NCEER-87-0017 "Digital Simulation of Seismic Ground Motion," by M. Shinozuka, G. Deodatis and T. Harada, 8/31/87, (PB88-155197, A04, MF-A01). This report is available only through NTIS (see address given above).
- NCEER-87-0018 "Practical Considerations for Structural Control: System Uncertainty, System Time Delay and Truncation of Small Control Forces," J.N. Yang and A. Akbarpour, 8/10/87, (PB88-163738, A08, MF-A01). This report is only available through NTIS (see address given above).
- NCEER-87-0019 "Modal Analysis of Nonclassically Damped Structural Systems Using Canonical Transformation," by J.N. Yang, S. Sarkani and F.X. Long, 9/27/87, (PB88-187851, A04, MF-A01).
- NCEER-87-0020 "A Nonstationary Solution in Random Vibration Theory," by J.R. Red-Horse and P.D. Spanos, 11/3/87, (PB88-163746, A03, MF-A01).
- NCEER-87-0021 "Horizontal Impedances for Radially Inhomogeneous Viscoelastic Soil Layers," by A.S. Veletsos and K.W. Dotson, 10/15/87, (PB88-150859, A04, MF-A01).
- NCEER-87-0022 "Seismic Damage Assessment of Reinforced Concrete Members," by Y.S. Chung, C. Meyer and M. Shinozuka, 10/9/87, (PB88-150867, A05, MF-A01). This report is available only through NTIS (see address given above).
- NCEER-87-0023 "Active Structural Control in Civil Engineering," by T.T. Soong, 11/11/87, (PB88-187778, A03, MF-A01).
- NCEER-87-0024 "Vertical and Torsional Impedances for Radially Inhomogeneous Viscoelastic Soil Layers," by K.W. Dotson and A.S. Veletsos, 12/87, (PB88-187786, A03, MF-A01).
- NCEER-87-0025 "Proceedings from the Symposium on Seismic Hazards, Ground Motions, Soil-Liquefaction and Engineering Practice in Eastern North America," October 20-22, 1987, edited by K.H. Jacob, 12/87, (PB88-188115, A23, MF-A01). This report is available only through NTIS (see address given above).
- NCEER-87-0026 "Report on the Whittier-Narrows, California, Earthquake of October 1, 1987," by J. Pantelic and A. Reinhorn, 11/87, (PB88-187752, A03, MF-A01). This report is available only through NTIS (see address given above).
- NCEER-87-0027 "Design of a Modular Program for Transient Nonlinear Analysis of Large 3-D Building Structures," by S. Srivastav and J.F. Abel, 12/30/87, (PB88-187950, A05, MF-A01). This report is only available through NTIS (see address given above).
- NCEER-87-0028 "Second-Year Program in Research, Education and Technology Transfer," 3/8/88, (PB88-219480, A04, MF-A01).
- NCEER-88-0001 "Workshop on Seismic Computer Analysis and Design of Buildings With Interactive Graphics," by W. McGuire, J.F. Abel and C.H. Conley, 1/18/88, (PB88-187760, A03, MF-A01). This report is only available through NTIS (see address given above).
- NCEER-88-0002 "Optimal Control of Nonlinear Flexible Structures," by J.N. Yang, F.X. Long and D. Wong, 1/22/88, (PB88-213772, A06, MF-A01).
- NCEER-88-0003 "Substructuring Techniques in the Time Domain for Primary-Secondary Structural Systems," by G.D. Manolis and G. Juhn, 2/10/88, (PB88-213780, A04, MF-A01).
- NCEER-88-0004 "Iterative Seismic Analysis of Primary-Secondary Systems," by A. Singhal, L.D. Lutes and P.D. Spanos, 2/23/88, (PB88-213798, A04, MF-A01).
- NCEER-88-0005 "Stochastic Finite Element Expansion for Random Media," by P.D. Spanos and R. Ghanem, 3/14/88, (PB88-213806, A03, MF-A01).

- NCEER-88-0006 "Combining Structural Optimization and Structural Control," by F.Y. Cheng and C.P. Pantelides, 1/10/88, (PB88-213814, A05, MF-A01).
- NCEER-88-0007 "Seismic Performance Assessment of Code-Designed Structures," by H.H-M. Hwang, J-W. Jaw and H-J. Shau, 3/20/88, (PB88-219423, A04, MF-A01). This report is only available through NTIS (see address given above).
- NCEER-88-0008 "Reliability Analysis of Code-Designed Structures Under Natural Hazards," by H.H-M. Hwang, H. Ushiba and M. Shinozuka, 2/29/88, (PB88-229471, A07, MF-A01). This report is only available through NTIS (see address given above).
- NCEER-88-0009 "Seismic Fragility Analysis of Shear Wall Structures," by J-W Jaw and H.H-M. Hwang, 4/30/88, (PB89-102867, A04, MF-A01).
- NCEER-88-0010 "Base Isolation of a Multi-Story Building Under a Harmonic Ground Motion - A Comparison of Performances of Various Systems," by F-G Fan, G. Ahmadi and I.G. Tadjbakhsh, 5/18/88, (PB89-122238, A06, MF-A01). This report is only available through NTIS (see address given above).
- NCEER-88-0011 "Seismic Floor Response Spectra for a Combined System by Green's Functions," by F.M. Lavelle, L.A. Bergman and P.D. Spanos, 5/1/88, (PB89-102875, A03, MF-A01).
- NCEER-88-0012 "A New Solution Technique for Randomly Excited Hysteretic Structures," by G.Q. Cai and Y.K. Lin, 5/16/88, (PB89-102883, A03, MF-A01).
- NCEER-88-0013 "A Study of Radiation Damping and Soil-Structure Interaction Effects in the Centrifuge," by K. Weissman, supervised by J.H. Prevost, 5/24/88, (PB89-144703, A06, MF-A01).
- NCEER-88-0014 "Parameter Identification and Implementation of a Kinematic Plasticity Model for Frictional Soils," by J.H. Prevost and D.V. Griffiths, not available.
- NCEER-88-0015 "Two- and Three- Dimensional Dynamic Finite Element Analyses of the Long Valley Dam," by D.V. Griffiths and J.H. Prevost, 6/17/88, (PB89-144711, A04, MF-A01).
- NCEER-88-0016 "Damage Assessment of Reinforced Concrete Structures in Eastern United States," by A.M. Reinhorn, M.J. Seidel, S.K. Kunnath and Y.J. Park, 6/15/88, (PB89-122220, A04, MF-A01). This report is only available through NTIS (see address given above).
- NCEER-88-0017 "Dynamic Compliance of Vertically Loaded Strip Foundations in Multilayered Viscoelastic Soils," by S. Ahmad and A.S.M. Israil, 6/17/88, (PB89-102891, A04, MF-A01).
- NCEER-88-0018 "An Experimental Study of Seismic Structural Response With Added Viscoelastic Dampers," by R.C. Lin, Z. Liang, T.T. Soong and R.H. Zhang, 6/30/88, (PB89-122212, A05, MF-A01). This report is available only through NTIS (see address given above).
- NCEER-88-0019 "Experimental Investigation of Primary - Secondary System Interaction," by G.D. Manolis, G. Juhn and A.M. Reinhorn, 5/27/88, (PB89-122204, A04, MF-A01).
- NCEER-88-0020 "A Response Spectrum Approach For Analysis of Nonclassically Damped Structures," by J.N. Yang, S. Sarkani and F.X. Long, 4/22/88, (PB89-102909, A04, MF-A01).
- NCEER-88-0021 "Seismic Interaction of Structures and Soils: Stochastic Approach," by A.S. Veletsos and A.M. Prasad, 7/21/88, (PB89-122196, A04, MF-A01). This report is only available through NTIS (see address given above).
- NCEER-88-0022 "Identification of the Serviceability Limit State and Detection of Seismic Structural Damage," by E. DiPasquale and A.S. Cakmak, 6/15/88, (PB89-122188, A05, MF-A01). This report is available only through NTIS (see address given above).
- NCEER-88-0023 "Multi-Hazard Risk Analysis: Case of a Simple Offshore Structure," by B.K. Bhartia and E.H. Vanmarcke, 7/21/88, (PB89-145213, A05, MF-A01).

- NCEER-88-0024 "Automated Seismic Design of Reinforced Concrete Buildings," by Y.S. Chung, C. Meyer and M. Shinozuka, 7/5/88, (PB89-122170, A06, MF-A01). This report is available only through NTIS (see address given above).
- NCEER-88-0025 "Experimental Study of Active Control of MDOF Structures Under Seismic Excitations," by L.L. Chung, R.C. Lin, T.T. Soong and A.M. Reinhorn, 7/10/88, (PB89-122600, A04, MF-A01).
- NCEER-88-0026 "Earthquake Simulation Tests of a Low-Rise Metal Structure," by J.S. Hwang, K.C. Chang, G.C. Lee and R.L. Ketter, 8/1/88, (PB89-102917, A04, MF-A01).
- NCEER-88-0027 "Systems Study of Urban Response and Reconstruction Due to Catastrophic Earthquakes," by F. Kozin and H.K. Zhou, 9/22/88, (PB90-162348, A04, MF-A01).
- NCEER-88-0028 "Seismic Fragility Analysis of Plane Frame Structures," by H.H-M. Hwang and Y.K. Low, 7/31/88, (PB89-131445, A06, MF-A01).
- NCEER-88-0029 "Response Analysis of Stochastic Structures," by A. Kardara, C. Bucher and M. Shinozuka, 9/22/88, (PB89-174429, A04, MF-A01).
- NCEER-88-0030 "Nonnormal Accelerations Due to Yielding in a Primary Structure," by D.C.K. Chen and L.D. Lutes, 9/19/88, (PB89-131437, A04, MF-A01).
- NCEER-88-0031 "Design Approaches for Soil-Structure Interaction," by A.S. Veletsos, A.M. Prasad and Y. Tang, 12/30/88, (PB89-174437, A03, MF-A01). This report is available only through NTIS (see address given above).
- NCEER-88-0032 "A Re-evaluation of Design Spectra for Seismic Damage Control," by C.J. Turkstra and A.G. Tallin, 11/7/88, (PB89-145221, A05, MF-A01).
- NCEER-88-0033 "The Behavior and Design of Noncontact Lap Splices Subjected to Repeated Inelastic Tensile Loading," by V.E. Sagan, P. Gergely and R.N. White, 12/8/88, (PB89-163737, A08, MF-A01).
- NCEER-88-0034 "Seismic Response of Pile Foundations," by S.M. Mamoon, P.K. Banerjee and S. Ahmad, 11/1/88, (PB89-145239, A04, MF-A01).
- NCEER-88-0035 "Modeling of R/C Building Structures With Flexible Floor Diaphragms (IDARC2)," by A.M. Reinhorn, S.K. Kunnath and N. Panahshahi, 9/7/88, (PB89-207153, A07, MF-A01).
- NCEER-88-0036 "Solution of the Dam-Reservoir Interaction Problem Using a Combination of FEM, BEM with Particular Integrals, Modal Analysis, and Substructuring," by C-S. Tsai, G.C. Lee and R.L. Ketter, 12/31/88, (PB89-207146, A04, MF-A01).
- NCEER-88-0037 "Optimal Placement of Actuators for Structural Control," by F.Y. Cheng and C.P. Pantelides, 8/15/88, (PB89-162846, A05, MF-A01).
- NCEER-88-0038 "Teflon Bearings in Aseismic Base Isolation: Experimental Studies and Mathematical Modeling," by A. Mokha, M.C. Constantinou and A.M. Reinhorn, 12/5/88, (PB89-218457, A10, MF-A01). This report is available only through NTIS (see address given above).
- NCEER-88-0039 "Seismic Behavior of Flat Slab High-Rise Buildings in the New York City Area," by P. Weidlinger and M. Ettouney, 10/15/88, (PB90-145681, A04, MF-A01).
- NCEER-88-0040 "Evaluation of the Earthquake Resistance of Existing Buildings in New York City," by P. Weidlinger and M. Ettouney, 10/15/88, not available.
- NCEER-88-0041 "Small-Scale Modeling Techniques for Reinforced Concrete Structures Subjected to Seismic Loads," by W. Kim, A. El-Attar and R.N. White, 11/22/88, (PB89-189625, A05, MF-A01).
- NCEER-88-0042 "Modeling Strong Ground Motion from Multiple Event Earthquakes," by G.W. Ellis and A.S. Cakmak, 10/15/88, (PB89-174445, A03, MF-A01).

- NCEER-88-0043 "Nonstationary Models of Seismic Ground Acceleration," by M. Grigoriu, S.E. Ruiz and E. Rosenblueth, 7/15/88, (PB89-189617, A04, MF-A01).
- NCEER-88-0044 "SARCF User's Guide: Seismic Analysis of Reinforced Concrete Frames," by Y.S. Chung, C. Meyer and M. Shinozuka, 11/9/88, (PB89-174452, A08, MF-A01).
- NCEER-88-0045 "First Expert Panel Meeting on Disaster Research and Planning," edited by J. Pantelic and J. Stoyke, 9/15/88, (PB89-174460, A05, MF-A01).
- NCEER-88-0046 "Preliminary Studies of the Effect of Degrading Infill Walls on the Nonlinear Seismic Response of Steel Frames," by C.Z. Chrysostomou, P. Gergely and J.F. Abel, 12/19/88, (PB89-208383, A05, MF-A01).
- NCEER-88-0047 "Reinforced Concrete Frame Component Testing Facility - Design, Construction, Instrumentation and Operation," by S.P. Pessiki, C. Conley, T. Bond, P. Gergely and R.N. White, 12/16/88, (PB89-174478, A04, MF-A01).
- NCEER-89-0001 "Effects of Protective Cushion and Soil Compliancy on the Response of Equipment Within a Seismically Excited Building," by J.A. HoLung, 2/16/89, (PB89-207179, A04, MF-A01).
- NCEER-89-0002 "Statistical Evaluation of Response Modification Factors for Reinforced Concrete Structures," by H.H-M. Hwang and J-W. Jaw, 2/17/89, (PB89-207187, A05, MF-A01).
- NCEER-89-0003 "Hysteretic Columns Under Random Excitation," by G-Q. Cai and Y.K. Lin, 1/9/89, (PB89-196513, A03, MF-A01).
- NCEER-89-0004 "Experimental Study of 'Elephant Foot Bulge' Instability of Thin-Walled Metal Tanks," by Z-H. Jia and R.L. Ketter, 2/22/89, (PB89-207195, A03, MF-A01).
- NCEER-89-0005 "Experiment on Performance of Buried Pipelines Across San Andreas Fault," by J. Isenberg, E. Richardson and T.D. O'Rourke, 3/10/89, (PB89-218440, A04, MF-A01). This report is available only through NTIS (see address given above).
- NCEER-89-0006 "A Knowledge-Based Approach to Structural Design of Earthquake-Resistant Buildings," by M. Subramani, P. Gergely, C.H. Conley, J.F. Abel and A.H. Zaghaw, 1/15/89, (PB89-218465, A06, MF-A01).
- NCEER-89-0007 "Liquefaction Hazards and Their Effects on Buried Pipelines," by T.D. O'Rourke and P.A. Lane, 2/1/89, (PB89-218481, A09, MF-A01).
- NCEER-89-0008 "Fundamentals of System Identification in Structural Dynamics," by H. Imai, C-B. Yun, O. Maruyama and M. Shinozuka, 1/26/89, (PB89-207211, A04, MF-A01).
- NCEER-89-0009 "Effects of the 1985 Michoacan Earthquake on Water Systems and Other Buried Lifelines in Mexico," by A.G. Ayala and M.J. O'Rourke, 3/8/89, (PB89-207229, A06, MF-A01).
- NCEER-89-R010 "NCEER Bibliography of Earthquake Education Materials," by K.E.K. Ross, Second Revision, 9/1/89, (PB90-125352, A05, MF-A01). This report is replaced by NCEER-92-0018.
- NCEER-89-0011 "Inelastic Three-Dimensional Response Analysis of Reinforced Concrete Building Structures (IDARC-3D), Part I - Modeling," by S.K. Kunnath and A.M. Reinhorn, 4/17/89, (PB90-114612, A07, MF-A01). This report is available only through NTIS (see address given above).
- NCEER-89-0012 "Recommended Modifications to ATC-14," by C.D. Poland and J.O. Malley, 4/12/89, (PB90-108648, A15, MF-A01).
- NCEER-89-0013 "Repair and Strengthening of Beam-to-Column Connections Subjected to Earthquake Loading," by M. Corazao and A.J. Durrani, 2/28/89, (PB90-109885, A06, MF-A01).
- NCEER-89-0014 "Program EXKAL2 for Identification of Structural Dynamic Systems," by O. Maruyama, C-B. Yun, M. Hoshiya and M. Shinozuka, 5/19/89, (PB90-109877, A09, MF-A01).

- NCEER-89-0015 "Response of Frames With Bolted Semi-Rigid Connections, Part I - Experimental Study and Analytical Predictions," by P.J. DiCorso, A.M. Reinhorn, J.R. Dickerson, J.B. Radzimirski and W.L. Harper, 6/1/89, not available.
- NCEER-89-0016 "ARMA Monte Carlo Simulation in Probabilistic Structural Analysis," by P.D. Spanos and M.P. Mignolet, 7/10/89, (PB90-109893, A03, MF-A01).
- NCEER-89-P017 "Preliminary Proceedings from the Conference on Disaster Preparedness - The Place of Earthquake Education in Our Schools," Edited by K.E.K. Ross, 6/23/89, (PB90-108606, A03, MF-A01).
- NCEER-89-0017 "Proceedings from the Conference on Disaster Preparedness - The Place of Earthquake Education in Our Schools," Edited by K.E.K. Ross, 12/31/89, (PB90-207895, A012, MF-A02). This report is available only through NTIS (see address given above).
- NCEER-89-0018 "Multidimensional Models of Hysteretic Material Behavior for Vibration Analysis of Shape Memory Energy Absorbing Devices, by E.J. Graesser and F.A. Cozzarelli, 6/7/89, (PB90-164146, A04, MF-A01).
- NCEER-89-0019 "Nonlinear Dynamic Analysis of Three-Dimensional Base Isolated Structures (3D-BASIS)," by S. Nagarajaiah, A.M. Reinhorn and M.C. Constantinou, 8/3/89, (PB90-161936, A06, MF-A01). This report has been replaced by NCEER-93-0011.
- NCEER-89-0020 "Structural Control Considering Time-Rate of Control Forces and Control Rate Constraints," by F.Y. Cheng and C.P. Pantelides, 8/3/89, (PB90-120445, A04, MF-A01).
- NCEER-89-0021 "Subsurface Conditions of Memphis and Shelby County," by K.W. Ng, T-S. Chang and H-H.M. Hwang, 7/26/89, (PB90-120437, A03, MF-A01).
- NCEER-89-0022 "Seismic Wave Propagation Effects on Straight Jointed Buried Pipelines," by K. Elhmadi and M.J. O'Rourke, 8/24/89, (PB90-162322, A10, MF-A02).
- NCEER-89-0023 "Workshop on Serviceability Analysis of Water Delivery Systems," edited by M. Grigoriu, 3/6/89, (PB90-127424, A03, MF-A01).
- NCEER-89-0024 "Shaking Table Study of a 1/5 Scale Steel Frame Composed of Tapered Members," by K.C. Chang, J.S. Hwang and G.C. Lee, 9/18/89, (PB90-160169, A04, MF-A01).
- NCEER-89-0025 "DYNA1D: A Computer Program for Nonlinear Seismic Site Response Analysis - Technical Documentation," by Jean H. Prevost, 9/14/89, (PB90-161944, A07, MF-A01). This report is available only through NTIS (see address given above).
- NCEER-89-0026 "1:4 Scale Model Studies of Active Tendon Systems and Active Mass Dampers for Aseismic Protection," by A.M. Reinhorn, T.T. Soong, R.C. Lin, Y.P. Yang, Y. Fukao, H. Abe and M. Nakai, 9/15/89, (PB90-173246, A10, MF-A02). This report is available only through NTIS (see address given above).
- NCEER-89-0027 "Scattering of Waves by Inclusions in a Nonhomogeneous Elastic Half Space Solved by Boundary Element Methods," by P.K. Hadley, A. Askar and A.S. Cakmak, 6/15/89, (PB90-145699, A07, MF-A01).
- NCEER-89-0028 "Statistical Evaluation of Deflection Amplification Factors for Reinforced Concrete Structures," by H.H.M. Hwang, J-W. Jaw and A.L. Ch'ng, 8/31/89, (PB90-164633, A05, MF-A01).
- NCEER-89-0029 "Bedrock Accelerations in Memphis Area Due to Large New Madrid Earthquakes," by H.H.M. Hwang, C.H.S. Chen and G. Yu, 11/7/89, (PB90-162330, A04, MF-A01).
- NCEER-89-0030 "Seismic Behavior and Response Sensitivity of Secondary Structural Systems," by Y.Q. Chen and T.T. Soong, 10/23/89, (PB90-164658, A08, MF-A01).
- NCEER-89-0031 "Random Vibration and Reliability Analysis of Primary-Secondary Structural Systems," by Y. Ibrahim, M. Grigoriu and T.T. Soong, 11/10/89, (PB90-161951, A04, MF-A01).

- NCEER-89-0032 "Proceedings from the Second U.S. - Japan Workshop on Liquefaction, Large Ground Deformation and Their Effects on Lifelines, September 26-29, 1989," Edited by T.D. O'Rourke and M. Hamada, 12/1/89, (PB90-209388, A22, MF-A03).
- NCEER-89-0033 "Deterministic Model for Seismic Damage Evaluation of Reinforced Concrete Structures," by J.M. Bracci, A.M. Reinhorn, J.B. Mander and S.K. Kunnath, 9/27/89, (PB91-108803, A06, MF-A01).
- NCEER-89-0034 "On the Relation Between Local and Global Damage Indices," by E. DiPasquale and A.S. Cakmak, 8/15/89, (PB90-173865, A05, MF-A01).
- NCEER-89-0035 "Cyclic Undrained Behavior of Nonplastic and Low Plasticity Silts," by A.J. Walker and H.E. Stewart, 7/26/89, (PB90-183518, A10, MF-A01).
- NCEER-89-0036 "Liquefaction Potential of Surficial Deposits in the City of Buffalo, New York," by M. Budhu, R. Giese and L. Baumgrass, 1/17/89, (PB90-208455, A04, MF-A01).
- NCEER-89-0037 "A Deterministic Assessment of Effects of Ground Motion Incoherence," by A.S. Veletsos and Y. Tang, 7/15/89, (PB90-164294, A03, MF-A01).
- NCEER-89-0038 "Workshop on Ground Motion Parameters for Seismic Hazard Mapping," July 17-18, 1989, edited by R.V. Whitman, 12/1/89, (PB90-173923, A04, MF-A01).
- NCEER-89-0039 "Seismic Effects on Elevated Transit Lines of the New York City Transit Authority," by C.J. Costantino, C.A. Miller and E. Heymsfield, 12/26/89, (PB90-207887, A06, MF-A01).
- NCEER-89-0040 "Centrifugal Modeling of Dynamic Soil-Structure Interaction," by K. Weissman, Supervised by J.H. Prevost, 5/10/89, (PB90-207879, A07, MF-A01).
- NCEER-89-0041 "Linearized Identification of Buildings With Cores for Seismic Vulnerability Assessment," by I-K. Ho and A.E. Aktan, 11/1/89, (PB90-251943, A07, MF-A01).
- NCEER-90-0001 "Geotechnical and Lifeline Aspects of the October 17, 1989 Loma Prieta Earthquake in San Francisco," by T.D. O'Rourke, H.E. Stewart, F.T. Blackburn and T.S. Dickerman, 1/90, (PB90-208596, A05, MF-A01).
- NCEER-90-0002 "Nonnormal Secondary Response Due to Yielding in a Primary Structure," by D.C.K. Chen and L.D. Lutes, 2/28/90, (PB90-251976, A07, MF-A01).
- NCEER-90-0003 "Earthquake Education Materials for Grades K-12," by K.E.K. Ross, 4/16/90, (PB91-251984, A05, MF-A05). This report has been replaced by NCEER-92-0018.
- NCEER-90-0004 "Catalog of Strong Motion Stations in Eastern North America," by R.W. Busby, 4/3/90, (PB90-251984, A05, MF-A01).
- NCEER-90-0005 "NCEER Strong-Motion Data Base: A User Manual for the GeoBase Release (Version 1.0 for the Sun3)," by P. Friberg and K. Jacob, 3/31/90 (PB90-258062, A04, MF-A01).
- NCEER-90-0006 "Seismic Hazard Along a Crude Oil Pipeline in the Event of an 1811-1812 Type New Madrid Earthquake," by H.H.M. Hwang and C-H.S. Chen, 4/16/90, (PB90-258054, A04, MF-A01).
- NCEER-90-0007 "Site-Specific Response Spectra for Memphis Sheahan Pumping Station," by H.H.M. Hwang and C.S. Lee, 5/15/90, (PB91-108811, A05, MF-A01).
- NCEER-90-0008 "Pilot Study on Seismic Vulnerability of Crude Oil Transmission Systems," by T. Ariman, R. Dobry, M. Grigoriu, F. Kozin, M. O'Rourke, T. O'Rourke and M. Shinozuka, 5/25/90, (PB91-108837, A06, MF-A01).
- NCEER-90-0009 "A Program to Generate Site Dependent Time Histories: EQGEN," by G.W. Ellis, M. Srinivasan and A.S. Cakmak, 1/30/90, (PB91-108829, A04, MF-A01).
- NCEER-90-0010 "Active Isolation for Seismic Protection of Operating Rooms," by M.E. Talbott, Supervised by M. Shinozuka, 6/8/9, (PB91-110205, A05, MF-A01).

- NCEER-90-0011 "Program LINEARID for Identification of Linear Structural Dynamic Systems," by C-B. Yun and M. Shinozuka, 6/25/90, (PB91-110312, A08, MF-A01).
- NCEER-90-0012 "Two-Dimensional Two-Phase Elasto-Plastic Seismic Response of Earth Dams," by A.N. Yiagos, Supervised by J.H. Prevost, 6/20/90, (PB91-110197, A13, MF-A02).
- NCEER-90-0013 "Secondary Systems in Base-Isolated Structures: Experimental Investigation, Stochastic Response and Stochastic Sensitivity," by G.D. Manolis, G. Juhn, M.C. Constantinou and A.M. Reinhorn, 7/1/90, (PB91-110320, A08, MF-A01).
- NCEER-90-0014 "Seismic Behavior of Lightly-Reinforced Concrete Column and Beam-Column Joint Details," by S.P. Pessiki, C.H. Conley, P. Gergely and R.N. White, 8/22/90, (PB91-108795, A11, MF-A02).
- NCEER-90-0015 "Two Hybrid Control Systems for Building Structures Under Strong Earthquakes," by J.N. Yang and A. Daniellians, 6/29/90, (PB91-125393, A04, MF-A01).
- NCEER-90-0016 "Instantaneous Optimal Control with Acceleration and Velocity Feedback," by J.N. Yang and Z. Li, 6/29/90, (PB91-125401, A03, MF-A01).
- NCEER-90-0017 "Reconnaissance Report on the Northern Iran Earthquake of June 21, 1990," by M. Mehrain, 10/4/90, (PB91-125377, A03, MF-A01).
- NCEER-90-0018 "Evaluation of Liquefaction Potential in Memphis and Shelby County," by T.S. Chang, P.S. Tang, C.S. Lee and H. Hwang, 8/10/90, (PB91-125427, A09, MF-A01).
- NCEER-90-0019 "Experimental and Analytical Study of a Combined Sliding Disc Bearing and Helical Steel Spring Isolation System," by M.C. Constantinou, A.S. Mokha and A.M. Reinhorn, 10/4/90, (PB91-125385, A06, MF-A01). This report is available only through NTIS (see address given above).
- NCEER-90-0020 "Experimental Study and Analytical Prediction of Earthquake Response of a Sliding Isolation System with a Spherical Surface," by A.S. Mokha, M.C. Constantinou and A.M. Reinhorn, 10/11/90, (PB91-125419, A05, MF-A01).
- NCEER-90-0021 "Dynamic Interaction Factors for Floating Pile Groups," by G. Gazetas, K. Fan, A. Kaynia and E. Kausel, 9/10/90, (PB91-170381, A05, MF-A01).
- NCEER-90-0022 "Evaluation of Seismic Damage Indices for Reinforced Concrete Structures," by S. Rodriguez-Gomez and A.S. Cakmak, 9/30/90, PB91-171322, A06, MF-A01).
- NCEER-90-0023 "Study of Site Response at a Selected Memphis Site," by H. Desai, S. Ahmad, E.S. Gazetas and M.R. Oh, 10/11/90, (PB91-196857, A03, MF-A01).
- NCEER-90-0024 "A User's Guide to Strongmo: Version 1.0 of NCEER's Strong-Motion Data Access Tool for PCs and Terminals," by P.A. Friberg and C.A.T. Susch, 11/15/90, (PB91-171272, A03, MF-A01).
- NCEER-90-0025 "A Three-Dimensional Analytical Study of Spatial Variability of Seismic Ground Motions," by L-L. Hong and A.H.-S. Ang, 10/30/90, (PB91-170399, A09, MF-A01).
- NCEER-90-0026 "MUMOID User's Guide - A Program for the Identification of Modal Parameters," by S. Rodriguez-Gomez and E. DiPasquale, 9/30/90, (PB91-171298, A04, MF-A01).
- NCEER-90-0027 "SARCF-II User's Guide - Seismic Analysis of Reinforced Concrete Frames," by S. Rodriguez-Gomez, Y.S. Chung and C. Meyer, 9/30/90, (PB91-171280, A05, MF-A01).
- NCEER-90-0028 "Viscous Dampers: Testing, Modeling and Application in Vibration and Seismic Isolation," by N. Makris and M.C. Constantinou, 12/20/90 (PB91-190561, A06, MF-A01).
- NCEER-90-0029 "Soil Effects on Earthquake Ground Motions in the Memphis Area," by H. Hwang, C.S. Lee, K.W. Ng and T.S. Chang, 8/2/90, (PB91-190751, A05, MF-A01).

- NCEER-91-0001 "Proceedings from the Third Japan-U.S. Workshop on Earthquake Resistant Design of Lifeline Facilities and Countermeasures for Soil Liquefaction, December 17-19, 1990," edited by T.D. O'Rourke and M. Hamada, 2/1/91, (PB91-179259, A99, MF-A04).
- NCEER-91-0002 "Physical Space Solutions of Non-Proportionally Damped Systems," by M. Tong, Z. Liang and G.C. Lee, 1/15/91, (PB91-179242, A04, MF-A01).
- NCEER-91-0003 "Seismic Response of Single Piles and Pile Groups," by K. Fan and G. Gazetas, 1/10/91, (PB92-174994, A04, MF-A01).
- NCEER-91-0004 "Damping of Structures: Part 1 - Theory of Complex Damping," by Z. Liang and G. Lee, 10/10/91, (PB92-197235, A12, MF-A03).
- NCEER-91-0005 "3D-BASIS - Nonlinear Dynamic Analysis of Three Dimensional Base Isolated Structures: Part II," by S. Nagarajaiah, A.M. Reinhorn and M.C. Constantinou, 2/28/91, (PB91-190553, A07, MF-A01). This report has been replaced by NCEER-93-0011.
- NCEER-91-0006 "A Multidimensional Hysteretic Model for Plasticity Deforming Metals in Energy Absorbing Devices," by E.J. Graesser and F.A. Cozzarelli, 4/9/91, (PB92-108364, A04, MF-A01).
- NCEER-91-0007 "A Framework for Customizable Knowledge-Based Expert Systems with an Application to a KBES for Evaluating the Seismic Resistance of Existing Buildings," by E.G. Ibarra-Anaya and S.J. Fenves, 4/9/91, (PB91-210930, A08, MF-A01).
- NCEER-91-0008 "Nonlinear Analysis of Steel Frames with Semi-Rigid Connections Using the Capacity Spectrum Method," by G.G. Deierlein, S-H. Hsieh, Y-J. Shen and J.F. Abel, 7/2/91, (PB92-113828, A05, MF-A01).
- NCEER-91-0009 "Earthquake Education Materials for Grades K-12," by K.E.K. Ross, 4/30/91, (PB91-212142, A06, MF-A01). This report has been replaced by NCEER-92-0018.
- NCEER-91-0010 "Phase Wave Velocities and Displacement Phase Differences in a Harmonically Oscillating Pile," by N. Makris and G. Gazetas, 7/8/91, (PB92-108356, A04, MF-A01).
- NCEER-91-0011 "Dynamic Characteristics of a Full-Size Five-Story Steel Structure and a 2/5 Scale Model," by K.C. Chang, G.C. Yao, G.C. Lee, D.S. Hao and Y.C. Yeh, 7/2/91, (PB93-116648, A06, MF-A02).
- NCEER-91-0012 "Seismic Response of a 2/5 Scale Steel Structure with Added Viscoelastic Dampers," by K.C. Chang, T.T. Soong, S-T. Oh and M.L. Lai, 5/17/91, (PB92-110816, A05, MF-A01).
- NCEER-91-0013 "Earthquake Response of Retaining Walls; Full-Scale Testing and Computational Modeling," by S. Alampalli and A-W.M. Elgamal, 6/20/91, not available.
- NCEER-91-0014 "3D-BASIS-M: Nonlinear Dynamic Analysis of Multiple Building Base Isolated Structures," by P.C. Tsopelas, S. Nagarajaiah, M.C. Constantinou and A.M. Reinhorn, 5/28/91, (PB92-113885, A09, MF-A02).
- NCEER-91-0015 "Evaluation of SEAOC Design Requirements for Sliding Isolated Structures," by D. Theodossiou and M.C. Constantinou, 6/10/91, (PB92-114602, A11, MF-A03).
- NCEER-91-0016 "Closed-Loop Modal Testing of a 27-Story Reinforced Concrete Flat Plate-Core Building," by H.R. Somaprasad, T. Toksoy, H. Yoshiyuki and A.E. Aktan, 7/15/91, (PB92-129980, A07, MF-A02).
- NCEER-91-0017 "Shake Table Test of a 1/6 Scale Two-Story Lightly Reinforced Concrete Building," by A.G. El-Attar, R.N. White and P. Gergely, 2/28/91, (PB92-222447, A06, MF-A02).
- NCEER-91-0018 "Shake Table Test of a 1/8 Scale Three-Story Lightly Reinforced Concrete Building," by A.G. El-Attar, R.N. White and P. Gergely, 2/28/91, (PB93-116630, A08, MF-A02).
- NCEER-91-0019 "Transfer Functions for Rigid Rectangular Foundations," by A.S. Veletsos, A.M. Prasad and W.H. Wu, 7/31/91, not available.

- NCEER-91-0020 "Hybrid Control of Seismic-Excited Nonlinear and Inelastic Structural Systems," by J.N. Yang, Z. Li and A. Daniellians, 8/1/91, (PB92-143171, A06, MF-A02).
- NCEER-91-0021 "The NCEER-91 Earthquake Catalog: Improved Intensity-Based Magnitudes and Recurrence Relations for U.S. Earthquakes East of New Madrid," by L. Seeber and J.G. Armbruster, 8/28/91, (PB92-176742, A06, MF-A02).
- NCEER-91-0022 "Proceedings from the Implementation of Earthquake Planning and Education in Schools: The Need for Change - The Roles of the Changemakers," by K.E.K. Ross and F. Winslow, 7/23/91, (PB92-129998, A12, MF-A03).
- NCEER-91-0023 "A Study of Reliability-Based Criteria for Seismic Design of Reinforced Concrete Frame Buildings," by H.H.M. Hwang and H-M. Hsu, 8/10/91, (PB92-140235, A09, MF-A02).
- NCEER-91-0024 "Experimental Verification of a Number of Structural System Identification Algorithms," by R.G. Ghanem, H. Gavin and M. Shinozuka, 9/18/91, (PB92-176577, A18, MF-A04).
- NCEER-91-0025 "Probabilistic Evaluation of Liquefaction Potential," by H.H.M. Hwang and C.S. Lee," 11/25/91, (PB92-143429, A05, MF-A01).
- NCEER-91-0026 "Instantaneous Optimal Control for Linear, Nonlinear and Hysteretic Structures - Stable Controllers," by J.N. Yang and Z. Li, 11/15/91, (PB92-163807, A04, MF-A01).
- NCEER-91-0027 "Experimental and Theoretical Study of a Sliding Isolation System for Bridges," by M.C. Constantinou, A. Kartoum, A.M. Reinhorn and P. Bradford, 11/15/91, (PB92-176973, A10, MF-A03).
- NCEER-92-0001 "Case Studies of Liquefaction and Lifeline Performance During Past Earthquakes, Volume 1: Japanese Case Studies," Edited by M. Hamada and T. O'Rourke, 2/17/92, (PB92-197243, A18, MF-A04).
- NCEER-92-0002 "Case Studies of Liquefaction and Lifeline Performance During Past Earthquakes, Volume 2: United States Case Studies," Edited by T. O'Rourke and M. Hamada, 2/17/92, (PB92-197250, A20, MF-A04).
- NCEER-92-0003 "Issues in Earthquake Education," Edited by K. Ross, 2/3/92, (PB92-222389, A07, MF-A02).
- NCEER-92-0004 "Proceedings from the First U.S. - Japan Workshop on Earthquake Protective Systems for Bridges," Edited by I.G. Buckle, 2/4/92, (PB94-142239, A99, MF-A06).
- NCEER-92-0005 "Seismic Ground Motion from a Haskell-Type Source in a Multiple-Layered Half-Space," A.P. Theoharis, G. Deodatis and M. Shinozuka, 1/2/92, not available.
- NCEER-92-0006 "Proceedings from the Site Effects Workshop," Edited by R. Whitman, 2/29/92, (PB92-197201, A04, MF-A01).
- NCEER-92-0007 "Engineering Evaluation of Permanent Ground Deformations Due to Seismically-Induced Liquefaction," by M.H. Baziar, R. Dobry and A-W.M. Elgamal, 3/24/92, (PB92-222421, A13, MF-A03).
- NCEER-92-0008 "A Procedure for the Seismic Evaluation of Buildings in the Central and Eastern United States," by C.D. Poland and J.O. Malley, 4/2/92, (PB92-222439, A20, MF-A04).
- NCEER-92-0009 "Experimental and Analytical Study of a Hybrid Isolation System Using Friction Controllable Sliding Bearings," by M.Q. Feng, S. Fujii and M. Shinozuka, 5/15/92, (PB93-150282, A06, MF-A02).
- NCEER-92-0010 "Seismic Resistance of Slab-Column Connections in Existing Non-Ductile Flat-Plate Buildings," by A.J. Durrani and Y. Du, 5/18/92, (PB93-116812, A06, MF-A02).
- NCEER-92-0011 "The Hysteretic and Dynamic Behavior of Brick Masonry Walls Upgraded by Ferrocement Coatings Under Cyclic Loading and Strong Simulated Ground Motion," by H. Lee and S.P. Prawel, 5/11/92, not available.
- NCEER-92-0012 "Study of Wire Rope Systems for Seismic Protection of Equipment in Buildings," by G.F. Demetriades, M.C. Constantinou and A.M. Reinhorn, 5/20/92, (PB93-116655, A08, MF-A02).

- NCEER-92-0013 "Shape Memory Structural Dampers: Material Properties, Design and Seismic Testing," by P.R. Witting and F.A. Cozzarelli, 5/26/92, (PB93-116663, A05, MF-A01).
- NCEER-92-0014 "Longitudinal Permanent Ground Deformation Effects on Buried Continuous Pipelines," by M.J. O'Rourke, and C. Nordberg, 6/15/92, (PB93-116671, A08, MF-A02).
- NCEER-92-0015 "A Simulation Method for Stationary Gaussian Random Functions Based on the Sampling Theorem," by M. Grigoriu and S. Balopoulou, 6/11/92, (PB93-127496, A05, MF-A01).
- NCEER-92-0016 "Gravity-Load-Designed Reinforced Concrete Buildings: Seismic Evaluation of Existing Construction and Detailing Strategies for Improved Seismic Resistance," by G.W. Hoffmann, S.K. Kunnath, A.M. Reinhorn and J.B. Mander, 7/15/92, (PB94-142007, A08, MF-A02).
- NCEER-92-0017 "Observations on Water System and Pipeline Performance in the Limón Area of Costa Rica Due to the April 22, 1991 Earthquake," by M. O'Rourke and D. Ballantyne, 6/30/92, (PB93-126811, A06, MF-A02).
- NCEER-92-0018 "Fourth Edition of Earthquake Education Materials for Grades K-12," Edited by K.E.K. Ross, 8/10/92, (PB93-114023, A07, MF-A02).
- NCEER-92-0019 "Proceedings from the Fourth Japan-U.S. Workshop on Earthquake Resistant Design of Lifeline Facilities and Countermeasures for Soil Liquefaction," Edited by M. Hamada and T.D. O'Rourke, 8/12/92, (PB93-163939, A99, MF-E11).
- NCEER-92-0020 "Active Bracing System: A Full Scale Implementation of Active Control," by A.M. Reinhorn, T.T. Soong, R.C. Lin, M.A. Riley, Y.P. Wang, S. Aizawa and M. Higashino, 8/14/92, (PB93-127512, A06, MF-A02).
- NCEER-92-0021 "Empirical Analysis of Horizontal Ground Displacement Generated by Liquefaction-Induced Lateral Spreads," by S.F. Bartlett and T.L. Youd, 8/17/92, (PB93-188241, A06, MF-A02).
- NCEER-92-0022 "IDARC Version 3.0: Inelastic Damage Analysis of Reinforced Concrete Structures," by S.K. Kunnath, A.M. Reinhorn and R.F. Lobo, 8/31/92, (PB93-227502, A07, MF-A02).
- NCEER-92-0023 "A Semi-Empirical Analysis of Strong-Motion Peaks in Terms of Seismic Source, Propagation Path and Local Site Conditions, by M. Kamiyama, M.J. O'Rourke and R. Flores-Berrones, 9/9/92, (PB93-150266, A08, MF-A02).
- NCEER-92-0024 "Seismic Behavior of Reinforced Concrete Frame Structures with Nonductile Details, Part I: Summary of Experimental Findings of Full Scale Beam-Column Joint Tests," by A. Beres, R.N. White and P. Gergely, 9/30/92, (PB93-227783, A05, MF-A01).
- NCEER-92-0025 "Experimental Results of Repaired and Retrofitted Beam-Column Joint Tests in Lightly Reinforced Concrete Frame Buildings," by A. Beres, S. El-Borgi, R.N. White and P. Gergely, 10/29/92, (PB93-227791, A05, MF-A01).
- NCEER-92-0026 "A Generalization of Optimal Control Theory: Linear and Nonlinear Structures," by J.N. Yang, Z. Li and S. Vongchavalitkul, 11/2/92, (PB93-188621, A05, MF-A01).
- NCEER-92-0027 "Seismic Resistance of Reinforced Concrete Frame Structures Designed Only for Gravity Loads: Part I - Design and Properties of a One-Third Scale Model Structure," by J.M. Bracci, A.M. Reinhorn and J.B. Mander, 12/1/92, (PB94-104502, A08, MF-A02).
- NCEER-92-0028 "Seismic Resistance of Reinforced Concrete Frame Structures Designed Only for Gravity Loads: Part II - Experimental Performance of Subassemblages," by L.E. Aycaardi, J.B. Mander and A.M. Reinhorn, 12/1/92, (PB94-104510, A08, MF-A02).
- NCEER-92-0029 "Seismic Resistance of Reinforced Concrete Frame Structures Designed Only for Gravity Loads: Part III - Experimental Performance and Analytical Study of a Structural Model," by J.M. Bracci, A.M. Reinhorn and J.B. Mander, 12/1/92, (PB93-227528, A09, MF-A01).

- NCEER-92-0030 "Evaluation of Seismic Retrofit of Reinforced Concrete Frame Structures: Part I - Experimental Performance of Retrofitted Subassemblages," by D. Choudhuri, J.B. Mander and A.M. Reinhorn, 12/8/92, (PB93-198307, A07, MF-A02).
- NCEER-92-0031 "Evaluation of Seismic Retrofit of Reinforced Concrete Frame Structures: Part II - Experimental Performance and Analytical Study of a Retrofitted Structural Model," by J.M. Bracci, A.M. Reinhorn and J.B. Mander, 12/8/92, (PB93-198315, A09, MF-A03).
- NCEER-92-0032 "Experimental and Analytical Investigation of Seismic Response of Structures with Supplemental Fluid Viscous Dampers," by M.C. Constantinou and M.D. Symans, 12/21/92, (PB93-191435, A10, MF-A03). This report is available only through NTIS (see address given above).
- NCEER-92-0033 "Reconnaissance Report on the Cairo, Egypt Earthquake of October 12, 1992," by M. Khater, 12/23/92, (PB93-188621, A03, MF-A01).
- NCEER-92-0034 "Low-Level Dynamic Characteristics of Four Tall Flat-Plate Buildings in New York City," by H. Gavin, S. Yuan, J. Grossman, E. Pekelis and K. Jacob, 12/28/92, (PB93-188217, A07, MF-A02).
- NCEER-93-0001 "An Experimental Study on the Seismic Performance of Brick-Infilled Steel Frames With and Without Retrofit," by J.B. Mander, B. Nair, K. Wojtkowski and J. Ma, 1/29/93, (PB93-227510, A07, MF-A02).
- NCEER-93-0002 "Social Accounting for Disaster Preparedness and Recovery Planning," by S. Cole, E. Pantoja and V. Razak, 2/22/93, (PB94-142114, A12, MF-A03).
- NCEER-93-0003 "Assessment of 1991 NEHRP Provisions for Nonstructural Components and Recommended Revisions," by T.T. Soong, G. Chen, Z. Wu, R-H. Zhang and M. Grigoriu, 3/1/93, (PB93-188639, A06, MF-A02).
- NCEER-93-0004 "Evaluation of Static and Response Spectrum Analysis Procedures of SEAOC/UBC for Seismic Isolated Structures," by C.W. Winters and M.C. Constantinou, 3/23/93, (PB93-198299, A10, MF-A03).
- NCEER-93-0005 "Earthquakes in the Northeast - Are We Ignoring the Hazard? A Workshop on Earthquake Science and Safety for Educators," edited by K.E.K. Ross, 4/2/93, (PB94-103066, A09, MF-A02).
- NCEER-93-0006 "Inelastic Response of Reinforced Concrete Structures with Viscoelastic Braces," by R.F. Lobo, J.M. Bracci, K.L. Shen, A.M. Reinhorn and T.T. Soong, 4/5/93, (PB93-227486, A05, MF-A02).
- NCEER-93-0007 "Seismic Testing of Installation Methods for Computers and Data Processing Equipment," by K. Kosar, T.T. Soong, K.L. Shen, J.A. HoLung and Y.K. Lin, 4/12/93, (PB93-198299, A07, MF-A02).
- NCEER-93-0008 "Retrofit of Reinforced Concrete Frames Using Added Dampers," by A. Reinhorn, M. Constantinou and C. Li, not available.
- NCEER-93-0009 "Seismic Behavior and Design Guidelines for Steel Frame Structures with Added Viscoelastic Dampers," by K.C. Chang, M.L. Lai, T.T. Soong, D.S. Hao and Y.C. Yeh, 5/1/93, (PB94-141959, A07, MF-A02).
- NCEER-93-0010 "Seismic Performance of Shear-Critical Reinforced Concrete Bridge Piers," by J.B. Mander, S.M. Waheed, M.T.A. Chaudhary and S.S. Chen, 5/12/93, (PB93-227494, A08, MF-A02).
- NCEER-93-0011 "3D-BASIS-TABS: Computer Program for Nonlinear Dynamic Analysis of Three Dimensional Base Isolated Structures," by S. Nagarajaiah, C. Li, A.M. Reinhorn and M.C. Constantinou, 8/2/93, (PB94-141819, A09, MF-A02).
- NCEER-93-0012 "Effects of Hydrocarbon Spills from an Oil Pipeline Break on Ground Water," by O.J. Helweg and H.H.M. Hwang, 8/3/93, (PB94-141942, A06, MF-A02).
- NCEER-93-0013 "Simplified Procedures for Seismic Design of Nonstructural Components and Assessment of Current Code Provisions," by M.P. Singh, L.E. Suarez, E.E. Matheu and G.O. Maldonado, 8/4/93, (PB94-141827, A09, MF-A02).
- NCEER-93-0014 "An Energy Approach to Seismic Analysis and Design of Secondary Systems," by G. Chen and T.T. Soong, 8/6/93, (PB94-142767, A11, MF-A03).

- NCEER-93-0015 "Proceedings from School Sites: Becoming Prepared for Earthquakes - Commemorating the Third Anniversary of the Loma Prieta Earthquake," Edited by F.E. Winslow and K.E.K. Ross, 8/16/93, (PB94-154275, A16, MF-A02).
- NCEER-93-0016 "Reconnaissance Report of Damage to Historic Monuments in Cairo, Egypt Following the October 12, 1992 Dahshur Earthquake," by D. Sykora, D. Look, G. Croci, E. Karaesmen and E. Karaesmen, 8/19/93, (PB94-142221, A08, MF-A02).
- NCEER-93-0017 "The Island of Guam Earthquake of August 8, 1993," by S.W. Swan and S.K. Harris, 9/30/93, (PB94-141843, A04, MF-A01).
- NCEER-93-0018 "Engineering Aspects of the October 12, 1992 Egyptian Earthquake," by A.W. Elgamal, M. Amer, K. Adalier and A. Abul-Fadl, 10/7/93, (PB94-141983, A05, MF-A01).
- NCEER-93-0019 "Development of an Earthquake Motion Simulator and its Application in Dynamic Centrifuge Testing," by I. Krstelj, Supervised by J.H. Prevost, 10/23/93, (PB94-181773, A-10, MF-A03).
- NCEER-93-0020 "NCEER-Taisei Corporation Research Program on Sliding Seismic Isolation Systems for Bridges: Experimental and Analytical Study of a Friction Pendulum System (FPS)," by M.C. Constantinou, P. Tsopelas, Y-S. Kim and S. Okamoto, 11/1/93, (PB94-142775, A08, MF-A02).
- NCEER-93-0021 "Finite Element Modeling of Elastomeric Seismic Isolation Bearings," by L.J. Billings, Supervised by R. Shepherd, 11/8/93, not available.
- NCEER-93-0022 "Seismic Vulnerability of Equipment in Critical Facilities: Life-Safety and Operational Consequences," by K. Porter, G.S. Johnson, M.M. Zadeh, C. Scawthorn and S. Eder, 11/24/93, (PB94-181765, A16, MF-A03).
- NCEER-93-0023 "Hokkaido Nansei-oki, Japan Earthquake of July 12, 1993, by P.I. Yanev and C.R. Scawthorn, 12/23/93, (PB94-181500, A07, MF-A01).
- NCEER-94-0001 "An Evaluation of Seismic Serviceability of Water Supply Networks with Application to the San Francisco Auxiliary Water Supply System," by I. Markov, Supervised by M. Grigoriu and T. O'Rourke, 1/21/94, (PB94-204013, A07, MF-A02).
- NCEER-94-0002 "NCEER-Taisei Corporation Research Program on Sliding Seismic Isolation Systems for Bridges: Experimental and Analytical Study of Systems Consisting of Sliding Bearings, Rubber Restoring Force Devices and Fluid Dampers," Volumes I and II, by P. Tsopelas, S. Okamoto, M.C. Constantinou, D. Ozaki and S. Fujii, 2/4/94, (PB94-181740, A09, MF-A02 and PB94-181757, A12, MF-A03).
- NCEER-94-0003 "A Markov Model for Local and Global Damage Indices in Seismic Analysis," by S. Rahman and M. Grigoriu, 2/18/94, (PB94-206000, A12, MF-A03).
- NCEER-94-0004 "Proceedings from the NCEER Workshop on Seismic Response of Masonry Infills," edited by D.P. Abrams, 3/1/94, (PB94-180783, A07, MF-A02).
- NCEER-94-0005 "The Northridge, California Earthquake of January 17, 1994: General Reconnaissance Report," edited by J.D. Goltz, 3/11/94, (PB94-193943, A10, MF-A03).
- NCEER-94-0006 "Seismic Energy Based Fatigue Damage Analysis of Bridge Columns: Part I - Evaluation of Seismic Capacity," by G.A. Chang and J.B. Mander, 3/14/94, (PB94-219185, A11, MF-A03).
- NCEER-94-0007 "Seismic Isolation of Multi-Story Frame Structures Using Spherical Sliding Isolation Systems," by T.M. Al-Hussaini, V.A. Zayas and M.C. Constantinou, 3/17/94, (PB94-193745, A09, MF-A02).
- NCEER-94-0008 "The Northridge, California Earthquake of January 17, 1994: Performance of Highway Bridges," edited by I.G. Buckle, 3/24/94, (PB94-193851, A06, MF-A02).
- NCEER-94-0009 "Proceedings of the Third U.S.-Japan Workshop on Earthquake Protective Systems for Bridges," edited by I.G. Buckle and I. Friedland, 3/31/94, (PB94-195815, A99, MF-A06).

- NCEER-94-0010 "3D-BASIS-ME: Computer Program for Nonlinear Dynamic Analysis of Seismically Isolated Single and Multiple Structures and Liquid Storage Tanks," by P.C. Tsopelas, M.C. Constantinou and A.M. Reinhorn, 4/12/94, (PB94-204922, A09, MF-A02).
- NCEER-94-0011 "The Northridge, California Earthquake of January 17, 1994: Performance of Gas Transmission Pipelines," by T.D. O'Rourke and M.C. Palmer, 5/16/94, (PB94-204989, A05, MF-A01).
- NCEER-94-0012 "Feasibility Study of Replacement Procedures and Earthquake Performance Related to Gas Transmission Pipelines," by T.D. O'Rourke and M.C. Palmer, 5/25/94, (PB94-206638, A09, MF-A02).
- NCEER-94-0013 "Seismic Energy Based Fatigue Damage Analysis of Bridge Columns: Part II - Evaluation of Seismic Demand," by G.A. Chang and J.B. Mander, 6/1/94, (PB95-18106, A08, MF-A02).
- NCEER-94-0014 "NCEER-Taisei Corporation Research Program on Sliding Seismic Isolation Systems for Bridges: Experimental and Analytical Study of a System Consisting of Sliding Bearings and Fluid Restoring Force/Damping Devices," by P. Tsopelas and M.C. Constantinou, 6/13/94, (PB94-219144, A10, MF-A03).
- NCEER-94-0015 "Generation of Hazard-Consistent Fragility Curves for Seismic Loss Estimation Studies," by H. Hwang and J-R. Huo, 6/14/94, (PB95-181996, A09, MF-A02).
- NCEER-94-0016 "Seismic Study of Building Frames with Added Energy-Absorbing Devices," by W.S. Pong, C.S. Tsai and G.C. Lee, 6/20/94, (PB94-219136, A10, A03).
- NCEER-94-0017 "Sliding Mode Control for Seismic-Excited Linear and Nonlinear Civil Engineering Structures," by J. Yang, J. Wu, A. Agrawal and Z. Li, 6/21/94, (PB95-138483, A06, MF-A02).
- NCEER-94-0018 "3D-BASIS-TABS Version 2.0: Computer Program for Nonlinear Dynamic Analysis of Three Dimensional Base Isolated Structures," by A.M. Reinhorn, S. Nagarajaiah, M.C. Constantinou, P. Tsopelas and R. Li, 6/22/94, (PB95-182176, A08, MF-A02).
- NCEER-94-0019 "Proceedings of the International Workshop on Civil Infrastructure Systems: Application of Intelligent Systems and Advanced Materials on Bridge Systems," Edited by G.C. Lee and K.C. Chang, 7/18/94, (PB95-252474, A20, MF-A04).
- NCEER-94-0020 "Study of Seismic Isolation Systems for Computer Floors," by V. Lambrou and M.C. Constantinou, 7/19/94, (PB95-138533, A10, MF-A03).
- NCEER-94-0021 "Proceedings of the U.S.-Italian Workshop on Guidelines for Seismic Evaluation and Rehabilitation of Unreinforced Masonry Buildings," Edited by D.P. Abrams and G.M. Calvi, 7/20/94, (PB95-138749, A13, MF-A03).
- NCEER-94-0022 "NCEER-Taisei Corporation Research Program on Sliding Seismic Isolation Systems for Bridges: Experimental and Analytical Study of a System Consisting of Lubricated PTFE Sliding Bearings and Mild Steel Dampers," by P. Tsopelas and M.C. Constantinou, 7/22/94, (PB95-182184, A08, MF-A02).
- NCEER-94-0023 "Development of Reliability-Based Design Criteria for Buildings Under Seismic Load," by Y.K. Wen, H. Hwang and M. Shinozuka, 8/1/94, (PB95-211934, A08, MF-A02).
- NCEER-94-0024 "Experimental Verification of Acceleration Feedback Control Strategies for an Active Tendon System," by S.J. Dyke, B.F. Spencer, Jr., P. Quast, M.K. Sain, D.C. Kaspari, Jr. and T.T. Soong, 8/29/94, (PB95-212320, A05, MF-A01).
- NCEER-94-0025 "Seismic Retrofitting Manual for Highway Bridges," Edited by I.G. Buckle and I.F. Friedland, published by the Federal Highway Administration (PB95-212676, A15, MF-A03).
- NCEER-94-0026 "Proceedings from the Fifth U.S.-Japan Workshop on Earthquake Resistant Design of Lifeline Facilities and Countermeasures Against Soil Liquefaction," Edited by T.D. O'Rourke and M. Hamada, 11/7/94, (PB95-220802, A99, MF-E08).

- NCEER-95-0001 “Experimental and Analytical Investigation of Seismic Retrofit of Structures with Supplemental Damping: Part 1 - Fluid Viscous Damping Devices,” by A.M. Reinhorn, C. Li and M.C. Constantinou, 1/3/95, (PB95-266599, A09, MF-A02).
- NCEER-95-0002 “Experimental and Analytical Study of Low-Cycle Fatigue Behavior of Semi-Rigid Top-And-Seat Angle Connections,” by G. Pekcan, J.B. Mander and S.S. Chen, 1/5/95, (PB95-220042, A07, MF-A02).
- NCEER-95-0003 “NCEER-ATC Joint Study on Fragility of Buildings,” by T. Anagnos, C. Rojahn and A.S. Kiremidjian, 1/20/95, (PB95-220026, A06, MF-A02).
- NCEER-95-0004 “Nonlinear Control Algorithms for Peak Response Reduction,” by Z. Wu, T.T. Soong, V. Gattulli and R.C. Lin, 2/16/95, (PB95-220349, A05, MF-A01).
- NCEER-95-0005 “Pipeline Replacement Feasibility Study: A Methodology for Minimizing Seismic and Corrosion Risks to Underground Natural Gas Pipelines,” by R.T. Eguchi, H.A. Seligson and D.G. Honegger, 3/2/95, (PB95-252326, A06, MF-A02).
- NCEER-95-0006 “Evaluation of Seismic Performance of an 11-Story Frame Building During the 1994 Northridge Earthquake,” by F. Naeim, R. DiSulio, K. Benuska, A. Reinhorn and C. Li, not available.
- NCEER-95-0007 “Prioritization of Bridges for Seismic Retrofitting,” by N. Basöz and A.S. Kiremidjian, 4/24/95, (PB95-252300, A08, MF-A02).
- NCEER-95-0008 “Method for Developing Motion Damage Relationships for Reinforced Concrete Frames,” by A. Singhal and A.S. Kiremidjian, 5/11/95, (PB95-266607, A06, MF-A02).
- NCEER-95-0009 “Experimental and Analytical Investigation of Seismic Retrofit of Structures with Supplemental Damping: Part II - Friction Devices,” by C. Li and A.M. Reinhorn, 7/6/95, (PB96-128087, A11, MF-A03).
- NCEER-95-0010 “Experimental Performance and Analytical Study of a Non-Ductile Reinforced Concrete Frame Structure Retrofitted with Elastomeric Spring Dampers,” by G. Pekcan, J.B. Mander and S.S. Chen, 7/14/95, (PB96-137161, A08, MF-A02).
- NCEER-95-0011 “Development and Experimental Study of Semi-Active Fluid Damping Devices for Seismic Protection of Structures,” by M.D. Symans and M.C. Constantinou, 8/3/95, (PB96-136940, A23, MF-A04).
- NCEER-95-0012 “Real-Time Structural Parameter Modification (RSPM): Development of Innervated Structures,” by Z. Liang, M. Tong and G.C. Lee, 4/11/95, (PB96-137153, A06, MF-A01).
- NCEER-95-0013 “Experimental and Analytical Investigation of Seismic Retrofit of Structures with Supplemental Damping: Part III - Viscous Damping Walls,” by A.M. Reinhorn and C. Li, 10/1/95, (PB96-176409, A11, MF-A03).
- NCEER-95-0014 “Seismic Fragility Analysis of Equipment and Structures in a Memphis Electric Substation,” by J-R. Huo and H.H.M. Hwang, 8/10/95, (PB96-128087, A09, MF-A02).
- NCEER-95-0015 “The Hanshin-Awaji Earthquake of January 17, 1995: Performance of Lifelines,” Edited by M. Shinozuka, 11/3/95, (PB96-176383, A15, MF-A03).
- NCEER-95-0016 “Highway Culvert Performance During Earthquakes,” by T.L. Youd and C.J. Beckman, available as NCEER-96-0015.
- NCEER-95-0017 “The Hanshin-Awaji Earthquake of January 17, 1995: Performance of Highway Bridges,” Edited by I.G. Buckle, 12/1/95, not available.
- NCEER-95-0018 “Modeling of Masonry Infill Panels for Structural Analysis,” by A.M. Reinhorn, A. Madan, R.E. Valles, Y. Reichmann and J.B. Mander, 12/8/95, (PB97-110886, MF-A01, A06).
- NCEER-95-0019 “Optimal Polynomial Control for Linear and Nonlinear Structures,” by A.K. Agrawal and J.N. Yang, 12/11/95, (PB96-168737, A07, MF-A02).

- NCEER-95-0020 "Retrofit of Non-Ductile Reinforced Concrete Frames Using Friction Dampers," by R.S. Rao, P. Gergely and R.N. White, 12/22/95, (PB97-133508, A10, MF-A02).
- NCEER-95-0021 "Parametric Results for Seismic Response of Pile-Supported Bridge Bents," by G. Mylonakis, A. Nikolaou and G. Gazetas, 12/22/95, (PB97-100242, A12, MF-A03).
- NCEER-95-0022 "Kinematic Bending Moments in Seismically Stressed Piles," by A. Nikolaou, G. Mylonakis and G. Gazetas, 12/23/95, (PB97-113914, MF-A03, A13).
- NCEER-96-0001 "Dynamic Response of Unreinforced Masonry Buildings with Flexible Diaphragms," by A.C. Costley and D.P. Abrams, 10/10/96, (PB97-133573, MF-A03, A15).
- NCEER-96-0002 "State of the Art Review: Foundations and Retaining Structures," by I. Po Lam, not available.
- NCEER-96-0003 "Ductility of Rectangular Reinforced Concrete Bridge Columns with Moderate Confinement," by N. Wehbe, M. Saiidi, D. Sanders and B. Douglas, 11/7/96, (PB97-133557, A06, MF-A02).
- NCEER-96-0004 "Proceedings of the Long-Span Bridge Seismic Research Workshop," edited by I.G. Buckle and I.M. Friedland, not available.
- NCEER-96-0005 "Establish Representative Pier Types for Comprehensive Study: Eastern United States," by J. Kulicki and Z. Prucz, 5/28/96, (PB98-119217, A07, MF-A02).
- NCEER-96-0006 "Establish Representative Pier Types for Comprehensive Study: Western United States," by R. Imbsen, R.A. Schamber and T.A. Osterkamp, 5/28/96, (PB98-118607, A07, MF-A02).
- NCEER-96-0007 "Nonlinear Control Techniques for Dynamical Systems with Uncertain Parameters," by R.G. Ghanem and M.I. Bujakov, 5/27/96, (PB97-100259, A17, MF-A03).
- NCEER-96-0008 "Seismic Evaluation of a 30-Year Old Non-Ductile Highway Bridge Pier and Its Retrofit," by J.B. Mander, B. Mahmoodzadegan, S. Bhadra and S.S. Chen, 5/31/96, (PB97-110902, MF-A03, A10).
- NCEER-96-0009 "Seismic Performance of a Model Reinforced Concrete Bridge Pier Before and After Retrofit," by J.B. Mander, J.H. Kim and C.A. Ligozio, 5/31/96, (PB97-110910, MF-A02, A10).
- NCEER-96-0010 "IDARC2D Version 4.0: A Computer Program for the Inelastic Damage Analysis of Buildings," by R.E. Valles, A.M. Reinhorn, S.K. Kunnath, C. Li and A. Madan, 6/3/96, (PB97-100234, A17, MF-A03).
- NCEER-96-0011 "Estimation of the Economic Impact of Multiple Lifeline Disruption: Memphis Light, Gas and Water Division Case Study," by S.E. Chang, H.A. Seligson and R.T. Eguchi, 8/16/96, (PB97-133490, A11, MF-A03).
- NCEER-96-0012 "Proceedings from the Sixth Japan-U.S. Workshop on Earthquake Resistant Design of Lifeline Facilities and Countermeasures Against Soil Liquefaction, Edited by M. Hamada and T. O'Rourke, 9/11/96, (PB97-133581, A99, MF-A06).
- NCEER-96-0013 "Chemical Hazards, Mitigation and Preparedness in Areas of High Seismic Risk: A Methodology for Estimating the Risk of Post-Earthquake Hazardous Materials Release," by H.A. Seligson, R.T. Eguchi, K.J. Tierney and K. Richmond, 11/7/96, (PB97-133565, MF-A02, A08).
- NCEER-96-0014 "Response of Steel Bridge Bearings to Reversed Cyclic Loading," by J.B. Mander, D-K. Kim, S.S. Chen and G.J. Premus, 11/13/96, (PB97-140735, A12, MF-A03).
- NCEER-96-0015 "Highway Culvert Performance During Past Earthquakes," by T.L. Youd and C.J. Beckman, 11/25/96, (PB97-133532, A06, MF-A01).
- NCEER-97-0001 "Evaluation, Prevention and Mitigation of Pounding Effects in Building Structures," by R.E. Valles and A.M. Reinhorn, 2/20/97, (PB97-159552, A14, MF-A03).
- NCEER-97-0002 "Seismic Design Criteria for Bridges and Other Highway Structures," by C. Rojahn, R. Mayes, D.G. Anderson, J. Clark, J.H. Hom, R.V. Nutt and M.J. O'Rourke, 4/30/97, (PB97-194658, A06, MF-A03).

- NCEER-97-0003 "Proceedings of the U.S.-Italian Workshop on Seismic Evaluation and Retrofit," Edited by D.P. Abrams and G.M. Calvi, 3/19/97, (PB97-194666, A13, MF-A03).
- NCEER-97-0004 "Investigation of Seismic Response of Buildings with Linear and Nonlinear Fluid Viscous Dampers," by A.A. Seleemah and M.C. Constantinou, 5/21/97, (PB98-109002, A15, MF-A03).
- NCEER-97-0005 "Proceedings of the Workshop on Earthquake Engineering Frontiers in Transportation Facilities," edited by G.C. Lee and I.M. Friedland, 8/29/97, (PB98-128911, A25, MR-A04).
- NCEER-97-0006 "Cumulative Seismic Damage of Reinforced Concrete Bridge Piers," by S.K. Kunnath, A. El-Bahy, A. Taylor and W. Stone, 9/2/97, (PB98-108814, A11, MF-A03).
- NCEER-97-0007 "Structural Details to Accommodate Seismic Movements of Highway Bridges and Retaining Walls," by R.A. Imbsen, R.A. Schamber, E. Thorkildsen, A. Kartoum, B.T. Martin, T.N. Rosser and J.M. Kulicki, 9/3/97, (PB98-108996, A09, MF-A02).
- NCEER-97-0008 "A Method for Earthquake Motion-Damage Relationships with Application to Reinforced Concrete Frames," by A. Singhal and A.S. Kiremidjian, 9/10/97, (PB98-108988, A13, MF-A03).
- NCEER-97-0009 "Seismic Analysis and Design of Bridge Abutments Considering Sliding and Rotation," by K. Fishman and R. Richards, Jr., 9/15/97, (PB98-108897, A06, MF-A02).
- NCEER-97-0010 "Proceedings of the FHWA/NCEER Workshop on the National Representation of Seismic Ground Motion for New and Existing Highway Facilities," edited by I.M. Friedland, M.S. Power and R.L. Mayes, 9/22/97, (PB98-128903, A21, MF-A04).
- NCEER-97-0011 "Seismic Analysis for Design or Retrofit of Gravity Bridge Abutments," by K.L. Fishman, R. Richards, Jr. and R.C. Divito, 10/2/97, (PB98-128937, A08, MF-A02).
- NCEER-97-0012 "Evaluation of Simplified Methods of Analysis for Yielding Structures," by P. Tsopelas, M.C. Constantinou, C.A. Kircher and A.S. Whittaker, 10/31/97, (PB98-128929, A10, MF-A03).
- NCEER-97-0013 "Seismic Design of Bridge Columns Based on Control and Repairability of Damage," by C-T. Cheng and J.B. Mander, 12/8/97, (PB98-144249, A11, MF-A03).
- NCEER-97-0014 "Seismic Resistance of Bridge Piers Based on Damage Avoidance Design," by J.B. Mander and C-T. Cheng, 12/10/97, (PB98-144223, A09, MF-A02).
- NCEER-97-0015 "Seismic Response of Nominally Symmetric Systems with Strength Uncertainty," by S. Balopoulou and M. Grigoriu, 12/23/97, (PB98-153422, A11, MF-A03).
- NCEER-97-0016 "Evaluation of Seismic Retrofit Methods for Reinforced Concrete Bridge Columns," by T.J. Wipf, F.W. Klaiber and F.M. Russo, 12/28/97, (PB98-144215, A12, MF-A03).
- NCEER-97-0017 "Seismic Fragility of Existing Conventional Reinforced Concrete Highway Bridges," by C.L. Mullen and A.S. Cakmak, 12/30/97, (PB98-153406, A08, MF-A02).
- NCEER-97-0018 "Loss Assessment of Memphis Buildings," edited by D.P. Abrams and M. Shinozuka, 12/31/97, (PB98-144231, A13, MF-A03).
- NCEER-97-0019 "Seismic Evaluation of Frames with Infill Walls Using Quasi-static Experiments," by K.M. Mosalam, R.N. White and P. Gergely, 12/31/97, (PB98-153455, A07, MF-A02).
- NCEER-97-0020 "Seismic Evaluation of Frames with Infill Walls Using Pseudo-dynamic Experiments," by K.M. Mosalam, R.N. White and P. Gergely, 12/31/97, (PB98-153430, A07, MF-A02).
- NCEER-97-0021 "Computational Strategies for Frames with Infill Walls: Discrete and Smeared Crack Analyses and Seismic Fragility," by K.M. Mosalam, R.N. White and P. Gergely, 12/31/97, (PB98-153414, A10, MF-A02).

- NCEER-97-0022 "Proceedings of the NCEER Workshop on Evaluation of Liquefaction Resistance of Soils," edited by T.L. Youd and I.M. Idriss, 12/31/97, (PB98-155617, A15, MF-A03).
- MCEER-98-0001 "Extraction of Nonlinear Hysteretic Properties of Seismically Isolated Bridges from Quick-Release Field Tests," by Q. Chen, B.M. Douglas, E.M. Maragakis and I.G. Buckle, 5/26/98, (PB99-118838, A06, MF-A01).
- MCEER-98-0002 "Methodologies for Evaluating the Importance of Highway Bridges," by A. Thomas, S. Eshenaur and J. Kulicki, 5/29/98, (PB99-118846, A10, MF-A02).
- MCEER-98-0003 "Capacity Design of Bridge Piers and the Analysis of Overstrength," by J.B. Mander, A. Dutta and P. Goel, 6/1/98, (PB99-118853, A09, MF-A02).
- MCEER-98-0004 "Evaluation of Bridge Damage Data from the Loma Prieta and Northridge, California Earthquakes," by N. Basoz and A. Kiremidjian, 6/2/98, (PB99-118861, A15, MF-A03).
- MCEER-98-0005 "Screening Guide for Rapid Assessment of Liquefaction Hazard at Highway Bridge Sites," by T. L. Youd, 6/16/98, (PB99-118879, A06, not available on microfiche).
- MCEER-98-0006 "Structural Steel and Steel/Concrete Interface Details for Bridges," by P. Ritchie, N. Kauh and J. Kulicki, 7/13/98, (PB99-118945, A06, MF-A01).
- MCEER-98-0007 "Capacity Design and Fatigue Analysis of Confined Concrete Columns," by A. Dutta and J.B. Mander, 7/14/98, (PB99-118960, A14, MF-A03).
- MCEER-98-0008 "Proceedings of the Workshop on Performance Criteria for Telecommunication Services Under Earthquake Conditions," edited by A.J. Schiff, 7/15/98, (PB99-118952, A08, MF-A02).
- MCEER-98-0009 "Fatigue Analysis of Unconfined Concrete Columns," by J.B. Mander, A. Dutta and J.H. Kim, 9/12/98, (PB99-123655, A10, MF-A02).
- MCEER-98-0010 "Centrifuge Modeling of Cyclic Lateral Response of Pile-Cap Systems and Seat-Type Abutments in Dry Sands," by A.D. Gadre and R. Dobry, 10/2/98, (PB99-123606, A13, MF-A03).
- MCEER-98-0011 "IDARC-BRIDGE: A Computational Platform for Seismic Damage Assessment of Bridge Structures," by A.M. Reinhorn, V. Simeonov, G. Mylonakis and Y. Reichman, 10/2/98, (PB99-162919, A15, MF-A03).
- MCEER-98-0012 "Experimental Investigation of the Dynamic Response of Two Bridges Before and After Retrofitting with Elastomeric Bearings," by D.A. Wendichansky, S.S. Chen and J.B. Mander, 10/2/98, (PB99-162927, A15, MF-A03).
- MCEER-98-0013 "Design Procedures for Hinge Restrainers and Hinge Sear Width for Multiple-Frame Bridges," by R. Des Roches and G.L. Fenves, 11/3/98, (PB99-140477, A13, MF-A03).
- MCEER-98-0014 "Response Modification Factors for Seismically Isolated Bridges," by M.C. Constantinou and J.K. Quarshie, 11/3/98, (PB99-140485, A14, MF-A03).
- MCEER-98-0015 "Proceedings of the U.S.-Italy Workshop on Seismic Protective Systems for Bridges," edited by I.M. Friedland and M.C. Constantinou, 11/3/98, (PB2000-101711, A22, MF-A04).
- MCEER-98-0016 "Appropriate Seismic Reliability for Critical Equipment Systems: Recommendations Based on Regional Analysis of Financial and Life Loss," by K. Porter, C. Scawthorn, C. Taylor and N. Blais, 11/10/98, (PB99-157265, A08, MF-A02).
- MCEER-98-0017 "Proceedings of the U.S. Japan Joint Seminar on Civil Infrastructure Systems Research," edited by M. Shinozuka and A. Rose, 11/12/98, (PB99-156713, A16, MF-A03).
- MCEER-98-0018 "Modeling of Pile Footings and Drilled Shafts for Seismic Design," by I. PoLam, M. Kapuskar and D. Chaudhuri, 12/21/98, (PB99-157257, A09, MF-A02).

- MCEER-99-0001 "Seismic Evaluation of a Masonry Infilled Reinforced Concrete Frame by Pseudodynamic Testing," by S.G. Buonopane and R.N. White, 2/16/99, (PB99-162851, A09, MF-A02).
- MCEER-99-0002 "Response History Analysis of Structures with Seismic Isolation and Energy Dissipation Systems: Verification Examples for Program SAP2000," by J. Scheller and M.C. Constantinou, 2/22/99, (PB99-162869, A08, MF-A02).
- MCEER-99-0003 "Experimental Study on the Seismic Design and Retrofit of Bridge Columns Including Axial Load Effects," by A. Dutta, T. Kokorina and J.B. Mander, 2/22/99, (PB99-162877, A09, MF-A02).
- MCEER-99-0004 "Experimental Study of Bridge Elastomeric and Other Isolation and Energy Dissipation Systems with Emphasis on Uplift Prevention and High Velocity Near-source Seismic Excitation," by A. Kasalanati and M. C. Constantinou, 2/26/99, (PB99-162885, A12, MF-A03).
- MCEER-99-0005 "Truss Modeling of Reinforced Concrete Shear-flexure Behavior," by J.H. Kim and J.B. Mander, 3/8/99, (PB99-163693, A12, MF-A03).
- MCEER-99-0006 "Experimental Investigation and Computational Modeling of Seismic Response of a 1:4 Scale Model Steel Structure with a Load Balancing Supplemental Damping System," by G. Pekcan, J.B. Mander and S.S. Chen, 4/2/99, (PB99-162893, A11, MF-A03).
- MCEER-99-0007 "Effect of Vertical Ground Motions on the Structural Response of Highway Bridges," by M.R. Button, C.J. Cronin and R.L. Mayes, 4/10/99, (PB2000-101411, A10, MF-A03).
- MCEER-99-0008 "Seismic Reliability Assessment of Critical Facilities: A Handbook, Supporting Documentation, and Model Code Provisions," by G.S. Johnson, R.E. Sheppard, M.D. Quilici, S.J. Eder and C.R. Scawthorn, 4/12/99, (PB2000-101701, A18, MF-A04).
- MCEER-99-0009 "Impact Assessment of Selected MCEER Highway Project Research on the Seismic Design of Highway Structures," by C. Rojahn, R. Mayes, D.G. Anderson, J.H. Clark, D'Appolonia Engineering, S. Gloyd and R.V. Nutt, 4/14/99, (PB99-162901, A10, MF-A02).
- MCEER-99-0010 "Site Factors and Site Categories in Seismic Codes," by R. Dobry, R. Ramos and M.S. Power, 7/19/99, (PB2000-101705, A08, MF-A02).
- MCEER-99-0011 "Restrainer Design Procedures for Multi-Span Simply-Supported Bridges," by M.J. Randall, M. Saiidi, E. Maragakis and T. Isakovic, 7/20/99, (PB2000-101702, A10, MF-A02).
- MCEER-99-0012 "Property Modification Factors for Seismic Isolation Bearings," by M.C. Constantinou, P. Tsopelas, A. Kasalanati and E. Wolff, 7/20/99, (PB2000-103387, A11, MF-A03).
- MCEER-99-0013 "Critical Seismic Issues for Existing Steel Bridges," by P. Ritchie, N. Kauh and J. Kulicki, 7/20/99, (PB2000-101697, A09, MF-A02).
- MCEER-99-0014 "Nonstructural Damage Database," by A. Kao, T.T. Soong and A. Vender, 7/24/99, (PB2000-101407, A06, MF-A01).
- MCEER-99-0015 "Guide to Remedial Measures for Liquefaction Mitigation at Existing Highway Bridge Sites," by H.G. Cooke and J. K. Mitchell, 7/26/99, (PB2000-101703, A11, MF-A03).
- MCEER-99-0016 "Proceedings of the MCEER Workshop on Ground Motion Methodologies for the Eastern United States," edited by N. Abrahamson and A. Becker, 8/11/99, (PB2000-103385, A07, MF-A02).
- MCEER-99-0017 "Quindío, Colombia Earthquake of January 25, 1999: Reconnaissance Report," by A.P. Asfura and P.J. Flores, 10/4/99, (PB2000-106893, A06, MF-A01).
- MCEER-99-0018 "Hysteretic Models for Cyclic Behavior of Deteriorating Inelastic Structures," by M.V. Sivaselvan and A.M. Reinhorn, 11/5/99, (PB2000-103386, A08, MF-A02).

- MCEER-99-0019 "Proceedings of the 7th U.S.- Japan Workshop on Earthquake Resistant Design of Lifeline Facilities and Countermeasures Against Soil Liquefaction," edited by T.D. O'Rourke, J.P. Bardet and M. Hamada, 11/19/99, (PB2000-103354, A99, MF-A06).
- MCEER-99-0020 "Development of Measurement Capability for Micro-Vibration Evaluations with Application to Chip Fabrication Facilities," by G.C. Lee, Z. Liang, J.W. Song, J.D. Shen and W.C. Liu, 12/1/99, (PB2000-105993, A08, MF-A02).
- MCEER-99-0021 "Design and Retrofit Methodology for Building Structures with Supplemental Energy Dissipating Systems," by G. Pekcan, J.B. Mander and S.S. Chen, 12/31/99, (PB2000-105994, A11, MF-A03).
- MCEER-00-0001 "The Marmara, Turkey Earthquake of August 17, 1999: Reconnaissance Report," edited by C. Scawthorn; with major contributions by M. Bruneau, R. Eguchi, T. Holzer, G. Johnson, J. Mander, J. Mitchell, W. Mitchell, A. Papageorgiou, C. Scaethorn, and G. Webb, 3/23/00, (PB2000-106200, A11, MF-A03).
- MCEER-00-0002 "Proceedings of the MCEER Workshop for Seismic Hazard Mitigation of Health Care Facilities," edited by G.C. Lee, M. Ettouney, M. Grigoriu, J. Hauer and J. Nigg, 3/29/00, (PB2000-106892, A08, MF-A02).
- MCEER-00-0003 "The Chi-Chi, Taiwan Earthquake of September 21, 1999: Reconnaissance Report," edited by G.C. Lee and C.H. Loh, with major contributions by G.C. Lee, M. Bruneau, I.G. Buckle, S.E. Chang, P.J. Flores, T.D. O'Rourke, M. Shinozuka, T.T. Soong, C-H. Loh, K-C. Chang, Z-J. Chen, J-S. Hwang, M-L. Lin, G-Y. Liu, K-C. Tsai, G.C. Yao and C-L. Yen, 4/30/00, (PB2001-100980, A10, MF-A02).
- MCEER-00-0004 "Seismic Retrofit of End-Sway Frames of Steel Deck-Truss Bridges with a Supplemental Tendon System: Experimental and Analytical Investigation," by G. Pekcan, J.B. Mander and S.S. Chen, 7/1/00, (PB2001-100982, A10, MF-A02).
- MCEER-00-0005 "Sliding Fragility of Unrestrained Equipment in Critical Facilities," by W.H. Chong and T.T. Soong, 7/5/00, (PB2001-100983, A08, MF-A02).
- MCEER-00-0006 "Seismic Response of Reinforced Concrete Bridge Pier Walls in the Weak Direction," by N. Abo-Shadi, M. Saiidi and D. Sanders, 7/17/00, (PB2001-100981, A17, MF-A03).
- MCEER-00-0007 "Low-Cycle Fatigue Behavior of Longitudinal Reinforcement in Reinforced Concrete Bridge Columns," by J. Brown and S.K. Kunnath, 7/23/00, (PB2001-104392, A08, MF-A02).
- MCEER-00-0008 "Soil Structure Interaction of Bridges for Seismic Analysis," I. PoLam and H. Law, 9/25/00, (PB2001-105397, A08, MF-A02).
- MCEER-00-0009 "Proceedings of the First MCEER Workshop on Mitigation of Earthquake Disaster by Advanced Technologies (MEDAT-1), edited by M. Shinozuka, D.J. Inman and T.D. O'Rourke, 11/10/00, (PB2001-105399, A14, MF-A03).
- MCEER-00-0010 "Development and Evaluation of Simplified Procedures for Analysis and Design of Buildings with Passive Energy Dissipation Systems, Revision 01," by O.M. Ramirez, M.C. Constantinou, C.A. Kircher, A.S. Whittaker, M.W. Johnson, J.D. Gomez and C. Chrysostomou, 11/16/01, (PB2001-105523, A23, MF-A04).
- MCEER-00-0011 "Dynamic Soil-Foundation-Structure Interaction Analyses of Large Caissons," by C-Y. Chang, C-M. Mok, Z-L. Wang, R. Settgast, F. Waggoner, M.A. Ketchum, H.M. Gonnermann and C-C. Chin, 12/30/00, (PB2001-104373, A07, MF-A02).
- MCEER-00-0012 "Experimental Evaluation of Seismic Performance of Bridge Restrainers," by A.G. Vlassis, E.M. Maragakis and M. Saiid Saiidi, 12/30/00, (PB2001-104354, A09, MF-A02).
- MCEER-00-0013 "Effect of Spatial Variation of Ground Motion on Highway Structures," by M. Shinozuka, V. Saxena and G. Deodatis, 12/31/00, (PB2001-108755, A13, MF-A03).
- MCEER-00-0014 "A Risk-Based Methodology for Assessing the Seismic Performance of Highway Systems," by S.D. Werner, C.E. Taylor, J.E. Moore, II, J.S. Walton and S. Cho, 12/31/00, (PB2001-108756, A14, MF-A03).

- MCEER-01-0001 “Experimental Investigation of P-Delta Effects to Collapse During Earthquakes,” by D. Vian and M. Bruneau, 6/25/01, (PB2002-100534, A17, MF-A03).
- MCEER-01-0002 “Proceedings of the Second MCEER Workshop on Mitigation of Earthquake Disaster by Advanced Technologies (MEDAT-2),” edited by M. Bruneau and D.J. Inman, 7/23/01, (PB2002-100434, A16, MF-A03).
- MCEER-01-0003 “Sensitivity Analysis of Dynamic Systems Subjected to Seismic Loads,” by C. Roth and M. Grigoriu, 9/18/01, (PB2003-100884, A12, MF-A03).
- MCEER-01-0004 “Overcoming Obstacles to Implementing Earthquake Hazard Mitigation Policies: Stage 1 Report,” by D.J. Alesch and W.J. Petak, 12/17/01, (PB2002-107949, A07, MF-A02).
- MCEER-01-0005 “Updating Real-Time Earthquake Loss Estimates: Methods, Problems and Insights,” by C.E. Taylor, S.E. Chang and R.T. Eguchi, 12/17/01, (PB2002-107948, A05, MF-A01).
- MCEER-01-0006 “Experimental Investigation and Retrofit of Steel Pile Foundations and Pile Bents Under Cyclic Lateral Loadings,” by A. Shama, J. Mander, B. Blabac and S. Chen, 12/31/01, (PB2002-107950, A13, MF-A03).
- MCEER-02-0001 “Assessment of Performance of Bolu Viaduct in the 1999 Duzce Earthquake in Turkey” by P.C. Roussis, M.C. Constantinou, M. Erdik, E. Durukal and M. Dicleli, 5/8/02, (PB2003-100883, A08, MF-A02).
- MCEER-02-0002 “Seismic Behavior of Rail Counterweight Systems of Elevators in Buildings,” by M.P. Singh, Rildova and L.E. Suarez, 5/27/02. (PB2003-100882, A11, MF-A03).
- MCEER-02-0003 “Development of Analysis and Design Procedures for Spread Footings,” by G. Mylonakis, G. Gazetas, S. Nikolaou and A. Chauncey, 10/02/02, (PB2004-101636, A13, MF-A03, CD-A13).
- MCEER-02-0004 “Bare-Earth Algorithms for Use with SAR and LIDAR Digital Elevation Models,” by C.K. Huyck, R.T. Eguchi and B. Houshmand, 10/16/02, (PB2004-101637, A07, CD-A07).
- MCEER-02-0005 “Review of Energy Dissipation of Compression Members in Concentrically Braced Frames,” by K.Lee and M. Bruneau, 10/18/02, (PB2004-101638, A10, CD-A10).
- MCEER-03-0001 “Experimental Investigation of Light-Gauge Steel Plate Shear Walls for the Seismic Retrofit of Buildings” by J. Berman and M. Bruneau, 5/2/03, (PB2004-101622, A10, MF-A03, CD-A10).
- MCEER-03-0002 “Statistical Analysis of Fragility Curves,” by M. Shinozuka, M.Q. Feng, H. Kim, T. Uzawa and T. Ueda, 6/16/03, (PB2004-101849, A09, CD-A09).
- MCEER-03-0003 “Proceedings of the Eighth U.S.-Japan Workshop on Earthquake Resistant Design of Lifeline Facilities and Countermeasures Against Liquefaction,” edited by M. Hamada, J.P. Bardet and T.D. O’Rourke, 6/30/03, (PB2004-104386, A99, CD-A99).
- MCEER-03-0004 “Proceedings of the PRC-US Workshop on Seismic Analysis and Design of Special Bridges,” edited by L.C. Fan and G.C. Lee, 7/15/03, (PB2004-104387, A14, CD-A14).
- MCEER-03-0005 “Urban Disaster Recovery: A Framework and Simulation Model,” by S.B. Miles and S.E. Chang, 7/25/03, (PB2004-104388, A07, CD-A07).
- MCEER-03-0006 “Behavior of Underground Piping Joints Due to Static and Dynamic Loading,” by R.D. Meis, M. Maragakis and R. Siddharthan, 11/17/03, (PB2005-102194, A13, MF-A03, CD-A00).
- MCEER-04-0001 “Experimental Study of Seismic Isolation Systems with Emphasis on Secondary System Response and Verification of Accuracy of Dynamic Response History Analysis Methods,” by E. Wolff and M. Constantinou, 1/16/04 (PB2005-102195, A99, MF-E08, CD-A00).
- MCEER-04-0002 “Tension, Compression and Cyclic Testing of Engineered Cementitious Composite Materials,” by K. Kesner and S.L. Billington, 3/1/04, (PB2005-102196, A08, CD-A08).

- MCEER-04-0003 “Cyclic Testing of Braces Laterally Restrained by Steel Studs to Enhance Performance During Earthquakes,” by O.C. Celik, J.W. Berman and M. Bruneau, 3/16/04, (PB2005-102197, A13, MF-A03, CD-A00).
- MCEER-04-0004 “Methodologies for Post Earthquake Building Damage Detection Using SAR and Optical Remote Sensing: Application to the August 17, 1999 Marmara, Turkey Earthquake,” by C.K. Huyck, B.J. Adams, S. Cho, R.T. Eguchi, B. Mansouri and B. Houshmand, 6/15/04, (PB2005-104888, A10, CD-A00).
- MCEER-04-0005 “Nonlinear Structural Analysis Towards Collapse Simulation: A Dynamical Systems Approach,” by M.V. Sivaselvan and A.M. Reinhorn, 6/16/04, (PB2005-104889, A11, MF-A03, CD-A00).
- MCEER-04-0006 “Proceedings of the Second PRC-US Workshop on Seismic Analysis and Design of Special Bridges,” edited by G.C. Lee and L.C. Fan, 6/25/04, (PB2005-104890, A16, CD-A00).
- MCEER-04-0007 “Seismic Vulnerability Evaluation of Axially Loaded Steel Built-up Laced Members,” by K. Lee and M. Bruneau, 6/30/04, (PB2005-104891, A16, CD-A00).
- MCEER-04-0008 “Evaluation of Accuracy of Simplified Methods of Analysis and Design of Buildings with Damping Systems for Near-Fault and for Soft-Soil Seismic Motions,” by E.A. Pavlou and M.C. Constantinou, 8/16/04, (PB2005-104892, A08, MF-A02, CD-A00).
- MCEER-04-0009 “Assessment of Geotechnical Issues in Acute Care Facilities in California,” by M. Lew, T.D. O’Rourke, R. Dobry and M. Koch, 9/15/04, (PB2005-104893, A08, CD-A00).
- MCEER-04-0010 “Scissor-Jack-Damper Energy Dissipation System,” by A.N. Sigaher-Boyle and M.C. Constantinou, 12/1/04 (PB2005-108221).
- MCEER-04-0011 “Seismic Retrofit of Bridge Steel Truss Piers Using a Controlled Rocking Approach,” by M. Pollino and M. Bruneau, 12/20/04 (PB2006-105795).
- MCEER-05-0001 “Experimental and Analytical Studies of Structures Seismically Isolated with an Uplift-Restraint Isolation System,” by P.C. Roussis and M.C. Constantinou, 1/10/05 (PB2005-108222).
- MCEER-05-0002 “A Versatile Experimentation Model for Study of Structures Near Collapse Applied to Seismic Evaluation of Irregular Structures,” by D. Kusumastuti, A.M. Reinhorn and A. Rutenberg, 3/31/05 (PB2006-101523).
- MCEER-05-0003 “Proceedings of the Third PRC-US Workshop on Seismic Analysis and Design of Special Bridges,” edited by L.C. Fan and G.C. Lee, 4/20/05, (PB2006-105796).
- MCEER-05-0004 “Approaches for the Seismic Retrofit of Braced Steel Bridge Piers and Proof-of-Concept Testing of an Eccentrically Braced Frame with Tubular Link,” by J.W. Berman and M. Bruneau, 4/21/05 (PB2006-101524).
- MCEER-05-0005 “Simulation of Strong Ground Motions for Seismic Fragility Evaluation of Nonstructural Components in Hospitals,” by A. Wanitkorkul and A. Filiatrault, 5/26/05 (PB2006-500027).
- MCEER-05-0006 “Seismic Safety in California Hospitals: Assessing an Attempt to Accelerate the Replacement or Seismic Retrofit of Older Hospital Facilities,” by D.J. Alesch, L.A. Arendt and W.J. Petak, 6/6/05 (PB2006-105794).
- MCEER-05-0007 “Development of Seismic Strengthening and Retrofit Strategies for Critical Facilities Using Engineered Cementitious Composite Materials,” by K. Kesner and S.L. Billington, 8/29/05 (PB2006-111701).
- MCEER-05-0008 “Experimental and Analytical Studies of Base Isolation Systems for Seismic Protection of Power Transformers,” by N. Murota, M.Q. Feng and G-Y. Liu, 9/30/05 (PB2006-111702).
- MCEER-05-0009 “3D-BASIS-ME-MB: Computer Program for Nonlinear Dynamic Analysis of Seismically Isolated Structures,” by P.C. Tsopelas, P.C. Roussis, M.C. Constantinou, R. Buchanan and A.M. Reinhorn, 10/3/05 (PB2006-111703).
- MCEER-05-0010 “Steel Plate Shear Walls for Seismic Design and Retrofit of Building Structures,” by D. Vian and M. Bruneau, 12/15/05 (PB2006-111704).

- MCEER-05-0011 "The Performance-Based Design Paradigm," by M.J. Astrella and A. Whittaker, 12/15/05 (PB2006-111705).
- MCEER-06-0001 "Seismic Fragility of Suspended Ceiling Systems," H. Badillo-Almaraz, A.S. Whittaker, A.M. Reinhorn and G.P. Cimellaro, 2/4/06 (PB2006-111706).
- MCEER-06-0002 "Multi-Dimensional Fragility of Structures," by G.P. Cimellaro, A.M. Reinhorn and M. Bruneau, 3/1/06 (PB2007-106974, A09, MF-A02, CD A00).
- MCEER-06-0003 "Built-Up Shear Links as Energy Dissipators for Seismic Protection of Bridges," by P. Dusicka, A.M. Itani and I.G. Buckle, 3/15/06 (PB2006-111708).
- MCEER-06-0004 "Analytical Investigation of the Structural Fuse Concept," by R.E. Vargas and M. Bruneau, 3/16/06 (PB2006-111709).
- MCEER-06-0005 "Experimental Investigation of the Structural Fuse Concept," by R.E. Vargas and M. Bruneau, 3/17/06 (PB2006-111710).
- MCEER-06-0006 "Further Development of Tubular Eccentrically Braced Frame Links for the Seismic Retrofit of Braced Steel Truss Bridge Piers," by J.W. Berman and M. Bruneau, 3/27/06 (PB2007-105147).
- MCEER-06-0007 "REDARS Validation Report," by S. Cho, C.K. Huyck, S. Ghosh and R.T. Eguchi, 8/8/06 (PB2007-106983).
- MCEER-06-0008 "Review of Current NDE Technologies for Post-Earthquake Assessment of Retrofitted Bridge Columns," by J.W. Song, Z. Liang and G.C. Lee, 8/21/06 (PB2007-106984).
- MCEER-06-0009 "Liquefaction Remediation in Silty Soils Using Dynamic Compaction and Stone Columns," by S. Thevanayagam, G.R. Martin, R. Nashed, T. Shenthan, T. Kanagalingam and N. Ecemis, 8/28/06 (PB2007-106985).
- MCEER-06-0010 "Conceptual Design and Experimental Investigation of Polymer Matrix Composite Infill Panels for Seismic Retrofitting," by W. Jung, M. Chiewanichakorn and A.J. Aref, 9/21/06 (PB2007-106986).
- MCEER-06-0011 "A Study of the Coupled Horizontal-Vertical Behavior of Elastomeric and Lead-Rubber Seismic Isolation Bearings," by G.P. Warn and A.S. Whittaker, 9/22/06 (PB2007-108679).
- MCEER-06-0012 "Proceedings of the Fourth PRC-US Workshop on Seismic Analysis and Design of Special Bridges: Advancing Bridge Technologies in Research, Design, Construction and Preservation," Edited by L.C. Fan, G.C. Lee and L. Ziang, 10/12/06 (PB2007-109042).
- MCEER-06-0013 "Cyclic Response and Low Cycle Fatigue Characteristics of Plate Steels," by P. Dusicka, A.M. Itani and I.G. Buckle, 11/1/06 06 (PB2007-106987).
- MCEER-06-0014 "Proceedings of the Second US-Taiwan Bridge Engineering Workshop," edited by W.P. Yen, J. Shen, J-Y. Chen and M. Wang, 11/15/06 (PB2008-500041).
- MCEER-06-0015 "User Manual and Technical Documentation for the REDARSTM Import Wizard," by S. Cho, S. Ghosh, C.K. Huyck and S.D. Werner, 11/30/06 (PB2007-114766).
- MCEER-06-0016 "Hazard Mitigation Strategy and Monitoring Technologies for Urban and Infrastructure Public Buildings: Proceedings of the China-US Workshops," edited by X.Y. Zhou, A.L. Zhang, G.C. Lee and M. Tong, 12/12/06 (PB2008-500018).
- MCEER-07-0001 "Static and Kinetic Coefficients of Friction for Rigid Blocks," by C. Kafali, S. Fathali, M. Grigoriu and A.S. Whittaker, 3/20/07 (PB2007-114767).
- MCEER-07-0002 "Hazard Mitigation Investment Decision Making: Organizational Response to Legislative Mandate," by L.A. Arendt, D.J. Alesch and W.J. Petak, 4/9/07 (PB2007-114768).
- MCEER-07-0003 "Seismic Behavior of Bidirectional-Resistant Ductile End Diaphragms with Unbonded Braces in Straight or Skewed Steel Bridges," by O. Celik and M. Bruneau, 4/11/07 (PB2008-105141).

- MCEER-07-0004 “Modeling Pile Behavior in Large Pile Groups Under Lateral Loading,” by A.M. Dodds and G.R. Martin, 4/16/07(PB2008-105142).
- MCEER-07-0005 “Experimental Investigation of Blast Performance of Seismically Resistant Concrete-Filled Steel Tube Bridge Piers,” by S. Fujikura, M. Bruneau and D. Lopez-Garcia, 4/20/07 (PB2008-105143).
- MCEER-07-0006 “Seismic Analysis of Conventional and Isolated Liquefied Natural Gas Tanks Using Mechanical Analogs,” by I.P. Christovasilis and A.S. Whittaker, 5/1/07, not available.
- MCEER-07-0007 “Experimental Seismic Performance Evaluation of Isolation/Restraint Systems for Mechanical Equipment – Part 1: Heavy Equipment Study,” by S. Fathali and A. Filiatrault, 6/6/07 (PB2008-105144).
- MCEER-07-0008 “Seismic Vulnerability of Timber Bridges and Timber Substructures,” by A.A. Sharma, J.B. Mander, I.M. Friedland and D.R. Allicock, 6/7/07 (PB2008-105145).
- MCEER-07-0009 “Experimental and Analytical Study of the XY-Friction Pendulum (XY-FP) Bearing for Bridge Applications,” by C.C. Marin-Artieda, A.S. Whittaker and M.C. Constantinou, 6/7/07 (PB2008-105191).
- MCEER-07-0010 “Proceedings of the PRC-US Earthquake Engineering Forum for Young Researchers,” Edited by G.C. Lee and X.Z. Qi, 6/8/07 (PB2008-500058).
- MCEER-07-0011 “Design Recommendations for Perforated Steel Plate Shear Walls,” by R. Purba and M. Bruneau, 6/18/07, (PB2008-105192).
- MCEER-07-0012 “Performance of Seismic Isolation Hardware Under Service and Seismic Loading,” by M.C. Constantinou, A.S. Whittaker, Y. Kalpakidis, D.M. Fenz and G.P. Warn, 8/27/07, (PB2008-105193).
- MCEER-07-0013 “Experimental Evaluation of the Seismic Performance of Hospital Piping Subassemblies,” by E.R. Goodwin, E. Maragakis and A.M. Itani, 9/4/07, (PB2008-105194).
- MCEER-07-0014 “A Simulation Model of Urban Disaster Recovery and Resilience: Implementation for the 1994 Northridge Earthquake,” by S. Miles and S.E. Chang, 9/7/07, (PB2008-106426).
- MCEER-07-0015 “Statistical and Mechanistic Fragility Analysis of Concrete Bridges,” by M. Shinozuka, S. Banerjee and S-H. Kim, 9/10/07, (PB2008-106427).
- MCEER-07-0016 “Three-Dimensional Modeling of Inelastic Buckling in Frame Structures,” by M. Schachter and AM. Reinhorn, 9/13/07, (PB2008-108125).
- MCEER-07-0017 “Modeling of Seismic Wave Scattering on Pile Groups and Caissons,” by I. Po Lam, H. Law and C.T. Yang, 9/17/07 (PB2008-108150).
- MCEER-07-0018 “Bridge Foundations: Modeling Large Pile Groups and Caissons for Seismic Design,” by I. Po Lam, H. Law and G.R. Martin (Coordinating Author), 12/1/07 (PB2008-111190).
- MCEER-07-0019 “Principles and Performance of Roller Seismic Isolation Bearings for Highway Bridges,” by G.C. Lee, Y.C. Ou, Z. Liang, T.C. Niu and J. Song, 12/10/07 (PB2009-110466).
- MCEER-07-0020 “Centrifuge Modeling of Permeability and Pinning Reinforcement Effects on Pile Response to Lateral Spreading,” by L.L Gonzalez-Lagos, T. Abdoun and R. Dobry, 12/10/07 (PB2008-111191).
- MCEER-07-0021 “Damage to the Highway System from the Pisco, Perú Earthquake of August 15, 2007,” by J.S. O’Connor, L. Mesa and M. Nykamp, 12/10/07, (PB2008-108126).
- MCEER-07-0022 “Experimental Seismic Performance Evaluation of Isolation/Restraint Systems for Mechanical Equipment – Part 2: Light Equipment Study,” by S. Fathali and A. Filiatrault, 12/13/07 (PB2008-111192).
- MCEER-07-0023 “Fragility Considerations in Highway Bridge Design,” by M. Shinozuka, S. Banerjee and S.H. Kim, 12/14/07 (PB2008-111193).

- MCEER-07-0024 "Performance Estimates for Seismically Isolated Bridges," by G.P. Warn and A.S. Whittaker, 12/30/07 (PB2008-112230).
- MCEER-08-0001 "Seismic Performance of Steel Girder Bridge Superstructures with Conventional Cross Frames," by L.P. Carden, A.M. Itani and I.G. Buckle, 1/7/08, (PB2008-112231).
- MCEER-08-0002 "Seismic Performance of Steel Girder Bridge Superstructures with Ductile End Cross Frames with Seismic Isolators," by L.P. Carden, A.M. Itani and I.G. Buckle, 1/7/08 (PB2008-112232).
- MCEER-08-0003 "Analytical and Experimental Investigation of a Controlled Rocking Approach for Seismic Protection of Bridge Steel Truss Piers," by M. Pollino and M. Bruneau, 1/21/08 (PB2008-112233).
- MCEER-08-0004 "Linking Lifeline Infrastructure Performance and Community Disaster Resilience: Models and Multi-Stakeholder Processes," by S.E. Chang, C. Pasion, K. Tatebe and R. Ahmad, 3/3/08 (PB2008-112234).
- MCEER-08-0005 "Modal Analysis of Generally Damped Linear Structures Subjected to Seismic Excitations," by J. Song, Y-L. Chu, Z. Liang and G.C. Lee, 3/4/08 (PB2009-102311).
- MCEER-08-0006 "System Performance Under Multi-Hazard Environments," by C. Kafali and M. Grigoriu, 3/4/08 (PB2008-112235).
- MCEER-08-0007 "Mechanical Behavior of Multi-Spherical Sliding Bearings," by D.M. Fenz and M.C. Constantinou, 3/6/08 (PB2008-112236).
- MCEER-08-0008 "Post-Earthquake Restoration of the Los Angeles Water Supply System," by T.H.P. Tabucchi and R.A. Davidson, 3/7/08 (PB2008-112237).
- MCEER-08-0009 "Fragility Analysis of Water Supply Systems," by A. Jacobson and M. Grigoriu, 3/10/08 (PB2009-105545).
- MCEER-08-0010 "Experimental Investigation of Full-Scale Two-Story Steel Plate Shear Walls with Reduced Beam Section Connections," by B. Qu, M. Bruneau, C-H. Lin and K-C. Tsai, 3/17/08 (PB2009-106368).
- MCEER-08-0011 "Seismic Evaluation and Rehabilitation of Critical Components of Electrical Power Systems," S. Ersoy, B. Feizi, A. Ashrafi and M. Ala Saadeghvaziri, 3/17/08 (PB2009-105546).
- MCEER-08-0012 "Seismic Behavior and Design of Boundary Frame Members of Steel Plate Shear Walls," by B. Qu and M. Bruneau, 4/26/08 . (PB2009-106744).
- MCEER-08-0013 "Development and Appraisal of a Numerical Cyclic Loading Protocol for Quantifying Building System Performance," by A. Filiatrault, A. Wanitkorkul and M. Constantinou, 4/27/08 (PB2009-107906).
- MCEER-08-0014 "Structural and Nonstructural Earthquake Design: The Challenge of Integrating Specialty Areas in Designing Complex, Critical Facilities," by W.J. Petak and D.J. Alesch, 4/30/08 (PB2009-107907).
- MCEER-08-0015 "Seismic Performance Evaluation of Water Systems," by Y. Wang and T.D. O'Rourke, 5/5/08 (PB2009-107908).
- MCEER-08-0016 "Seismic Response Modeling of Water Supply Systems," by P. Shi and T.D. O'Rourke, 5/5/08 (PB2009-107910).
- MCEER-08-0017 "Numerical and Experimental Studies of Self-Centering Post-Tensioned Steel Frames," by D. Wang and A. Filiatrault, 5/12/08 (PB2009-110479).
- MCEER-08-0018 "Development, Implementation and Verification of Dynamic Analysis Models for Multi-Spherical Sliding Bearings," by D.M. Fenz and M.C. Constantinou, 8/15/08 (PB2009-107911).
- MCEER-08-0019 "Performance Assessment of Conventional and Base Isolated Nuclear Power Plants for Earthquake Blast Loadings," by Y.N. Huang, A.S. Whittaker and N. Luco, 10/28/08 (PB2009-107912).

- MCEER-08-0020 “Remote Sensing for Resilient Multi-Hazard Disaster Response – Volume I: Introduction to Damage Assessment Methodologies,” by B.J. Adams and R.T. Eguchi, 11/17/08 (PB2010-102695).
- MCEER-08-0021 “Remote Sensing for Resilient Multi-Hazard Disaster Response – Volume II: Counting the Number of Collapsed Buildings Using an Object-Oriented Analysis: Case Study of the 2003 Bam Earthquake,” by L. Gusella, C.K. Huyck and B.J. Adams, 11/17/08 (PB2010-100925).
- MCEER-08-0022 “Remote Sensing for Resilient Multi-Hazard Disaster Response – Volume III: Multi-Sensor Image Fusion Techniques for Robust Neighborhood-Scale Urban Damage Assessment,” by B.J. Adams and A. McMillan, 11/17/08 (PB2010-100926).
- MCEER-08-0023 “Remote Sensing for Resilient Multi-Hazard Disaster Response – Volume IV: A Study of Multi-Temporal and Multi-Resolution SAR Imagery for Post-Katrina Flood Monitoring in New Orleans,” by A. McMillan, J.G. Morley, B.J. Adams and S. Chesworth, 11/17/08 (PB2010-100927).
- MCEER-08-0024 “Remote Sensing for Resilient Multi-Hazard Disaster Response – Volume V: Integration of Remote Sensing Imagery and VIEWS™ Field Data for Post-Hurricane Charley Building Damage Assessment,” by J.A. Womble, K. Mehta and B.J. Adams, 11/17/08 (PB2009-115532).
- MCEER-08-0025 “Building Inventory Compilation for Disaster Management: Application of Remote Sensing and Statistical Modeling,” by P. Sarabandi, A.S. Kiremidjian, R.T. Eguchi and B. J. Adams, 11/20/08 (PB2009-110484).
- MCEER-08-0026 “New Experimental Capabilities and Loading Protocols for Seismic Qualification and Fragility Assessment of Nonstructural Systems,” by R. Retamales, G. Mosqueda, A. Filiatrault and A. Reinhorn, 11/24/08 (PB2009-110485).
- MCEER-08-0027 “Effects of Heating and Load History on the Behavior of Lead-Rubber Bearings,” by I.V. Kalpakidis and M.C. Constantinou, 12/1/08 (PB2009-115533).
- MCEER-08-0028 “Experimental and Analytical Investigation of Blast Performance of Seismically Resistant Bridge Piers,” by S.Fujikura and M. Bruneau, 12/8/08 (PB2009-115534).
- MCEER-08-0029 “Evolutionary Methodology for Aseismic Decision Support,” by Y. Hu and G. Dargush, 12/15/08.
- MCEER-08-0030 “Development of a Steel Plate Shear Wall Bridge Pier System Conceived from a Multi-Hazard Perspective,” by D. Keller and M. Bruneau, 12/19/08 (PB2010-102696).
- MCEER-09-0001 “Modal Analysis of Arbitrarily Damped Three-Dimensional Linear Structures Subjected to Seismic Excitations,” by Y.L. Chu, J. Song and G.C. Lee, 1/31/09 (PB2010-100922).
- MCEER-09-0002 “Air-Blast Effects on Structural Shapes,” by G. Ballantyne, A.S. Whittaker, A.J. Aref and G.F. Dargush, 2/2/09 (PB2010-102697).
- MCEER-09-0003 “Water Supply Performance During Earthquakes and Extreme Events,” by A.L. Bonneau and T.D. O’Rourke, 2/16/09 (PB2010-100923).
- MCEER-09-0004 “Generalized Linear (Mixed) Models of Post-Earthquake Ignitions,” by R.A. Davidson, 7/20/09 (PB2010-102698).
- MCEER-09-0005 “Seismic Testing of a Full-Scale Two-Story Light-Frame Wood Building: NEESWood Benchmark Test,” by I.P. Christovasilis, A. Filiatrault and A. Wanitkorkul, 7/22/09 (PB2012-102401).
- MCEER-09-0006 “IDARC2D Version 7.0: A Program for the Inelastic Damage Analysis of Structures,” by A.M. Reinhorn, H. Roh, M. Sivaselvan, S.K. Kunnath, R.E. Valles, A. Madan, C. Li, R. Lobo and Y.J. Park, 7/28/09 (PB2010-103199).
- MCEER-09-0007 “Enhancements to Hospital Resiliency: Improving Emergency Planning for and Response to Hurricanes,” by D.B. Hess and L.A. Arendt, 7/30/09 (PB2010-100924).

- MCEER-09-0008 "Assessment of Base-Isolated Nuclear Structures for Design and Beyond-Design Basis Earthquake Shaking," by Y.N. Huang, A.S. Whittaker, R.P. Kennedy and R.L. Mayes, 8/20/09 (PB2010-102699).
- MCEER-09-0009 "Quantification of Disaster Resilience of Health Care Facilities," by G.P. Cimellaro, C. Fumo, A.M. Reinhorn and M. Bruneau, 9/14/09 (PB2010-105384).
- MCEER-09-0010 "Performance-Based Assessment and Design of Squat Reinforced Concrete Shear Walls," by C.K. Gulec and A.S. Whittaker, 9/15/09 (PB2010-102700).
- MCEER-09-0011 "Proceedings of the Fourth US-Taiwan Bridge Engineering Workshop," edited by W.P. Yen, J.J. Shen, T.M. Lee and R.B. Zheng, 10/27/09 (PB2010-500009).
- MCEER-09-0012 "Proceedings of the Special International Workshop on Seismic Connection Details for Segmental Bridge Construction," edited by W. Phillip Yen and George C. Lee, 12/21/09 (PB2012-102402).
- MCEER-10-0001 "Direct Displacement Procedure for Performance-Based Seismic Design of Multistory Woodframe Structures," by W. Pang and D. Rosowsky, 4/26/10 (PB2012-102403).
- MCEER-10-0002 "Simplified Direct Displacement Design of Six-Story NEESWood Capstone Building and Pre-Test Seismic Performance Assessment," by W. Pang, D. Rosowsky, J. van de Lindt and S. Pei, 5/28/10 (PB2012-102404).
- MCEER-10-0003 "Integration of Seismic Protection Systems in Performance-Based Seismic Design of Woodframed Structures," by J.K. Shinde and M.D. Symans, 6/18/10 (PB2012-102405).
- MCEER-10-0004 "Modeling and Seismic Evaluation of Nonstructural Components: Testing Frame for Experimental Evaluation of Suspended Ceiling Systems," by A.M. Reinhorn, K.P. Ryu and G. Maddaloni, 6/30/10 (PB2012-102406).
- MCEER-10-0005 "Analytical Development and Experimental Validation of a Structural-Fuse Bridge Pier Concept," by S. El-Bahey and M. Bruneau, 10/1/10 (PB2012-102407).
- MCEER-10-0006 "A Framework for Defining and Measuring Resilience at the Community Scale: The PEOPLES Resilience Framework," by C.S. Renschler, A.E. Frazier, L.A. Arendt, G.P. Cimellaro, A.M. Reinhorn and M. Bruneau, 10/8/10 (PB2012-102408).
- MCEER-10-0007 "Impact of Horizontal Boundary Elements Design on Seismic Behavior of Steel Plate Shear Walls," by R. Purba and M. Bruneau, 11/14/10 (PB2012-102409).
- MCEER-10-0008 "Seismic Testing of a Full-Scale Mid-Rise Building: The NEESWood Capstone Test," by S. Pei, J.W. van de Lindt, S.E. Pryor, H. Shimizu, H. Isoda and D.R. Rammer, 12/1/10 (PB2012-102410).
- MCEER-10-0009 "Modeling the Effects of Detonations of High Explosives to Inform Blast-Resistant Design," by P. Sherkar, A.S. Whittaker and A.J. Aref, 12/1/10 (PB2012-102411).
- MCEER-10-0010 "L'Aquila Earthquake of April 6, 2009 in Italy: Rebuilding a Resilient City to Withstand Multiple Hazards," by G.P. Cimellaro, I.P. Christovasilis, A.M. Reinhorn, A. De Stefano and T. Kirova, 12/29/10.
- MCEER-11-0001 "Numerical and Experimental Investigation of the Seismic Response of Light-Frame Wood Structures," by I.P. Christovasilis and A. Filiatrault, 8/8/11 (PB2012-102412).
- MCEER-11-0002 "Seismic Design and Analysis of a Precast Segmental Concrete Bridge Model," by M. Anagnostopoulou, A. Filiatrault and A. Aref, 9/15/11.
- MCEER-11-0003 "Proceedings of the Workshop on Improving Earthquake Response of Substation Equipment," Edited by A.M. Reinhorn, 9/19/11 (PB2012-102413).
- MCEER-11-0004 "LRFD-Based Analysis and Design Procedures for Bridge Bearings and Seismic Isolators," by M.C. Constantinou, I. Kalpakidis, A. Filiatrault and R.A. Ecker Lay, 9/26/11.

- MCEER-11-0005 “Experimental Seismic Evaluation, Model Parameterization, and Effects of Cold-Formed Steel-Framed Gypsum Partition Walls on the Seismic Performance of an Essential Facility,” by R. Davies, R. Retamales, G. Mosqueda and A. Filiatrault, 10/12/11.
- MCEER-11-0006 “Modeling and Seismic Performance Evaluation of High Voltage Transformers and Bushings,” by A.M. Reinhorn, K. Oikonomou, H. Roh, A. Schiff and L. Kempner, Jr., 10/3/11.
- MCEER-11-0007 “Extreme Load Combinations: A Survey of State Bridge Engineers,” by G.C. Lee, Z. Liang, J.J. Shen and J.S. O’Connor, 10/14/11.
- MCEER-12-0001 “Simplified Analysis Procedures in Support of Performance Based Seismic Design,” by Y.N. Huang and A.S. Whittaker.
- MCEER-12-0002 “Seismic Protection of Electrical Transformer Bushing Systems by Stiffening Techniques,” by M. Koliou, A. Filiatrault, A.M. Reinhorn and N. Oliveto, 6/1/12.
- MCEER-12-0003 “Post-Earthquake Bridge Inspection Guidelines,” by J.S. O’Connor and S. Alampalli, 6/8/12.
- MCEER-12-0004 “Integrated Design Methodology for Isolated Floor Systems in Single-Degree-of-Freedom Structural Fuse Systems,” by S. Cui, M. Bruneau and M.C. Constantinou, 6/13/12.
- MCEER-12-0005 “Characterizing the Rotational Components of Earthquake Ground Motion,” by D. Basu, A.S. Whittaker and M.C. Constantinou, 6/15/12.
- MCEER-12-0006 “Bayesian Fragility for Nonstructural Systems,” by C.H. Lee and M.D. Grigoriu, 9/12/12.
- MCEER-12-0007 “A Numerical Model for Capturing the In-Plane Seismic Response of Interior Metal Stud Partition Walls,” by R.L. Wood and T.C. Hutchinson, 9/12/12.
- MCEER-12-0008 “Assessment of Floor Accelerations in Yielding Buildings,” by J.D. Wieser, G. Pekcan, A.E. Zaghi, A.M. Itani and E. Maragakis, 10/5/12.
- MCEER-13-0001 “Experimental Seismic Study of Pressurized Fire Sprinkler Piping Systems,” by Y. Tian, A. Filiatrault and G. Mosqueda, 4/8/13.
- MCEER-13-0002 “Enhancing Resource Coordination for Multi-Modal Evacuation Planning,” by D.B. Hess, B.W. Conley and C.M. Farrell, 2/8/13.
- MCEER-13-0003 “Seismic Response of Base Isolated Buildings Considering Pounding to Moat Walls,” by A. Masroor and G. Mosqueda, 2/26/13.
- MCEER-13-0004 “Seismic Response Control of Structures Using a Novel Adaptive Passive Negative Stiffness Device,” by D.T.R. Pasala, A.A. Sarlis, S. Nagarajaiah, A.M. Reinhorn, M.C. Constantinou and D.P. Taylor, 6/10/13.
- MCEER-13-0005 “Negative Stiffness Device for Seismic Protection of Structures,” by A.A. Sarlis, D.T.R. Pasala, M.C. Constantinou, A.M. Reinhorn, S. Nagarajaiah and D.P. Taylor, 6/12/13.
- MCEER-13-0006 “Emilia Earthquake of May 20, 2012 in Northern Italy: Rebuilding a Resilient Community to Withstand Multiple Hazards,” by G.P. Cimellaro, M. Chiriatti, A.M. Reinhorn and L. Tirca, June 30, 2013.
- MCEER-13-0007 “Precast Concrete Segmental Components and Systems for Accelerated Bridge Construction in Seismic Regions,” by A.J. Aref, G.C. Lee, Y.C. Ou and P. Sideris, with contributions from K.C. Chang, S. Chen, A. Filiatrault and Y. Zhou, June 13, 2013.
- MCEER-13-0008 “A Study of U.S. Bridge Failures (1980-2012),” by G.C. Lee, S.B. Mohan, C. Huang and B.N. Fard, June 15, 2013.
- MCEER-13-0009 “Development of a Database Framework for Modeling Damaged Bridges,” by G.C. Lee, J.C. Qi and C. Huang, June 16, 2013.

- MCEER-13-0010 “Model of Triple Friction Pendulum Bearing for General Geometric and Frictional Parameters and for Uplift Conditions,” by A.A. Sarlis and M.C. Constantinou, July 1, 2013.
- MCEER-13-0011 “Shake Table Testing of Triple Friction Pendulum Isolators under Extreme Conditions,” by A.A. Sarlis, M.C. Constantinou and A.M. Reinhorn, July 2, 2013.
- MCEER-13-0012 “Theoretical Framework for the Development of MH-LRFD,” by G.C. Lee (coordinating author), H.A. Capers, Jr., C. Huang, J.M. Kulicki, Z. Liang, T. Murphy, J.J.D. Shen, M. Shinozuka and P.W.H. Yen, July 31, 2013.
- MCEER-13-0013 “Seismic Protection of Highway Bridges with Negative Stiffness Devices,” by N.K.A. Attary, M.D. Symans, S. Nagarajaiah, A.M. Reinhorn, M.C. Constantinou, A.A. Sarlis, D.T.R. Pasala, and D.P. Taylor, September 3, 2014.
- MCEER-14-0001 “Simplified Seismic Collapse Capacity-Based Evaluation and Design of Frame Buildings with and without Supplemental Damping Systems,” by M. Hamidia, A. Filiatrault, and A. Aref, May 19, 2014.
- MCEER-14-0002 “Comprehensive Analytical Seismic Fragility of Fire Sprinkler Piping Systems,” by Siavash Soroushian, Emmanuel “Manos” Maragakis, Arash E. Zaghi, Alicia Echevarria, Yuan Tian and Andre Filiatrault, August 26, 2014.
- MCEER-14-0003 “Hybrid Simulation of the Seismic Response of a Steel Moment Frame Building Structure through Collapse,” by M. Del Carpio Ramos, G. Mosqueda and D.G. Lignos, October 30, 2014.
- MCEER-14-0004 “Blast and Seismic Resistant Concrete-Filled Double Skin Tubes and Modified Steel Jacketed Bridge Columns,” by P.P. Fouche and M. Bruneau, June 30, 2015.
- MCEER-14-0005 “Seismic Performance of Steel Plate Shear Walls Considering Various Design Approaches,” by R. Purba and M. Bruneau, October 31, 2014.
- MCEER-14-0006 “Air-Blast Effects on Civil Structures,” by Jinwon Shin, Andrew S. Whittaker, Amjad J. Aref and David Cormie, October 30, 2014.
- MCEER-14-0007 “Seismic Performance Evaluation of Precast Girders with Field-Cast Ultra High Performance Concrete (UHPC) Connections,” by G.C. Lee, C. Huang, J. Song, and J. S. O’Connor, July 31, 2014.
- MCEER-14-0008 “Post-Earthquake Fire Resistance of Ductile Concrete-Filled Double-Skin Tube Columns,” by Reza Imani, Gilberto Mosqueda and Michel Bruneau, December 1, 2014.
- MCEER-14-0009 “Cyclic Inelastic Behavior of Concrete Filled Sandwich Panel Walls Subjected to In-Plane Flexure,” by Y. Alzeni and M. Bruneau, December 19, 2014.
- MCEER-14-0010 “Analytical and Experimental Investigation of Self-Centering Steel Plate Shear Walls,” by D.M. Dowden and M. Bruneau, December 19, 2014.
- MCEER-15-0001 “Seismic Analysis of Multi-story Unreinforced Masonry Buildings with Flexible Diaphragms,” by J. Aleman, G. Mosqueda and A.S. Whittaker, June 12, 2015.
- MCEER-15-0002 “Site Response, Soil-Structure Interaction and Structure-Soil-Structure Interaction for Performance Assessment of Buildings and Nuclear Structures,” by C. Bolisetti and A.S. Whittaker, June 15, 2015.
- MCEER-15-0003 “Stress Wave Attenuation in Solids for Mitigating Impulsive Loadings,” by R. Rafiee-Dehkharghani, A.J. Aref and G. Dargush, August 15, 2015.
- MCEER-15-0004 “Computational, Analytical, and Experimental Modeling of Masonry Structures,” by K.M. Dolatshahi and A.J. Aref, November 16, 2015.
- MCEER-15-0005 “Property Modification Factors for Seismic Isolators: Design Guidance for Buildings,” by W.J. McVitty and M.C. Constantinou, June 30, 2015.

- MCEER-15-0006 “Seismic Isolation of Nuclear Power Plants using Sliding Bearings,” by Manish Kumar, Andrew S. Whittaker and Michael C. Constantinou, December 27, 2015.
- MCEER-15-0007 “Quintuple Friction Pendulum Isolator Behavior, Modeling and Validation,” by Donghun Lee and Michael C. Constantinou, December 28, 2015.
- MCEER-15-0008 “Seismic Isolation of Nuclear Power Plants using Elastomeric Bearings,” by Manish Kumar, Andrew S. Whittaker and Michael C. Constantinou, December 29, 2015.
- MCEER-16-0001 “Experimental, Numerical and Analytical Studies on the Seismic Response of Steel-Plate Concrete (SC) Composite Shear Walls,” by Siamak Epackachi and Andrew S. Whittaker, June 15, 2016.
- MCEER-16-0002 “Seismic Demand in Columns of Steel Frames,” by Lisa Shrestha and Michel Bruneau, June 17, 2016.
- MCEER-16-0003 “Development and Evaluation of Procedures for Analysis and Design of Buildings with Fluidic Self-Centering Systems” by Shoma Kitayama and Michael C. Constantinou, July 21, 2016.
- MCEER-16-0004 “Real Time Control of Shake Tables for Nonlinear Hysteretic Systems,” by Ki Pung Ryu and Andrei M. Reinhorn, October 22, 2016.
- MCEER-16-0006 “Seismic Isolation of High Voltage Electrical Power Transformers,” by Kostis Oikonomou, Michael C. Constantinou, Andrei M. Reinhorn and Leon Kemper, Jr., November 2, 2016.
- MCEER-16-0007 “Open Space Damping System Theory and Experimental Validation,” by Erkan Polat and Michael C. Constantinou, December 13, 2016.
- MCEER-16-0008 “Seismic Response of Low Aspect Ratio Reinforced Concrete Walls for Buildings and Safety-Related Nuclear Applications,” by Bismarck N. Luna and Andrew S. Whittaker.
- MCEER-16-0009 “Buckling Restrained Braces Applications for Superstructure and Substructure Protection in Bridges,” by Xiaone Wei and Michel Bruneau, December 28, 2016.
- MCEER-16-0010 “Procedures and Results of Assessment of Seismic Performance of Seismically Isolated Electrical Transformers with Due Consideration for Vertical Isolation and Vertical Ground Motion Effects,” by Shoma Kitayama, Michael C. Constantinou and Donghun Lee, December 31, 2016.



EARTHQUAKE ENGINEERING TO EXTREME EVENTS

University at Buffalo, The State University of New York

133A Ketter Hall ■ Buffalo, New York 14260-4300

Phone: (716) 645-3391 ■ Fax: (716) 645-3399

Email: mceer@buffalo.edu ■ Web: <http://mceer.buffalo.edu>



University at Buffalo *The State University of New York*

ISSN 1520-295X